BIOLOGICAL STRATEGIES TO ENHANCE THE ANAEROBIC DIGESTION PERFORMANCE: FUNDAMENTALS AND PROCESS DEVELOPMENT

EDITED BY: Shanfei Fu, Irini Angelidaki, Zeynep Cetecioglu, Qiang Kong, Yi Zheng and Panagiotis Tsapekos

PUBLISHED IN: Frontiers in Microbiology

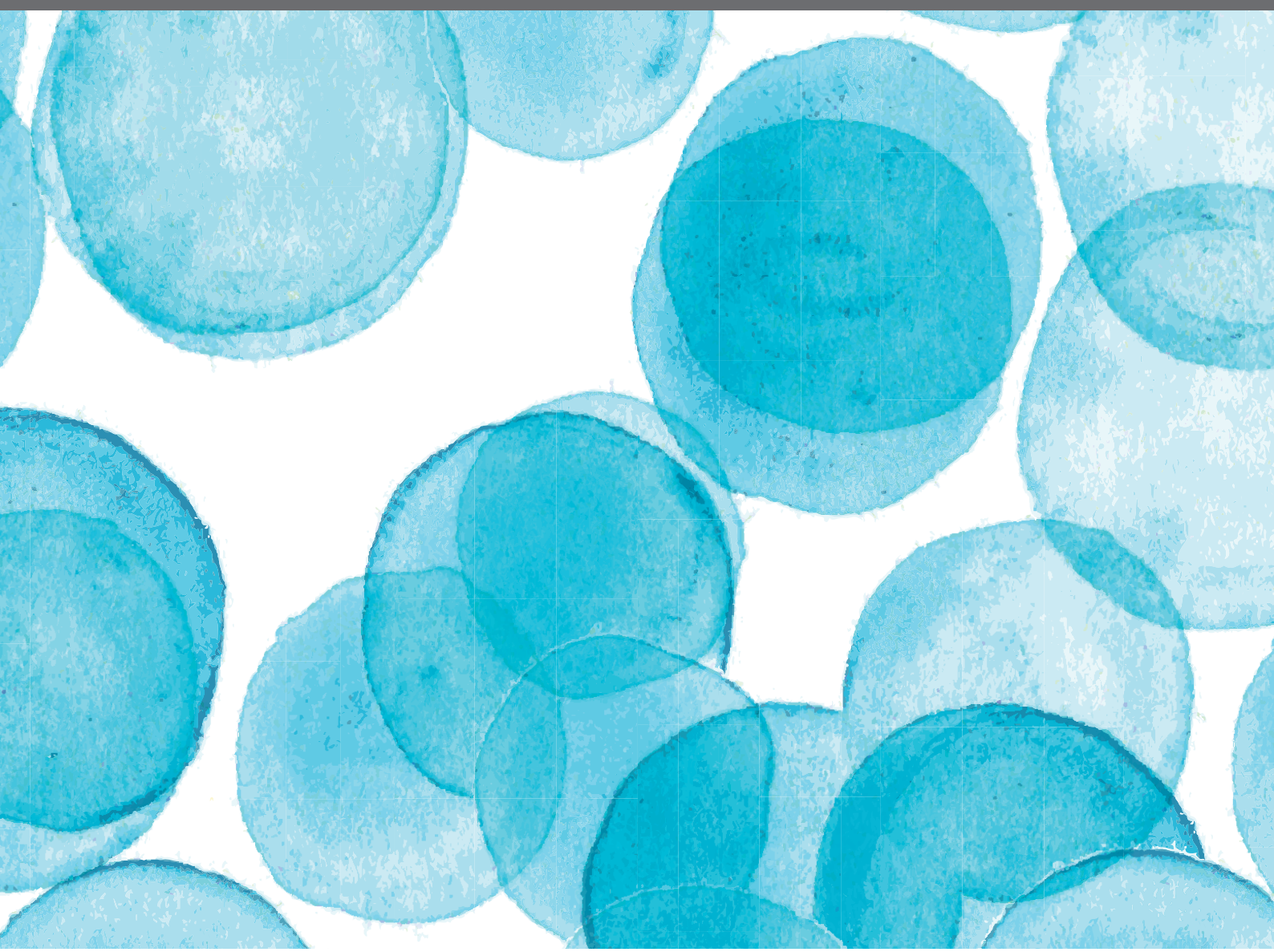

frontiers Research Topics

frontiers

ISSN 1664-8714
ISBN 978-2-88971-937-2
DOI 10.3389/978-2-88971-937-2

About Frontiers

Frontiers is more than just an open-access publisher of scholarly articles: it is a pioneering approach to the world of academia, radically improving the way scholarly research is managed. The grand vision of Frontiers is a world where all people have an equal opportunity to seek, share and generate knowledge. Frontiers provides immediate and permanent online open access to all its publications, but this alone is not enough to realize our grand goals.

Frontiers Journal Series

The Frontiers Journal Series is a multi-tier and interdisciplinary set of open-access, online journals, promising a paradigm shift from the current review, selection and dissemination processes in academic publishing. All Frontiers journals are driven by researchers for researchers; therefore, they constitute a service to the scholarly community. At the same time, the Frontiers Journal Series operates on a revolutionary invention, the tiered publishing system, initially addressing specific communities of scholars, and gradually climbing up to broader public understanding, thus serving the interests of the lay society, too.

Dedication to Quality

Each Frontiers article is a landmark of the highest quality, thanks to genuinely collaborative interactions between authors and review editors, who include some of the world's best academicians. Research must be certified by peers before entering a stream of knowledge that may eventually reach the public - and shape society; therefore, Frontiers only applies the most rigorous and unbiased reviews.
Frontiers revolutionizes research publishing by freely delivering the most outstanding research, evaluated with no bias from both the academic and social point of view. By applying the most advanced information technologies, Frontiers is catapulting scholarly publishing into a new generation.

What are Frontiers Research Topics?

Frontiers Research Topics are very popular trademarks of the Frontiers Journals Series: they are collections of at least ten articles, all centered on a particular subject. With their unique mix of varied contributions from Original Research to Review Articles, Frontiers Research Topics unify the most influential researchers, the latest key findings and historical advances in a hot research area! Find out more on how to host your own Frontiers Research Topic or contribute to one as an author by contacting the Frontiers Editorial Office: frontiersin.org/about/contact

BIOLOGICAL STRATEGIES TO ENHANCE THE ANAEROBIC DIGESTION PERFORMANCE: FUNDAMENTALS AND PROCESS DEVELOPMENT

Topic Editors:
Shanfei Fu, Jiangnan University, China
Irini Angelidaki, Technical University of Denmark, Denmark
Zeynep Cetecioglu, Royal Institute of Technology, Sweden
Qiang Kong, Shandong Normal University, China
Yi Zheng, Kansas State University, United States
Panagiotis Tsapekos, Technical University of Denmark, Denmark

Citation: Fu, S., Angelidaki, I., Cetecioglu, Z., Kong, Q., Zheng, Y., Tsapekos, P., eds. (2021). Biological Strategies to Enhance the Anaerobic Digestion Performance: Fundamentals and Process Development. Lausanne: Frontiers Media SA. doi: 10.3389/978-2-88971-937-2

Table of Contents

frontiers in Microbiology

EDITORIAL
published: 05 November 2021
doi: 10.3389/fmicb.2021.762875

Editorial: Biological Strategies to Enhance the Anaerobic Digestion Performance: Fundamentals and Process Development

Shanfei Fu[1]*, *Irini Angelidaki*[2], *Zeynep Cetecioglu*[3], *Qiang Kong*[4], *Yi Zheng*[5] and *Panagiotis Tsapekos*[2]

[1] School of Environmental and Civil Engineering, Jiangnan University, Wuxi, China, [2] Department of Chemical and Biochemical Engineering, Technical University of Denmark, Kongens Lyngby, Denmark, [3] Department of Chemical Engineering, Royal Institute of Technology, Stockholm, Sweden, [4] College of Geography and Environment, Shandong Normal University, Jinan, China, [5] Department of Grain Science and Industry, Kansas State University, Manhattan, KS, United States

Keywords: anaerobic digestion, biological pre-treatment, bioaugmentation, direct interspecies electron transfer, biogas plant surveillance

OPEN ACCESS

Edited by:
Eric Altermann,
AgResearch Ltd, New Zealand

Reviewed by:
Marcell Nikolausz,
Helmholtz Centre for Environmental Research (UFZ), Germany
Serge R. Guiot,
Université de Montréal, Canada

***Correspondence:**
Shanfei Fu
fusf@jiangnan.edu.cn

Specialty section:
This article was submitted to Microbiotechnology, a section of the journal Frontiers in Microbiology

Received: *23 August 2021*
Accepted: *06 October 2021*
Published: *05 November 2021*

Citation:
Fu S, Angelidaki I, Cetecioglu Z, Kong Q, Zheng Y and Tsapekos P (2021) Editorial: Biological Strategies to Enhance the Anaerobic Digestion Performance: Fundamentals and Process Development. Front. Microbiol. 12:762875. doi: 10.3389/fmicb.2021.762875

Editorial on the Research Topic

Biological Strategies to Enhance the Anaerobic Digestion Performance: Fundamentals and Process Development

Anaerobic digestion (AD) is a well-recognized process for organic waste reduction, stabilization, and bioenergy recovery (Niu et al., 2021). During the AD process, organic substrate is converted into biogas through four main biological steps: hydrolysis, acidogenesis, acetogenesis, and methanogenesis (Wu et al., 2021). Biogas is the end-product of AD, which is considered an important renewable energy carrier. Though promising, some key challenges, such as low biogas production efficiency, long digestion period, limited volumetric efficiency, and high capital cost, still exist in the AD process. In addition to these challenges, the microbial compositions and synergy mechanisms in the AD systems could also be affected by many factors including operational parameters, ammonia, volatile fatty acids (VFAs) concentration, and salinity.

Within the AD process, steering microbiological processes could potentially be an economical, highly efficient, and environmentally friendly solution (Detman et al., 2021). Microbial resource management was introduced originally by Vestraete et al. as an efficient way to influence the outcome of the AD process by managing or altering the microbial community composition to achieve specific goals (Verstraete et al., 2007). Microbial community composition has been altered to mitigate ammonia inhibition, to achieve resilience and balance of the AD process, to avoid inhibition of specific toxicants, and to improve acetogenesis. Several approaches have been applied to microbial community management as a means of influencing microbial composition (**Figure 1**). Bioaugmentation is a method wherein specific microorganisms, either as pure cultures or as mixed cultures, have been added either once or over a period of time to increase the tolerance to ammonia (Yang et al., 2019) and lipid-rich substrate (Cirne et al., 2006) and enhance the biodegradation of lignocellulosic materials (Martin-Ryals et al., 2015; Tsapekos et al., 2017). Other biological strategies include enrichment and/or stimulation of special indigenous microorganisms to increase the competitiveness of these microorganisms by providing the preferred substrate or operating

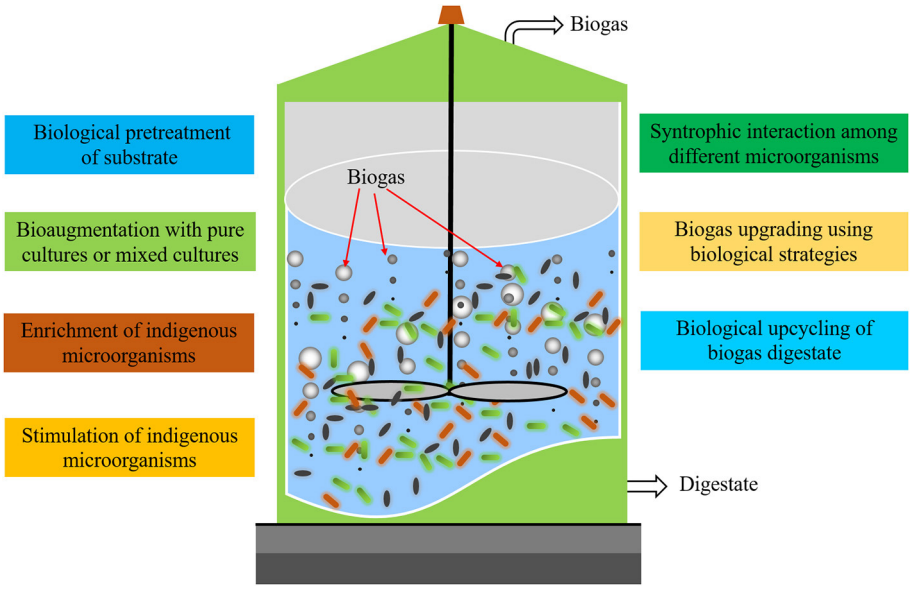

FIGURE 1 | Biological strategies to enhance the anaerobic digestion performance.

AD at specific conditions (e.g., temperature, pH, specific nutrients, and micro-aeration), which have been reported as promising methods to improve AD efficiency. However, further research is still needed to advance the AD process based on both fundamental understanding of the process and process engineering. Additionally, the studies on the variations of microbial communities and interactions among various microorganisms when the AD systems are subjected to certain external factors are also crucial to further unraveling the science of AD.

This Research Topic aims to cover promising and novel research into biological strategies to enhance AD performance, surveillance of biogas plants, and promote AD commercialization. Song et al. tried to enhance the AD performance of paper waste by novel biological pre-treatment, which provides an efficient and environmentally friendly solution to low hydrolysis efficiency existing in AD of cellulosic substrate; Atasoy and Cetecioglu showed the bioaugmentation of AD to treat cheese production wastewater with *Clostridium aceticum* could significantly increase the total VFA production as well as acetic acid concentration in the VFA mixture. García Rea et al. focused on increasing the phenol conversion rate in anaerobic systems by adding high sodium, which promoted the enrichment of phenol degrader *Syntrophorhabdus* sp. and the acetoclastic methanogen *Methanosaeta* sp.; Logroño et al. reported inoculum enriched in *Methanobacterium* genus can have functional resilience in terms of hydrogen consumption and methane production upon starvation periods. Xu et al. reported that a hydrothermal pre-treatment (HPT) combined with the addition of hydrochar could promote the actual biogas yield of anaerobic digestion of dead pig carcasses, since HPT considerably increased lipid decomposition and, to a lesser extent, proteins, and that hydrochar reduced ammonia inhibition by different mechanisms; Ceron-Chafla et al. showed the limited propionate conversion at elevated pCO_2 could be promoted by alternative and more resilient syntrophic propionate oxidizing bacteria and building up biomass adaptation to environmental conditions via directional selection of microbial community. Zhang et al. found that *Lactobacillus plantarum* QZ227 was a suitable silage additive to accumulate lactic acid and protect lignocellulosic biomass from contamination under freezing and thawing at low temperatures; Pang et al. demonstrated that the protease activity, protein-degrading bacteria, and acidogens were improved, while the α-glucosidase activity and the carbohydrate-degrading bacteria were inhibited under high salinity during AD. Singh et al. developed a strategy wherein a high-throughput microbiological surveillance approach was used to visualize the potential acetogenic population in commercial biogas digesters by using formyltetrahydrofolate synthetase (FTHFS) gene amplicons and unsupervised data analysis with the AcetoScan pipeline, which could assist in management of stable AD operations.

Overall, the published articles revealed biologically-based strategies to overcome barriers existing in anaerobic environments and enhance AD process performance. Though many papers are published on this topic every year, and the subject is attracting increasing attention, breakthroughs are still limited. More efforts should be made to reveal and understand fundamental mechanisms using advanced technologies (e.g., genome-centric metatranscriptomics, isotope tracing techniques, high-throughput sequencing, etc.). Subsequently, the generated knowledge can pave the way for the construction of highly efficient AD systems.

AUTHOR CONTRIBUTIONS

All authors listed have made a substantial, direct and intellectual contribution to the work, and approved it for publication.

ACKNOWLEDGMENTS

We would like to thank all authors for their valuable contributions, and the reviewers for assuring the quality of the papers in this topic.

REFERENCES

Cirne, D. G., Björnsson, L., Alves, M., and Mattiasson, B. (2006). Effects of bioaugmentation by an anaerobic lipolytic bacterium on anaerobic digestion of lipid-rich waste. *J. Chem. Technol. Biotechnol.* 81, 1745–1752. doi: 10.1002/jctb.1597

Detman, A., Laubitz, D., Chojnacka, A., Kiela, P. R., Salamon, A., Barberan, A., et al. (2021). Dynamics of dark fermentation microbial communities in the light of lactate and butyrate production. *Microbiome* 9:158. doi: 10.1186/s40168-021-01105-x

Martin-Ryals, A., Schideman, L., Li, P., Wilkinson, H., and Wagner, R. (2015). Improving anaerobic digestion of a cellulosic waste via routine bioaugmentation with cellulolytic microorganisms. *Bioresour. Technol.* 189, 62–70. doi: 10.1016/j.biortech.2015.03.069

Niu, C., Cai, T., Lu, X., Zhen, G., Pan, Y., Ren, X., et al. (2021). Nano zero-valent iron regulates the enrichment of organics-degrading and hydrogenotrophic microbes to stimulate methane bioconversion of waste activated sludge. *Chem. Eng. J.* 418:129511. doi: 10.1016/j.cej.2021.129511

Tsapekos, P., Kougias, P. G., Vasileiou, S. A., Treu, L., Campanaro, S., Lyberatos, G., et al. (2017). Bioaugmentation with hydrolytic microbes to improve the anaerobic biodegradability of lignocellulosic agricultural residues. *Bioresour. Technol.* 234, 350–359. doi: 10.1016/j.biortech.2017.03.043

Verstraete, W., Wittebolle, L., Heylen, K., Vanparys, B., van de Wiele, P., Boon, N. (2007). Microbial resource management: the road to go for environmental biotechnology.pdf. *Eng. Life Sci.* 7, 117–126. doi: 10.1002/elsc.200620176

Wu, D., Li, L., Peng, Y., Yang, P., Peng, X., Sun, Y., et al. (2021). State indicators of anaerobic digestion: a critical review on process monitoring and diagnosis. *Renew. Sustain. Energy Rev.* 148:111260. doi: 10.1016/j.rser.2021.111260

Yang, Z., Wang, W., Liu, C., Zhang, R., and Liu, G. (2019). Mitigation of ammonia inhibition through bioaugmentation with different microorganisms during anaerobic digestion: selection of strains and reactor performance evaluation. *Water Res.* 155, 214–224. doi: 10.1016/j.watres.2019.02.048

Conflict of Interest: The authors declare that the research was conducted in the absence of any commercial or financial relationships that could be construed as a potential conflict of interest.

Publisher's Note: All claims expressed in this article are solely those of the authors and do not necessarily represent those of their affiliated organizations, or those of the publisher, the editors and the reviewers. Any product that may be evaluated in this article, or claim that may be made by its manufacturer, is not guaranteed or endorsed by the publisher.

frontiers in Microbiology

ORIGINAL RESEARCH
published: 09 October 2020
doi: 10.3389/fmicb.2020.589222

Effect of NaCl Concentration on Microbiological Properties in NaCl Assistant Anaerobic Fermentation: Hydrolase Activity and Microbial Community Distribution

Heliang Pang[2], Xiaodong Xin[3], Junguo He[4], Baihui Cui[5], Dabin Guo[1,5], Shiming Liu[1], Zhongsen Yan[6], Chong Liu[7], Xinyu Wang[2] and Jun Nan[2]*

[1]School of Environmental Science and Engineering, Huazhong University of Science and Technology, Wuhan, China, [2]School of Environment, Harbin Institute of Technology, Harbin, China, [3]Department of Environmental Science and Engineering, Huaqiao University, Xiamen, China, [4]School of Civil Engineering, Guangzhou University, Guangzhou, China, [5]Advanced Environmental Biotechnology Centre, Nanyang Environment and Water Research Institute, Nanyang Technological University, Singapore, Singapore, [6]College of Civil Engineering, Fuzhou University, Fuzhou, China, [7]Frog Biotechnology Co., LTD, Harbin, China

OPEN ACCESS

Edited by:
Qiang Kong,
Shandong Normal University, China

Reviewed by:
Qinglian Wu,
National University of Singapore, Singapore
Guozhi Fan,
Wuhan Polytechnic University, China
Shihai Deng,
National University of Singapore, Singapore

***Correspondence:**
Dabin Guo
dabin@hust.edu.cn

Specialty section:
This article was submitted to Microbiotechnology, a section of the journal Frontiers in Microbiology

Received: 30 July 2020
Accepted: 14 September 2020
Published: 09 October 2020

Citation:
Pang H, Xin X, He J, Cui B, Guo D, Liu S, Yan Z, Liu C, Wang X and Nan J (2020) Effect of NaCl Concentration on Microbiological Properties in NaCl Assistant Anaerobic Fermentation: Hydrolase Activity and Microbial Community Distribution. Front. Microbiol. 11:589222. doi: 10.3389/fmicb.2020.589222

Previous studies have demonstrated that sludge hydrolysis and short-chain fatty acids (SCFAs) production were improved through NaCl assistant anaerobic fermentation. However, the effect of NaCl concentrations on hydrolase activity and microbial community structure was rarely reported. In this study, it was found that α-glucosidase activity and some carbohydrate-degrading bacteria were inhibited in NaCl tests, owing to their vulnerability to high NaCl concentration. Correspondingly, the microbial community richness and diversity were reduced compared with the control test, while the evenness was not affected by NaCl concentration. By contrast, the protease activity was increased in the presence of NaCl and reached the highest activity at the NaCl concentration of 20 g/L. The protein-degrading and SCFAs-producing bacteria (e.g., *Clostridium algidicarnis* and *Proteiniclasticum*) were enriched in the presence of NaCl, which were salt-tolerant.

Keywords: sodium chloride, anaerobic fermentation, hydrolase activity, waste activated sludge, microbial community

INTRODUCTION

It is estimated that China's total waste activated sludge (WAS) production will reach 60 million tons by 2020 (Li et al., 2018). The disposal of WAS has become a global problem. The yield of WAS had reached or even exceeded the environmental load, which increased environmental risks and disposal costs (Sun et al., 2015; Chen et al., 2019; He et al., 2019; Zhang et al., 2019). In recent years, carbon recovery in anaerobic fermentation has attracted wide attention (Cheng et al., 2020; Pang et al., 2020d). Through anaerobic fermentation process, biodegradable organic matter in WAS can be converted into short-chain fatty acids (SCFA), which was a promising carbon source with a wide range of applications (Zhang et al., 2018, 2020; Xin et al., 2020). For example, it could be used as an external carbon source to supplement

the carbon gap in wastewater treatment plants (WWTPs) and to promote the biological production of electricity/polyhydroxyalkanoate (PHA; Cai et al., 2009; Li et al., 2011; Chen et al., 2013). Generally, hydrolysis and acidification were involved in anaerobic fermentation for SCFAs production (Luo et al., 2019). The hydrolysis step was regarded as the rate-limiting stage, as the biodegradable organic matters were wrapped in WAS flocs, which reduced their usability for microorganism (Lv et al., 2010). As such, WAS solubilization with the aim of organic matter release was necessary for improving anaerobic fermentation efficiency.

NaCl (sodium chloride) is an inexpensive chemical with a wide range of sources. It has been reported that high NaCl concentration could induce sludge solubilization and deteriorate floc structure (Reid et al., 2006; Cui et al., 2015; Su et al., 2016; Lu et al., 2019). In our previous research, a novel and efficient NaCl assistant anaerobic fermentation strategy was developed for bio-production of SCFAs (Pang et al., 2020e). In the process of NaCl assistant anaerobic fermentation, the addition of NaCl resulted in significant osmotic pressure difference between the sludge phase and the liquid phase, which caused the decomposition of WAS flocs and the breakdown of extracellular polymeric substances (EPS). As such, the sludge flocs were dissolved with release of biodegradable organic matter. Thereby, the efficiencies of sludge hydrolysis and the subsequent SCFAs production were improved. It was reported that numerous soluble chemical oxygen demand (SCOD) of 4,092 mg/L was released into the supernatant at the optimal NaCl concentration of 20 g/L, meanwhile considerable SCFAs of 288.2 mg COD/g VSS was produced through a 4-day anaerobic fermentation (Pang et al., 2020e). Such performances on sludge solubilization and SCFAs yield in NaCl assistant anaerobic fermentation were comparable to the anaerobic fermentation with chemical pretreatments (e.g., surfactants, enzymes, cation-exchange resin, etc.; Huang et al., 2015; He et al., 2018; Pang et al., 2020a,b, 2021).

Furthermore, numerous NaCl was remained in the fermented sludge, which was feasible for reuse once the produced SCFAs could be utilized and consumed. As declared in previous study, the NaCl assistant anaerobic fermentation was indeed a green and efficient approach with some advantages, e.g., none irresistibly consumed chemicals, considerably reduced treatment costs and avoided environmental risks of remained NaCl. After NaCl assistant anaerobic fermentation, the fermentative liquid with numerous SCFAs could be used as external carbon source, e.g., the substrate for biological electricity production through microbial fuel cell (MFC) or the external carbon source for supplementing the carbon gap in municipal wastewater. The feasibility of these utilization approaches were discussed in our previous study (Pang et al., 2020e). After utilization of the soluble organic matters, the fermentative liquid could be reused for NaCl assistant anaerobic fermentation since there is numerous NaCl existed in the fermentative liquid. In this way, the treatment agent (i.e., NaCl) could be recycled, implying that considerable chemical agent and treatment costs could be saved.

Despite the sludge solubilization, EPS disruption, SCFA yield, and relevant mechanism were explored in our previous study (Pang et al., 2020e); the effects of NaCl concentration on enzyme activity and microbial community structure are still unfathomed. Actually, the tolerance of bacteria for high salinity condition is different. The harsh condition of high NaCl concentration might not be conducive to the survival of some microorganism in WAS, which was related to microbial community structure and might lead to shift of dominant bacterial community (Duan et al., 2016). In ecosystem, the functional bacteria distribution is critical to the system functions (Xin et al., 2015; Xu et al., 2018, 2019; Ji et al., 2020). In the anaerobic fermentation process, both the biodegradation of dissolved organic matters (DOMs) and the consumption of SCFAs mainly rely on appropriate microbial communities. As such, exploring the hydrolase activity and microbial community structure under different NaCl concentrations were beneficial to completely understand the NaCl assistant anaerobic fermentation process and optimize the process parameters. Furthermore, the evolutions of microbial community structure and metabolic activity at different NaCl concentrations during anaerobic fermentation process have rarely attracted our attention. Under this circumstance, the functional characteristics of the sludge ecosystem and the biodegradation pathway of DOMs were seriously affected, which might be varying at different NaCl concentrations and be dissimilar to that in conventional anaerobic fermentation (without NaCl addition). The microbial and enzymic characteristics of sludge related to different NaCl concentration in NaCl assistant anaerobic fermentation might be an interesting issue.

In this study, the microbiological characteristics at different NaCl concentrations were explored in the anaerobic fermentation system. The main objectives of this research include (1) investigating the effect of NaCl concentrations on hydrolase activity in anaerobic fermentation process; (2) exploring the microbial community structure and identifying main species at different NaCl concentrations; and (3) analyzing biodegradation pathway of DOMs for SCFAs accumulation in NaCl assistant anaerobic fermentation process. Through this research work, we can further understand the metabolic activity and microbial community structure related to different NaCl concentrations during anaerobic fermentation, which improved the knowledge of community ecology.

MATERIALS AND METHODS

Characteristics of Thickened WAS

The WAS samples were obtained from a municipal WWTP locating in Harbin city, Heilongjiang province, China. The collected WAS samples were thickened at 4°C for 12 h, which was then used for the anaerobic fermentation experiments. The total suspended solids (TSS), volatile suspended solids (VSS), and total chemical oxygen demand (TCOD) of the thickened WAS were 19.2 ± 0.2, 13.2 ± 0.1, and 17.1 ± 0.3 g/L, respectively. The sludge pH was 6.95 ± 0.15. In the initial supernatant, the SCOD concentration, soluble proteins content,

soluble polysaccharides content, and SCFAs concentration were 240 ± 85, 62.2 ± 12.7, 26.6 ± 5.8, and 45.7 ± 30.0 mg COD/L, respectively.

Anaerobic Fermentation Experiment

The NaCl assistant anaerobic fermentation was performed in four batch reactors (working volume = 500 ml) and 450 ml thickened WAS was filled each. The NaCl agent (AR) was added into these batch reactors to adjust the NaCl concentrations to 0 (control), 10, 20, and 30 g/L, respectively. Then, these reactors were flushed with N_2 and were stirred in an air-bath shaker at 120 rpm (35 ± 1°C). The sludge samples were collected on day 4 of the anaerobic fermentation for the analyses of hydrolase activity and microbial community. The sludge pH during the NaCl assistant anaerobic fermentation process was in the range of 6.7–7.0, without adjustment. The fermentation period (4 days) was selected according to our previous study, in which the sludge samples and experimental conditions were the same. In our previous study, the optimal period of NaCl assistant anaerobic fermentation was found to be 4 days (Pang et al., 2020e). The experimental results are averaged in triplicates.

Hydrolase Activities

The protease and α-glucosidase activities were measured following the procedures in existing literatures (Liu et al., 2015). The Tris-HCl buffer (pH = 8) and Triton X-100 were employed for extracting the protease from sludge samples. The protease extraction solution was used for protease activity quantification, while the sludge samples were used for α-glucosidase activity measurement. The measurement procedure of hydrolase activity was the same for different sludge samples.

Denaturing Gradient Gel Electrophoresis Analysis

The Fast DNA Spin Kit-EZ-10 was used to extract total DNA according to the method described in specification. After the successful extraction by gel electrophoresis, the DNA was stored in a refrigerator (−20°C) for further processing. The GeneAmp PCR System 9700 (PE9700, ABI, USA) was used to amplify 16S rRNA genes, the steps were as follows: denaturation (95°C, 30 s), denaturation (94°C, 45 s), annealing (60°C, 45 s), extension (72°C, 60 s), and extension (72°C, 600 s). Primers 338F (FACTCCTACGGGAGGCAGC) and 518R (ATTACCGCG GCTGCTGG) were used for gene amplification. Electrophoresis was carried out using buffer (1 × TAE, 80 V, 60°C, 720 min). Then, the gel was stained with SDNA-nucleic acid staining dye (Bio Basic Inc., Canada), followed by washing with sterile water and scanning using a projection scanner (PowerLook 1,000, Umax, China). Finally, the samples were sequenced on DNA sequencing system (ABI3730XL).

In order to assess the microbial community structure at different NaCl concentrations, the richness and diversity indexes were analyzed. The denaturing gradient gel electrophoresis (DGGE) band results were analyzed by Quantity One version 4.6.2 analysis software, i.e., the band numbers and strength were determined, followed by calculation according to the procedure in previous study (Polli et al., 2018). The DGGE technology is economical and dependable, which is sufficient for analyzing the difference of microbial community structure between sludge samples. In this study, the DGGE results were expected to provide some valuable conclusions.

RESULTS AND DISCUSSION

Effect of NaCl Concentration on Hydrolase Activity

The enzyme activity was closely related to metabolic activity of functional microorganism in sludge system, especially the hydrolase activity, which directly affects sludge hydrolysis and DOMs biodegradation in anaerobic fermentation process. During the NaCl assistant anaerobic fermentation, the additional NaCl caused remarkable osmotic pressure difference, resulting in EPS disruption and cell lysis (Pang et al., 2020d). Sludge solubilization was thereby triggered, which enhanced sludge hydrolysis and SCFAs production. Meanwhile, the high salinity environment significantly affected the survival of some microorganism, which modified microbial community structure and changed functional characteristics of sludge system. The enzyme activity was also remarkably affected. The **Figure 1** presents the relative activity of hydrolase (i.e., protease and α-glucosidase) after 4-day anaerobic fermentation at different NaCl concentrations. Compared with the control test (i.e., without NaCl addition), the protease activity was significantly increased at the NaCl concentrations in range of 10–30 g/L, while the α-glucosidase activity was decreased. Overall, the presence of NaCl facilitated protease and inhibited α-glucosidase in the anaerobic fermentation system. Moreover, it was noticeable that the relative activity of protease was increased with the rising NaCl concentration from 0 to 20 g/L, afterward the protease activity

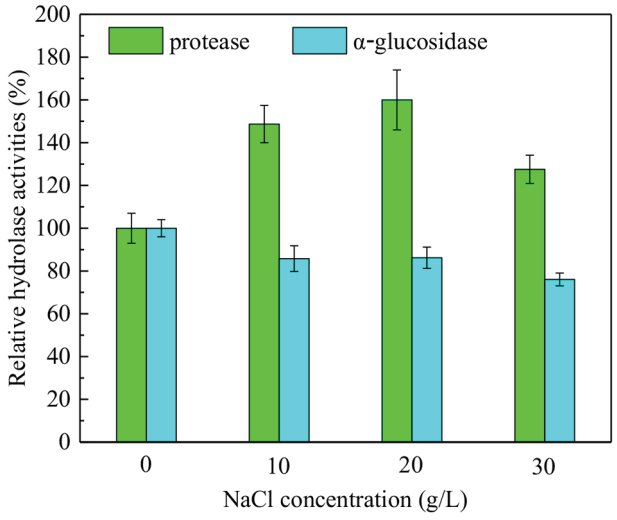

FIGURE 1 | Relative activities of protease and α-glucosidase after 4-day NaCl assistant anaerobic fermentation at the NaCl concentrations of 0 (control), 10, 20, and 30 g/L.

gradually decreased with the further increase in NaCl concentration to 30 g/L. Apparently, 20 g/L was the optimal NaCl concentration for protease activity and hydrolysis of protein-like substances. The increasing NaCl concentration within 0–20 g/L facilitated protease secretion and improved protease activity, further increasing NaCl concentration might injure some function microbes and inhibits protease activity. In contrast, the relative α-glucosidase activity presented decrease trend with the increasing NaCl concentration. Obviously, the protease was resistant to the NaCl presence when the NaCl concentration was less than 20 g/L, whereas α-glucosidase was vulnerable to the high salinity condition. The hydrolase activity was associated with the hydrolysis efficiency of DOMs. It could be inferred that the hydrolysis of proteins was improved and the hydrolysis of carbohydrates inhibited in the NaCl assistant anaerobic fermentation.

Functional Microbial Community Identification: DGGE Band Analysis

To explore the effects of NaCl concentration on microbial community in NaCl assistant anaerobic fermentation process, the DGGE analysis was employed. The DGGE fingerprint at different NaCl concentrations (0–30 g/L) is presented in **Figure 2A**, and the DGGE diagram is provided in **Figure 2B** for more clear demonstration. The location and lightness of the bands represent the bacteria species and abundance, respectively. Obvious differences of bacterial species between the samples at different NaCl concentrations were observed. Moreover, the color depth and the line roughness of bands could be used for assessing bacterial abundance, i.e., the deeper color in **Figure 2A** and the more rough line in **Figure 2B** were associated with the higher bacteria abundance. This implied that the relative abundances of each bacteria

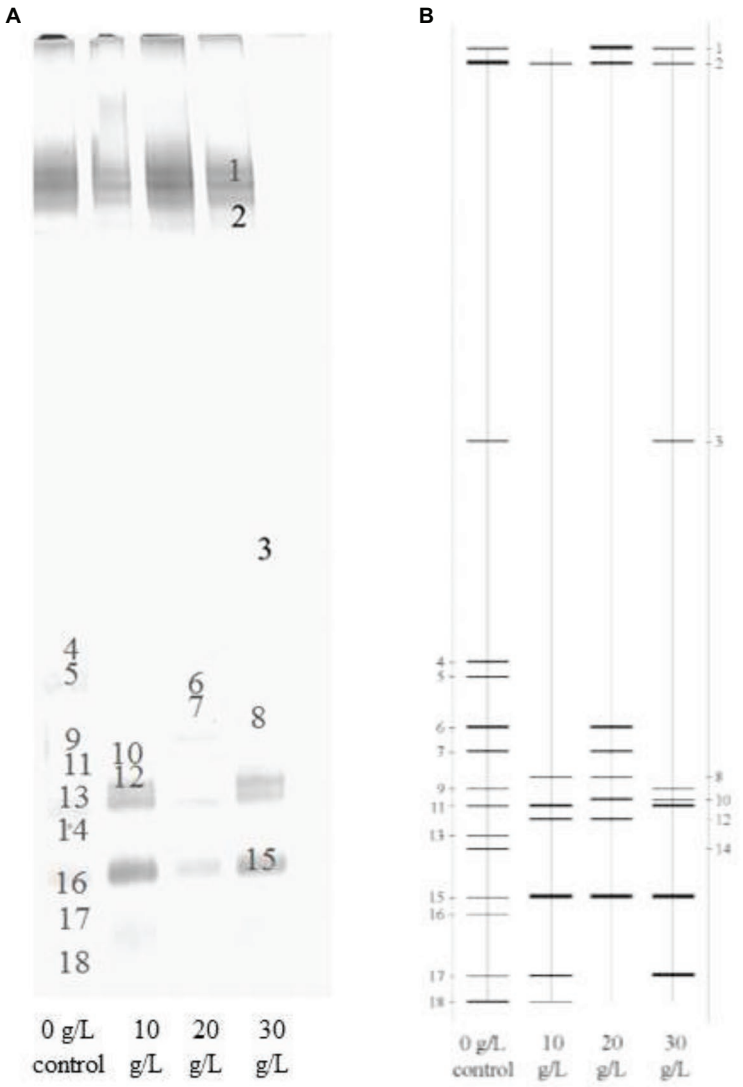

FIGURE 2 | DGGE fingerprint of microbial communities at different NaCl concentrations of 0 (control), 10, 20, and 30 g/L: **(A)** DGGE profiles and **(B)** DGGE diagram.

were diverse with different NaCl concentrations. **Figure 3** displays the microbial community distribution of the sludge samples, which also proved the diverse evolution of microbial community at different NaCl concentrations. According to the band strength and bacteria distribution in **Figures 2**, **3**, it was observed that the bacteria species were reduced with the presence of NaCl. The abundances of the bacteria related to Band 2, 4, 5, 6, 7, 9, 13, 14, 16, and 18 were reduced with the rising NaCl concentrations, while the abundances of bacteria related to Band 1, 8, 10, 11, 12, 15, and 17 were increased.

The bacteria identification of the bands from DGGE profile is shown in **Table 1**, and the main physiological functions of these functional bacteria are summarized in **Table 2**. Moreover, the neighbor-joining tree was analyzed for identifying the bacterial affiliation from DGGE band sequences to the database sequences as shown in **Figure 4**. The bacteria with closed distance in neighbor-joining tree implied that these two bacteria might be affiliated to the same phylum or class with similar functions. It can be seen in **Figure 4** that the major phyla in the sludge system after 4-day anaerobic fermentation include Firmicutes, Bacteroidetes, Proteobacteria, Synergistetes, and Actinobacteria, which were reported to widely present in anaerobic digestion processes (Pang et al., 2020c). It was found that the phylum Proteobacteria was responsible for cell lysis, intracellular material release, and organic compound degradation (Kim et al., 2009), while Bacteroidetes could utilize the released intracellular material to carry out hydrolytic fermentation and possibly release proteinaceous EPS (Han et al., 2015). It was also reported that the Phylym Firmicutes includes extremely resistant microorganisms and endospores, which could also trigger the biodegradation of some organic compounds (Garcia et al., 2011).

	0 g/L	10 g/L	20 g/L	30 g/L
Band 1	+	-	+	+
Band 2	+	+	+	+
Band 3	+	-	-	+
Band 4	+	-	-	-
Band 5	+	-	-	-
Band 6	+	-	+	-
Band 7	+	-	+	-
Band 8	-	+	+	-
Band 9	+	-	-	+
Band 10	-	-	+	+
Band 11	+	+	-	+
Band 12	-	+	+	-
Band 13	+	-	-	-
Band 14	+	-	-	-
Band 15	+	+	+	+
Band 16	+	-	-	-
Band 17	+	+	-	+
Band 18	+	+	-	-

FIGURE 3 | Illustration of bacteria distribution in NaCl assistant anaerobic fermentation system at different NaCl concentrations.

Obviously, the phyla in the four sludge samples were mainly responsible for sludge hydrolysis and anaerobic fermentation. The reduced bacteria abundances might attribute to the inhibition of NaCl on bacteria growth. The inhibited bacteria were vulnerable to high salinity condition, i.e., *Parabacteroides chartae*, *Parabacteroides*, *Macellibacteroides fermentans*, *Petrimonas mucosa*, ammonia-oxidizing beta proteobacterium, and *Burkholderia*. It indicated that many bacteria in these genera were eliminated because they were more susceptible to the high NaCl concentration. Some research have reported that the major ecological function of *Parabacteroides chartae*, *Macellibacteroides fermentans*, and *Petrimonas mucosa* was the degradation of carbohydrates, which was consistent with the decreased α-glucosidase activity in **Figure 1**. Compared with control test (0 g/L), the genera, including *Clostridium algidicarnis*, *Propionivibrio* sp. canine oral taxon 223, uncultured *Acetomicrobium* sp., uncultured actinobacterium, and *Proteiniclasticum* sp., were enriched, which were salt-tolerant and were mostly associated with proteins biodegradation and SCFAs production. The above results revealed that the presence of NaCl during the 4-day anaerobic fermentation period caused bacteria abundance variations. The long-term exposure to high salinity condition resulted in significant reductions in some certain bacteria abundances related to carbohydrate hydrolysis, while some protein-hydrolysis bacteria and SCFAs producers were survived. The enrichment of these resistant bacteria contributed to the bio-production of SCFA and the biodegradation of proteins during the NaCl assistant anaerobic fermentation. These results indicated that the presence of NaCl changed the structural composition of microbial community, which created a good favorable environment for anaerobic fermentation. Under the condition with different NaCl concentrations, the NaCl assistant anaerobic fermentation was related to the evolution of microbial community composition. Besides, it could be inferred that the SCFAs was mainly produced from the biodegradation of proteins, while the hydrolysis of carbohydrates was inhibited. The migration and shift of microbial community would promote the efficient enrichments of protein-degrading and SCFAs-producing bacteria, resulting in the accumulation of a large amount of SCFAs during NaCl assistant anaerobic fermentation process.

Although the anaerobic microbes would be impacted when the NaCl concentration is too high, both the SCFAs production and the SCFAs-producing bacteria abundance were significantly improved in NaCl assistant anaerobic fermentation process. The anaerobic fermentation (i.e., SCFAs production) includes three steps: sludge hydrolysis, acidification, and methanogenesis. On the one hand, although the high NaCl concentration might inhibited metabolism of microbes, the sludge solubilization and hydrolysis were significantly improved, which provided

TABLE 1 | Phylogenetic affiliation of the bacteria from DGGE bands.

Bands	Nearest sequence	Accession No.	Similarity (%)	Class	Phylum
1	*Clostridium algidicarnis*	MN646976	87.23	Clostridia	Firmicutes
2	Uncultured bacterium	AB514039	100	-	-
3	*Dysgonomonas oryzarvi*	MN646999	94.81	Bacteroidia	Bacteroidetes
4	*Parabacteroides chartae*	MN646998	96.32	Bacteroidia	Bacteroidetes
5	*Parabacteroides sp. enrichment culture*	KP076661	98.61	Bacteroidia	Bacteroidetes
6	Uncultured Bacteroidetes bacterium	KX380777	90.21	-	Bacteroidetes
7	*Macellibacteroides fermentans*	MF800883	98.05	Bacteroidia	Bacteroidetes
8	*Propionivibrio sp. canine oral taxon 223*	JN713386	91.3	Betaproteobacteria	Proteobacteria
9	*Petrimonas mucosa*	LT608328	98.25	Bacteroidia	Bacteroidetes
10	*Uncultured Bacteroidetes bacterium clone*	JN371402	100	-	Bacteroidetes
11	Uncultured *Acetomicrobium sp.*	MF162838	100	Synergistia	Synergistetes
12	Uncultured bacterium	AJ630308	86.32	-	-
13	Uncultured ammonia-oxidizing beta proteobacterium	JQ725756	85.84	Betaproteobacteria	Proteobacteria
14	*Burkholderia sp. enrichment culture clone Sa3_4.3*	GQ181155	85.84	Betaproteobacteria	Proteobacteria
15	Uncultured actinobacterium	KP724729	93.68	-	Actinobacteria
16	Uncultured bacterium isolate DGGE gel	KT351685	87.5	-	-
17	*Proteiniclasticum sp.*	MN699083	93.55	Clostridia	Firmicutes
18	Uncultured bacterium	MG240376	94.57	-	-

TABLE 2 | Main functions of the key bacteria.

Nearest sequence	Bands	Main functions	Specific functions	References
Clostridium algidicarnis	1	Fermentation bacteria for DOMs biodegradation and SCFAs production	Bio-production of SCFAs and hydrogen.	Lawson et al., 1994
Dysgonomonas oryzarvi	3		Biodegradation of glucose, galactose, xylose, cellobiose, lactose, sucrose, D-ribose, fructose to produce SCFAs (especially acetic acid).	Kodama et al., 2012
Parabacteroides chartae	4		Biodegradation of glucose, lactose, sucrose, maltose, xylose, cellobiose to produce lactic acid, propionic acid, formic acid and acetic acid.	Tan et al., 2012
Parabacteroides sp. enrichment culture	5			
Macellibacteroides fermentans	7		Biogradation of carbohydrates to produce SCFAs	Wang et al., 2019
Propionivibrio sp. canine oral taxon 223	8		Bio-production of SCFAs (especially acetic and propionic acids)	Brune et al., 2002
Petrimonas mucosa	9		Biogradation of carbohydrates to produce SCFAs	Wang et al., 2019
Uncultured *Acetomicrobium sp.*	11		Biogradation of carbohydrates to produce SCFAs	Soutschek et al., 1984
Uncultured ammonia-oxidizing beta proteobacterium	13		Ammonia oxidization, degradation of proteins and amino acids	Wittebolle et al., 2005
Burkholderia sp. enrichment culture clone Sa3_4.3	14		Biodegradation of lipid	Lee et al., 2014
Proteiniclasticum sp.	17		Biodegradation of proteins to produce SCFAs	Wang et al., 2019

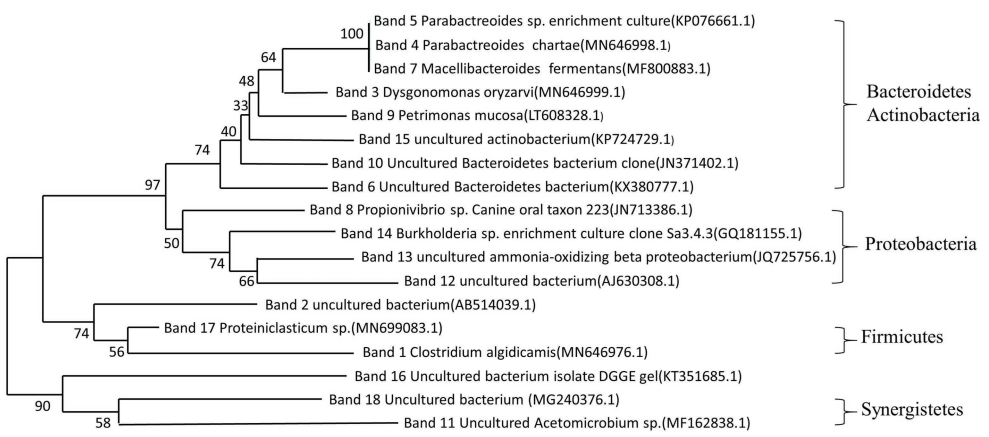

FIGURE 4 | Neighbor-joining tree for phylogenetic identities of the bacteria in DGGE bands.

more substrates for SCFAs production. On the other hand, the methanogenesis was inhibited by NaCl, which reduced SCFAs consumption and was beneficial for the anaerobic fermentation performance. The inhibition of sodium on methanogens might be greater than that on SCFAs-producing bacteria, indicating that high NaCl concentration was beneficial for SCFAs accumulation. Furthermore, the improvement of NaCl addition on SCFAs-producing bacteria was resulted from two aspects: (1) the NaCl-caused sludge solubilization provided numerous biodegradable organic matters, which facilitated the acidification step in anaerobic fermentation process and promoted the growth of SCFAs-producing bacteria and (2) the high salinity condition seriously inhibited methanogens rather than SCFAs-producing bacteria, i.e., the inhibited growth of other bacteria increased the abundances of SCFAs-producing bacteria. Similar phenomenon has been observed in previous studies (Su et al., 2016).

Richness and Diversity of Microbial Community

According to the DGGE fingerprint and bacteria identification in **Figure 2** and **Table 1**, phyla Bacteroidetes and Proteobacteria were mostly inhibited. It was observed that the band numbers of DGGE profiles in the presence of NaCl were less than that in the control, while the band number and location were also diverse, which implied varied microbial community richness and diversity at different NaCl concentrations. In order to explore the effects of NaCl concentration on microbial community structure, the richness, diversity, and evenness of microbial community were analyzed as shown in **Table 3**. The microbial community richness was used for evaluating the specie numbers in microbial community (Pang et al., 2020c), which was calculated using the bank amounts in this study. It was found that the microbial community richness was significantly reduced in the presence of NaCl, which was in the range of 7–8 at the NaCl concentrations of 10–30 g/L, while the higher richness value of 15 was observed in the control. In the anaerobic fermentation process, the sludge sample without NaCl addition has higher species abundance than those with NaCl addition. Apparently, high NaCl concentration inhibited the survival of some microbes in sludge system, i.e., the species abundance was reduced with the NaCl presence, which decreased the microbial community richness. It should be realized that the microbial community richness at the different NaCl concentrations (10–30 g/L) were similar, implying that the varying NaCl concentrations have similar inhibition effects on microbial growth and have similar species reduction performance in the anaerobic fermentation process.

The Shannon and Pielou indexes could assess the diversity and evenness of the microbial community related to different NaCl concentrations (Xin et al., 2015). The relative abundance and the number of species impacted the Shannon index (Miura et al., 2007). In this study, the Shannon index and the Pielou index were calculated according to the band numbers and the relative abundance of each frequency band. It is found in **Table 3** that the diversity of microbial communities at the NaCl concentrations of 10–30 g/L were much lower than that in the control, indicating the microbial community diversity was decreased owing to the inhibition of additional NaCl on the microbial species growth. Moreover, it was noticeable that the microbial community diversities at the NaCl concentrations of 20 and 30 g/L were similar, which were bother higher than that at the NaCl concentration of 10 g/L. Although the additional salinity was unfavorable for the growth of some microbes, the higher NaCl concentration might facilitate microbial activity compared with low NaCl concentration, i.e., increased NaCl concentration was beneficial for microbial community diversity when the NaCl concentration was higher than 10 g/L. The increased diversity was beneficial for the stability of microbial community structure and the comprehensive functions of sludge system. The reduction of microbial community diversity was a response of the microbial community to resist the perturbed conditions (i.e., high NaCl concentration). The release of lysed nuclear matters owing to NaCl-caused EPS disruption and cell lysis might also contribute to decrease the biodiversity of sludge bio-samples. In contrast, the evenness of microbial communities at different NaCl concentrations did not significantly differ to each other. The NaCl concentration has little effect on microbial community evenness. In consequence, the attack of additional NaCl performed a significantly negative effect on richness and diversity of microbial community, and the increased NaCl concentration (10–30 g/L) facilitated to improve microbial community diversity, while the microbial community evenness was not affected by NaCl concentration.

TABLE 3 | The richness, diversity, and evenness of microbial communities at different NaCl concentrations.

	Richness	Diversity	Evenness
0 g/L (control)	15	2.7046	0.998726
10 g/L	7	1.9372	0.995524
20 g/L	8	2.0767	0.998682
30 g/L	8	2.0754	0.998056

TABLE 4 | The similarity coefficient (%) between sludge samples at different NaCl concentrations.

	0 g/L (control)	10 g/L	20 g/L	30 g/L
0 g/L (control)	100.0	-	-	-
10 g/L	29.2	100.0	-	-
20 g/L	39.4	46.5	100.0	-
30 g/L	32.7	58.2	34.8	100.0

The Similarity of Microbial Communities Related to Different NaCl Concentrations

As shown in **Table 4**, the Dice coefficient was used to quantify the similarity of DGGE spectra between the microbial communities at different NaCl concentrations. It was observed that the similarity of the sludge samples with each other was low, the similarity coefficients were all below 60%, which implied that the varied NaCl concentrations triggered significant microbial community evolution. Moreover, it was noticeable that the similarity coefficients

of the 10 g/L test with the 20 and 30 g/L tests were 46.5 and 58.2%, respectively, which were a bit higher than the similarity coefficients among other tests. The microbial community at the NaCl concentration of 10 g/L was a bit similar to those at 20 and 30 g/L. Similar results could be also observed by the clustering analysis (**Figure 5**). Apparently, the presence of NaCl significantly changed microbial community composition, whereas the microbial community evolutions between different NaCl concentrations (10–30 g/L) were less obvious. The dissimilarity of microbial communities at different NaCl concentrations might attribute to the decreased microbial community richness and diversity (**Table 2**). The above results suggested that (1) evolution of microbial community existed obviously with the presence of NaCl; (2) increase in NaCl concentration had a positive impact on the dissimilarity of microbial communities; and (3) the dissimilarity among the control test with the NaCl tests was the most significant, i.e., the microbial community dissimilarity with the "NaCl grow out of nothing" was more obvious than the "further increase NaCl concentration" one.

Microbial Dynamic Implications

According to the findings in this study, the hydrolytic bacteria and acidogens were enriched with the presence of NaCl, especially at the optimal NaCl concentration of 20 g/L, which facilitated the hydrolysis stage and acidification stages. In contrast, the bacteria responsible for SCFAs consumption and methane production were inhibited with decreased abundance due to the attack of high salinity condition on SCFAs-consuming bacteria, which was beneficial for reducing SCFAs consumption and facilitating SCFAs accumulation in anaerobic fermentation. Moreover, the increased protease activity and decreased α-glucosidase activity with rising NaCl concentration are observed in **Figure 1**. It could be inferred that the hydrolysis of protein-like substances was improved with NaCl assistance, while the hydrolysis of carbohydrates might be a bit poor. During the NaCl assistant anaerobic fermentation, the bacteria responsible for DOMs biodegradation and SCFAs production were enriched, these bacteria were resistant to high NaCl concentration. On contrary, the SCFAs consumers (e.g., methanogens, etc.) were inhibited, which were vulnerable to high salinity condition. Obviously, the external NaCl modified microbial community structure by richness, diversity, and evenness, which created a liquid environment favorable for acidogenic fermentation.

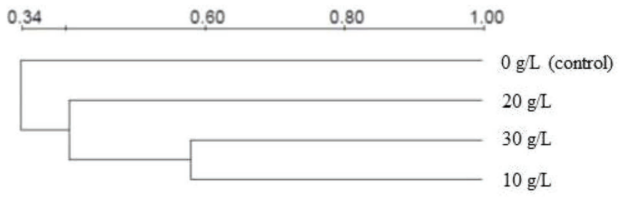

FIGURE 5 | Clustering analysis for evaluating the similarity between microbial communities at different NaCl concentrations.

Although the optimal NaCl concentration of 20 g/L was high, the NaCl could be recovered and reused after utilization of the produced SCFAs in fermentative liquid, which reduced the treatment costs and environmental hazard. The fermentative liquid could be used as external carbon source for biological electricity production (MFC) or hydrogen production (microbial electrolysis cells). In this way, the effluent with numerous NaCl could be reused for NaCl assistant anaerobic fermentation process.

CONCLUSION

This study demonstrated that NaCl could modify hydrolase activity and microbial community structure in 4-day anaerobic fermentation. With the rising NaCl concentrations (0–30 g/L), the protease activity was increased to 127.6–160%, while the α-glucosidase activity was reduced to 76.1–86.2%. Some carbohydrate-hydrolysis bacteria (e.g., *Parabacteroides chartae*, *Macellibacteroides fermentans*, and *Petrimonas mucosa*) were inhibited by high salinity condition, while the protein-degrading and SCFAs-producing bacteria were resistive and enriched. Compared with control test, the microbial community richness and diversity were reduced in NaCl test (10–30 g/L), while the evenness was almost changeless. The similarity between communities was low. Moreover, the pathway of DOMs biodegradation and SCFAs production in NaCl assistant anaerobic fermentation was illustrated.

DATA AVAILABILITY STATEMENT

The raw data supporting the conclusions of this article will be made available by the authors, without undue reservation.

AUTHOR CONTRIBUTIONS

HP: writing-original draft and data curation. XX: investigation. ZY: methodology. BC: writing-original draft. CL: data curation. XW: software. DG: writing-original draft, conceptualization, and formal analysis. JH: supervision. JN: conceptualization. All authors contributed to the article and approved the submitted version.

FUNDING

Thanks for the support from National Natural Science Foundation of China – China (No.51778179) and National key research and development program of China – China (2018YFD1100603).

ACKNOWLEDGMENTS

The authors thank the funders, and Dr. Qin for the support and enlightenment.

REFERENCES

Brune, A., Ludwig, W., and Schink, B. (2002). Propionivibrio limicola sp. nov., a fermentative bacterium specialized in the degradation of hydroaromatic compounds, reclassification of Propionibacter pelophilus as Propionivibrio pelophilus comb. nov. and amended description of the genus Propionivibrio. *Int. J. Syst. Evol. Microbiol.* 52, 441–444. doi: 10.1099/00207713-52-2-441

Cai, M. M., Chua, H., Zhao, Q. L., Shirley, S. N., and Ren, J. (2009). Optimal production of polyhydroxyalkanoates (PHA) in activated sludge fed by volatile fatty acids (VFAs) generated from alkaline excess sludge fermentation. *Bioresour. Technol.* 100, 1399–1405. doi: 10.1016/j.biortech.2008.09.014

Chen, Y., Luo, J., Yan, Y., and Feng, L. (2013). Enhanced production of short-chain fatty acid by co-fermentation of waste activated sludge and kitchen waste under alkaline conditions and its application to microbial fuel cells. *Appl. Energy* 102, 1197–1204. doi: 10.1016/j.apenergy.2012.06.056

Chen, Y., Zhu, R., Jiang, Q., Sun, T., Li, M., Shi, J., et al. (2019). Effects of green waste participation on the co-digestion of residual sludge and kitchen waste: a preliminary study. *Sci. Total Environ.* 671, 838–849. doi: 10.1016/j.scitotenv.2019.03.339

Cheng, Q., Xu, C., Huang, W., Jiang, M., Yan, J., Fan, G., et al. (2020). Improving anaerobic digestion of piggery wastewater by alleviating stress of ammonia using biochar derived from rice straw. *Environ. Technol. Innov.* 19:100948. doi: 10.1016/j.eti.2020.100948

Cui, Y., Su, H., Chen, Y., Chen, Y., and Peng, Y. (2015). Mechanism of activated sludge Floc disintegration induced by excess addition of NaCl. *Clean (Weinh)* 43, 1197–1206. doi: 10.1002/clen.201400219

Duan, X., Wang, X., Xie, J., Feng, L., Yan, Y., and Zhou, Q. (2016). Effect of nonylphenol on volatile fatty acids accumulation during anaerobic fermentation of waste activated sludge. *Water Res.* 105, 209–217. doi: 10.1016/j.watres.2016.08.062

Garcia, S. L., Jangid, K., Whitman, W. B., and Das, K. C. (2011). Transition of microbial communities during the adaption to anaerobic digestion of carrot waste. *Bioresour. Technol.* 102, 7249–7256. doi: 10.1016/j.biortech.2011.04.098

Han, X., Wang, Z., Ma, J., Zhu, C., Li, Y., and Wu, Z. (2015). Membrane bioreactors fed with different COD/N ratio wastewater: impacts on microbial community, microbial products, and membrane fouling. *Environ. Sci. Pollut. Res.* 22, 11436–11445. doi: 10.1007/s11356-015-4376-z

He, Z. W., Liu, W. Z., Gao, Q., Tang, C. C., Wang, L., Guo, Z. C., et al. (2018). Potassium ferrate addition as an alternative pre-treatment to enhance short-chain fatty acids production from waste activated sludge. *Bioresour. Technol.* 247, 174–181. doi: 10.1016/j.biortech.2017.09.073

He, Z. W., Tang, C. C., Liu, W. Z., Ren, Y. X., Guo, Z. C., Zhou, A. J., et al. (2019). Enhanced short-chain fatty acids production from waste activated sludge with alkaline followed by potassium ferrate treatment. *Bioresour. Technol.* 289:121642. doi: 10.1016/j.biortech.2019.121642

Huang, X., Shen, C., Liu, J., and Lu, L. (2015). Improved volatile fatty acid production during waste activated sludge anaerobic fermentation by different bio-surfactants. *Chem. Eng. J.* 264, 280–290. doi: 10.1016/j.cej.2014.11.078

Ji, B., Zhang, M., Gu, J., Ma, Y., and Liu, Y. (2020). A self-sustaining synergetic microalgal-bacterial granular sludge process towards energy-efficient and environmentally sustainable municipal wastewater treatment. *Water Res.* 179:115884. doi: 10.1016/j.watres.2020.115884

Kim, S., Seol, E., Oh, Y. -K., Wang, G. Y., and Park, S. (2009). Hydrogen production and metabolic flux analysis of metabolically engineered Escherichia coli strains. *Int. J. Hydrog. Energy* 34, 7417–7427. doi: 10.1016/j.ijhydene.2009.05.053

Kodama, Y., Shimoyama, T., and Watanabe, K. (2012). Dysgonomonas oryzarvi sp. nov., isolated from a microbial fuel cell. *Int. J. Syst. Evol. Microbiol.* 62, 3055–3059. doi: 10.1099/ijs.0.039040-0

Lawson, P., Dainty, R. H., Kristiansen, N., Berg, J., and Collins, M. D. (1994). Characterization of a psychrotrophic Clostridium causing spoilage in vacuum-packed cooked pork: description of Clostridium algidicarnis sp. nov. *Lett. Appl. Microbiol.* 19, 153–157. doi: 10.1111/j.1472-765x.1994.tb00930.x

Lee, S., Park, S., Park, C., Pack, S. P., and Lee, J. (2014). Enhanced free fatty acid production by codon-optimized Lactococcus lactis acyl-ACP thioesterase gene expression in *Escherichia coli* using crude glycerol. *Enzym. Microb. Technol.* 67, 8–16. doi: 10.1016/j.enzmictec.2014.08.004

Li, X., Chen, H., Hu, L., Yu, L., Chen, Y., and Gu, G. (2011). Pilot-scale waste activated sludge alkaline fermentation, fermentation liquid separation, and application of fermentation liquid to improve biological nutrient removal. *Environ. Sci. Technol.* 45, 1834–1839. doi: 10.1021/es1031882

Li, X., Chen, L., Mei, Q., Dong, B., Dai, X., Ding, G., et al. (2018). Microplastics in sewage sludge from the wastewater treatment plants in China. *Water Res.* 142, 75–85. doi: 10.1016/j.watres.2018.05.034

Liu, K., Chen, Y., Xiao, N., Zheng, X., and Li, M. (2015). Effect of humic acids with different characteristics on fermentative short-chain fatty acids production from waste activated sludge. *Environ. Sci. Technol.* 49, 4929–4936. doi: 10.1021/acs.est.5b00200

Lu, H., Li, Y., Shan, X., Abbas, G., Zeng, Z., Kang, D., et al. (2019). A holistic analysis of ANAMMOX process in response to salinity: from adaptation to collapse. *Sep. Purif. Technol.* 215, 342–350. doi: 10.1016/j.seppur.2019.01.016

Luo, K., Pang, Y., Yang, Q., Wang, D., Li, X., Lei, M., et al. (2019). A critical review of volatile fatty acids produced from waste activated sludge: enhanced strategies and its applications. *Environ. Sci. Pollut. Res.* 26, 13984–13998. doi: 10.1007/s11356-019-04798-8

Lv, W., Schanbacher, F. L., and Yu, Z. T. (2010). Putting microbes to work in sequence: recent advances in temperature-phased anaerobic digestion processes. *Bioresour. Technol.* 101, 9409–9414. doi: 10.1016/j.biortech.2010.07.100

Miura, Y., Hiraiwa, M. N., Ito, T., Itonaga, T., Watanabe, Y., and Okabe, S. (2007). Bacterial community structures in MBRs treating municipal wastewater: relationship between community stability and reactor performance. *Water Res.* 41, 627–637. doi: 10.1016/j.watres.2006.11.005

Pang, H., Chen, Y., He, J., Guo, D., Pan, X., Ma, Y., et al. (2020a). Cation exchange resin-induced hydrolysis for improving biodegradability of waste activated sludge: characterization of dissolved organic matters and microbial community. *Bioresour. Technol.* 302:122870. doi: 10.1016/j.biortech.2020.122870

Pang, H., He, J., Ma, Y., Pan, X., Zheng, Y., Yu, H., et al. (2021). Enhancing volatile fatty acids production from waste activated sludge by a novel cation-exchange resin assistant strategy. *J. Clean. Prod.* 278:123236. doi: 10.1016/j.jclepro.2020.123236

Pang, H., Li, L., He, J., Yan, Z., Ma, Y., Nan, J., et al. (2020b). New insight into enhanced production of short-chain fatty acids from waste activated sludge by cation exchange resin-induced hydrolysis. *Chem. Eng. J.* 388:124235. doi: 10.1016/j.cej.2020.124235

Pang, H., Ma, W., He, J., Pan, X., Ma, Y., Guo, D., et al. (2020c). Hydrolase activity and microbial community dynamic shift related to the lack in multivalent cations during cation exchange resin-enhanced anaerobic fermentation of waste activated sludge. *J. Hazard. Mater.* 398:122930. doi: 10.1016/j.jhazmat.2020.122930

Pang, H., Pan, X., Li, L., He, J., Zheng, Y., Qu, F., et al. (2020d). An innovative alkaline protease-based pretreatment approach for enhanced short-chain fatty acids production via a short-term anaerobic fermentation of waste activated sludge. *Bioresour. Technol.* 312:123397. doi: 10.1016/j.biortech.2020.123397

Pang, H., Xu, J., He, J., Pan, X., Ma, Y., Li, L., et al. (2020e). Enhanced anaerobic fermentation of waste activated sludge by NaCl assistant hydrolysis strategy: improved bio-production of short-chain fatty acids and feasibility of NaCl reuse. *Bioresour. Technol.* 312:123303. doi: 10.1016/j.biortech.2020.123303

Polli, F., Zingaretti, D., Crognale, S., Pesciaroli, L., D'Annibale, A., Petruccioli, M., et al. (2018). Impact of the Fenton-like treatment on the microbial community of a diesel-contaminated soil. *Chemosphere* 191, 580–588. doi: 10.1016/j.chemosphere.2017.10.081

Reid, E., Liu, X., and Judd, S. J. (2006). Effect of high salinity on activated sludge characteristics and membrane permeability in an immersed membrane bioreactor. *J. Membr. Sci.* 283, 164–171. doi: 10.1016/j.memsci.2006.06.021

Soutschek, E., Winter, J., Schindler, F., and Kandler, O. (1984). Acetomicrobium flavidum, gen. Nov., sp. nov., a thermophilic, anaerobic bacterium from sewage sludge, forming acetate, CO_2 and H_2 from glucose. *System* 5, 377–390. doi: 10.1016/S0723-2020(84)80039-9

Su, G., Wang, S., Yuan, Z., and Peng, Y. (2016). Enhanced volatile fatty acids production of waste activated sludge under salinity conditions: performance and mechanisms. *J. Biosci. Bioeng.* 121, 293–298. doi: 10.1016/j.jbiosc.2015.07.009

Sun, R., Zhou, A., Jia, J., Liang, Q., Liu, Q., Xing, D., et al. (2015). Characterization of methane production and microbial community shifts during waste activated

sludge degradation in microbial electrolysis cells. *Bioresour. Technol.* 175, 68–74. doi: 10.1016/j.biortech.2014.10.052

Tan, H. Q., Li, T. T., Zhu, C., Zhang, X. Q., Wu, M., and Zhu, X. F. (2012). Parabacteroides chartae sp. nov., an obligately anaerobic species from wastewater of a paper mill. *Int. J. Syst. Evol. Microbiol.* 62, 2613–2617. doi: 10.1099/ijs.0.038000-0

Wang, L., He, Z., Guo, Z., Sangeetha, T., Yang, C., Gao, L., et al. (2019). Microbial community development on different cathode metals in a bioelectrolysis enhanced methane production system. *J. Power Sources* 444:227306. doi: 10.1016/j.jpowsour.2019.227306

Wittebolle, L., Boon, N., Vanparys, B., Heylen, K., Vos, P. D., and Verstraete, W. (2005). Failure of the ammonia oxidation process in two pharmaceutical wastewater treatment plants is linked to shifts in the bacterial communities. *J. Appl. Microbiol.* 99, 997–1006. doi: 10.1111/j.1365-2672.2005.02731.x

Xin, X. D., He, J. G., Qiu, W., Tang, J., and Liu, T. T. (2015). Microbial community related to lysozyme digestion process for boosting waste activated sludge biodegradability. *Bioresour. Technol.* 175, 112–119. doi: 10.1016/j.biortech.2014.10.042

Xin, S., Shen, J., Liu, G., Chen, Q., Xiao, Z., Zhang, G., et al. (2020). Electricity generation and microbial community of single-chamber microbial fuel cells in response to Cu_2O nanoparticles/reduced graphene oxide as cathode catalyst. *Chem. Eng. J.* 380:122446. doi: 10.1016/j.cej.2019.122446

Xu, F., Cao, F., Kong, Q., Zhou, L., Yuan, Q., Zhu, Y., et al. (2018). Electricity production and evolution of microbial community in the constructed wetland-microbial fuel cell. *Chem. Eng. J.* 339, 479–486. doi: 10.1016/j.cej.2018.02.003

Xu, F., Ouyang, D., Rene, E. R., Ng, H. Y., Guo, L., Zhu, Y., et al. (2019). Electricity production enhancement in a constructed wetland-microbial fuel cell system for treating saline wastewater. *Bioresour. Technol.* 288:121462. doi: 10.1016/j.biortech.2019.121462

Zhang, M., Gu, J., and Liu, Y. (2019). Engineering feasibility, economic viability and environmental sustainability of energy recovery from nitrous oxide in biological wastewater treatment plant. *Bioresour. Technol.* 282, 514–519. doi: 10.1016/j.biortech.2019.03.040

Zhang, Q., Wang, L., Yu, Z., Zhou, T., Gu, Z., Huang, Q., et al. (2020). Pine sawdust as algal biofilm biocarrier for wastewater treatment and algae-based byproducts production. *J. Clean. Prod.* 256:120449. doi: 10.1016/j.jclepro.2020.120449

Zhang, Q., Yu, Z., Zhu, L., Ye, T., Zuo, J., Li, X., et al. (2018). Vertical-algal-biofilm enhanced raceway pond for cost-effective wastewater treatment and value-added products production. *Water Res.* 139, 144–157. doi: 10.1016/j.watres.2018.03.076

Conflict of Interest: CL was employed by the company Frog Biotechnology Co., LTD, Harbin, 350116, China.

The remaining authors declare that the research was conducted in the absence of any commercial or financial relationships that could be construed as a potential conflict of interest.

frontiers in Microbiology

ORIGINAL RESEARCH
published: 30 November 2020
doi: 10.3389/fmicb.2020.604173

Enhancing Phenol Conversion Rates in Saline Anaerobic Membrane Bioreactor Using Acetate and Butyrate as Additional Carbon and Energy Sources

Víctor S. García Rea[1], Julian D. Muñoz Sierra[1,2], Laura M. Fonseca Aponte[1], Daniel Cerqueda-Garcia[3], Kiyan M. Quchani[1], Henri Spanjers[1] and Jules B. van Lier[1]*

[1] Sanitary Engineering Section, Department of Water Management, Delft University of Technology, Delft, Netherlands, [2] KWR Water Research Institute, Nieuwegein, Netherlands, [3] Institute of Ecology, National Autonomous University of Mexico, Mexico City, Mexico

OPEN ACCESS

Edited by:
Zeynep Cetecioglu, Royal Institute of Technology, Sweden

Reviewed by:
Ioannis Vyrides, Cyprus University of Technology, Cyprus
Seung Gu Shin, Pohang University of Science and Technology, South Korea

***Correspondence:**
Victor S. Garcia Rea
V.S.GarciaRea@tudelft.nl; serman13@hotmail.com

Specialty section:
This article was submitted to Microbiotechnology, a section of the journal Frontiers in Microbiology

Received: *08 September 2020*
Accepted: *29 October 2020*
Published: *30 November 2020*

Citation:
García Rea VS, Muñoz Sierra JD, Fonseca Aponte LM, Cerqueda-Garcia D, Quchani KM, Spanjers H and van Lier JB (2020) Enhancing Phenol Conversion Rates in Saline Anaerobic Membrane Bioreactor Using Acetate and Butyrate as Additional Carbon and Energy Sources. Front. Microbiol. 11:604173. doi: 10.3389/fmicb.2020.604173

Phenolic industrial wastewater, such as those from coal gasification, are considered a challenge for conventional anaerobic wastewater treatment systems because of its extreme characteristics such as presence of recalcitrant compounds, high toxicity, and salinity. However, anaerobic membrane bioreactors (AnMBRs) are considered of potential interest since they retain all micro-organism that are required for conversion of the complex organics. In this study, the degradation of phenol as main carbon and energy source (CES) in AnMBRs at high salinity (8.0 g $Na^{+}{\cdot}L^{-1}$) was evaluated, as well as the effect of acetate and an acetate-butyrate mixture as additional CES on the specific phenol conversion rate and microbial community structure. Three different experiments in two lab-scale (6.5 L) AnMBRs (35°C) were conducted. The first reactor (R1) was fed with phenol as the main CES, the second reactor was fed with phenol and either acetate [2 g $COD{\cdot}L^{-1}$], or a 2:1 acetate-butyrate [2 g $COD{\cdot}L^{-1}$] mixture as additional CES. Results showed that phenol conversion could not be sustained when phenol was the sole CES. In contrast, when the reactor was fed with acetate or an acetate-butyrate mixture, specific phenol conversion rates of 115 and 210 $mgPh{\cdot}gVSS^{-1}\ d^{-1}$, were found, respectively. The syntrophic phenol degrader *Syntrophorhabdus* sp. and the acetoclastic methanogen *Methanosaeta* sp. were the dominant bacteria and archaea, respectively, with corresponding relative abundances of up to 63 and 26%. The findings showed that dosage of additional CES allowed the development of a highly active phenol-degrading biomass, potentially improving the treatment of industrial and chemical wastewaters.

Keywords: phenol, anaerobic membrane bioreactor, enhanced phenol conversion rate, acetate, butyrate, microbial community, *Syntrophorhabdus* sp.

INTRODUCTION

Rapid industrialization has generated many industrial effluents that constitute a major source of pollution (Lin et al., 2013). Currently, many of these industrial effluents are successfully treated using anaerobic high-rate treatment processes (Van Lier et al., 2015). However, some industrial wastewaters represent a challenge for conventional anaerobic wastewater treatment systems. Wastewater characteristics that are considered extreme, such as high organic pollutant concentration, presence of recalcitrant or refractory as well as toxic or inhibitory compounds, and high salinity, reduce the performance of conventional anaerobic systems, which leads to process imbalance or reactor failure (Dereli et al., 2012). Dereli et al. (2012), proposed the use of anaerobic membrane bioreactors (AnMBR) to treat industrial wastewater with extreme characteristics, especially because of their effective biomass retention and the production of suspended-solids-free effluents, making them suitable for water reclamation.

Chemical and petrochemical wastewater, such as coal gasification, is an example of an industrial effluent with toxic phenolics as the major organic pollutants (Li et al., 2017). Nevertheless, other compounds such as acetate or butyrate, which could be used by microorganisms as carbon and energy sources (CES), are also present in coal gasification wastewater as common contaminants (Singer et al., 1978; Blum et al., 1986; Ji et al., 2016). Besides, it has been reported that coal-related industries wastewaters have a high concentration of total dissolved solids, ranging from 174 to 2,000 $mg{\cdot}L^{-1}$ (Maiti et al., 2019). Furthermore, under closed-water-loops, increasing salinity in the wastewater is expected.

Several studies have researched the anaerobic degradation of phenol, as well in some studies different CES have been used to promote or enhance the degradation of phenol under anaerobic conditions (Liang and Fang, 2010), e.g., glucose (Tay et al., 2001), volatile fatty acids (VFAs) (Carbajo et al., 2010), or acetate (Muñoz Sierra et al., 2017). Additional CES have been used as well during the reactor start-up, or for the degradation of mixtures of phenolic compounds. However, in most of these studies, it remains unclear how and to what extent these substrates promoted or increased phenol degradation.

We have identified four possible mechanisms that could explain the effect of additional CES on the degradation of toxic or inhibitory compounds: 1. Co-metabolism, a process that was initially defined as the catabolic degradation of a recalcitrant substrate without using the generated energy to promote or sustain cell growth (Horvath, 1972). In this process, the degradation of the non-easily degradable compound is dependent on the presence of a main substrate, or primary source, which is commonly an easily degradable compound (Horvath, 1972; Bertrand et al., 2015). However, (Wackett, 1996) attributed the enhancement in the conversion rate to an unknown or unidentified effect in the metabolic net between the different microbial populations, which are present in non-defined mixed cultures.

2. Direct usage of additional CES by the toxicant degraders to increase their metabolic capability (Kennes et al., 1997; Tay et al., 2001; Gali et al., 2006). Meaning that: a) additional CES could be used as a substrate to increase the anabolism of the degraders, promoting its growth, thus increasing its fraction in the biomass. b) Increasing the catabolic activity (i.e., uptake rate) of the degraders; or c) both processes are increased (**Supplementary Material S1**). This would imply, e.g., for phenol, that phenol degraders could use another (easily biodegradable) CES. The latter contrasts to the general comprehension that in anaerobic digestion (AD) process, specific (physiological) microbial populations have well-defined narrow substrate ranges (Batstone et al., 2002).

3. Effect of syntrophy on the thermodynamics of compound degradation. In the case of phenol conversion, a constant level of hydrogen consumption is required, which serves as an electron sink for favorable thermodynamics conditions (Qiu et al., 2008). Therefore, the development of a sound hydrogenotrophic methanogenic subpopulation is indispensable for establishing efficient anaerobic oxidation of aromatics and/or their degradation products.

4. An increase in intermediate compounds involved in the conversion of phenolics. Phenol degradation under anoxic conditions occurs via carboxylation of the phenolic ring to form 4-hydroxybenzoate (Schink et al., 2000; Gibson and Harwood, 2002; Fuchs et al., 2011). It has been reported that under strict anaerobic (methanogenic) conditions, phenol degradation is dependent on a sufficiently high CO_2/HCO_3^- and H_2 concentration (Knoll and Winter, 1987; Karlsson et al., 1999; Fuchs, 2008). Veeresh et al. (2005) reported that dosage of additional CES increased the phenol-degrading activity of the biomass, hypothesizing that this was due to a higher phenol hydrogenation rate, resulting in a better cleavage of the phenolic ring.

In contrast to these four mechanisms, addition of an extra CES, such as acetate, has been shown to inhibit the anaerobic degradation of terephthalic acid (Kleerebezem, 1999.), which even though is not a phenolic compound, shares the same degradation pathway (under anoxic/anaerobic conditions) with phenol (Nobu et al., 2015). So, the effect of CESs' dosage on the degradation of recalcitrant and toxic or inhibitory compounds is not fully understood. Moreover, there is few information regarding the effect of the dosage of CES on the specific phenol conversion rate (sPhCR), especially in AnMBRs under saline conditions.

As well, little is known regarding the microbial community structure and dynamics in AnMBRs under saline conditions treating toxic compounds such as phenol. Furthermore, no study has been conducted to determine how the microbial community is shifted by either the increase in the loading rates and/or the addition of extra CES, especially in suspended biomass systems as the one present in the AnMBR.

This study researched the effect of the addition of acetate or a mixture of acetate-butyrate as additional CES on the sPhCR of AnMBRs and on the microbial community related to the degradation process, with particular focus on the phenol degraders and the methanogens. The effect of phenol on the acetotrophic specific methanogenic activity (SMA) and the sPhCR in batch experiments were assessed as well.

MATERIALS AND METHODS

Analytical Techniques

Chemical Oxygen Demand

During the operation of the reactors, COD in the feed and the permeate was measured using a spectrophotometer (DR3900, Hach Lange, Germany). Hach Lange Kits (Hach Lange, Germany) were used following the instructions of the manufacturer. Proper dilutions were done to avoid Cl^- interference.

Phenol, Volatile Fatty Acids, and Benzoate Concentrations

Phenol, VFAs, and benzoate were measured by a gas chromatograph (GC) (Agilent Technology) equipped with a flame ionization detector (FID) with a capillary column (type HP-PLOT/U) with a size of 25 m × 320 mm × 0.5 mm. Helium was used as carrier gas at a flow rate of 67 mL·min^{-1} and a split ratio of 25:1. The oven temperature was increased from 80 to 180°C in 10.5 min. Injector and detector temperatures were 80 and 240°C, respectively, and the injection volume was 1 μL.

For the preparation of the samples, approximately 1 mL of permeate was filtered through a 0.45 μm filter (Chromafil Xtra PES-45/25). Depending on the dilution required to have phenol, VFAs, and benzoate in the measurable range of the GC, a certain volume of the filtrate was mixed with pentanol (320 mg·L^{-1}) to obtain a final volume of 1.5 mL. Finally, 10 μL of formic acid (95%) (Merck, Germany) were added to the vial. Phenol concentration was double-checked with a spectrophotometer (Merck, Germany) using Merck – Spectroquant Phenol cell kits (Merck, Germany) following manufacturers' instructions.

Batch Tests

Specific Methanogenic Activity Inhibition by Phenol

Batch tests with initial phenol concentrations of 50 (n = 2), 200 (n = 6), and 500 (n = 6) mg·L^{-1} were carried out in 250 mL Schott glass (Schott, Germany) reactors. Biomass samples (60–80 mL) were taken from the AnMBR to have a final volume of 200 mL at a VSS concentration of 4 g·L^{-1} (Inoculum/Substrate = 2 for the control with 2.0 gAc-COD·L^{-1}). Macro- and micronutrients, phosphate buffer solutions, and Na^+ as NaCl were dosed as specified in section "Experimental Setup and Reactors Operation." A shaker (New Brunswick™, Eppendorf, Germany) at 130 rpm and at 35°C was used for the incubation. Methane production was continuously measured by an AMPTS (Bioprocess Control, Sweden) following manufacturer's instruction. The tests were stopped when the acetate was completely depleted after 48–72 h approximately.

Phenol Degradation Tests

Batch tests with a phenol concentration of 500 mg·L^{-1} (n = 5) were performed. The batch tests were conducted in 250 mL Schott (Schott, Germany) glass reactors. Biomass was taken from the AnMBR to have a final VSS concentration of 4 g · L^{-1}. The batch reactors were supplemented with macro- and micronutrient solution, phosphate buffer solutions, and Na^+ (as NaCl) as specified in section "Experimental Setup and Reactors Operation." The bottles were incubated at 35°C and 130 rpm. Samples (1–2 mL) were periodically taken, and phenol concentration was measured.

Experimental Setup and Reactors Operation

Anaerobic Membrane Bioreactor Setup

Two AnMBRs (6.5 L working volume) were used for the continuous experiment. **Figure 1** depicts a scheme of the reactors' setup. The temperature of the reactors was kept at 35.0 ± 1.0°C by a water bath (Tamson Instruments, Netherlands) circulating warm water through the reactor double-jacketed wall. Mixing in the reactor was ensured by internal sludge circulation with a reactor turnover of approximately 200 times·d^{-1}. The setup used two peristaltic pumps (Watson Marlow 12 U/DV, 220 Du) for the feeding solution and permeate extraction, respectively, and one pump (Watson Marlow 620U) for the sludge recirculation. Temperature and pH were measured online by pH/temperature probes (Endress & Hauser Memosens and Mettler Toledo). The biogas production rate was measured by a gas meter counter MGC-1 PMMA (Ritter, Milligas, and MGC-10).

Each reactor was coupled to an external pressure-driven ultrafiltration (nominal pore size of 30 nm) PVDF membrane module (X-Flow, Pentair). Membranes were 64 cm length and 0.52 cm diameter, and were operated at a cross-flow velocity of 0.8 m·s^{-1} ($Q \approx$ 1,450 L·d^{-1}). Reactors worked at a constant flux of 6 L·m^{-2} · h^{-1}. The transmembrane pressure (TMP) was measured by three different pressure sensors (AE Sensors, The Netherlands), with a range of −800 to 600 mbar, that were located at the entrance and outlet of the membrane, and at the permeate side. Reactor volume was controlled by two pressure sensors (AE Sensors, The Netherlands) with a range of 0 to 100 mbar, one was located on top of the reactor to measure the gas pressure, and the other at the bottom of the reactor, to measure the hydrostatic pressure plus the gas pressure.

Biomass was already acclimated to high sodium concentration, and phenol and acetate degradation (Muñoz Sierra et al., 2018). Before starting the continuous experiments, the biomass was mixed and then evenly distributed between the two reactors.

AnMBRs Operation and Model Wastewater Composition

In the first reactor (R1), phenol was targeted to be, besides the yeast extract, the sole CES. For the second reactor (R2), acetate and a 2:1 acetate-butyrate mixture were added as additional CES (**Table 1**). Besides the first 10 days of operation of R1 where the HRT was decreased from 7 to 4 d, the HRT in the AnMBRs was maintained at 4 d. The average SRT was calculated as SRT = $X_{reactor}ave$ [gVSS]/$X_{removed}$[gVSS·d^{-1}], where $X_{removed}$ resulted from the biomass withdrawn for samplings divided by the days between each determination of solids. SRT values of 4,300 ± 1,600 (R1), 4,500 ± 1,700 d (R2a), and 5,300 + 2,040 d (R2b) were found.

For the model wastewater composition, and based on a modification to Hendriks et al. (2018) and Muñoz Sierra et al. (2018), per each gram of COD in the feeding solution, 1.5 mL of macronutrients solution, 0.76 mL of micronutrients solution,

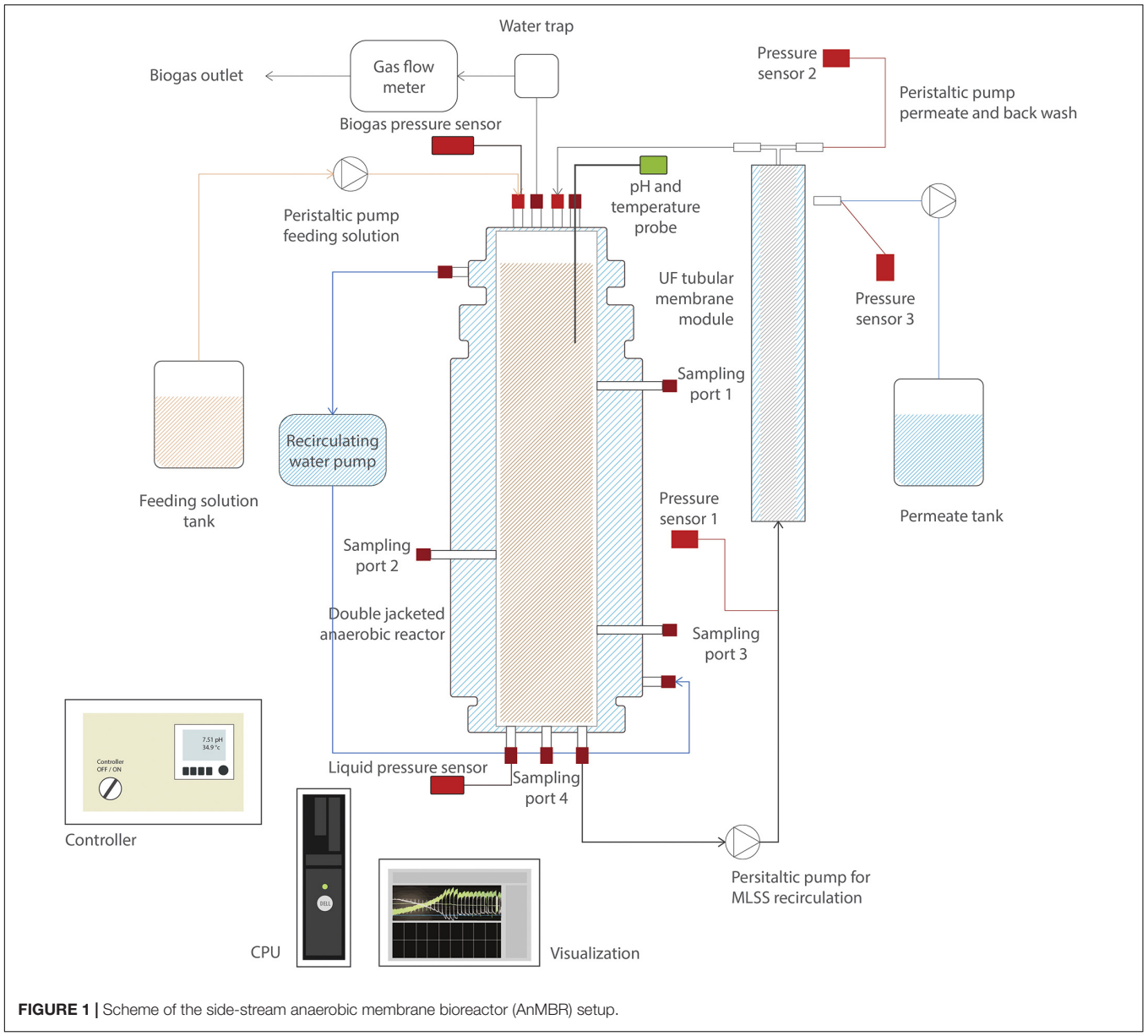

FIGURE 1 | Scheme of the side-stream anaerobic membrane bioreactor (AnMBR) setup.

2.2 mL of buffer phosphate solution A, 3.4 mL of buffer phosphate solution B, and 50 mg of yeast extract (Sigma Aldrich) were added, as well, to the feeding solution (**Table 2**). Enough NaCl was added to the feeding to keep a Na^+ concentration of 8.0 $g{\cdot}L^{-1}$.

Microbial Community Analysis

DNA Extraction, Quantification, and Amplification

Biomass samples corresponding to 1.5–2.0 mL of MLSS were regularly taken from the AnMBRs during the operation of the reactors. The biomass was transferred to Eppendorf tubes (Eppendorf, Germany) and centrifuged in a microcentrifuge (Eppendorf, Germany) at 10,000 *g* for 5 min. The supernatant was discarded and the biomass pellets were frozen and stored at −80°C. For the DNA extraction, the biomass pellet were thawed, and the DNA was extracted with the DNeasy UltraClean Microbial Kit (Qiagen, Germany). Qubit3.0 DNA detection (Qubit dsDNA HS assay kit, Life Technologies, United States) was used to verify DNA quality and quantity.

DNA (16S rRNA gene) amplification was done by Illumina Novaseq 6000 platform by Novogene. The hypervariable regions V3–V4 were amplified using the primer set 341F [(5′–3′) CCTAYGGGRBGCASCAG] and 806R [(5′–3′) GGACTACNNGGGTATCTAAT]. The PCR reactions were carried out with Phusion High- Fidelity PCR Master Mix (New England Biolabs).

DNA Data Processing

The paired-end reads (2 × 250) were processed in the QIIME2 pipeline (Bolyen et al., 2019). After manual inspection, the forward and reverse reads were truncated in the position 250

TABLE 1 | Influent concentration and loading rates of the different carbon sources during the operation of the AnMBRs.

Reactor	*Stages*	*Operation day*	*Phenol [g·L^{-1}]*	*Phenol loading rate [mgPh·gVSS^{-1}d^{-1}]*	*Acetate [gCOD·L^{-1}]*	*Acetate loading rate [gCOD-Ac·gVSS^{-1}d^{-1}]*	*Butyrate [gCOD·L^{-1}]*	*Butyrate loading rate [gCOD-Bu·gVSS^{-1}d^{-1}]*
R1	I	0–59	0.5	10, 28, 42	4.7, 3.5, 1.2, 0.3, 0	100, 76, 25, 7, 0	N/A	N/A
	II	60–99	0.5, 0.9, 0.5	42, 52, 31	0	0	N/A	N/A
	III	100–115	0	0	2.5	54	N/A	N/A
R2 (a)	I	0–43	0.5	25	4.7, 3.5, 2.3, 2.0	236, 177, 113, 100	N/A	N/A
	II	44–100	0.5, 1.5, 3.0, 6.0, 8.2	25, 75, 115, 230, 317	2.0	100, 75	N/A	N/A
	III	101–115	0.0	0	9.1	350	N/A	N/A
R2 (b)	I	0–30	0.5	≈17	1.33	≈48	0.66	≈24
	II	31–110	0.75, 1.0, 1.5, 2.7, 6.5, 11.1	30, 42, 62, 108, 195, 265	1.33	≈48	0.66	≈24

TABLE 2 | Micro- and macro nutrient and buffer solutions dosed in the AnMBRs.

Solution	*Composition*
Micronutrient	EDTA-Na_2 [1.0 g·L^{-1}], H_3BO_3 [0.050 g · L^{-1}], $MnCl_2{\cdot}4H_2O$ [0.50 g · L^{-1}], $FeCl_3{\cdot}6H_2O$ [2.0 g · L^{-1}], $ZnCl_2$ [0.050 g · L^{-1}], $NiCl_2{\cdot}6H_2O$ [0.050 g · L^{-1}], $CuCl_2{\cdot}2H_2O$ [0.030 g · L^{-1}], Na_2SeO_3 [0.10 g · L^{-1}], $(NH_4)_6Mo_7O_2{\cdot}4H_2O$ [0.090 g · L^{-1}], Na_2WO_4 [0.080 g · L^{-1}], and $CoCl_2{\cdot}6H_2O$ [2.0 g · L^{-1}].
Macronutrient	NH_4Cl [170 g·L^{-1}], $CaCl_2{\cdot}2H_2O$ [8 g·L^{-1}], and $MgSO_4{\cdot}7H_2O$ [9 g · L^{-1}].
Buffer solution A	$K_2HPO_4{\cdot}3H_2O$ [45.6 g·L^{-1}].
Buffer solution B	$NaH_2PO_4{\cdot}2H_2O$ [31.2 g·L^{-1}].

in the 3′ end, and the forward reads were trimmed in the position 35 in the 5′ end. Then, the reads were denoised, and the amplicon sequences variants were resolved with the DADA2 plugin (Callahan et al., 2016) removing chimeric sequences with the "consensus" method. The taxonomy of the representative sequences of the amplicon sequences variants was assigned with the classify-consensus-vsearch plugin (Rognes et al., 2016), using the SILVA 132 database (Quast et al., 2013) as reference. The feature table was exported to the R environment to perform the statistical analysis with the phyloseq library (Mcmurdie and Holmes, 2013). The sequences were deposited in the SRA (NCBI) database under the accession number PRJNA663299.

Canonical Correspondence Analysis

A canonical correspondence analysis (CCA) was calculated, using the Weighted Unifrac distance metric and the specific phenol loading rate (sPhLR) and sPhCR as explanatory variables. The statistical significance of the ordination in the CCA was tested with an ANOVA at a p-value <0.05.

RESULTS AND DISCUSSION

Acetoclastic SMA Inhibition by Phenol, and Butyrate Degradation Tests

Batch tests with initial phenol concentrations of 50, 200, and 500 mg·L^{-1} were performed to determine a possible inhibition by phenol on the acetoclastic SMA of the AnMBR biomass (**Figure 2**) (**Supplementary Material S2, Supplementary Table S1**). At initial phenol concentrations of 50 and 200 mg·L^{-1}, the SMA values were 3.4 ± 4.8% and 4.3 ± 23.6%, respectively, higher than the control (acetate 2.0 g COD·L^{-1}), meaning that at these concentrations, there was no inhibition in the acetoclastic methanogens due to phenol. On the other hand, the SMA at an initial phenol concentration of 500 mg·L^{-1} was 27.0 ± 6.6% lower than the control SMA, meaning that the methanogens were inhibited by phenol.

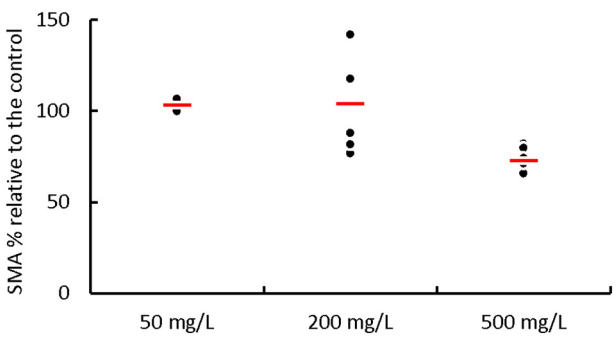

FIGURE 2 | Effect of the phenol addition on the percentage of the acetoclastic SMA of the AnMBR sludge. Each point represents the percentage of the SMA value when phenol, at different concentrations, was added in comparison to the value of the control SMA (acetate at 2 g COD · L^{-1}). The thick red line represents the average SMA value for the different phenol concentrations.

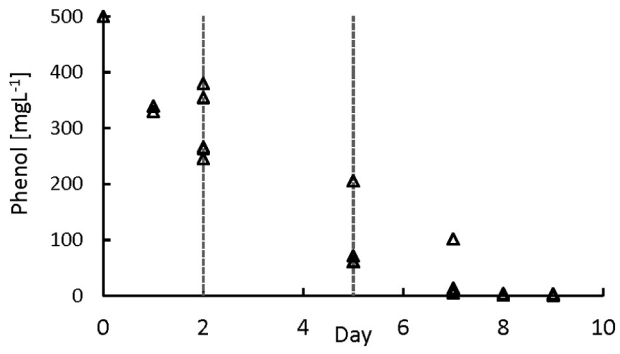

FIGURE 3 | Phenol degradation batch assays. The lines represent the period used for the determination of the specific phenol conversion rate.

AD inhibition by phenol is a phenomenon reported in literature (Olguin-Lora et al., 2003; Liang and Fang, 2010). Although phenol may affect all main physiological microbial populations of the AD process, it is reported, as with other inhibitory or toxic substances (Astals et al., 2015), that the acetoclastic methanogenic population could be the most affected group (Chen et al., 2008). Half maximum inhibitory concentration (IC_{50}) ranges between 50 and 1,750 mg·L^{-1} for non-adapted and phenol-degrading biomass have been reported (Fang and Chan, 1997; Olguin-Lora et al., 2003; Collins et al., 2005; Muñoz Sierra et al., 2017).

Furthermore, we performed all batch experiments at 8.0 g Na^{+}·L^{-1} which might have had an impact as well, even though the biomass was adapted to this Na^{+} concentration. In agreement with literature (Fang and Chan, 1997; Olguin-Lora et al., 2003; Collins et al., 2005; Muñoz Sierra et al., 2017), the results obtained in this research showed that a phenol concentration of 50 mg·L^{-1} caused no negative effect on the SMA when compared to the control without phenol. As well, the average SMA at phenol concentration of 200 mg·L^{-1} was not affected, but phenol concentration of 500 mg·L^{-1} decreased the SMA with 27%. Butyrate at a concentration up to 3.0 g COD·L^{-1} did not cause inhibition problems (**Supplementary Material S3**).

Phenol Degradation in Batch Assays

To further study the phenol degradation kinetics, a series of batch tests with phenol concentrations of 500 mgPh·L^{-1} were performed (**Figure 3**). For calculating the sPhCR, the period between day 2 and day 5 of the assays was chosen to get

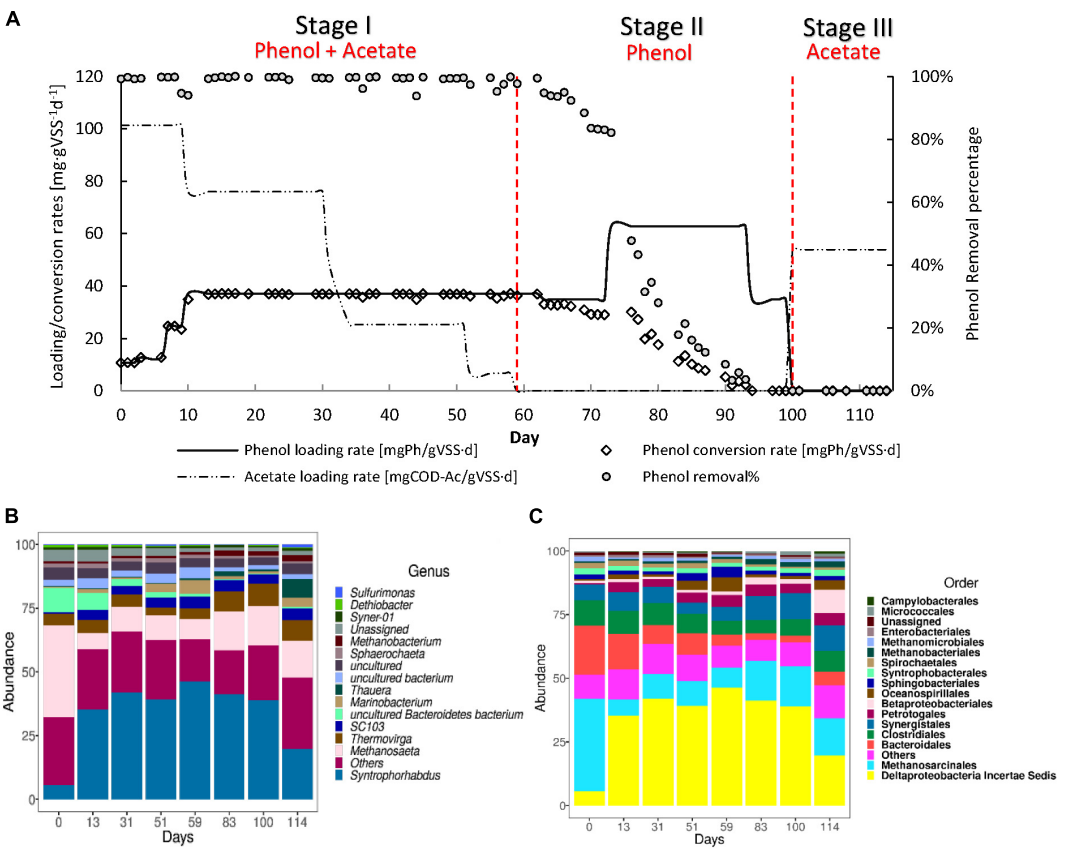

FIGURE 4 | Operation **(A)** and microbial community dynamics **(B,C)** of the R1 toward the usage of phenol as the main carbon and energy source (CES). The graph in **(A)** shows the phenol loading and conversion rates, the acetate loading rate, and the phenol removal percentage during the AnMBR operation. **(B,C)** shows the microbial community dynamics, as the more abundant microbial order **(B)** or genus **(C)** during the different operational days.

the part of the curve that avoids a possible inhibition of the phenol degraders by high phenol concentration (**Supplementary Material S1**). The average sPhCRs calculated during the batch test were 17.8 ± 2.6 mgPh·gVSS^{-1} d^{-1}.

Several sPhCR values for granular biomass have been reported in batch tests, such as 126 (Tay et al., 2000), 65 (Razo-Flores et al., 2003), and 38–93 (Fang et al., 2004) mgPh·gVSS^{-1} d^{-1} which are higher than the average value of 16.6 ± 1.9 mgPh·gVSS^{-1} d^{-1} that we obtained. However, in our study, the sPhCRs assessed in the batch tests were lower than the sPhCRs determined in the continuous experiment (section "AnMBR Operation").

AnMBR Operation

AnMBR Operation Toward Phenol as the Main Carbon and Energy Source

R1 was operated to assess whether phenol could serve as the sole CES (**Figure 4A**) and the maximum sPhCR that could be achieved. During stage I, in which acetate was stepwise decreased and the sPhLR was stepwise increased in ten days from 12 to 42 mgPh·gVSS^{-1} d^{-1}. During this period, the sPhCR remained the same as the sPhLR, i.e., 42 mgPh·gVSS^{-1} d^{-1}, corresponding to a phenol removal efficiency exceeding 99%. In stage II, after the exclusion of acetate from the feeding, the sPhCR decreased to 29 mgPh·gVSS^{-1} d^{-1} during the days 59–72. When the phenol loading was increased to 62 mgPh·gVSS^{-1} d^{-1}, the sPhCR and the removal percentage started to decrease, and on day 94, the sPhCR and the phenol removal efficiency were 0. During stage III, phenol was excluded from the influent because no phenol conversion was observed, and further intoxication of the reactor biomass was unwanted. Hence, the COD was replaced with acetate.

In our present study, it was not possible to achieve long-time AnMBR operation with phenol as the sole CES. This was confirmed with a second experiment (**Supplementary Material S4**, **Supplementary Figure S1**). Possibly, this inability might be attributed to the applied sodium concentration of 8 g·L^{-1}, which has been hypothesized to decrease the phenol conversion (Wang et al., 2017). Under saline conditions, more of the catabolically generated energy from the substrate conversion, in this case phenol, will be spent on regulating a higher maintenance energy in the biomass, because of the increased osmotic pressure (Russell and Cook, 1995; He et al., 2017). A maximum sPhCR of 40 mgPh·gVSS^{-1} L^{-1} was determined from days 49 to 62 (Stage I) when phenol was the main CES, representing 80% of the total COD while acetate contributed to 20% of the COD. However, this sPhCR could not be sustained for more than five days after the acetate was excluded from the influent (Stage II).

For continuous reactor operation, anaerobic degradation of phenol as sole CES at different sPhCRs (6–690 mgPh·gVSS^{-1}d^{-1}) has been reported (Fang et al., 1996; Kennes et al., 1997; Zhou and Fang, 1997; Razo-Flores et al., 2003; Ramakrishnan and Gupta, 2008; Liang and Fang, 2010) (**Table 3**). Most of these studies refer to granular-sludge-based reactors, such as upflow anaerobic sludge blanket (UASB) reactors, under non-saline conditions. As an exception, Suidan et al. (1988), reported the successful continuous operation of a chemostat (suspended biomass) with phenol as the only CES.

An anaerobic granule consists of several populations of microorganisms forming an ecosystem, in which the products of a specific population serves as the substrate for others in a very close vicinity. Moreover, methanogens and phenol-degraders in the inside are only exposed to very low phenol concentrations when phenol is indeed readily degraded in the continuous system. Subsequent phenol conversion in the granule interior provides the conversion intermediates as a substrate for the other populations, allowing the use of phenol as the sole CES. In suspended biomass systems, such as an AnMBR, the phenol concentration is the same for all biomass, while distances between microbial species are much larger, making these systems much more sensitive to increased phenol concentrations.

Effect of the Addition of Acetate on the Specific Phenol Conversion Rate

R2(a) was operated to determine the effect of the addition of acetate as an extra CES on the sPhCR (**Figure 5A**). In stage I, the acetate-COD concentration in the influent was decreased from 4.7 to 2.0 gCOD L^{-1}, corresponding to an acetate loading rate of 100 mgAc-COD·gVSS^{-1} d^{-1}, while the sPhLR was maintained at 25 mgPh·gVSS^{-1} d^{-1}, corresponding to a phenol concentration in the influent of 0.5 gPh·L^{-1}. During this stage, the sPhCR was 25 mgPh·gVSS^{-1} d^{-1}, corresponding to a phenol removal percentage of ≈100%.

In stage II, the sPhLR was stepwise increased from 75 to 230 mgPh·gVSS^{-1} d^{-1}, corresponding to phenol concentrations in the influent of 1.5 and 8.2 g·L^{-1}, respectively. Phenol removal of 100% was observed with phenol loading rates of 75 and 115 mgPh·gVSS^{-1} d^{-1}. At a loading rate of 230 mgPh·gVSS^{-1} d^{-1}, the sPhCR and the removal efficiency decreased to 86 mgPhg·VSS^{-1} d^{-1} and 55%, respectively. The further increase in the sPhLR (320 mgPh·gVSS^{-1} d^{-1}) on day 87 caused an intoxication of the AnMBR, which was observed as a decreased sPhCR that was eventually halted. During days 94 to 100, phenol in the feeding solution was excluded and acetate concentration was kept at 2.0 g COD·L^{-1}. In stage III, the reactor was fed with only acetate at a concentration of 9.1 g COD·L^{-1} to avoid further intoxication of the biomass.

Acetate has been used as an additional CES in the process of biological phenol degradation under anaerobic conditions, either during the reactor start-up (Razo-Flores et al., 2003) or operation (Wang et al., 2017; Muñoz Sierra et al., 2018, 2019) (**Table 3**). Wang et al. (2017) reported UASB reactors treating synthetic wastewater with acetate concentration of 3.6 g COD·L^{-1} and phenol concentrations ranging from 0.1 to 2.0 g·L^{-1}, operating under saline conditions with Na^+ concentration of 10 g · L^{-1}. They reported

TABLE 3 | Studies dealing with phenol degradation either as main/unique carbon and energy source or with the dosage of additional carbon and energy sources.

Substrate [mg·L^{-1}]	Sludge PhLR [gPh·gVSS^{-1} d^{-1}]	Total Removal	sCH$_4$ rate [L·gVSS^{-1} d^{-1}]	CH$_4$ yield [LCH$_4$·gCOD^{-1}]	gCH$_4$-COD·gCOD^{-1}	HRT	Vol [L]	Reactor type	References
Phenol degradation with no additional carbon and energy source									
Phenol (400)		90%		0.21	*53%*	0.14 d	0.66	rUASB	Chang et al. (1995)
Phenol (420–1,260)	*0.03-0.09*	98%	*0.075*	*0.35*	*89%*	12 h	2.8	rUASB	Fang et al. (1996)
Phenol (2,000)After rec (250 to 500)	*0.58*	99%	*0.001*	*0.47*	*117%*	6 h	35	rUASB	Lay and Cheng (1998)
Phenolics (600)	0.0182	30%	*0.001*	*0.02*	*5%*	24 h	7	UASB	Wang et al. (2010)
Phenol (50–700)	*0.024*	85%	*0.024*	0.415	*69%*	24 h	2.8	AFBR	De Amorim et al. (2015)
Additional carbon and energy source dosage for reactor start-up or biomass reactivation									
Phenol (234)	*0.006*	*92%*	*0.008*	0.338	*86%*	48 h	13.4	rAF	Li et al. (2016)
Phenol (1,260)	*0.26*	94%		0.308	*80%*	12 h	2.8	UASB	Fang et al. (2004)
Phenol (1,260)	*0.315*	86%	*0.304*	0.284	*72%*	12 h	2	UASB	Tay et al. (2000)
Phenol degradation with additional carbon and energy source dosage									
Phenol (105–1,260) + Glucose	*0.06–0.28*	98%				12 h	2	UASB	Tay et al. (2001)
Phenol (625)+ acetate (3,850)+ Na (10 g L^{-1})	0.1042	100%				48 h	3.5	rUASB-AF	Wang et al. (2017)
Phenol (1,000)+ Acetate (1,000)		99%		0.39	*100%*	5–2.5 h	10	GAC-AFBR	Lao (2002)
Phenol (500–1,000) + VFAs	0.07–0.14	98%		0.32	*87%*	12 h	3.5	rEGSB-AF	Scully et al. (2006)
Phenol (672)+ VFAs		95%		0.28	*72%*	0.43 d	1.8	AFBR	Carbajo et al. (2010)
Phenol (500) + Acetate + NaCl [4.7–20 g Na^{+}·L^{-1}]	0.012	99%				6.5 d	6.5	AnMBR	Muñoz Sierra et al. (2018)
Phenol (500) + NaCl (8 gNa^{+}·L^{-1})	*0.042*	*97%*	*0.036*	–	–	*4 d*	*6*	*AnMBR*	*This study*
Phenol (3,000)+ Acetate (2 gCOD·L^{-1}) + NaCl (8 gNa^{+}·L^{-1})	*0.115*	*100%*	*0.114*	*0.27*	*68%*	*4 d*	*6*	*AnMBR*	*This study*
Phenol (6,500)+ Acetate-Butyrate (2:1) (2 gCOD·L^{-1}) + NaCl (8 gNa^{+}·L^{-1})	*0.200*	*100%*	–	–	–	*4 d*	*6*	*AnMBR*	*This study*

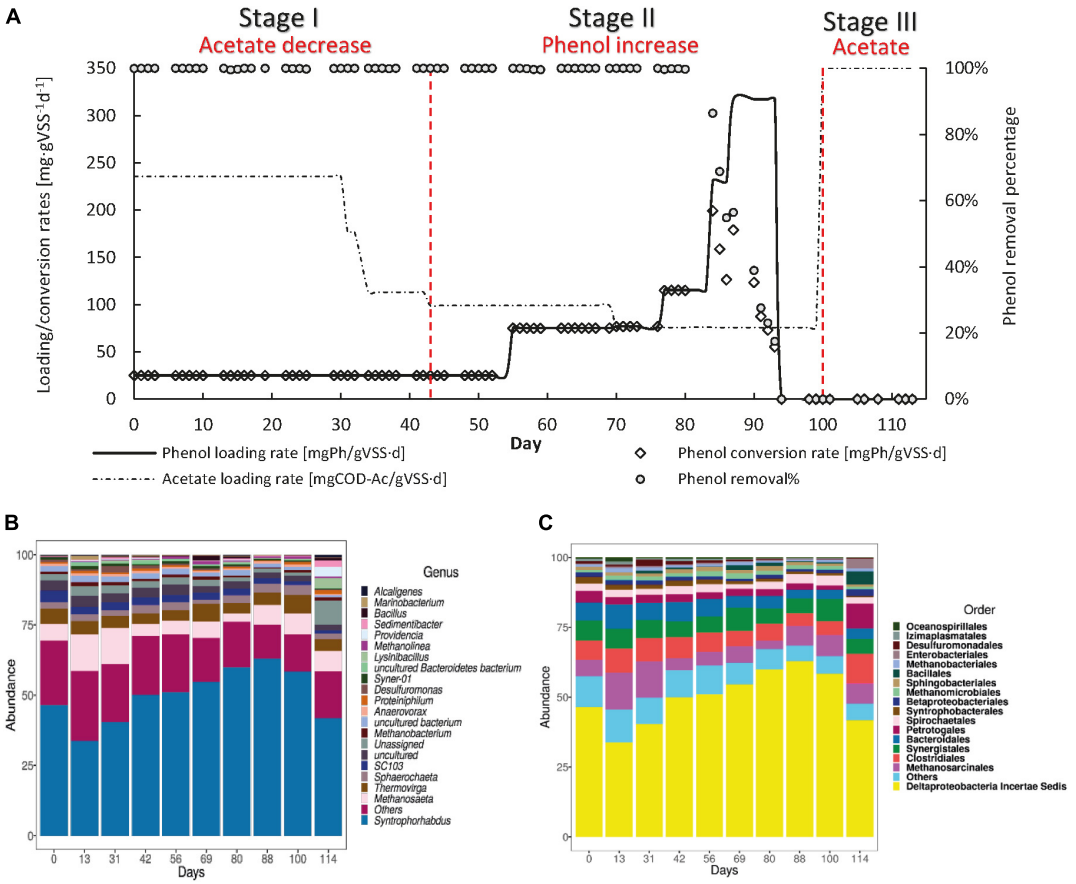

FIGURE 5 | Operation **(A)** and microbial community dynamics **(B)** of the R2(a) with acetate [2 g COD $\cdot L^{-1}$] as an additional carbon and energy source. The graph in **(A)** shows the phenol loading and conversion rates, the acetate loading rate, and the phenol removal percentage during the AnMBR operation. **(B,C)** show the microbial community dynamics, as the more abundant microbial order **(B)** or genus **(C)** during the different operational days.

maximum sPhCR of 20 and 13 mgPh $\cdot$ gVSS^{-1} d^{-1} for batch and continuous reactors, respectively. Working with AnMBRs, Muñoz Sierra et al. (2019), reported maximum sPhCRs of 87 mgPh·gVSS^{-1} d^{-1} at a sodium concentration of 18 g $\cdot$ L^{-1}, corresponding to concentrations in the influent of 5 g Phenol·L^{-1} and an acetate concentration of approximately 30 g COD $\cdot$ L^{-1}. For comparison, in this experiment, we found a maximum stable sPhCR of 115 mgPh·gVSS^{-1} L^{-1} when acetate [2 g COD·L^{-1}] was used as additional CES.

Effect of the Addition of the Acetate-Butyrate on the Specific Phenol Conversion Rate

After the recovery of the biomass from phenol intoxication, R2 was fed with a 2:1 acetate-butyrate mixture at a concentration of 2 g COD·L^{-1} to determine the effect of the dosage of an additional CES that intrinsically generates H_2 during its conversion on the sPhCR and the phenol degraders and methanogens (**Figure 6A**). During stage I, the sPhLR was kept at an average value of 17.1 $\pm$ 1.31 mgPh·gVSS^{-1} d^{-1}, corresponding to an average phenol concentration in the influent of 0.5 g·L^{-1}. On day 10 after the dosage of butyrate, the sPhCR and the phenol removal efficiency decreased to 8.4 mgPh·gVSS^{-1} d^{-1} and 64%, respectively. Possibly, the increased butyrate concentration impacted the phenol conversion pathway. Nobu et al. (2017) indicated that phenol converting microorganisms such as *Syntrophorhabdus* sp., have an alternative phenol degradation pathway, which yields one molecule of butyrate and one of acetate. Therefore, the increased butyrate concentration in the AnMBR could have decreased phenol degradation by product inhibition (**Figure 6A**).

During stage II, from day 32 to 98, a phenol removal efficiency of 100% was found up to a sPhLR (and sPhCR) of 200 mgPh·gVSS^{-1} d^{-1} (influent concentration 6.5 gPh·L^{-1}), being amongst the highest anaerobic sPhCRs' reported in the literature, and the highest value reported for suspended biomass under anaerobic and saline conditions (**Table 3**). When the sPhLR was increased to 265 mgPh·gVSS^{-1} d^{-1} (phenol concentration in the influent = 11.1 g·L^{-1}), on day 99, the sPhCR and the phenol removal efficiency started to decrease. On day 110 the sPhCR and the removal efficiency had already decreased to 130 mgPh·gVSS^{-1} d^{-1} and 45%, respectively, meaning a reactor failure due to biomass intoxication.

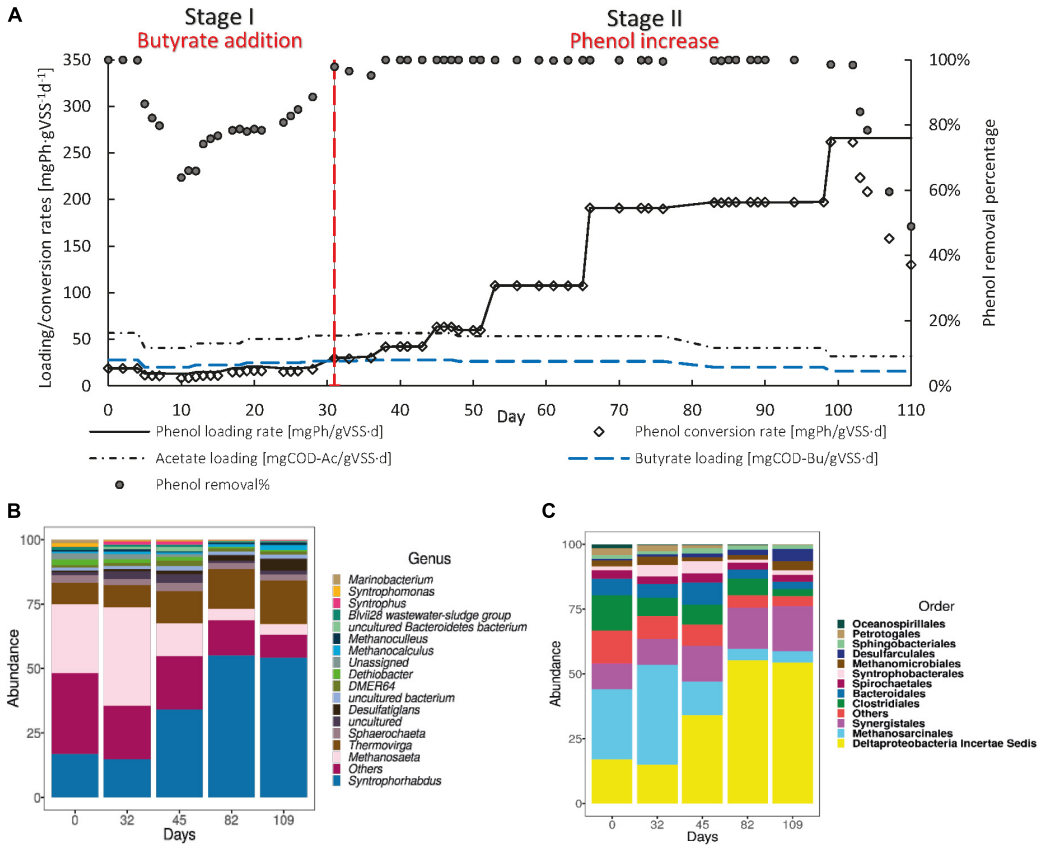

FIGURE 6 | Operation **(A)** and microbial community dynamics **(B)** of the R2(b) with a 2 g COD·L^{-1} 2:1 acetate-butyrate mixture as an additional carbon and energy source. The graph in **(A)** shows the phenol loading and conversion rates, the acetate and butyrate loading rates, and the phenol removal percentage during the AnMBR operation. **(B,C)** show the microbial community dynamics, as the more abundant microbial order **(B)** or genus **(C)** during the different operational days.

Analysis of the Microbial Community Dynamics During the Operation of the Reactors

Microbial Community Dynamics in the AnMBR Toward Phenol as the Main Carbon and Energy Source

To get an insight into the microbial community structure in the AnMBR biomass during the reactor operation and to determine what was the effect of the sPhLRs on this structure, we analyzed the V3–V4 regions of the 16S rRNA gene of several biomass samples. The analysis showed that during the whole reactor operation, the more abundant microorganisms at genus level, were the Deltaproteobacteria *Syntrophorhabdus* sp. (**Figures 4B,C**), which is a reported anaerobic syntrophic phenol degrader (Qiu et al., 2008; Nobu et al., 2015; Franchi et al., 2018), and the acetoclastic methanogen *Methanosaeta* sp. Together, these microorganisms represented ≈50% of the total microbial community; remarkably, no other genus had a relative abundance higher than 6% (**Supplementary Material**). However, other microorganisms such as *Thermovirga* sp. (5.8 ± 2.1%), *Marinobacterium* (2.1 ± 1.8%) (**Figure 4C**), and *Thauera* (1.5 ± 2.5%) were constantly present during the different stages. In this regard, *Thermovirga* sp., belonging to the order Clostridiales, has been reported in the microbial community of saline matrixes with either petrochemical (Dahle and Birkeland, 2006) or phenolic compounds (Wang et al., 2020). However, there are no studies suggesting phenol-degrading activity by this microorganism. *Marinobacterium* sp. has been reported as well as a community member of phenol-degrading reactors (Muñoz Sierra et al., 2019); although, most of the members of this genus are strictly aerobic, whereas *M. zhoushanense* is reported as facultative and halophilic microorganism (Han et al., 2016). *Thauera* sp. is a known phenol degrader, however, it has been reported as nitrate reducer.

During stage I, at day 0, the relative percentage of *Syntrophorhabdus* sp. was 5.6%, which increased to a maximum of 46.3% in the last period of this first stage (day 59) and had an average relative abundance of 40.7 ± 4.6%. For the methanogens, *Methanosaeta* sp. started at a relative abundance of 36.2%, and during the stage, it remained at an average of 8.4 ± 1.7%.

In stage II, the relative abundance of *Syntrophorhabdus* sp. decreased to 41.2% (day 83) and 38.9% (day 100), which seemed to correlate with the decrease in the sPhCR (section "Canonical Correspondence Analysis") and therefore, the removal percentage. The acetoclastic methanogen *Methanosaeta* sp.

remained as the most abundant methanogenic microorganism, with an average relative abundance of 15% (days 83 and 100).

During stage III corresponding to the intoxication period (section "AnMBR Operation Toward Phenol as the Main Carbon and Energy Source"), the relative abundance of *Syntrophorhabdus* sp. kept decreasing with respect to the previous stage to a value of 19.7%, while the methanogen *Methanosaeta* sp. had a relative abundance of 14.3%. For this stage, the low abundance of *Syntrophorhabdus* sp. coincided with the observed toxic effect of phenol and the fact that no more phenol but only acetate was present in the influent.

Microbial Community Dynamics in the AnMBR With Acetate as Additional Carbon and Energy Source

To determine the effect of the increase in the sPhLR and the dosage of acetate as additional CES on the microbial community structure, with a focus on the reported phenol degraders and the methanogens, we analyzed the microbial community structure of the R2(a) during different stages of its operation. We found, similar to R1, that the most abundant bacteria and archaea were *Syntrophorhabdus* sp. and *Methanosaeta*, respectively (**Figures 5B,C**). Same as in the operation of R1, no other genus had a relative abundance higher than 5%; although, *Thermovirga* sp. (4.7 ± 1.0%), was the next genus regarding relative abundance.

During stage I, the most abundant microorganism was the phenol degrader *Syntrophorhabdus* sp. with an average relative abundance of 40.2 ± 6.4%. The methanogens were mainly represented by *Methanosaeta* with an average abundance of 10.6 ± 4.1%. During stage II, after the sPhLR was increased, the relative abundance of *Syntrophorhabdus* sp. was increased, as well, to a maximum of 62.9% on day 88. However, on day 100, a decrease to 58.3% was observed, which correlated with the decrease in the phenol removal percentage (section "Canonical Correspondence Analysis"). For the methanogens, *Methanosaeta* sp. was the main microorganism during this stage with a maximum relative abundance of 7.5%.

During stage III, on day 114, a further decrease in the relative abundance of *Syntrophorhabdus* sp. to 41.8% was observed. However, the methanogen *Methanosaeta* sp. remained at a similar relative abundance as during stage II.

Microbial Community Dynamics in the AnMBR With the Acetate-Butyrate Mixture

To determine the effect of the sPhLR and an hydrogen-generating additional CES on the microbial community structure, with a focus on the reported phenol degraders and the methanogens, we analyzed the microbial community structure of the R2(b) during different stages of its operation (**Figures 6B,C**). For this reactor, the community was, again, mostly represented by the phenol degrader *Syntrophorhabdus* sp. and the acetoclastic *Methanosaeta* (>50%). As it was found in R1 and R2(a), there were no other genera with more than (5%) of relative abundance. However, in this reactor, the average relative abundance of *Thermovirga* sp. was 12.3 ± 3.9%, which suggests that this microorganisms could potentially have a role in the phenol degradation process.

At the beginning of stage I, *Syntrophorhabdus* sp. and *Methanosaeta* sp. represented 17.0 and 32.5% of the microbial community, respectively. On day 32, after the start of the butyrate dosage, and the observed decrease in the phenol removal percentage, there was a slight decrease in *Syntrophorhabdus* sp. to 14.9%; that, as discussed in section "Discussion on the Possible Phenol-Degrading-Enhancing Mechanisms," it could possibly be related to an adverse effect of butyrate on the phenol degraders.

During stage II, on day 82, the relative abundance of *Syntrophorhabdus* sp. reached a maximum of 55.2%, which was 7% lower compared to the highest relative abundance of this bacteria when the maximum sPhCR in the reactor operation with acetate as additional CES was reached. Nonetheless, the sPhCR achieved with the acetate-butyrate mixture was 73% higher than that with only acetate (115 $mgPh{\cdot}gVSS^{-1}\ d^{-1}$). For the methanogens, the acetoclastic *Methanosaeta* sp. remained as the main microorganism. On day 109, the relative abundance of *Syntrophorhabdus* sp. remained at 54%.

Canonical Correspondence Analysis

Canonical (or constrained) correspondence analyses (CCA) were performed to assess the changes in the microbial community structure during the operation of the reactors; and therefore, to correlate the effect of the increase in the sPhLR, and the dosage of acetate or the acetate-butyrate mixture with the different microbial communities in R1, R2(a), and R2(b) (**Figure 7**). CCA is an ordination technique that recovers the response of the community structure to different physical environmental variables, in this case the sPhLR and the sPhCR (Palmer, 1993).

The biplots for each reactor (**Figure 7A**), in which the vectors indicate the importance of either sPhLR and sPhCR in the ordination process, showed a significant correlation ($p < 0.05$) between the community structures of the biomass of the reactors and the two variables. As it is seen in **Figures 7A,B**, the community structures at different days (R1 = 13, 31, 51; R2(a) = 56, 69 and 80; R2(b) = 45, 82, 109), corresponding to the points at the right of the biplot, were correlated with a higher sPhLR and sPhCR. In the comparison of the three reactors (**Figure 7B**), it was noticed that the samples of R2(a) and R2(b) did not group together; however, because of the position of each sample respecting the vectors (sPhLR and sPhCR), it can be concluded that those community structures were more related to higher sPhLR and sPhCR. Regarding these two vectors explaining the environmental variables, it was decided to use both sPhLR and sPhCR, because even though sPhLR was the independent variable, sPhCR represented the biological activity of the biomass.

Discussion on the Possible Phenol-Degrading-Enhancing Mechanisms

Regarding to the four discussed mechanisms which could enhance the sPhCR, co-metabolism (1) and/or (2) direct usage of acetate as a catabolic substrate by the phenol degraders seems the less likely. As it has been reported, the phenol degrader *Syntrophorhabdus* sp., excretes acetate through a

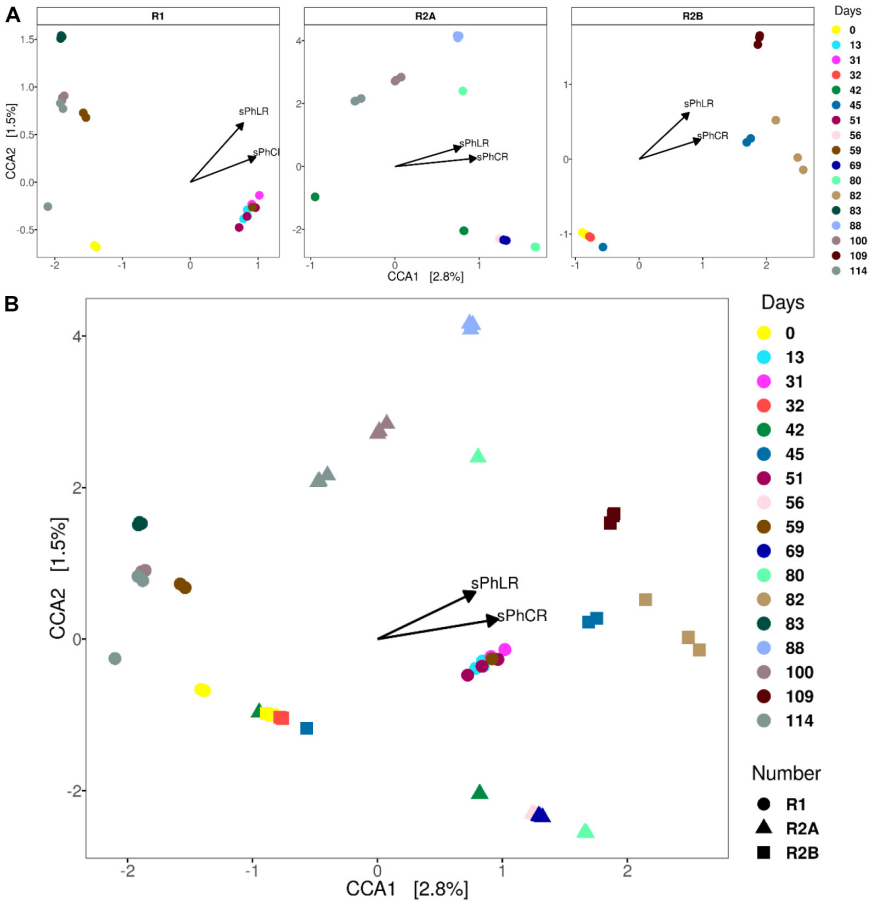

FIGURE 7 | CCAs' for each of the reactors **(A)** and for all three **(B)**. The samples that correspond to the reactors' operation with increased loading and conversion rates group to right of the biplots.

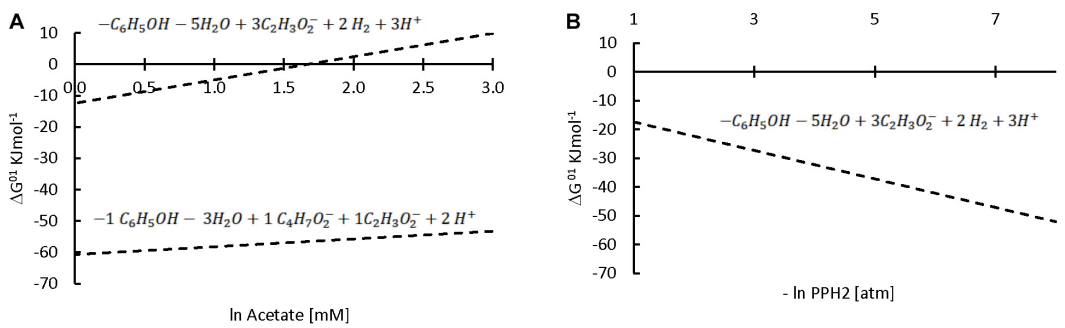

FIGURE 8 | Effect of acetate (upper line) or butyrate (lower line) concentrations **(A)** or hydrogen partial pressure **(B)** on the ΔG^{01} of the anaerobic phenol degradation reaction. The stoichiometry of each reaction is shown above the corresponding line. Note that the *x* axis on **(A)** is ln while in **(B)** is –ln; therefore, higher concentrations, but lower partial pressures are expected at the right of *x* axis.

cation-acetate symporter (Nobu et al., 2017). Furthermore, phenol degraders are a physiological population with defined substrates (Eq. S6) (Qiu et al., 2008), being in this case, phenol and not acetate. However, the microbial community analyses results clearly indicate that with an increase in the sPhLR, the percentage of the biomass corresponding to the (reported) phenol degraders increased, reaching values over 50% of the total relative abundance, either at the order and genus levels (*Syntrophorhabdus* sp.), of the biomass of R2(a) and R2(b) (**Figures 5**, **6B,C**). Note that the microbial community analyses were based on the study of the 16S rRNA gene, which may introduce inherent biases (Campanaro et al., 2018).

As well, this analysis does not offer information about the metabolic state of the microorganisms, therefore, presence does not mean activity. Even though, with the addition of acetate or butyrate, the relative abundance of *Syntrophorhabdus* sp. reached values higher than 50%, which coincided with the highest sPhCRs achieved by the reactor. This correlation of the microbial community structure with the enhanced conversion was statistically confirmed by the CCA analysis (section "Canonical Correspondence Analysis").

On the other hand, our hypothesis is that the third identified mechanism, syntrophic association, could have played a role in the increase in sPhCR. Two different syntrophic associations with the methanogens are considered, either with the acetoclastics, which were the main methanogens (section "Analysis of the Microbial Community Dynamics During the Operation of the Reactors") and with the hydrogenotrophic. Considering the acetoclastic methanogens, **Figure 8** shows the effect of the concentration of acetate on the Gibbs free energy change (ΔG^{01}, standard conditions and pH = 7) of phenol degradation under anaerobic conditions (section "Discussion on the Possible Phenol-Degrading-Enhancing Mechanisms," thermodynamic data **Supplementary Material S2**, **Supplementary Table S2**), which shows that a low acetate concentration makes the reaction thermodynamically more favorable. Therefore, an abundant phenol-adapted acetoclastic methanogen population could offer advantages over phenol degradation. Nevertheless, R1 had similar values of the relative abundance of the acetoclastic methanogens (**Supplementary Data Sheet S1**). Regarding reactor R2(b) and the second syntrophic process, it has been shown that anaerobic mineralization of phenol requires the presence of balanced (syntrophic) associations that guarantee efficient interspecies electron transfer. In these associations, hydrogen-consuming microorganisms, such as the hydrogenotrophic methanogens, may act as the required electron sink (Qiu et al., 2008). For this reason, butyrate was added as additional CES in AnMBR experiment R2(b). However, the reactor fed with butyrate did not show a higher relative abundance of hydrogenotrophic archaea in comparison to the operation of the other reactors (**Figure 9**). Hydrogenotrophic microorganisms such as *Methanoculleus* sp. and *Methanocalculus* sp. were present at an average of 1.76 ± 0.68%, whereas, when only acetate was dosed as additional CES, hydrogenotrophic methanogens such as *Methanobacterium* sp. and *Methanolinea* sp. were found in similar relative abundances (1.42 ± 0.42%). A similar percentage of 1.26 ± 0.68% was found for the hydrogenotrophic *Methanobacterium* in the operation of R1, in which phenol as the sole CES was investigated.

Therefore, we hypothesize that the development of the (acetoclastic) methanogenic population could have enhanced the phenol conversion by keeping the degradation products, e.g., acetate, in a low concentration, allowing the constant conversion of phenol, and consequently promoting an increase of the abundance of the phenol-degrading microorganisms or possibly their specific conversion rate (Eq. S6).

Finally, regarding to the fourth mechanism considered (i.e., an increase in intermediate compounds involved in the conversion of phenolics), it could be possible that an increase in the HCO_3^- concentration, due to the fermentation of acetate, could have played a role in the enhancement of the sPhCR by promoting the carboxylation step needed for phenol degradation. It has been reported that in the absence of HCO_3/CO_2 phenol degradation under anaerobic conditions is hampered (Karlsson et al., 1999) and that the phenylphosphate carboxylase found in *Syntrophorhabdus* sp. is highly dependent on HCO_3/CO_2 (Karlsson et al., 1999; Schühle and Fuchs, 2004; Nobu et al., 2015). However, this hypothesis should be further tested.

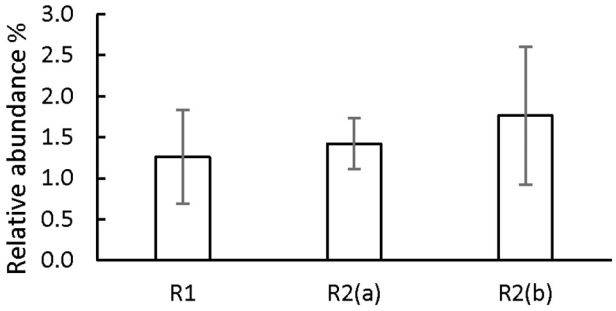

FIGURE 9 | Average relative abundance percentage of the hydrogenotrophic methanogens in the operation of the three AnMBRs. *n* = 5 to 10, bars CI 95%.

CONCLUSION

The present study showed the feasibility of using AnMBR for the treatment of phenolic wastewater at high sodium concentrations. From the conducted experiments, performed with previously acclimated biomass, the following conclusions can be derived:

- In batch reactors at 8 $gNa^+ \cdot L^{-1}$, phenol at a concentration of 0.5 $g \cdot L^{-1}$ decreased the SMA with 27% in comparison to the control tests without phenol. A maximum sPhCR of 17.8 ± 2.6 $mgPh \cdot gVSS^{-1}\ d^{-1}$ was determined for an initial phenol concentration of 500 $mg \cdot L^{-1}$.
- In the AnMBR, a stable sPhCR of 40 $mgPh \cdot gVSS^{-1}\ L^{-1}$ was measured when phenol contributed to 80% of the total COD. However, the sPhCR could not be maintained when phenol was the sole CES.
- In the AnMBR, when acetate was added as additional CES, a maximum sPhCR of 115 $mgPh \cdot gVSS^{-1}\ L^{-1}$ was determined.
- The highest sPhCR of 200 $mgPh \cdot gVSS^{-1}\ L^{-1}$ was found when a 2:1 acetate-butyrate mixture, based on COD, was fed to the AnMBR.
- During the operation of the reactors, the most abundant microorganisms were the phenol degrader *Syntrophorhabdus* sp. and the acetoclastic methanogen *Methanosaeta* sp., making more than 50% of the microbial community. Seemingly, there was a correlation ($p < 0.05$) between the increase in the sPhLR and the increase in the relative abundance of *Syntrophorhabdus* sp.

DATA AVAILABILITY STATEMENT

The original contributions presented in the study are publicly available. This data can be found in NCBI under accession number PRJNA663299.

AUTHOR CONTRIBUTIONS

VG conceptualized and designed the batch and reactor experiments, carried out the batch experiments, gathered, and analyzed the data, directed and supervised the operation of reactors, analyzed their data, planned and worked the samples for the microbial community analysis, and wrote the manuscript. JM conceptualized and designed the batch and reactor experiments, critically reviewed and provided feedback for the data analysis. LF designed and operated partially the reactor experiments, carried out analytical methods, and analyzed the data. KQ operated partially the reactors and performed laboratory analyses. DC-G did the bioinformatics analyses and performed the microbial community analysis. JM, HS, and JvL provided feedback that helped shape the research, experiments, and data analysis, and critically revised the manuscript. All authors have read and approved the final manuscript.

FUNDING

This research was supported by the Dutch Technology Foundation (STW, Project No 13348), which is 528 part of the Netherlands Organisation for Scientific Research (NWO), partly funded by the Dutch 529 Ministry of Economic Affairs. This research is co-sponsored by Evides Industriewater and Paques B.V.

ACKNOWLEDGMENTS

We thank the lab technicians Mohammed Jafar and Armand Middeldorp for their technical support, and Flor A. García Rea and Pamela S. Ceron Chafla for their help with the graphical design. VG thanks 1) Alexander Hendriks and Xuedong Zhang for all the discussions, and 2) the Mexican National Council of Science and Technology (CONACyT) for granting him the Ph.D. Scholarship No. 410669.

SUPPLEMENTARY MATERIAL

The Supplementary Material for this article can be found online at: https://www.frontiersin.org/articles/10.3389/fmicb.2020.604173/full#supplementary-material

REFERENCES

Astals, S., Batstone, D. J., Tait, S., and Jensen, P. D. (2015). Development and validation of a rapid test for anaerobic inhibition and toxicity. *Water Res.* 81, 208–215. doi: 10.1016/j.watres.2015.05.063

Batstone, D. J., Keller, J., Angelidaki, I., Kalyuzhnyi, S. V., Pavlostathis, S. G., Rozzi, A., et al. (2002). The IWA anaerobic digestion model no 1 (ADM1). *Water Sci. Technol.* 45, 65–73. doi: 10.2166/wst.2002.0292

Bertrand, J.-C., Doumenq, P., Guyoneaud, R., Marrot, B., Martin-Laurent, F., Matheron, R., et al. (2015). "Applied Microbial Ecology and Bioremediation," in *Environmental Microbiology: Fundamentals and Applications: Microbial Ecology*, eds J.-C. Bertrand, P. Caumette, P. Lebaron, R. Matheron, P. Normand, and T. Sime-Ngando (Dordrecht: Springer Netherlands), 659–753. doi: 10.1007/978-94-017-9118-2_16

Blum, D. J. W., Hergenroeder, R., Parkin, G. F., and Speece, R. E. (1986). Anaerobic treatment of coal conversion wastewater constituents: biodegradability and Toxicity. *J. (Water Pollut. Control Fed.)* 58, 122–131.

Bolaños, R. M. L., Varesche, M. B. A., Zaiat, M., and Foresti, E. (2001). Phenol degradation in horizontal-flow anaerobic immobilized biomass (HAIB) reactor under mesophilic conditions. *Water Sci. Technol.* 44, 167–174. doi: 10.2166/wst.2001.0212

Bolyen, E., Rideout, J. R., Dillon, M. R., Bokulich, N. A., Abnet, C. C., Al-Ghalith, G. A., et al. (2019). Reproducible, interactive, scalable and extensible microbiome data science using QIIME 2. *Nat. Biotechnol.* 37, 852–857. doi: 10.1038/s41587-019-0209-9

Callahan, B. J., Mcmurdie, P. J., Rosen, M. J., Han, A. W., Johnson, A. J., and Holmes, S. P. (2016). DADA2: high-resolution sample inference from Illumina amplicon data. *Nat. Methods* 13, 581–583. doi: 10.1038/nmeth.3869

Campanaro, S., Treu, L., Kougias, P. G., Zhu, X., and Angelidaki, I. (2018). Taxonomy of anaerobic digestion microbiome reveals biases associated with the applied high throughput sequencing strategies. *Sci. Rep.* 8:1926. doi: 10.1038/s41598-018-20414-0

Carbajo, J. B., Boltes, K., and Leton, P. (2010). Treatment of phenol in an anaerobic fluidized bed reactor (AFBR): continuous and batch regime. *Biodegradation* 21, 603–613. doi: 10.1007/s10532-010-9328-1

Chang, B. V., Chiang, F., and Yuan, S. Y. (2005). Anaerobic degradation of nonylphenol in sludge. *Chemosphere* 59, 1415–1420. doi: 10.1016/j.chemosphere.2004.12.055

Chang, Y.-J., Nishio, N., and Nagai, S. (1995). Characteristics of granular methanogenic sludge grown on phenol synthetic medium and methanogenic fermentation of phenolic wastewater in a UASB reactor. *J. Ferment. Bioeng.* 79, 348–353. doi: 10.1016/0922-338x(95)93993-t

Chen, Y., Cheng, J. J., and Creamer, K. S. (2008). Inhibition of anaerobic digestion process: a review. *Bioresour. Technol.* 99, 4044–4064. doi: 10.1016/j.biortech.2007.01.057

Collins, G., Foy, C., Mchugh, S., Mahony, T., and O'flaherty, V. (2005). Anaerobic biological treatment of phenolic wastewater at 15–18°C. *Water Res.* 39, 1614–1620. doi: 10.1016/j.watres.2005.01.017

Dahle, H., and Birkeland, N.-K. (2006). Thermovirga lienii gen. nov., sp. nov., a novel moderately thermophilic, anaerobic, amino-acid-degrading bacterium isolated from a North Sea oil well. *Int. J. Syst. Evol. Microbiol.* 56, 1539–1545. doi: 10.1099/ijs.0.63894-0

De Amorim, E. L. C., Sader, L. T., and Silva, E. L. (2015). Effects of the Organic-Loading rate on the performance of an Anaerobic Fluidized-Bed reactor treating synthetic wastewater containing phenol. *J. Environ. Eng.* 141, 04015022. doi: 10.1061/(asce)ee.1943-7870.0000952

Dereli, R. K., Ersahin, M. E., Ozgun, H., Ozturk, I., Jeison, D., Van Der Zee, F., et al. (2012). Potentials of anaerobic membrane bioreactors to overcome treatment limitations induced by industrial wastewaters. *Bioresour. Technol.* 122, 160–170. doi: 10.1016/j.biortech.2012.05.139

Fang, H. H., Liu, Y., Ke, S. Z., and Zhang, T. (2004). Anaerobic degradation of phenol in wastewater at ambient temperature. *Water Sci. Technol.* 49, 95–102. doi: 10.2166/wst.2004.0028

Fang, H. H., and Zhou, G.-M. (2000). Degradation of phenol and p-cresol in reactors. *Water Sci. Technol.* 42, 237–244. doi: 10.2166/wst.2000.0519

Fang, H. H. P., and Chan, O.-C. (1997). Toxicity of phenol towards anaerobic biogranules. *Water Res.* 31, 2229–2242. doi: 10.1016/S0043-1354(97)00069-9

Fang, H. H. P., Chen, T., Li, Y.-Y., and Chui, H.-K. (1996). Degradation of phenol in wastewater in an upflow anaerobic sludge blanket reactor. *Water Res.* 30, 1353–1360. doi: 10.1016/0043-1354(95)00309-6

Franchi, O., Rosenkranz, F., and Chamy, R. (2018). Key microbial populations involved in anaerobic degradation of phenol and p-cresol using different inocula. *Electron. J. Biotechnol.* 35, 33–38. doi: 10.1016/j.ejbt.2018.08.002

Fuchs, G. (2008). Anaerobic metabolism of aromatic compounds. *Ann. N. Y. Acad. Sci.* 1125, 82–99. doi: 10.1196/annals.1419.010

Fuchs, G., Boll, M., and Heider, J. (2011). Microbial degradation of aromatic compounds–from one strategy to four. *Nat. Rev. Microbiol.* 9, 803–816. doi: 10.1038/nrmicro2652

Gali, V. S., Kumar, P., and Mehrotra, I. (2006). Biodegradation of phenol with wastewater as a cosubstrate in upflow Anaerobic Sludge Blanket. *J. Environ. Eng.* 132, 1539–1542. doi: 10.1061/(ASCE)0733-93722006132:11(1539

Gibson, J., and Harwood, C. S. (2002). Metabolic diversity in aromatic compound utilization by Anaerobic Microbes. *Ann. Rev. Microbiol.* 56, 345–369. doi: 10.1146/annurev.micro.56.012302.160749

Guiot, S. R., Tawfiki-Hájji, K., and Lépine, F. (2000). Immobilization strategies for bioaugmentation of anaerobic reactors treating phenolic compounds. *Water Sci. Technol.* 42, 245–250. doi: 10.2166/wst.2000.0520

Han, S.-B., Wang, R.-J., Yu, X.-Y., Su, Y., Sun, C., Fu, G.-Y., et al. (2016). Marinobacterium zhoushanense sp. nov., isolated from surface seawater. *Int. J. Syst. Evol. Microbiol.* 66, 3437–3442. doi: 10.1099/ijsem.0.001213

Hanselmann, K. W. (1991). Microbial energetics applied to waste repositories. *Experientia* 47, 645–687. doi: 10.1007/BF01958816

He, H., Chen, Y., Li, X., Cheng, Y., Yang, C., and Zeng, G. (2017). Influence of salinity on microorganisms in activated sludge processes: a review. *Int. Biodeterior. Biodegradation* 119, 520–527. doi: 10.1016/j.ibiod.2016.10.007

Heijnen, J. J., and Kleerebezem, R. (2010). "Bioenergetics of Microbial Growth," in *Encyclopedia of Industrial Biotechnology*, ed. M. C. Flickinger (Hoboken, NJ: John Wiley & Sons), 1–66. doi: 10.1002/9780470054581.eib084

Hendriks, A. T. W. M., Van Lier, J. B., and De Kreuk, M. K. (2018). Growth media in anaerobic fermentative processes: The underestimated potential of thermophilic fermentation and anaerobic digestion. *Biotechnol. Adv.* 36, 1–13. doi: 10.1016/j.biotechadv.2017.08.004

Horvath, R. S. (1972). Microbial co-metabolism and the degradation of organic compounds in nature. *Bacteriol. Rev.* 36, 146–155. doi: 10.1128/mmbr.36.2.146-155.1972

Ji, Q., Tabassum, S., Hena, S., Silva, C. G., Yu, G., and Zhang, Z. (2016). A review on the coal gasification wastewater treatment technologies: past, present and future outlook. *J. Clean. Prod.* 126, 38–55. doi: 10.1016/j.jclepro.2016.02.147

Karlsson, A., Ejlertsson, J., Nezirevic, D., and Svensson, B. H. (1999). Degradation of phenol under meso- and thermophilic, anaerobic conditions. *Anaerobe* 5, 25–35. doi: 10.1006/anae.1998.0187

Kennes, C., Mendez, R., and Lema, J. M. (1997). Methanogenic degradation of p-cresol in batch and in continuous UASB reactors. *Water Res.* 31, 1549–1554. doi: 10.1016/S0043-1354(96)00156-X

Kleerebezem, R. (1999). *Anaerobic Treatmen of Phthalates, Microbiological and Technological Aspects*. PhD. thesis, WUR: Wageningen.

Knoll, G., and Winter, J. (1987). Anaerobic degradation of phenol in sewage sludge. *Appl. Microbiol. Biotechnol.* 25, 384–391. doi: 10.1007/bf00252552

Lao, S.-G. (2002). Mechanisms of granular activated carbon anaerobic fluidized-bed process for treating phenols wastewater. *J. Environ. Sci. (China)* 14, 132–135.

Lay, J.-J., and Cheng, S.-S. (1998). Influence of hydraulic loading rate on UASB reactor treating phenolic wastewater. *J. Environ. Eng.* 124, 829–837. doi: 10.1061/(asce)0733-9372(1998)124:9(829)

Li, Y., Tabassum, S., Chu, C., and Zhang, Z. (2017). Inhibitory effect of high phenol concentration in treating coal gasification wastewater in anaerobic biofilter. *J. Environ. Sci.* 64, 207–215. doi: 10.1016/j.jes.2017.06.001

Li, Y., Tabassum, S., and Zhang, Z. (2016). An advanced anaerobic biofilter with effluent recirculation for phenol removal and methane production in treatment of coal gasification wastewater. *J. Environ. Sci.* 47, 23–33. doi: 10.1016/j.jes.2016.03.012

Liang, D., and Fang, H. H. P. (2010). "Anaerobic Treatment of Phenolic Wastewaters," in *Environmental Anaerobic Technology*, ed. H. H. P. Fang (Singapore: World Scientific Publishing), 185–205. doi: 10.1142/9781848165434_0009

Lin, H., Peng, W., Zhang, M., Chen, J., Hong, H., and Zhang, Y. (2013). A review on anaerobic membrane bioreactors: applications, membrane fouling and future perspectives. *Desalination* 314, 169–188. doi: 10.1016/j.desal.2013.01.019

Maiti, D., Ansari, I., Rather, M. A., and Deepa, A. (2019). Comprehensive review on wastewater discharged from the coal-related industries–characteristics and treatment strategies. *Water Sci. Technol.* 79, 2023–2035. doi: 10.2166/wst.2019.195

Mcmurdie, P. J., and Holmes, S. (2013). phyloseq: an R package for reproducible interactive analysis and graphics of microbiome census data. *PLoS One* 8:e61217. doi: 10.1371/journal.pone.0061217

Muñoz Sierra, J. D., Lafita, C., Gabaldón, C., Spanjers, H., and Van Lier, J. B. (2017). Trace metals supplementation in anaerobic membrane bioreactors treating highly saline phenolic wastewater. *Bioresour. Technol.* 234, 106–114. doi: 10.1016/j.biortech.2017.03.032

Muñoz Sierra, J. D., Oosterkamp, M. J., Wang, W., Spanjers, H., and Van Lier, J. B. (2018). Impact of long-term salinity exposure in anaerobic membrane bioreactors treating phenolic wastewater: performance robustness and endured microbial community. *Water Res.* 141, 172–184. doi: 10.1016/j.watres.2018.05.006

Muñoz Sierra, J. D., Oosterkamp, M. J., Wang, W., Spanjers, H., and Van Lier, J. B. (2019). Comparative performance of upflow anaerobic sludge blanket reactor and anaerobic membrane bioreactor treating phenolic wastewater: overcoming high salinity. *Chem. Eng. J.* 366, 480–490. doi: 10.1016/j.cej.2019.02.097

Munoz Sierra, J. D., Wang, W., Cerqueda-Garcia, D., Oosterkamp, M. J., Spanjers, H., and Van Lier, J. B. (2018). Temperature susceptibility of a mesophilic anaerobic membrane bioreactor treating saline phenol-containing wastewater. *Chemosphere* 213, 92–102. doi: 10.1016/j.chemosphere.2018.09.023

Nobu, M. K., Narihiro, T., Hideyuki, T., Qiu, Y. L., Sekiguchi, Y., Woyke, T., et al. (2015). The genome of Syntrophorhabdus aromaticivorans strain UI provides new insights for syntrophic aromatic compound metabolism and electron flow. *Environ. Microbiol.* 17, 4861–4872. doi: 10.1111/1462-2920.12444

Nobu, M. K., Narihiro, T., Liu, M., Kuroda, K., Mei, R., and Liu, W. T. (2017). Thermodynamically diverse syntrophic aromatic compound catabolism. *Environ. Microbiol.* 19, 4576–4586. doi: 10.1111/1462-2920.13922

Olguin-Lora, P., Puig-Grajales, L., and Razo-Flores, E. (2003). Inhibition of the acetoclastic methanogenic activity by phenol and alkyl phenols. *Environ. Technol.* 24, 999–1006. doi: 10.1080/09593330309385638

Palmer, M. W. (1993). Putting things in even better order: the advantages of canonical correspondence analysis. *Ecology* 74, 2215–2230. doi: 10.2307/1939575

Puig-Grajales, L., Rodríguez-Nava, O., and Razo-Flores, E. (2003). Simultaneous biodegradation of a phenol and 3, 4-dimethylphenol mixture under denitrifying conditions. *Water Sci. Technol.* 48, 171–178. doi: 10.2166/wst.2003.0389

Qiu, Y. L., Hanada, S., Ohashi, A., Harada, H., Kamagata, Y., and Sekiguchi, Y. (2008). Syntrophorhabdus aromaticivorans gen. nov., sp. nov., the first cultured anaerobe capable of degrading phenol to acetate in obligate syntrophic associations with a hydrogenotrophic methanogen. *Appl. Environ. Microbiol.* 74, 2051–2058. doi: 10.1128/aem.02378-07

Quast, C., Pruesse, E., Yilmaz, P., Gerken, J., Schweer, T., Yarza, P., et al. (2013). The SILVA ribosomal RNA gene database project: improved data processing and web-based tools. *Nucleic Acids Res.* 41, D590–D596. doi: 10.1093/nar/gks1219

Ramakrishnan, A., and Gupta, S. K. (2008). Effect of hydraulic retention time on the biodegradation of complex phenolic mixture from simulated coal wastewater in hybrid UASB reactors. *J. Hazard. Mater.* 153, 843–851. doi: 10.1016/j.jhazmat.2007.09.034

Razo-Flores, E., Iniestra-González, M., Field, J. A., Olgu-Lora, P., and Puig-Grajales, L. (2003). Biodegradation of mixtures of phenolic compounds in an upward-flow anaerobic sludge blanket reactor. *J. Environ. Eng.* 129, 999–1006. doi: 10.1061/(asce)0733-9372(2003)129:11(999)

Rognes, T., Flouri, T., Nichols, B., Quince, C., and Mahe, F. (2016). VSEARCH: a versatile open source tool for metagenomics. *PeerJ* 4:e2584. doi: 10.7717/peerj.2584

Russell, J. B., and Cook, G. M. (1995). Energetics of bacterial growth: balance of anabolic and catabolic reactions. *Microbiol. Rev.* 59, 48–62. doi: 10.1128/mmbr.59.1.48-62.1995

Sancinetti, G. P., Sader, L., Varesche, M. B. A., Amorim, E. L. C. D., Omena, S. P. F. D., and Silva, E. (2012). Phenol degradation in an anaerobic fluidized bed reactor packed with low density support materials. *Braz. J. Chem. Eng.* 29, 87–98. doi: 10.1590/s0104-66322012000100010

Schink, B., Philipp, B., and Muller, J. (2000). Anaerobic degradation of phenolic compounds. *Naturwissenschaften* 87, 12–23. doi: 10.1007/s001140050002

Schühle, K., and Fuchs, G. (2004). Phenylphosphate carboxylase: a New C-C Lyase involved in anaerobic phenol metabolism in *Thauera Aromatica*. *J. Bacteriol.* 186, 4556–4567. doi: 10.1128/JB.186.14.4556-4567.2004

Scully, C., Collins, G., and O'flaherty, V. (2006). Anaerobic biological treatment of phenol at 9.5–15°C in an expanded granular sludge bed (EGSB)-based bioreactor. *Water Res.* 40, 3737–3744. doi: 10.1016/j.watres.2006.08.023

Singer, P. C., Pfaender, F. K., Chinchilli, J., Maciorowski Iii, A. F., and Lamb, J. C. III (1978). *Assessment of Coal Conversion Wastewaters: Characterization and Preliminary Biotreatability, Technical Report*. Chapel Hill, NC: University of North Carolina at Chapel Hill.

Suidan, M. T., Najm, I. N., Pfeffer, J. T., and Wang, Y. T. (1988). Anaerobic biodegradation of phenols inhibition kinetics and system stability. *J. Environ. Eng.* 114, 1359–1376. doi: 10.1061/(asce)0733-9372(1988)114:6(1359)

Tay, J.-H., He, Y.-X., and Yan, Y.-G. (2000). Anaerobic biogranulation using phenol as the sole carbon source. *Water Environ. Res.* 72, 189–194. doi: 10.2175/106143000x137275

Tay, J.-H., He, Y.-X., and Yan, Y.-G. (2001). Improved anaerobic degradation of phenol with supplemental glucose. *J. Environ. Eng.* 127, 38–45. doi: 10.1061/(asce)0733-9372(2001)127:1(38)

Van Lier, J., Van Der Zee, F., Frijters, C., and Ersahin, M. (2015). Celebrating 40 years anaerobic sludge bed reactors for industrial wastewater treatment. *Rev. Environ. Sci. Biotechnol.* 14, 681–702. doi: 10.1007/s11157-015-9375-5

Veeresh, G. S., Kumar, P., and Mehrotra, I. (2005). Treatment of phenol and cresols in upflow anaerobic sludge blanket (UASB) process: a review. *Water Res.* 39, 154–170. doi: 10.1016/j.watres.2004.07.028

Wackett, L. P. (1996). Co-metabolism: is the emperor wearing any clothes? *Curr. Opin. Biotechnol.* 7, 321–325. doi: 10.1016/S0958-1669(96)80038-3

Wang, J., Wu, B., Sierra, J. M., He, C., Hu, Z., and Wang, W. (2020). Influence of particle size distribution on anaerobic degradation of phenol and analysis of methanogenic microbial community. *Environ. Sci. Pollut. Res.* 27, 10391–10403. doi: 10.1007/s11356-020-07665-z

Wang, W., Han, H., Yuan, M., and Li, H. (2010). Enhanced anaerobic biodegradability of real coal gasification wastewater with methanol addition. *J. Environ. Sci.* 22, 1868–1874. doi: 10.1016/S1001-0742(09)60327-2

Wang, W., Wu, B., Pan, S., Yang, K., Hu, Z., and Yuan, S. (2017). Performance robustness of the UASB reactors treating saline phenolic wastewater and analysis of microbial community structure. *J. Hazard. Mater.* 331, 21–27. doi: 10.1016/j.jhazmat.2017.02.025

Zhou, G.-M., and Fang, H. H. P. (1997). Co-degradation of phenol and m-cresol in a UASB reactor. *Bioresour. Technol.* 61, 47–52. doi: 10.1016/S0960-8524(97)84698-6 doi: 10.1016/s0960-8524(97)84698-6

Conflict of Interest: The authors declare that the research was conducted in the absence of any commercial or financial relationships that could be construed as a potential conflict of interest.

frontiers in Microbiology

ORIGINAL RESEARCH
published: 11 February 2021
doi: 10.3389/fmicb.2021.619632

Microbial Communities in Flexible Biomethanation of Hydrogen Are Functionally Resilient Upon Starvation

*Washington Logroño, Denny Popp, Marcell Nikolausz, Paul Kluge, Hauke Harms and Sabine Kleinsteuber**

Department of Environmental Microbiology, Helmholtz Centre for Environmental Research – UFZ, Leipzig, Germany

Ex situ biomethanation allows the conversion of hydrogen produced from surplus electricity to methane. The flexibility of the process was recently demonstrated, yet it is unknown how intermittent hydrogen feeding impacts the functionality of the microbial communities. We investigated the effect of starvation events on the hydrogen consumption and methane production rates (MPRs) of two different methanogenic communities that were fed with hydrogen and carbon dioxide. Both communities showed functional resilience in terms of hydrogen consumption and MPRs upon starvation periods of up to 14 days. The origin of the inoculum, community structure and dominant methanogens were decisive for high gas conversion rates. Thus, pre-screening a well performing inoculum is essential to ensure the efficiency of biomethanation systems operating under flexible gas feeding regimes. Our results suggest that the type of the predominant hydrogenotrophic methanogen (here: *Methanobacterium*) is important for an efficient process. We also show that flexible biomethanation of hydrogen and carbon dioxide with complex microbiota is possible while avoiding the accumulation of acetate, which is relevant for practical implementation. In our study, the inoculum from an upflow anaerobic sludge blanket reactor treating wastewater from paper industry performed better compared to the inoculum from a plug flow reactor treating cow manure and corn silage. Therefore, the implementation of the power-to-gas concept in wastewater treatment plants of the paper industry, where biocatalytic biomass is readily available, may be a viable option to reduce the carbon footprint of the paper industry.

Keywords: power-to-gas, biomethane, biogas upgrading, hydrogenotrophic methanogenesis, wastewater treatment, anaerobic digester, intermittent feeding, *Methanobacterium*

OPEN ACCESS

Edited by:
Panagiotis Tsapekos, Technical University of Denmark, Denmark

Reviewed by:
Maria Westerholm, Swedish University of Agricultural Sciences, Sweden
Seung Gu Shin, Pohang University of Science and Technology, South Korea
Mariusz Kuglarz, University of Bielsko-Biała, Poland

***Correspondence:**
Sabine Kleinsteuber
sabine.kleinsteuber@ufz.de

Specialty section:
This article was submitted to Microbiotechnology, a section of the journal Frontiers in Microbiology

Received: *20 October 2020*
Accepted: *14 January 2021*
Published: *11 February 2021*

Citation:
Logroño W, Popp D, Nikolausz M, Kluge P, Harms H and Kleinsteuber S (2021) Microbial Communities in Flexible Biomethanation of Hydrogen Are Functionally Resilient Upon Starvation. Front. Microbiol. 12:619632. doi: 10.3389/fmicb.2021.619632

INTRODUCTION

The growing share of variable renewable energy, mainly photovoltaics and wind power, generates temporary surplus electricity that leads to an energy storage problem. To address this issue, energy storage and flexible energy conversion are required (Strübing et al., 2019). The power-to-gas (P2G) approach is an elegant way to store surplus electricity in the form of a chemical energy carrier that

can be consumed independently of electricity production, e.g., hydrogen or methane (Schiebahn et al., 2015). Hydrogen has various applications as fuel and chemical feedstock or can be stored in the natural gas grid though only up to certain limits (Bailera et al., 2017). Methane has also various applications as fuel or chemical building block, but compared to hydrogen it is more compatible with the existing infrastructure. It is easier to store and to transport due to its higher energy density and can be readily injected into the natural gas grid (Blanco et al., 2018).

The production of methane from surplus electricity is carried out in a two-step process: first hydrogen is produced by water electrolysis (Eq. 1), which is then used in the second step to reduce carbon dioxide to methane (Eq. 2) (Schaaf et al., 2014).

$$4H_2O \rightarrow 2O_2 + 4H_2 \quad (1)$$

$$4H_2 + CO_2 \rightarrow CH_4 + 2H_2O \quad (2)$$

Methanation can be performed by a catalyst-based chemical reaction, known as the Sabatier reaction, or in a microbial process employing the CO_2-reductive pathway of hydrogenotrophic methanogenesis. The latter seems advantageous over the Sabatier reaction in terms of catalyst regeneration and milder process conditions (Angelidaki et al., 2018). *Ex situ* biomethanation is a microbial process that uses point sources of CO_2 or the CO_2 fraction of biogas to produce high quality biomethane. It can be carried out by methanogenic pure cultures (Rittmann et al., 2015) or mixed cultures (Angelidaki et al., 2018). In a recent study comparing different reactor systems, the most efficient reactor produced methane of 98% purity (Kougias et al., 2017). During *ex situ* biomethanation with mixed cultures, volatile fatty acids (VFAs) such as acetate and propionate are produced (Burkhardt and Busch, 2013; Alitalo et al., 2015; Burkhardt et al., 2015, 2019; Rachbauer et al., 2016; Kougias et al., 2017; Savvas et al., 2017; Strübing et al., 2017, 2018; Yun et al., 2017; Ullrich et al., 2018). Acetate can be produced from hydrogen and CO_2 via the Wood–Ljungdahl pathway of acetogenic bacteria (Eq. 3), which competes with hydrogenotrophic methanogenesis for the electron donor and carbon source. However, if acetotrophic methanogens are present in the mixed culture, acetate is eventually converted to methane (Eq. 4) (Angelidaki et al., 2018). Alternatively, acetate can be converted to hydrogen and CO_2 by syntrophic acetate-oxidizing bacteria (SAOB), provided the hydrogen partial pressure is kept sufficiently low due to immediate consumption (Eq. 5). Hence, this reaction relies on the syntrophic cooperation of SAOB with hydrogenotrophic methanogens (Eq. 2) (Hattori, 2008). Acetate is also assimilated by bacteria and archaea to build microbial biomass.

$$4H_2 + 2CO_2 \rightarrow CH_3COOH + 2H_2O \quad (3)$$

$$CH_3COOH \rightarrow CH_4 + CO_2 \quad (4)$$

$$CH_3COO^- + 4H_2O \rightarrow 2HCO_3^- + H^+ + 4H_2 \quad (5)$$

Surplus electricity is fluctuating due to seasonal and diurnal changes; therefore, biomethanation requires a flexible process enduring idle periods without performance loss. Recently, the flexibility of the process was systematically investigated with standby periods of 1–8 days and at temperatures of 25 and 55°C (Strübing et al., 2018, 2019). However, the effect of starvation periods on the microbial communities in *ex situ* biomethanation is yet to be investigated. Here, we studied the impact of fluctuations in gas supply causing intermittent starvation of the hydrogenotrophic community in an *ex situ* biomethanation system. Process parameters, community profiles and changes in microbial diversity upon different starvation periods were analyzed in two methanogenic consortia from different origin. Further, we assessed the effect of the inoculum source on the performance of the biomethanation process and propose a concept to implement the P2G approach for biogas upgrading in wastewater treatment plants.

MATERIALS AND METHODS

Experimental Setup

Mesophilic anaerobic granular sludge from an industrial-scale upflow anaerobic sludge blanket (UASB) reactor treating wastewater from paper industry (designated as WW) was sampled and transported to the laboratory under anoxic conditions. The sludge granules were crushed upon inoculum preparation as described in **Supplementary Text 1**. The second mesophilic inoculum sludge was digestate from a pilot-scale plug-flow reactor digesting cow manure and corn silage (designated as PF). Both inocula were degassed for 5 days at 37°C. Reactor experiments were conducted in four biological replicates under strict anaerobic conditions in serum bottles (219.5 mL) filled with 50 mL of master inoculum mixture (**Supplementary Text 1**). The master inoculum mixtures were prepared with sludge sieved through 400 μm mesh size in mineral medium containing 0.2 g L^{-1} yeast extract. Medium supplemented with such low concentrations of yeast extract is regarded as mineral medium (Stams et al., 1993). The initial pH was set to 9.0 with a sterile anoxic stock solution of 2 M KOH. The bottles were incubated at 37°C. Liquid samples of 5 mL were withdrawn weekly and an equal volume of fresh medium was added. In the beginning the reactors were operated in fed-batch mode (feeding every 24 h, except weekends) with a gas mixture of H_2/CO_2 (4:1) and a total pressure of ∼2.2 bar. In each fed-batch cycle, the gas produced was withdrawn before feeding the gas mixture. Detailed information on flushing and pressurization procedures is given elsewhere (Logroño et al., 2020). The background biogas production from the inoculum was determined by setting up three biological controls with N_2/CO_2 (4:1) in the headspace.

The starvation experiment comprised five phases as illustrated in **Figure 1**: after a regular fed-batch phase with feeding every 24 h over 56 days (phase 1), one fed-batch cycle without shaking lasted 7 days (phase 2), followed by single fed-batch cycles (24 h each) after starvation periods of 7 days (phase 3), 14 days (phase 4), and 21 days (phase 5). The bottles were shaken at 200 rpm except in phase 2 to determine the effect of gas mass transfer limitation. Gas consumption and production rates were

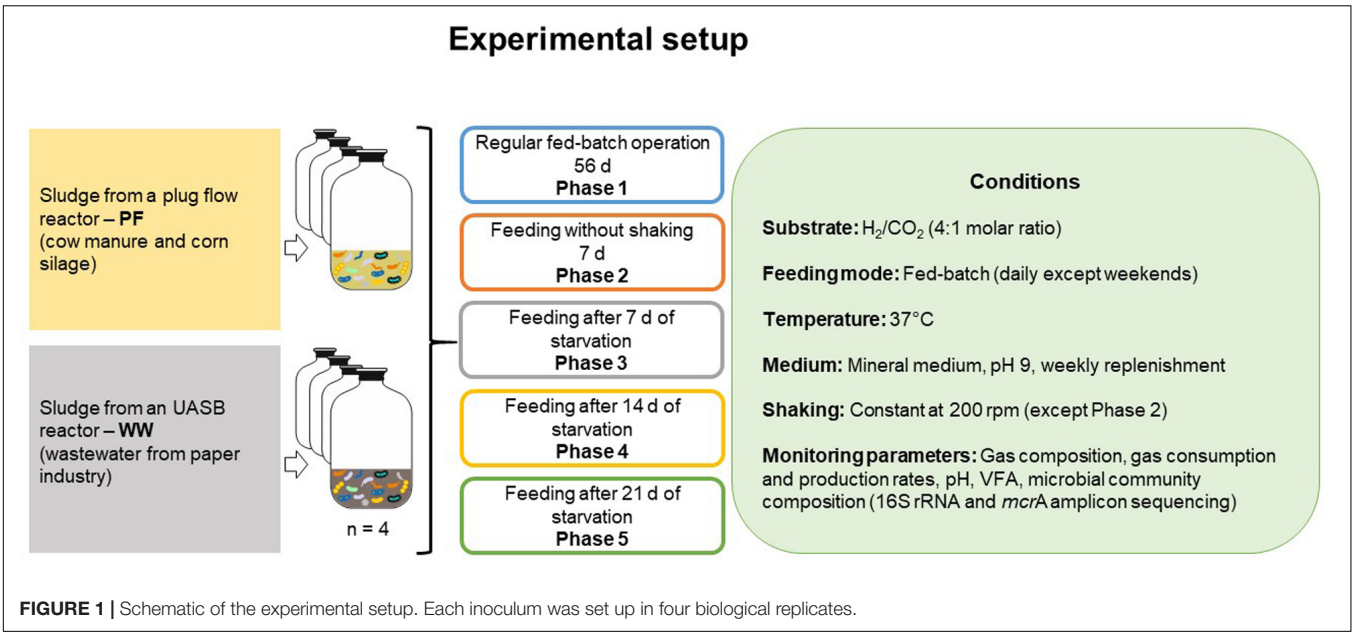

FIGURE 1 | Schematic of the experimental setup. Each inoculum was set up in four biological replicates.

determined at three sampling times during phase 1 (days 7, 21, and 53) and once during each of phases 2–5. Gas amounts are presented in mmol and were calculated as previously described (Logroño et al., 2020). The mean values of gas consumption and production rates in phase 1 were used as a reference for comparison with the other phases. Liquid samples were analyzed at the end of each phase.

Analytical Methods

The pressure was measured with a high resolution manometer (LEO 5, Keller, Switzerland) as described previously (Logroño et al., 2020). The gas composition was analyzed after every batch cycle in 1 mL gas samples via gas chromatography (GC). The pH value of the broth was recorded in 200 μL samples with a mini-pH meter (ISFET pH meter S2K922, ISFETCOM Co., Ltd., Hidaka, Japan). VFA concentrations in the liquid phase were analyzed by high performance liquid chromatography (HPLC). In brief, 1.5 mL samples were withdrawn, centrifuged at 20,817 × *g* and 4°C for 10 min, and subsequently filtered through cellulose acetate membrane filters with a pore size of 0.22 μm (13 mm; LABSOLUTE, Th. Geyer GmbH, Hamburg, Germany) and stored at −20°C if not measured immediately. Detailed information about the GC and HPLC setup was given in our previous study (Logroño et al., 2020).

Microbial Community Analysis

Liquid samples (1.5 mL) were taken at the start of the experiment and at the end of each experimental phase. The samples were centrifuged at 4°C and 20,817 × *g* for 10 min. Genomic DNA from the pellet was extracted with the NucleoSpin Soil kit (MACHEREY-NAGEL GmbH & Co., KG, Germany) using buffer SL2 and enhancer solution as indicated in the manufacturer's protocol. Extracted DNA was stored at −20°C until use. The microbial community composition was analyzed by amplicon sequencing of *mcrA* genes for methanogens and 16S rRNA genes for bacteria.

The V3–V4 region of the 16S rRNA genes was amplified using the primers 341f and 785r (Klindworth et al., 2013). For methanogens, the mlas and mcrA-rev primers were used (Steinberg and Regan, 2008). Amplicon sequencing was performed on the Illumina MiSeq platform using the MiSeq Reagent Kit v3 with 2 × 300 cycles. Bioinformatic analysis was done as described previously (Logroño et al., 2020). In brief, primer sequences were clipped from demultiplexed and adapter-free reads using Cutadapt v1.18 (Martin, 2013), and further sequence analysis was performed with the QIIME2 v2019.1 pipeline (Bolyen et al., 2019) using the dada2 plugin (Callahan et al., 2016). The resulting amplicon sequencing variants (ASVs) for 16S rRNA genes were classified against the MiDAS database v2.1 (McIlroy et al., 2017) trimmed to the region covered by the 341f and 785r primers. Archaeal 16S rRNA reads were removed from the dataset and bacterial read counts were normalized to 100%. For *mcrA* ASVs, a taxonomy database compiled by using *mcrA* sequences from the RDP FunGene database (Fish et al., 2013) was used.

Microbial Community Ecological Indices

Amplicon sequencing variant data was used to calculate indices quantifying α-diversity as described by Lucas et al. (2017). Briefly, the Shannon index (H) describes the uncertainty to predict the identity of an unknown individual randomly chosen from a community (Eq. 6), richness (R) reflects the number of present types regardless of their particular relative abundances (Eq. 7), diversity of order one (^{1}D) quantifies the community diversity by weighting all present types according to their particular abundances (Eq. 8), diversity of order two (^{2}D) quantifies the community diversity by weighting the most common types significantly more than the rare types (Eq. 9), evenness of order

one (^{1}E) reflects the abundance heterogeneity of the types in a community (Eq. 10).

$$H = -\sum_{i=1}^{R} p_i \ln p_i \quad (6)$$

$$^0D = \sum_{i=1}^{R} p_i^0 = R \quad (7)$$

$$^1D = \exp(H) \quad (8)$$

$$^2D = 1 \Big/ \left(\sum_{i=1}^{R} p_i^2\right) \quad (9)$$

$$^1E = {}^1D/R = \exp(H)/R \quad (10)$$

To quantify the β-diversity, the microbial community composition data was subjected to principal coordinate analysis (PCoA) based on Bray–Curtis distances using the phyloseq package (Bolyen et al., 2019) version 1.30.0. PCoA was plotted using the ggplot2 package (Wickham, 2016) version 3.2.1.

Statistical Analysis

Differences between phases were studied by analysis of variance (ANOVA). Tukey's *post-hoc* test was used for multiple comparisons and significant differences were denoted * when $p < 0.05$ [$p > 0.05$ (ns: not significant), $p < 0.05$ (*), $p < 0.01$ (**), $p < 0.001$ (***), and $p < 0.0001$ (****)]. Analysis of similarities (ANOSIM) was used to test if the intra-community variation could be explained by the experimental phases and calculated in R (R Core Team, 2019) version 3.6.1 using the Vegan package (Oksanen et al., 2019). Ecological indices were compared between phases with ANOVA and Tukey's *post-hoc* test as aforementioned. Graphpad (Graphpad Software, Inc., San Diego, CA, United States) or Microsoft Excel were used to compute the data.

RESULTS AND DISCUSSION

Effects of Starvation on the Process Performance

After the first feeding, the production of CH_4 from H_2/CO_2 in reactors WW was three times faster than that in PF, as the gaseous substrate was depleted after 24 and 72 h, respectively. Thereafter, all cultures converted the gaseous substrate within ∼24 h in a stable manner for 56 days during phase 1 (**Figure 2** and **Supplementary Figure 1**). Previous studies have also reported complete gas conversion within 24 h (Kern et al., 2016; Logroño et al., 2020).

In phase 1, the mean gas consumption (H_2 and CO_2) and production (CH_4) rates of WW were significantly higher than those of PF (**Table 1**) although the methane content was comparable for both inocula. When shaking was omitted in phase 2, all cultures suffered from gas mass transfer limitations as reflected by extremely low gas consumption and production rates (**Table 1**). In case of PF, the H_2 consumption rate in phase 3 and 5 were 2 and 11% lower than in phase 1. Similarly for WW, the H_2 conversion rate in phase 3 and 5 were 5 and 11% lower than in phase 1. Interestingly, the highest H_2 consumption rates were observed in phase 4 for both WW and PF (after 14 days of starvation) (**Table 1**). The trends of consumption and production rates in phases 2–5 are shown in **Figure 3**.

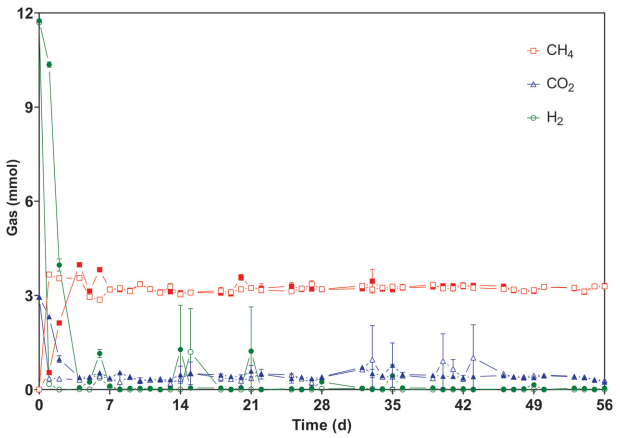

FIGURE 2 | Time course of consumed and produced gases during regular fed-batch operation (phase 1). The bottles were fed every 24 h (except weekends) and measurements were carried out at the end of each batch cycle. Open symbols: reactors WW (inoculated with anaerobic granular sludge from an industrial-scale UASB reactor treating wastewater from paper industry); filled symbols: reactors PF (inoculated with digestate from a pilot-scale plug flow reactor digesting cow manure and corn silage). The mean and standard deviation of $n = 4$ are depicted. Invisible error bars are smaller than the symbol.

Comparing the methane production rates (MPRs) in phase 1 (regular fed-batch) to those in phase 3 (7 days of starvation), phase 4 (14 days of starvation), and phase 5 (21 days of starvation) showed that both communities responded in a similar way (**Table 1**). The rates in phase 1 were significantly higher than those in phase 3 and 5. No differences in MPR between phase 1 and 4 (14 days of starvation) were observed, suggesting functional resilience of the microbiota. However, the MPR in phase 5 (21 days of starvation) was significantly lower than in phase 1, which may reflect the limits of resilience.

The pH values decreased from 9 to ∼8.3 in all cultures (**Table 1**). Previous studies where the pH was not controlled and the initial experimental pH was lower than in our study have also shown that the system stabilized to similar pH values (8–8.5) after H_2/CO_2 feeding (Bassani et al., 2017; Kougias et al., 2017; Logroño et al., 2020). When comparing the phase of regular feeding (phase 1) to the other phases, the two communities revealed a different behavior. In case of PF, the pH values in phases 2–5 were significantly lower than in phase 1 (**Table 1**). With WW, the pH did not drop significantly over phases 1–4 but the pH in phase 5 was significantly lower than in phase 1 (**Table 1**). Recently it was reported that pH variations change the energy yields of redox reactions under anoxic conditions (here: methanogenesis) and thereby can influence the structure and function of microbial communities (Jin and Kirk, 2018).

TABLE 1 | Summary of process performance during different experimental phases.

Inoculum	Phase	pH	CH_4 (%)	H_2 (mmol L^{-1} h^{-1})	CO_2 (mmol L^{-1} h^{-1})	CH_4 (mmol L^{-1} h^{-1})	H_2 consumption efficiency (%)
WW	Start	9.02 ± 0.00	–	–	–	–	–
	1 (56 days)	8.29 ± 0.03	97.56 ± 0.21[a]	25.02 ± 0.28[b] (****)	5.81 ± 0.08[b] (*)	6.73 ± 0.09[b] (*)	98.3 ± 10.3
	2 (7 days)	8.36 ± 0.04	91.66 ± 5.10	1.56 ± 0.03 (****)	0.38 ± 0.00 (****)	0.50 ± 0.01 (****)	98.3 ± 1.8
	3 (7 days)	8.18 ± 0.03	88.53 ± 0.58	23.83 ± 0.48 (****)	5.21 ± 0.14 (****)	6.34 ± 0.29 (**)	100.0 ± 0.0
	4 (14 days)	8.18 ± 0.03	88.80 ± 0.96	25.91 ± 0.34 (**)	5.54 ± 0.03 (**)	6.65 ± 0.15	100.0 ± 0.0
	5 (21 days)	8.08 ± 0.03 (*)	91.93 ± 0.71	22.26 ± 0.30 (****)	5.06 ± 0.10 (****)	5.83 ± 0.11 (****)	100.0 ± 0.0
PF	Start	9.00 ± 0.00	–	–	–	–	–
	1 (56 days)	8.39 ± 0.04	96.57 ± 0.23[a]	23.46 ± 0.20	5.61 ± 0.06	6.42 ± 0.05	97.6 ± 11.6
	2 (7 days)	8.06 ± 0.22 (****)	44.81 ± 3.57	1.20 ± 0.06 (****)	0.31 ± 0.01 (****)	0.34 ± 0.02 (****)	77.6 ± 2.7
	3 (7 days)	8.12 ± 0.10 (**)	87.79 ± 1.54	23.02 ± 0.23	4.96 ± 0.06 (****)	5.21 ± 0.14 (***)	99.7 ± 0.5
	4 (14 days)	8.00 ± 0.06 (****)	88.66 ± 1.28	25.09 ± 0.06 (****)	5.41 ± 0.10 (*)	6.39 ± 0.07	100.0 ± 0.0
	5 (21 days)	8.17 ± 0.04 (*)	91.69 ± 0.91	20.94 ± 0.24 (****)	4.78 ± 0.10 (****)	5.35 ± 0.10 (****)	100.0 ± 0.1

ND: not detected.
*The mean and standard deviation of n = 4 are given. Significant differences between phase 1 and other phases are indicated with * ($p < 0.05$), ** ($p < 0.01$), *** ($p < 0.001$) or **** ($p < 0.0001$) considering n = 4.*
[a]*The highest methane concentration in phase 1 is presented. The values of the other parameters were determined at the end of each phase.*
[b]*Comparison between the rates of WW and PF in phase 1 (regular fed-batch).*

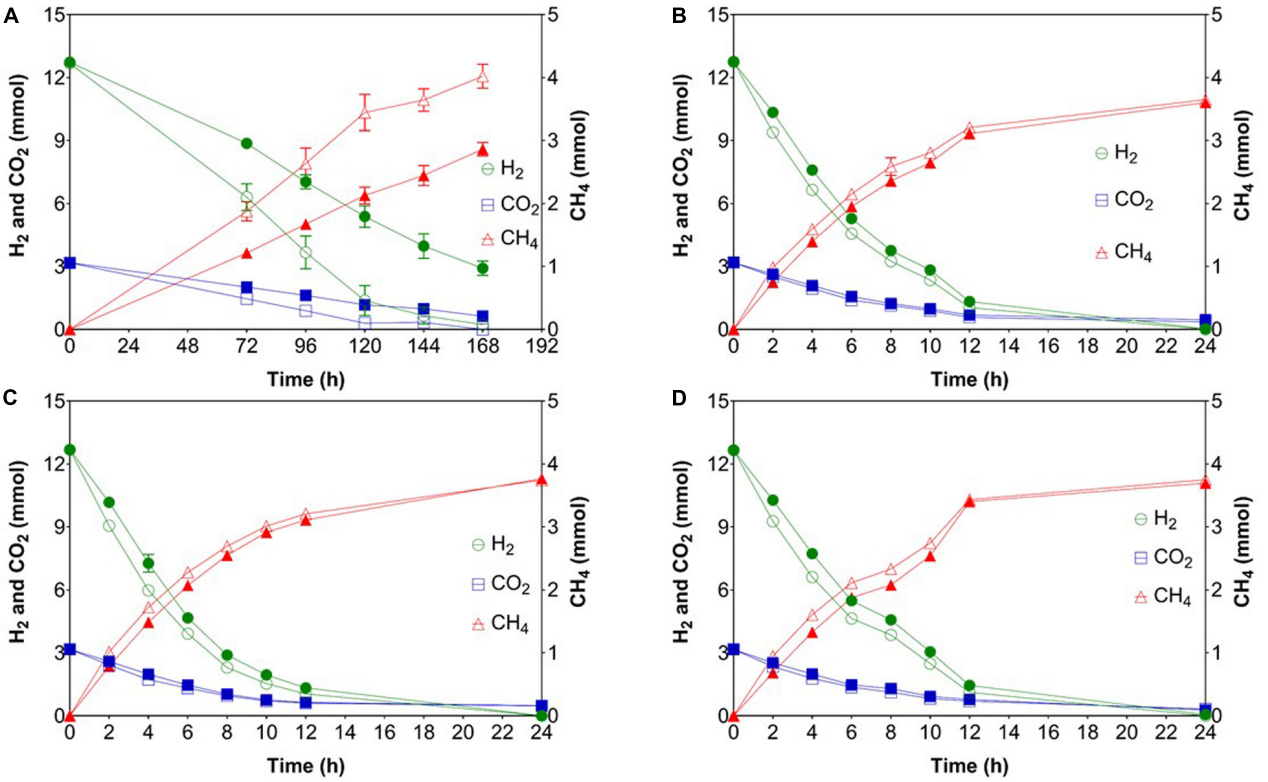

FIGURE 3 | Gas consumption (H_2 and CO_2) and production (CH_4) rates after starvation events. **(A)** Phase 2 (feeding without shaking), **(B)** phase 3 (after 7 days of starvation), **(C)** phase 4 (after 14 days of starvation), **(D)** phase 5 (after 21 days of starvation). Open symbols: reactors WW (inoculated with anaerobic granular sludge from an industrial-scale UASB reactor treating wastewater from paper industry); filled symbols: reactors PF (inoculated with digestate from a pilot-scale plug flow reactor digesting cow manure and corn silage). The mean and standard deviation of *n* = 4 are depicted.

Contrary to previous findings where acetate and propionate were produced (Savvas et al., 2017; Strübing et al., 2018), only traces of VFAs (below 10 mg L^{-1}) were detected in our experiments despite using complex microbiota. Several explanations for this observation are conceivable: Either homoacetogens could not compete with hydrogenotrophic

methanogens for H_2 and thus only low amounts of acetate were produced, or acetate produced by homoacetogens during sufficiently high H_2 levels was readily converted to CH_4 by acetotrophic methanogens, or by SAOB when the H_2 partial pressure was sufficiently low. The H_2 consumption efficiency was ∼100% in all phases except for PF in phase 2, when gas mass transfer limitation was reflected by the lowest H_2 consumption rates (**Table 1** and **Figure 3**). Such high H_2 consumption efficiency is consistent with the findings reported earlier (Strübing et al., 2018).

Effects of Starvation on the Microbial Community Diversity

The rarefaction curves from amplicon sequencing analysis of *mcr*A and 16S rRNA genes indicated that sufficient sequencing depth was reached in all samples (**Supplementary Figure 2**). To evaluate the α-diversity in the single phases of each community, we calculated the diversity and evenness of order one (**Figure 4**). ANOVA revealed significant differences in both indices for both bacteria and methanogens.

The methanogenic community from the start phase of the WW inoculum was significantly more diverse than that from the PF inoculum ($p < 0.0001$) (**Figure 4A**). Feeding stoichiometric H_2:CO_2 ratio required for hydrogenotrophic methanogenesis led to a significant decrease in diversity, which is evident when comparing the start phase to the other phases in both inocula. However, it is to note that even after starvation events no significant diversity changes in the methanogenic and bacterial communities were found when comparing phase 1 to the other phases. In the start phase, evenness of the WW methanogenic community was significantly higher ($p = 0.0345$) than that of the PF methanogenic community (**Figure 4B**). Evenness significantly decreased for WW when comparing the start phase to the other

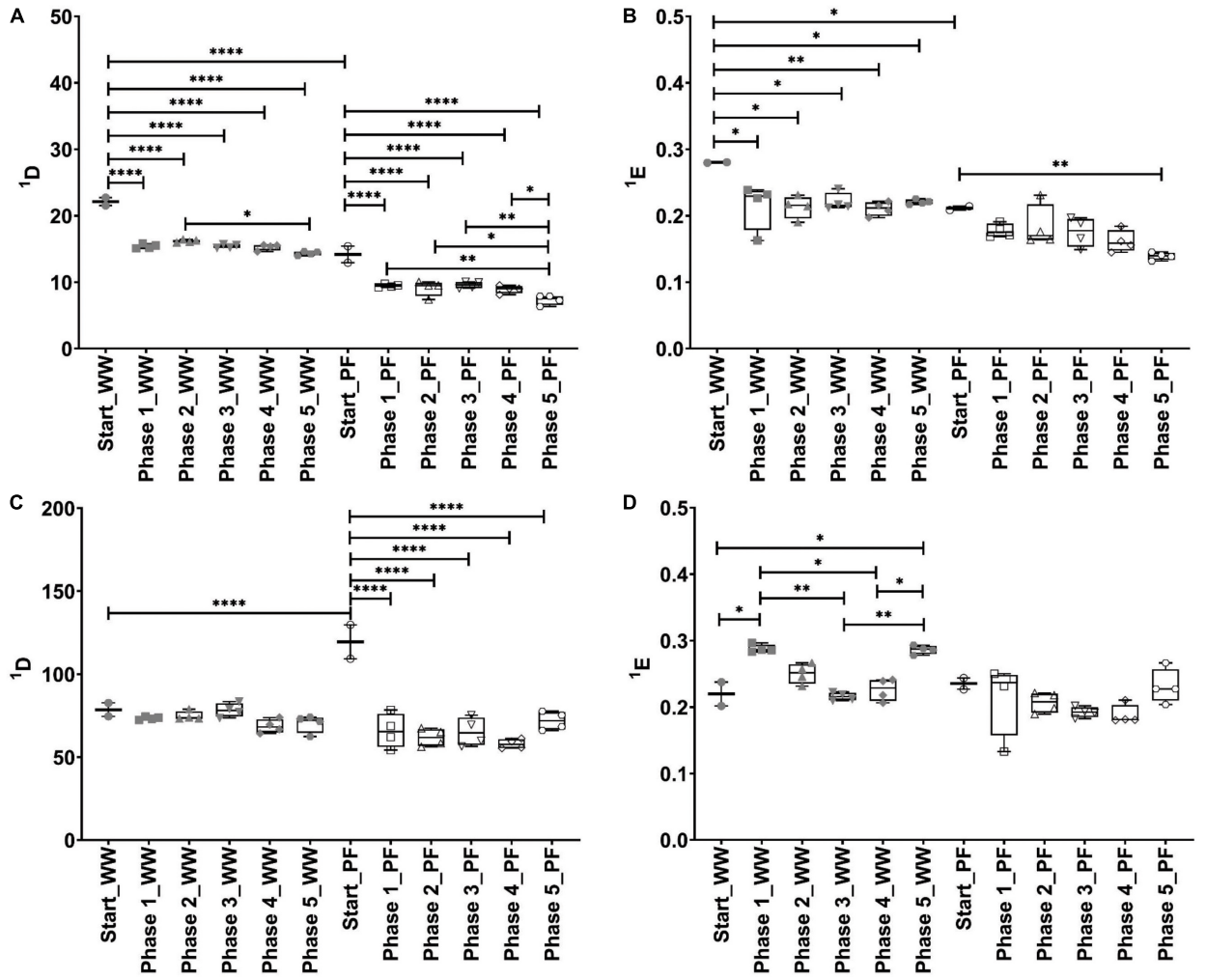

FIGURE 4 | Box plots of diversity **(A,C)** and evenness **(B,D)** for $q = 1$ in different phases. Methanogenic communities **(A,B)** and bacterial communities **(C,D)**. Significant differences between groups are indicated with * when $p < 0.05$, ** when $p < 0.01$, and **** when $p < 0.0001$. Note that for start $n = 2$ whereas for phases 1 to 5 $n = 4$. WW: reactors inoculated with anaerobic granular sludge from an industrial-scale UASB reactor treating wastewater from paper industry; PF: reactors inoculated with digestate from a pilot-scale plug-flow reactor digesting cow manure and corn silage.

phases but significant differences for PF were only observed between start and phase 5 ($p = 0.0026$). Additional α-diversity indices such as H, R, and ^{2}D of the methanogenic community are presented in **Supplementary Figures 3A–C**.

Comparing diversity of order one (^{1}D) from the start phase of WW and PF indicated that the bacterial community of PF was significantly more diverse than that of the WW inoculum ($p < 0.0001$) (**Figure 4C**). These differences can be explained by the low abundant taxa rather than the most abundant ones since diversity of order two (^{2}D) was not different between the start phases of the WW and PF inocula (**Supplementary Figure 3F**). Furthermore, ^{1}D remained unchanged for WW but it significantly decreased for PF when comparing the start phase to the other phases. **Figure 4D** shows that evenness of the bacterial communities was comparable for both inocula in the start phase. Evenness of the WW bacterial community was significantly higher than that of the PF bacterial community in phase 1 and 5 but not in the other phases. Other α-diversity indices (H, R, and ^{2}D) of the bacterial community are presented in **Supplementary Figures 3D–F**.

The functional resilience, i.e., the ability of microbial communities to return to a stable process state after a disturbance, was evaluated in terms of MPR. MPRs in phase 3 and 5 were significantly lower than in phase 1 for both inocula, indicating that sudden and extended disturbances result in a decreased performance, which is explained by lower resilience of the microbial communities. Considering that the MPR of WW was higher than that of PF (**Table 1**) even after starvation events, it can be hypothesized that this is linked to the type of hydrogenotrophic methanogens present in the community. By comparing diversity ^{2}D (which gives more weight to the most abundant taxa) between inocula for each independent phase we found that the diversity of the WW methanogenic community was significantly higher than that of the PF methanogenic community (**Supplementary Figure 3C**; $p < 0.0001$ for all comparisons). Therefore, it appears that the diversity of methanogens may play a role in coping with disturbances since the more diverse community (WW) was more functionally resilient than PF. A recent study by Figeac et al. (2020) evaluated the effect of temperature and origin of the inoculum on the performance and stability of *ex situ* biomethanation with mixed cultures. Although MPR of the thermophilic process was higher, the instability of the process increased along with temperature due to the unique dominance of *Methanothermobacter*.

Effects of Starvation on the Microbial Community Structure

The relative abundance of various methanogens throughout the experiment is presented in **Figure 5**. Hydrogenotrophic methanogenesis was the main pathway in the WW reactors as hydrogenotrophic genera dominated the methanogenic community with ∼62%. The most dominant genera in the WW inoculum were *Methanobacterium* (53%) followed by *Methanothrix* (36%), which suggests that also acetotrophic methanogenesis was active in this inoculum. In contrast, acetotrophic methanogenesis was the main pathway in the PF inoculum as *Methanothrix* (42%) was most dominant together with the versatile genus *Methanosarcina* (9%), which together summed up to more than 50% of all methanogens. In PF, *Methanoculleus* (27%) was the predominant hydrogenotrophic genus together with *Methanobacterium* (17%), whereas *Methanoculleus* (<1%) was underrepresented in WW. H_2/CO_2 fed-batch feeding favored *Methanobacterium* in all experimental phases with mean relative abundances of 93 and 77% in WW and PF, respectively. Other hydrogenotrophic methanogens (*Methanolinea*, *Methanospirillum*, and *Methanoculleus*) were strongly outcompeted by *Methanobacterium* in case of WW. The situation was different for PF where two hydrogenotrophic genera (*Methanobacterium* and *Methanoculleus*) dominated from the beginning and stayed predominant throughout the experiment, even though *Methanobacterium* was favored as well over *Methanoculleus*. The versatile genus *Methanosarcina* was outcompeted by strict hydrogenotrophic methanogens in PF likely due to its lower H_2 uptake rate (Feist et al., 2006; Goyal et al., 2015). However, *Methanosarcina* was still present in both communities until the end of the experiment at very low relative abundance. Our results are consistent with previous studies on H_2 biomethanation reporting the dominance of *Methanobacteriales* (Kougias et al., 2017; Rachbauer et al., 2017; Savvas et al., 2017). This indicates that methanogens affiliated to the *Methanobacteriales* have a selective advantage over other hydrogenotrophic methanogens in *ex situ* biomethanation. The relative abundance of *Methanothrix* decreased drastically in the end of phase 1 and then remained fairly stable in both communities. The persistence of this obligate acetotrophic throughout the entire experiment is remarkable considering the simple substrate (H_2/CO_2) supply and suggests homoacetogenesis as a competing hydrogenotrophic reaction. *Methanothrix* decreased in abundance from 36 to 5% and from 42% to less than 1% in WW and PF, respectively. Although the relative abundance was low, its presence could explain the low acetate concentrations (**Table 1**). The better performance of WW over PF may be explained by the fact that *Methanobacterium* was dominant initially and throughout the experiment. Hence, selecting an inoculum dominated by *Methanobacteriales* could be advantageous from the application point of view.

Regarding the bacterial community, WW and PF presented distinct community structures that reflected the origin of the inocula (**Supplementary Figure 4**). The most abundant genera at the start were T78 (*Chloroflexi*) (9 ± 4%) in WW and *Fastidiosipila* (16 ± 5%) in PF. *Petrimonas* was underrepresented in the inocula (<1%) but increased in relative abundance after H_2/CO_2 feeding in both communities and remained at comparable levels of around 11% throughout phases 1–5 for WW and PF. *Petrimonas* and *Fastidiosipila*, the latter being dominant throughout all phases in PF, were also found in enrichment cultures fed with H_2/CO_2 under similar operating conditions (mode of feeding and mineral medium) (Logroño et al., 2020). So far there are no species described as autotroph for the two aforementioned genera but their enrichment suggests a specific ecological niche in systems fed with H_2/CO_2. Further investigations, e.g., isolation or metagenomics, are needed to

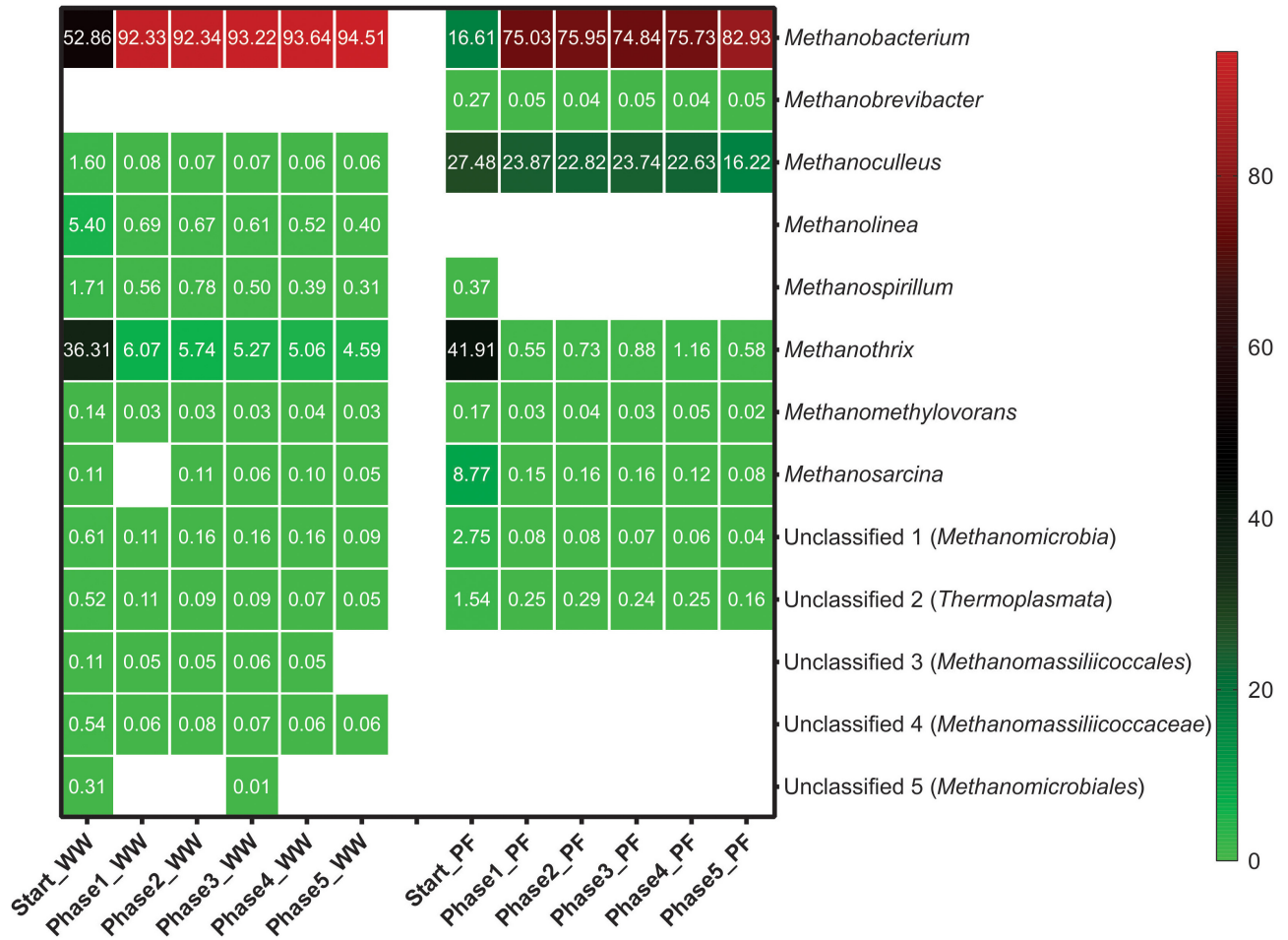

FIGURE 5 | Methanogenic community structure based on *mcr*A gene amplicon sequencing in different phases at genus level. Taxa with relative abundances less than 0.1% were filtered out. Numbers represent the relative abundance in percent and blank space indicates the absence of the respective taxon. Mean values of three biological replicates are presented for Start whereas four biological replicates were averaged for phase 1–5. WW: reactors (inoculated with anaerobic granular sludge from an industrial-scale UASB reactor treating wastewater from paper industry) and PF: reactors (inoculated with digestate from a pilot-scale plug-flow reactor digesting cow manure and corn silage).

elucidate their function. When analyzing the top 25 genera, only four genera were shared between WW and PF of which three were unclassified (**Supplementary Figure 4**). A recent meta-omics study on the genus *Petrimonas* revealed its function in sugar and amino acid fermentation pathways and its widespread occurrence in biogas reactors, particularly in biogas plants with process disorders (Maus et al., 2020). The dominance of this genus in the WW and PF communities might be related to microbial biomass turnover under stress conditions such as substrate shift in phase 1 and starvation in phases 2–5.

At the family level (**Supplementary Figure 5**), *Anaerolineaceae* (21 ± 3%) in WW and *Ruminococcaceae* (24 ± 4%) in PF dominated at the start. Throughout phases 1–5, *Porphyromonadaceae* remained at comparably high relative abundance in both communities. After H_2/CO_2 feeding, families with relative abundances of ≥5% were *Porphyromonadaceae*, *Synergistaceae*, *Anaerolineaceae*, and *Thermotogaceae* in WW, whereas PF was dominated by the families *Porphyromonadaceae*, *Ruminococcaceae*, Unclassified family 5 (*Cloacimonetes*), *Caldicoprobacteraceae*, and MBA03 (*Firmicutes*). The slight production of acetate might be attributed to the presence of *Thermoanaerobacteraceae* (>2%), a family that comprises acetogens (Bengelsdorf et al., 2018). Comparable relative abundances in WW and PF (phase 1–5) were observed. This observation is in accordance with our previous findings (Logroño et al., 2020).

Effects of Starvation on the Microbial Community Dynamics

Principal coordinate analysis of the Bray–Curtis distances between the communities in different phases and from different inocula revealed that the WW samples clustered distinct from PF samples but community specialization toward hydrogenotrophic metabolism was evident after H_2/CO_2 feeding (**Figure 6**). The distinct clustering of the communities can be explained by the

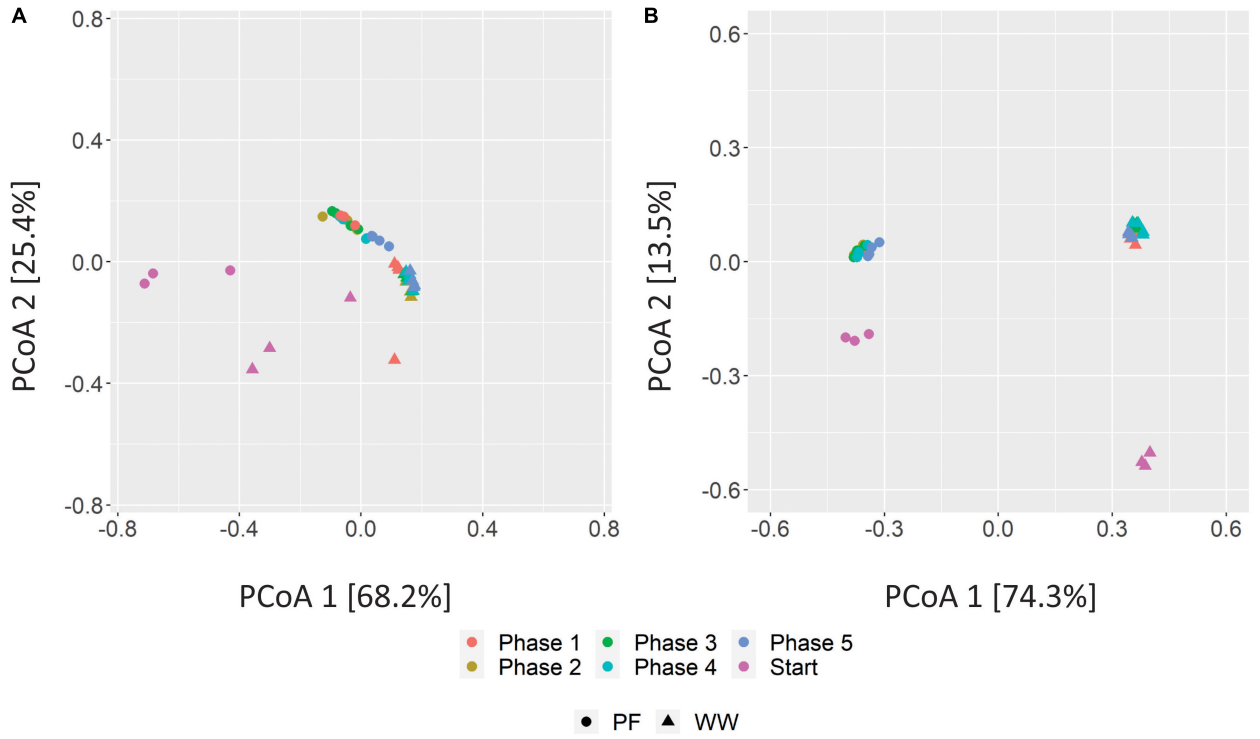

FIGURE 6 | PCoA plots of Bray–Curtis distances of methanogenic **(A)** and bacterial **(B)** communities based on amplicon sequencing of *mcr*A and 16 rRNA genes. Three biological replicates are presented for sludge inoculum (Start) whereas four biological replicates are presented for end of regular fed-batch (phase 1), feeding without shaking (phase 2), and feeding after 7 days (phase 3), 14 days (phase 4) and 21 days (phase 5) of starvation. WW: anaerobic granular sludge from an industrial-scale UASB reactor treating wastewater from paper industry; PF: digestate from a pilot-scale plug-flow reactor digesting cow manure and corn silage.

different substrates each sludge was originally digesting and likely by the different reactor configuration (UASB vs. plug-flow reactor) as suggested earlier (Mcateer et al., 2020) as well as different operational parameters leading to different process conditions. While the methanogenic communities converged over the phases to one cluster of similar communities for both WW and PF (**Figure 6A**), the bacterial communities stayed distinct for WW and PF but showed the same trend of community dynamics, reflecting the enrichment of different hydrogenotrophic communities (**Figure 6B**). In contrast to the strong community shifts caused by H_2/CO_2 feeding, the communities did not change much over the phases 1–5. A more detailed PCoA of these samples excluding the start samples is shown in **Supplementary Figure 6**.

Implications for P2G Applications in Industrial Wastewater Treatment

The results indicated that the WW inoculum led to the enrichment of the best performing community, which was most resilient to starvation disturbances, had the highest hydrogen consumption and methane production rates, and was dominated by hydrogenotrophic methanogens of the genus *Methanobacterium*. Admittedly, considerable differences in terms of hydrogen consumption and methane production rates were only observed in the beginning of phase 1 (**Figure 2** and **Supplementary Figure 1**), which indicates that hydrogenotrophs were more active in WW than in PF from the beginning, in agreement with the dominance of *Methanobacterium* in the WW inoculum. However, the WW community could also better cope with mass transfer limitations (phase 2) and performed slightly better after starvation periods (phases 3–5) as visible in **Figure 3**. The relative abundance of *Methanobacterium* increased in both communities after repeated starvation periods, which suggests that this genus could endure starvation and ensure efficient biomethanation better than other hydrogenotrophs. On the long run, the PF community might have adapted as reflected by the increasing share of *Methanobacterium*, but the WW inoculum originating from an UASB reactor treating wastewater from paper industry was immediately ready for efficient and resilient biomethanation. Considering the case scenario of a wastewater treatment plant in paper industry that produces biogas and performs biogas upgrading, we propose that biological *ex situ* biomethanation could be easily implemented due to the fact that biocatalytic biomass (granular sludge from an UASB reactor) is readily available from the wastewater treatment process, the reactor infrastructure may be available and oxygen resulting from water electrolysis could be used on site for improving the aerobic treatment step. The approach (**Figure 7**) could be implemented as *in situ* (partial biogas upgrading through hydrogen injection in the main anaerobic digester), *ex situ* (converting the CO_2 fraction of the biogas in facilities

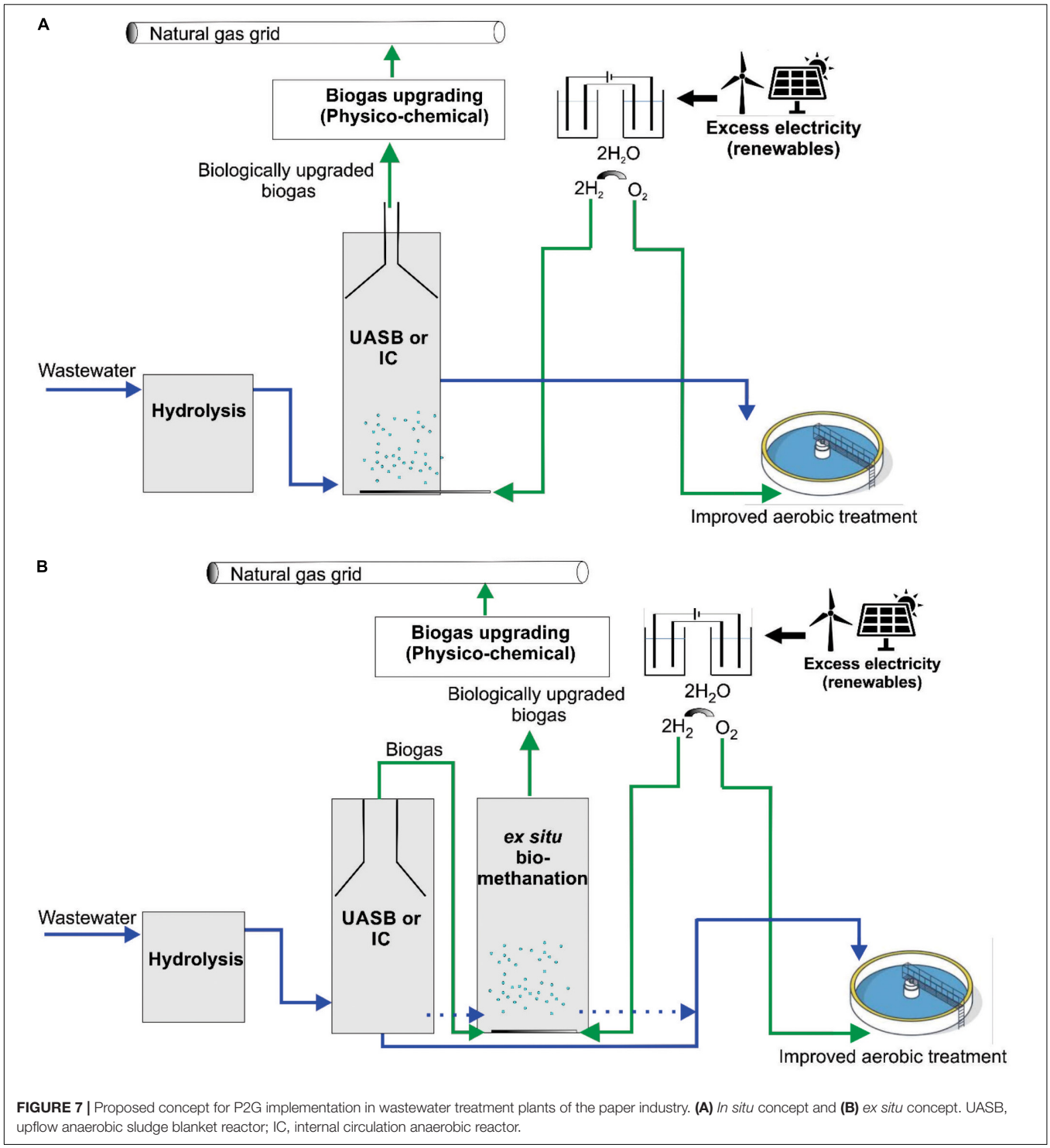

FIGURE 7 | Proposed concept for P2G implementation in wastewater treatment plants of the paper industry. **(A)** *In situ* concept and **(B)** *ex situ* concept. UASB, upflow anaerobic sludge blanket reactor; IC, internal circulation anaerobic reactor.

where physical or chemical biogas upgrading is already in operation) or hybrid approach, where the two aforementioned concepts are combined.

This study shows the effect of starvation on the hydrogen consumption and methane production rates and the microbial community changes in two different inocula that were fed with hydrogen and carbon dioxide. We found that microbial communities are functionally resilient upon starvation disturbances in flexible biomethanation of hydrogen, although long-term effects of repeated or prolonged starvation periods need to be studied in future studies with more replicates and controls. Our results suggest that type and origin of the inoculum, community structure and dominant methanogens are important for process performance. Pre-screening a well

performing inoculum is thus essential for functional resilience of flexible biomethanation. It appears that the dominance of the genus *Methanobacterium* was decisive for an efficient *ex situ* biomethanation process since the highest hydrogen consumption rates were observed for the inoculum with this property. We also demonstrated that it is possible to perform H_2/CO_2 biomethanation with complex microbiota while avoiding VFA accumulation, which is a relevant aspect for practical implementation. The implementation of the P2G concept in wastewater treatment plants of the paper industry, where biocatalytic biomass is readily available, could be a viable option to reduce the carbon footprint of the paper industry.

DATA AVAILABILITY STATEMENT

Demultiplexed raw sequence data were submitted to the NCBI Sequence Read Archive (SRA) (http://www.ncbi.nlm.nih.gov/Traces/sra/). The dataset for this study can be found under the study accession number PRJNA623376.

AUTHOR CONTRIBUTIONS

WL designed the experiments, analyzed the data, and drafted the manuscript. PK and WL conducted the experiments. DP contributed to the bioinformatic analysis, discussion of the results, and revision of the manuscript. SK and MN contributed to the experimental design, supervised the study, critically discussed the results, and revised the manuscript. HH contributed to the discussion of the results and revision of the manuscript. All authors have read and approved the final manuscript.

FUNDING

This research was funded by the Helmholtz Association (Research Program Renewable Energies).

ACKNOWLEDGMENTS

Ute Lohse is duly acknowledged for technical assistance in library preparation for MiSeq amplicon sequencing. Cloud computing facilities used for the analysis of sequencing data were provided by the BMBF-funded de.NBI Cloud within the German Network for Bioinformatics Infrastructure (de.NBI) (031A537B, 031A533A, 031A538A, 031A533B, 031A535A, 031A537C, 031A534A, and 031A532B).

SUPPLEMENTARY MATERIAL

The Supplementary Material for this article can be found online at: https://www.frontiersin.org/articles/10.3389/fmicb.2021.619632/full#supplementary-material

REFERENCES

Alitalo, A., Niskanen, M., and Aura, E. (2015). Biocatalytic methanation of hydrogen and carbon dioxide in a fixed bed bioreactor. *Bioresour. Technol.* 196, 600–605. doi: 10.1016/j.biortech.2015.08.021

Angelidaki, I., Treu, L., Tsapekos, P., Luo, G., Campanaro, S., Wenzel, H., et al. (2018). Biogas upgrading and utilization: current status and perspectives. *Biotechnol. Adv.* 36, 452–466. doi: 10.1016/j.biotechadv.2018.01.011

Bailera, M., Lisbona, P., Romeo, L. M., and Espatolero, S. (2017). Power to gas projects review: lab, pilot and demo plants for storing renewable energy and CO_2. *Renew. Sustain. Energy Rev.* 69, 292–312. doi: 10.1016/j.rser.2016.11.130

Bassani, I., Kougias, P. G., Treu, L., Porté, H., Campanaro, S., and Angelidaki, I. (2017). Optimization of hydrogen dispersion in thermophilic up-flow reactors for ex situ biogas upgrading. *Bioresour. Technol.* 234, 310–319. doi: 10.1016/j.biortech.2017.03.055

Bengelsdorf, F. R., Beck, M. H., Erz, C., Hoffmeister, S., Karl, M. M., Riegler, P., et al. (2018). Bacterial anaerobic synthesis gas (syngas) and $CO_2 + H_2$ fermentation. *Adv. Appl. Microbiol.* 103, 143–221. doi: 10.1016/bs.aambs.2018.01.002

Blanco, H., Nijs, W., Ruf, J., and Faaij, A. (2018). Potential of power-to-methane in the EU energy transition to a low carbon system using cost optimization. *Appl. Energy* 232, 323–340. doi: 10.1016/j.apenergy.2018.08.027

Bolyen, E., Rideout, J. R., Dillon, M. R., Bokulich, N. A., Abnet, C. C., Al-Ghalith, G. A., et al. (2019). Reproducible, interactive, scalable and extensible microbiome data science using QIIME 2. *Nat. Biotechnol.* 37, 852–857. doi: 10.1038/s41587-019-0209-9

Burkhardt, M., and Busch, G. (2013). Methanation of hydrogen and carbon dioxide. *Appl. Energy* 111, 74–79. doi: 10.1016/j.apenergy.2013.04.080

Burkhardt, M., Jordan, I., Heinrich, S., Behrens, J., Ziesche, A., and Busch, G. (2019). Long term and demand-oriented biocatalytic synthesis of highly concentrated methane in a trickle bed reactor. *Appl. Energy* 240, 818–826. doi: 10.1016/j.apenergy.2019.02.076

Burkhardt, M., Koschack, T., and Busch, G. (2015). Biocatalytic methanation of hydrogen and carbon dioxide in an anaerobic three-phase system. *Bioresour. Technol.* 178, 330–333. doi: 10.1016/j.biortech.2014.08.023

Callahan, B. J., McMurdie, P. J., Rosen, M. J., Han, A. W., Johnson, A. J. A., and Holmes, S. P. (2016). DADA2: high-resolution sample inference from Illumina amplicon data. *Nat. Methods* 13, 581–583. doi: 10.1038/nmeth.3869

Feist, A. M., Scholten, J. C. M., Palsson, B., Brockman, F. J., and Ideker, T. (2006). Modeling methanogenesis with a genome-scale metabolic reconstruction of *Methanosarcina barkeri*. *Mol. Syst. Biol.* 2, 1–14. doi: 10.1038/msb4100046

Figeac, N., Trably, E., Bernet, N., Delgenès, J.-P., and Escudié, R. (2020). Temperature and inoculum origin influence the performance of ex-situ biological hydrogen methanation. *Molecules* 25:5665. doi: 10.3390/molecules25235665

Fish, J. A., Chai, B., Wang, Q., Sun, Y., Brown, C. T., Tiedje, J. M., et al. (2013). FunGene: the functional gene pipeline and repository. *Front. Microbiol.* 4:291. doi: 10.3389/fmicb.2013.00291

Goyal, N., Padhiary, M., Karimi, I. A., and Zhou, Z. (2015). Flux measurements and maintenance energy for carbon dioxide utilization by *Methanococcus maripaludis*. *Microb. Cell Fact.* 14, 1–9. doi: 10.1186/s12934-015-0336-z

Hattori, S. (2008). Syntrophic acetate-oxidizing microbes in methanogenic environments. *Microb. Environ.* 23, 118–127. doi: 10.1264/jsme2.23.118

Jin, Q., and Kirk, M. F. (2018). pH as a primary control in environmental microbiology: 1. Thermodynamic perspective. *Front. Microbiol.* 6:21. doi: 10.3389/fenvs.2018.00021

Kern, T., Theiss, J., Röske, K., and Rother, M. (2016). Assessment of hydrogen metabolism in commercial anaerobic digesters. *Appl. Microbiol. Biotechnol.* 100, 4699–4710. doi: 10.1007/s00253-016-7436-5

Klindworth, A., Pruesse, E., Schweer, T., Peplies, J., Quast, C., Horn, M., et al. (2013). Evaluation of general 16S ribosomal RNA gene PCR primers for classical and next-generation sequencing-based diversity studies. *Nucleic Acids Res.* 41, 1–11. doi: 10.1093/nar/gks808

Kougias, P. G., Treu, L., Benavente, D. P., Boe, K., Campanaro, S., and Angelidaki, I. (2017). Ex-situ biogas upgrading and enhancement in different reactor systems. *Bioresour. Technol.* 225, 429–437. doi: 10.1016/j.biortech.2016.11.124

Logroño, W., Popp, D., Kleinsteuber, S., Sträuber, H., Harms, H., and Nikolausz, M. (2020). Microbial resource management for ex situ biomethanation of hydrogen at alkaline pH. *Microorganisms* 8:614. doi: 10.3390/microorganisms8040614

Lucas, R., Harms, H., Johst, K., Frank, K., and Kleinsteuber, S. (2017). A critical evaluation of ecological indices for the comparative analysis of microbial communities based on molecular datasets. *FEMS Microbiol. Ecol.* 93, 1–15. doi: 10.1093/femsec/fiw209

Martin, M. (2013). Cutadapt removes adapter sequences from high-throughput sequencing reads. *EMBnet. J.* 17, 10–12. doi: 10.14806/ej.17.1.200

Maus, I., Tubbesing, T., Wibberg, D., Heyer, R., Hassa, J., Tomazetto, G., et al. (2020). The role of *Petrimonas mucosa* ING2-E5AT in mesophilic biogas reactor systems as deduced from multiomics analyses. *Microorganisms* 8:2024. doi: 10.3390/microorganisms8122024

Mcateer, P. G., Christine, A., Thorn, C., Mahony, T., Abram, F., and Flaherty, V. O. (2020). Reactor configuration influences microbial community structure during high-rate, low-temperature anaerobic treatment of dairy wastewater. *Bioresour. Technol.* 307:123221. doi: 10.1016/j.biortech.2020.123221

McIlroy, S. J., Kirkegaard, R. H., McIlroy, B., Nierychlo, M., Kristensen, J. M., Karst, S. M., et al. (2017). MiDAS 2.0: an ecosystem-specific taxonomy and online database for the organisms of wastewater treatment systems expanded for anaerobic digester groups. *Database* 2017:bax016. doi: 10.1093/database/bax016

Oksanen, J., Blanchet, F. G., Friendly, M., Kindt, R., Legendre, P., McGlinn, D., et al. (2019). *Vegan: Community Ecology Package*. Available online at: https://cran.r-project.org/package=vegan (accessed March 30, 2020)

R Core Team (2019). *R: A Language and Environment for Statistical Computing*. Vienna: R Foundation for Statistical Computing.

Rachbauer, L., Beyer, R., Bochmann, G., and Fuchs, W. (2017). Characteristics of adapted hydrogenotrophic community during biomethanation. *Sci. Total Environ.* 595, 912–919. doi: 10.1016/j.scitotenv.2017.03.074

Rachbauer, L., Voitl, G., Bochmann, G., and Fuchs, W. (2016). Biological biogas upgrading capacity of a hydrogenotrophic community in a trickle-bed reactor. *Appl. Energy* 180, 483–490. doi: 10.1016/j.apenergy.2016.07.109

Rittmann, S., Seifert, A., and Herwig, C. (2015). Essential prerequisites for successful bioprocess development of biological CH_4 production from CO_2 and H_2. *Crit. Rev. Biotechnol.* 35, 141–151. doi: 10.3109/07388551.2013.820685

Savvas, S., Donnelly, J., Patterson, T., Chong, Z. S., and Esteves, S. R. (2017). Biological methanation of CO_2 in a novel biofilm plug-flow reactor: a high rate and low parasitic energy process. *Appl. Energy* 202, 238–247. doi: 10.1016/j.apenergy.2017.05.134

Schaaf, T., Grünig, J., Schuster, M. R., Rothenfluh, T., and Orth, A. (2014). Methanation of CO_2 - storage of renewable energy in a gas distribution system. *Energy Sustain. Soc.* 4, 1–14. doi: 10.1186/s13705-014-0029-1

Schiebahn, S., Grube, T., Robinius, M., Tietze, V., Kumar, B., and Stolten, D. (2015). Power to gas: technological overview, systems analysis and economic assessment for a case study in Germany. *Int. J. Hydrogen Energy* 40, 4285–4294. doi: 10.1016/j.ijhydene.2015.01.123

Stams, A. J. M., Van Dijk, J. B., Dijkema, C., and Plugge, C. M. (1993). Growth of syntrophic propionate-oxidizing bacteria with fumarate in the absence of methanogenic bacteria. *Appl. Environ. Microbiol.* 59, 1114–1119.

Steinberg, L. M., and Regan, J. M. (2008). Phylogenetic comparison of the methanogenic communities from an acidic, oligotrophic fen and an anaerobic digester treating municipal wastewater sludge. *Appl. Environ. Microbiol.* 74, 6663–6671. doi: 10.1128/AEM.00553-08

Strübing, D., Huber, B., Lebuhn, M., Drewes, J. E., and Koch, K. (2017). High performance biological methanation in a thermophilic anaerobic trickle bed reactor. *Bioresour. Technol.* 245, 1176–1183. doi: 10.1016/j.biortech.2017.08.088

Strübing, D., Moeller, A. B., Mößnang, B., Lebuhn, M., Drewes, J. E., and Koch, K. (2018). Anaerobic thermophilic trickle bed reactor as a promising technology for flexible and demand-oriented H_2/CO_2 biomethanation. *Appl. Energy* 232, 543–554. doi: 10.1016/j.apenergy.2018.09.225

Strübing, D., Moeller, A. B., Mößnang, B., Lebuhn, M., Drewes, J. E., and Koch, K. (2019). Load change capability of an anaerobic thermophilic trickle bed reactor for dynamic H_2/CO_2 biomethanation. *Bioresour. Technol.* 289:121735. doi: 10.1016/j.biortech.2019.121735

Ullrich, T., Lindner, J., Bär, K., Mörs, F., Graf, F., and Lemmer, A. (2018). Influence of operating pressure on the biological hydrogen methanation in trickle-bed reactors. *Bioresour. Technol.* 247, 7–13. doi: 10.1016/j.biortech.2017.09.069

Wickham, H. (2016). ggplot2: Elegant Graphics for Data Analysis. New York, NY: Springer.

Yun, Y. M., Sung, S., Kang, S., Kim, M. S., and Kim, D. H. (2017). Enrichment of hydrogenotrophic methanogens by means of gas recycle and its application in biogas upgrading. *Energy* 135, 294–302. doi: 10.1016/j.energy.2017.06.133

Conflict of Interest: The authors declare that the research was conducted in the absence of any commercial or financial relationships that could be construed as a potential conflict of interest.

frontiers in Microbiology

ORIGINAL RESEARCH
published: 12 April 2021
doi: 10.3389/fmicb.2021.622235

Effects of Hydrothermal Pretreatment and Hydrochar Addition on the Performance of Pig Carcass Anaerobic Digestion

Jie Xu[1,2], *Hongjian Lin*[2] *and Kuichuan Sheng*[2]*

[1] School of City and Architecture Engineering, Zaozhuang University, Zaozhuang, China, [2] College of Biosystems Engineering and Food Science, Zhejiang University, Hangzhou, China

Proper disposal and utilization of dead pig carcasses are problems of public concern. The combination of hydrothermal pretreatment (HTP) and anaerobic digestion is a promising method to treat these wastes, provided that digestion inhibition is reduced. For this reason, the aim of this work was to investigate the optimal HTP temperature (140–180°C) for biogas production during anaerobic digestion of dead pigs in batch systems. In addition, the effects of hydrochar addition (6 g/L) on anaerobic digestion of pork products after HTP in continuous stirred tank reactors (CSTR) were determined. According to the results, 90% of lipids and 10% of proteins present in the pork were decomposed by HTP. In addition, the highest chemical oxygen demand (COD) concentration in liquid products (LP) reached 192.6 g/L, and it was obtained after 170°C HTP. The biogas potential from the solid residue (SR) and LP was up to 478 mL/g-VS and 398 mL/g-COD, respectively. A temperature of 170°C was suitable for pork HTP, which promoted the practical biogas yield because of the synergistic effect between proteins and lipids. Ammonia inhibition was reduced by the addition of hydrochar to the CSTR during co-digestion of SR and LP, maximum ammonia concentration tolerated by methanogens increased from 2.68 to 3.38 g/L. This improved total biogas yield and degradation rate of substrates, reaching values of 28.62 and 36.06%, respectively. The acetate content in volatile fatty acids (VFA) may be used as an index that reflects the degree of methanogenesis of the system. The results of the present work may also provide guidance for the digestion of feedstock with high protein and lipid content.

Keywords: pig carcass, hydrothermal temperature, hydrochar addition, biogas production, ammonia inhibition

OPEN ACCESS

Edited by:
Yi Zheng,
Kansas State University, United States

Reviewed by:
Eldon R. Rene,
IHE Delft Institute for Water Education, Netherlands
Youjie Xu,
Iowa State University, United States

***Correspondence:**
Kuichuan Sheng
kcsheng@zju.edu.cn

Specialty section:
This article was submitted to Microbiotechnology, a section of the journal Frontiers in Microbiology

Received: *28 October 2020*
Accepted: *15 March 2021*
Published: *12 April 2021*

Citation:
Xu J, Lin H and Sheng K (2021) Effects of Hydrothermal Pretreatment and Hydrochar Addition on the Performance of Pig Carcass Anaerobic Digestion. Front. Microbiol. 12:622235. doi: 10.3389/fmicb.2021.622235

INTRODUCTION

China as a country displays an annual production of 451 million swines. For this reason, China is the largest pork producer in the world (National Bureau of Statistics of China [NBSC], 2018). Unfortunately, during the growing process, more than 22 million pigs (5%) die every year of different illnesses, because of inadequate feeding conditions and unadvanced medical technology (Bono et al., 2014). Since 2018, African swine fever (ASF) outbreaks have been a major threat to pig farmers because of an extraordinary variability, a rapid transmissibility and high antibiotics resistance (Blome et al., 2020). As of November 22, 2019, a total of 160 ASF outbreaks had been reported in China, events that caused the culling of 11.93 million hogs (Ding and Wang, 2020). These data emphasizes the importance of timely vaccination, improving the sanitary conditions

in piggeries, and reducing the stocking density of pigs. In this context, burial and burning are the usual methods used in China; however, reduced land resources and environmental safety are growing concerns. For this reason, during the last years, the use of biological treatments has been promoted by the government (Wei et al., 2015). Anaerobic digestion of animal carcass for the conversion of these organic wastes into biogas is attracting extensive attention (Russo and von Blottnitz, 2017). Nevertheless, since dead pigs may contain pathogens and some veterinary drugs, a hygienization pretreatment is obligatory before carcass disposal or utilization. According to the regulation published by the Chinese government, livestock carcass should be pretreated at 135°C and 3 bar for 30 min before anaerobic digestion (Ministry of Agriculture and Rural Affairs of The People's Republic of China [MARF], 2017). This sterilization condition is consistent with that prescribed by the European Community, which indicates conditions of 133°C and 3 bar for 30 min or 140°C and 5 bar for 20 min (Gwyther et al., 2011).

Hydrothermal pretreatment (HTP) has been widely applied before anaerobic digestion of different substrates including food waste, biomass, and municipal sludge (Ding et al., 2017; Li et al., 2017; Ahmad et al., 2018). This technology is also suitable for animal carcass disinfection before anaerobic digestion. Temperature is the dominant HTP factor affecting the decomposition of organic matter. Since organic components are converted into hydrochar at high temperatures, proper HTP temperature for food waste treatment should not exceed 180°C (Munir et al., 2018). Several works about the HTP treatment of slaughterhouse waste (SW) and anaerobic digestion have been published by 133 and 140°C (Eftaxias et al., 2018; Spyridonidis et al., 2018); however, the optimal HTP temperature for biogas production from animal carcass is still not well known. Moreover, the biogas production may be inhibited by ammonia and long chain fatty acids (LCFA), which result from the digestion of protein and lipids (Latifi et al., 2019). The inhibition of biogas production can be reduced by the addition of hydrochar, which contains different functional groups at the surface that promote electron transfer reactions. For example, −OH may increase the pH of the system after combination with H^+. Also, under alkaline conditions, different groups containing carbon (C≡C, C=O, and C−O) may promote the release of protons (Fagbohungbe et al., 2017). In addition, the porous structure and alkaline environment of hydrochar supports microbial proliferation and enhances buffer capacity, respectively (Choe et al., 2019; Usman et al., 2020).

The objectives of the present study were: (1) investigate the optimal HTP temperature for biogas production during anaerobic digestion of dead pigs; and (2) evaluate the effects of hydrochar addition on anaerobic digestion of pig carcass.

MATERIALS AND METHODS

Feedstock and Inoculum

Because of safety constraints, fresh pork from a market in Hangzhou, China, was used in the investigation as an alternative to dead pigs (Dai et al., 2015). The pork was homogenized using a blender (CPEL-23, Shanghai Guosheng, China) and later stored at −20°C until further use. Rice straw (RS) obtained from a farm in Hangzhoug was used as material for hydrochar preparation. In addition, raw sludge, which was used as inoculum, was collected from a mesophilic biogas plant located in Hangzhou, China. After sampling, the sludge was stored at room temperature (about 25°C) in an airtight container. Physicochemical properties of feedstock and inoculum are shown in **Table 1**. The functional groups present in raw sludge are shown in **Figure 1**.

Hydrothermal Pretreatment

A 2-L stainless reactor (Parr 4848, United States) was used to carry out the HTP and hydrothermal carbonization (HTC) experiments. For HTP, 250 g (wet base, w.b.) pork and 250 mL deionized water were treated at 140, 150, 160, 170, and 180°C for 30 min. For the hydrochar preparation, 100 g RS (dry base, d.b.) and 1,000 mL deionized water were heated at 260°C for 2 h. After cooling to ambient temperature, the solid and liquid final products were separately collected.

Batch Anaerobic Digestion System

The pork biogas production at different HTP was carried out in batch anaerobic digestion systems, which consisted of a 500-mL glass bottle, a 1-L glass bottle filled with a diluted hydrochloric acid solution (pH < 3), and a 500-mL plastic bottle acting as the bioreactor, the biogas collection bottle, and the liquid collection bottle, respectively.

TABLE 1 | Physicochemical properties of feedstock and inoculum.

	Total solids (TS) (%, w.b.)	Volatile solids (VS)/TS (%, d.b.)	Protein (%, w.b.)	Lipid (%, w.b.)	pH	C/N
Pork	45.9 ± 0.3	97.5 ± 0.1	16.4 ± 0.3	24.6 ± 0.5	6.1 ± 0.1	8.0 ± 0.5
Inoculum	12.9 ± 0.2	52.9 ± 0.2	ND	ND	6.9 ± 0.1	7.0 ± 0.5

ND, not determined.

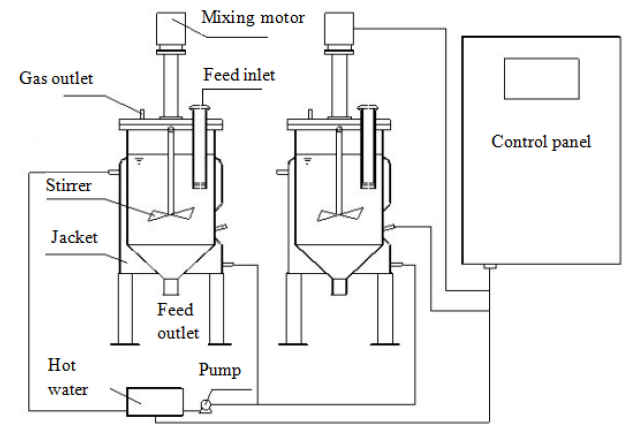

FIGURE 1 | Diagram of the continuous anaerobic digestion system used in the present research.

After HTP, 15 g (w.b.) solid residues (SRs), 25 mL liquid products (LP), and the mixtures of SR (2.81 g-VS, d.b.) and LP [0.22–1.97 g-chemical oxygen demand (COD)] were digested separately. 70 g inoculum (w.b.) was loaded into each bioreactor, and the corresponding ratios of inoculum to substrate (I/S) are displayed in **Table 2** (Xu et al., 2017). After loading with feedstock and inoculum, the working volume of the bioreactor was adjusted to 150 mL by adding deionized water and the top space was flushed with N_2 for 5 min. The bioreactors were kept at 35 ± 1°C on a water bath and manually shaken for 1 min twice a day. All the digestions were run in duplicate for 26 days until no biogas production was observed over a 5-day period.

Anaerobic Digestion With Continuous Stirred Tank Reactors

After completing the batch digestion, the optimal HTP temperature (170°C) was determined. Based on this temperature, the pretreated pork products were digested in continuous stirred tank reactors (CSTR). The schematic diagram of CSTR is displayed in **Figure 2**. The CTSR consisted of two reactors (30 L) and a central control. The reactors were set to operate at 37 ± 1°C and filled with 20 L inoculum before start-up.

Two sets of digestions were carried out. In order to determine the standard deviation of the biogas yield from the two reactors, the co-digestion of SR and LP were performed in duplicate for 20 days. After HTP of 250 g pork, the resulting products (35.85 g-VS SR and 48.15 g-COD LP) were added to each reactor on a daily basis. The amounts were equivalent to an organic loading rate (OLR) of 4.2 g-VS·(L·d)$^{-1}$. In addition, the reactors were stirred for 20 min at 35 rpm every 2 h, and the biogas production was measured using a drumtype gas flowmeter (Alpha LML-2, Changchun, China).

After data was collected to determine the standard deviation, the reactors were restarted with the same operational parameters. According to data reported in previous studies, hydrochar addition of 2–10 g/L resulted in 60.7–90.8% increase in biogas production from SR. This occurred because hydrochar increased the presence of functional groups as well as the buffer capacity of the system (Xu et al., 2018). In the present research, 6 g/L hydrochar were added to one reactor (A) to reduce process inhibition; in addition, another reactor (B), with no hydrochar addition, was set as the control group. During digestion and according to biogas production performance, the reactor was manually fed and discharged once a day between days 1 and 10, once every 2 days between days 12 and 18, and every 3 days between days 21 and 27. Digestate was collected from each reactor and subsequently analyzed.

Analytical Methods

Total solids (TS), volatile solids (VS), total ammonia nitrogen (TAN), and COD were measured according to the APHA (2006) standard method. The pH value was determined using a pH meter (PHS-3D, Shanghai, China). Total carbon and nitrogen content were measured with an elemental analyzer (EA 1112, CarloErba, Italy). Protein content was determined with a Kjeldahl nitrogen determination device (UDK152, Italy; protein = 6.25 × total nitrogen). For this purpose, the dry pork was digested with concentrated sulfuric acid at 420°C for 90 min; later, the solution was distilled with a sodium hydroxide and boric acid solution for 5 min. Finally, a titration with hydrochloric acid solution was performed. Lipid content was determined after Soxhlet extraction (SXT-06, Shanghai). Herein, the fat present in the pork was extracted using petroleum ether. Heating was provided with a water bath (80°C) for 4 h. Later, petroleum ether was evaporated and sample dried at 120°C. The composition of

TABLE 2 | The results for biogas production during batch digestion of pork products after HTP.

		140°C	150°C	160°C	170°C	180°C
I/S ratio	SR	1.30 ± 0.1	1.40 ± 0.1	1.53 ± 0.1	1.71 ± 0.1	1.95 ± 0.1
	LP	1.92 ± 0.1	1.58 ± 0.1	1.27 ± 0.1	0.99 ± 0.1	1.50 ± 0.1
	SR + LP	1.83 ± 0.1	1.50 ± 0.1	1.30 ± 0.1	1.00 ± 0.1	1.40 ± 0.1
Biogas yield (mL/g-VS)	SR	263.2 ± 13.9	289.3 ± 15.2	352.1 ± 15.1	422.2 ± 16.6	479.3 ± 18.9
	LP	398.1 ± 11.4	312.2 ± 13.3	235.3 ± 12.6	174.2 ± 11.2	291.4 ± 10.7
	SR + LP	392.4 ± 16.2	326.4 ± 15.6	272.4 ± 12.8	211.3 ± 14.4	315.3 ± 14.3
Methane content (%)	SR	69.4 ± 0.6	71.2 ± 0.6	71.8 ± 0.5	72.2 ± 0.5	73.3 ± 0.6
	LP	73.4 ± 0.6	71.8 ± 0.5	70.3 ± 0.6	69.7 ± 0.6	69.1 ± 0.8
	SR + LP	72.6 ± 0.4	71.2 ± 0.4	71.0 ± 0.5	70.3 ± 0.6	69.3 ± 0.7
TAN (g/L)	SR	2.06 ± 0.05	1.94 ± 0.04	1.75 ± 0.03	1.56 ± 0.02	1.42 ± 0.02
	LP	0.39 ± 0.02	0.51 ± 0.02	0.72 ± 0.03	0.89 ± 0.04	1.03 ± 0.05
	SR + LP	1.86 ± 0.03	2.01 ± 0.03	2.12 ± 0.03	2.27 ± 0.03	2.08 ± 0.03
pH	SR	7.49 ± 0.06	7.35 ± 0.06	7.23 ± 0.05	7.14 ± 0.08	7.03 ± 0.07
	LP	7.01 ± 0.08	6.85 ± 0.08	6.73 ± 0.07	6.64 ± 0.06	6.52 ± 0.07
	SR + LP	7.21 ± 0.06	7.15 ± 0.06	7.13 ± 0.07	7.08 ± 0.07	7.02 ± 0.08
Theoretical biogas yield (L)	SR	11.77 ± 0.46	10.48 ± 0.46	8.98 ± 0.46	6.87 ± 0.46	4.29 ± 0.46
	LP	3.97 ± 0.09	4.82 ± 0.09	5.97 ± 0.09	7.67 ± 0.09	5.09 ± 0.09
	SR + LP	15.74 ± 0.55	15.3 ± 0.55	14.95 ± 0.55	14.54 ± 0.55	9.38 ± 0.55

I/S ratio, the ratio of inoculum to substrate.

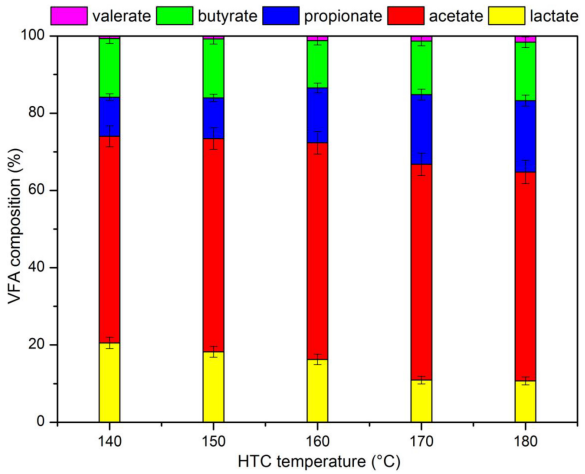

FIGURE 2 | Volatile fatty acids (VFA) composition of liquid products (LP) after hydrothermal pretreatment (HTP).

TABLE 3 | Characterization of solid residue (SR) and liquid products (LP) after different hydrothermal pretreatment (HTP) temperatures.

	140°C	150°C	160°C	170°C	180°C
TS (%, w.b.)	25.0 ± 0.2	23.3 ± 0.2	21.2 ± 0.3	19.0 ± 0.3	16.6 ± 0.4
VS/TS (%, d.b.)	98.3 ± 0.1	98.1 ± 0.2	98.7 ± 0.2	98.2 ± 0.1	98.5 ± 0.2
Lipid (%, w.b.)	3.3 ± 0.1	2.7 ± 0.1	2.4 ± 0.1	2.2 ± 0.1	2.1 ± 0.1
Protein (%, w.b.)	21.5 ± 0.3	20.1 ± 0.3	18.5 ± 0.3	16.4 ± 0.3	14.1 ± 0.3
Chemical oxygen demand (COD, g/L)	99.8 ± 0.3	121.2 ± 0.3	150.0 ± 0.3	192.6 ± 0.3	127.8 ± 0.3
Ammonia (g/L)	2.0 ± 0.2	3.8 ± 0.2	4.3 ± 0. 2	6.5 ± 0.2	4.9 ± 0.1
pH	6.32 ± 0.1	6.28 ± 0.1	6.25 ± 0.1	6.21 ± 0.1	6.19 ± 0.1
Volatile fatty acids (VFA, g/L)	15.2 ± 0.2	18.6 ± 0.2	21.2 ± 0.2	25.6 ± 0.2	20.6 ± 0.2

the biogas and volatile fatty acids (VFA) produced during the digestion were measured using gas chromatography (GC 2014, Shimadzu, Japan). In order to determine biogas composition, 10 μL gas were analyzed with a thermal conductivity detector. The temperatures of the column, injector port, and detector were 100, 120, and 120°C, respectively. The carrier gas was argon and was supplied at a flow rate of 30 mL/min. For VFA analysis, the fermentation liquid was centrifuged at 10,000 rpm for 15 min, acidified with metaphosphoric acid until reaching a pH value < 2.5, and filtered through a 0.22 μm membrane. After pretreatment, 0.4 μL of sample were analyzed using a hydrogen flame ionization detector. The temperatures of the injector port and detector were 250 and 280°C, respectively. The carrier gas was argon and was supplied at a flow rate of 30 mL/min. The functional groups present on the hydrochar and sludge were characterized at room temperature using Fourier transform infrared (FTIR) spectroscopy (Varian 640-IR, United States). For this purpose, the range of 400–4,000 cm^{-1} and KBr method were selected. Hydrochar surface area, pore volume, and pore size were measured with the Brunauer–Emmet–Teller (BET) method using an automatic nitrogen adsorption analyzer (JW-BK, China).

RESULTS AND DISCUSSION

Effects of Hydrothermal Temperature on Degradability and Biogas Production of Pork Products

Degradability of Pork Products After HTP

Characteristics of pork products after different HTP temperatures are shown in **Table 3**. According to the results, during HTP, the organics present in the pork presented a 50% reduction. Almost 90% of lipids were decomposed at 140°C, while at 180°C more than 85% of the protein was still preserved in the SR. The results were consistent with other study that indicated that most lipids were dissolved at 160°C and the soluble protein content increased as hydrothermal temperature increased (Pavlovič et al., 2013). This occurred because above 160°C, the cell walls are ruptured liberating the protein present inside the cell (Zhang et al., 2014). The COD concentrations in LP were 99.8–192.6 g/L after HTP, and the VFA content in LP was between 15.2 and 25.6 g/L. VFA only contributed to 13.2–19.1% of total COD, because the preliminary decomposition during HTP resulted in proteins and lipids hydrolization to produce polypeptides and LCFA, respectively. For example, a COD concentration of 149.6 g/L was achieved after SW was subjected to a HTP of 140°C. In addition, VFA accounted for less than 10% of total COD (Spyridonidis et al., 2018). Although the breakdown of organic compounds present in the biomass was accelerated at increasing HTP temperatures, the maximum values of COD and VFA were obtained after 170°C HTP. It is likely that some micromolecular organics such as VFA were converted into gas when temperature increased from 170 to 180°C. It has been reported that during HTP, soluble organics with molecular weight <10 kDa were easily converted into gas or refractory materials (Liu et al., 2012).

Figure 3 shows the VFA composition in the LP. Acetate accounted for about 50% of VFA, followed by lactate or propionate (10–20%), butyrate (10%), and valerate (1%). Part of the lactate was converted into propionate with increasing HTP temperatures. It was likely that propionate could be transformed from H_2 and lactate (Grause et al., 2012), and the hydrogen content in biomass was reduced with increasing temperatures during HTP (Yan et al., 2018); the increase in HTP temperature promoted the formation of H_2 and the conversion of lactate to propionate due to subcritical condition. The possible reaction for the conversion of lactate to propionate is displayed in **Table 4**.

Specific Biogas Yield of Pork Products After HTP

Table 2 displays the results for biogas production during batch digestion of pork products after HTP. The specific biogas yield

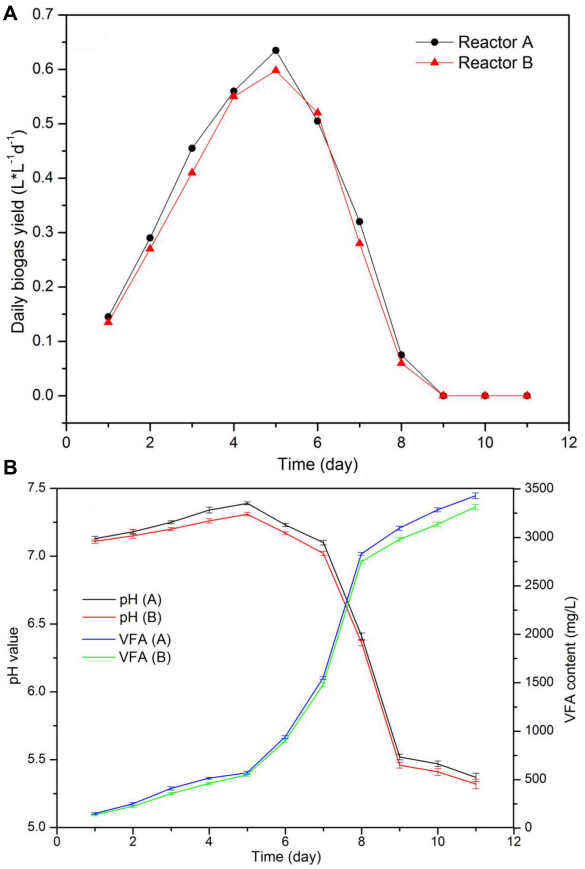

FIGURE 3 | Performance of continuous stirred tank reactors (CSTR) digestion of pork products after HTP: **(A)** daily biogas production; **(B)** pH value and VFA content.

TABLE 4 | Gibbs's energy of lactate converted to acetate, propionate and butyrate.

Equilibrium	ΔG° (kJ/mol)
Lactate + $2H_2O$ → acetate + HCO_3^- + H^+ + $2H_2$	−4.2
Lactate + H_2 → propionate + H_2O	−79.9
2Lactate + H^+ → butyrate + $2H_2$ + $2CO_2$	−64.1

from SR and from LP reached 479 mL/g-VS and 398 mL/g-COD at the I/S ratio of 1.95 and 1.92, respectively; both biogas yields decreased with reducing I/S ratio. The methane content in the biogas was between 69.1 and 73.4% during the whole digestion process, value that agree with the high theoretical methane content coefficient for lipids and proteins (Wu et al., 2009). Although the theoretical biogas potential of SW is above 740 mL/g-VS, because of the inhibition by excess ammonia and LCFA, the specific biogas yield normally depends on the operational conditions (Wu et al., 2015). Other studies have reported SW methane yields between 300 and 800 mL/g-VS. For example, a biogas yield of 443 mL/g-VS was obtained during the digestion of SW at a I/S ratio of 4 (Latifi et al., 2019). Also, a biogas yield of 425 mL/g-COD was obtained after SW water digestion with an OLR of 1.82 g·(L d)$^{-1}$ (Schmidt et al., 2018). These results are close to biogas yields obtained in this paper.

A TAN concentration of 1.7 g/L was considered as the threshold for ammonia inhibition during the digestion of substrates with high nitrogen content (Akindele and Sartaj, 2018). In the present experiments, the biogas yield decreased from 422 to 289 mL/g-VS when the TAN value increased from 1.53 to 1.94 g/L. This occurred because the protein content of the substrate increased from 16.4 to 20.1%. During the co-digestion of SR and LP and at the same I/S ratio, the biogas yield was higher than that obtained during mono-digestion of either SR or LP. Nevertheless, during co-digestion, the TAN value was higher. This has been attributed to the increasing buffer capacity resulting from the synergistic effect between VFA and ammonia (Zhang et al., 2013). Eq. 1 displays the formation of the buffer system.

$$C_xH_yCOOH + NH_3 \cdot H_2O \rightarrow C_xH_yCOO^- + NH_4^+ + H_2O \quad (1)$$

The calculation of the theoretical total biogas yield from pork products after HTP was based on the specific SR and LP biogas yield (479 mL/g-VS and 398 mL/g-COD, respectively). Results are shown in **Table 2**. According to the theoretical results, the highest biogas yield from pork products would be obtained after 140°C HTP. However, the risk of inhibition due to ammonium was present. It was also determined that, because of the synergistic effect between protein and lipid, a temperature of 170°C was the optimal value for pork HTP, which would promote the maximum value for practical biogas yield.

The Parallel CSTR Digestion of Pork Products After HTP

The daily biogas production and process stability from the two reactors running at the same conditions is shown in **Figure 4**. As data indicated, the biogas production increased during the first 5 days from 0.14 L·L^{-1}·d^{-1} to around 0.61 L L^{-1} d^{-1}, and it was rapidly reduced after day 6 and stopped after day 9. Moreover, VFA content augmented from around 920–3400 mg/L between days 6 and 9. According to pH values and VFA content, the reduction in biogas production was the result of the decrease in pH and VFA accumulation, a process that was caused by the addition of sour LP because of improper storage. It is known that the addition of sour substrate with pH values between 5.0 and 5.5 may cause digester instability. As a consequence, a rapid acidification and reaction failure may easily happen (Kong et al., 2016). When food waste was soaked and stored with no refrigeration for 12 h, pH decreased from 6.5–7.4 to 5.2–5.5, causing a rapid increase from 0.03 to 0.4 in the VFA/COD value (Kuruti et al., 2017).

Although the biogas production only occurred during the first 8 days of the process, the values for daily biogas yield, pH, and VFA content in the two reactors were very close during this period. Total biogas production reached 59.7 and 56.46 L in each reactor, the difference in biogas production between the two reactors was less than 7%.

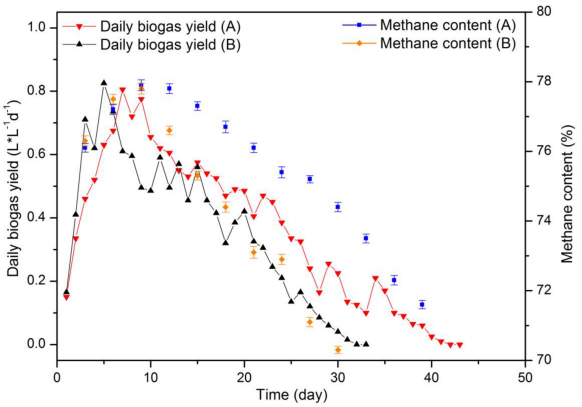

FIGURE 4 | Biogas yield and methane content in CSTR digestion of pork products after HTP.

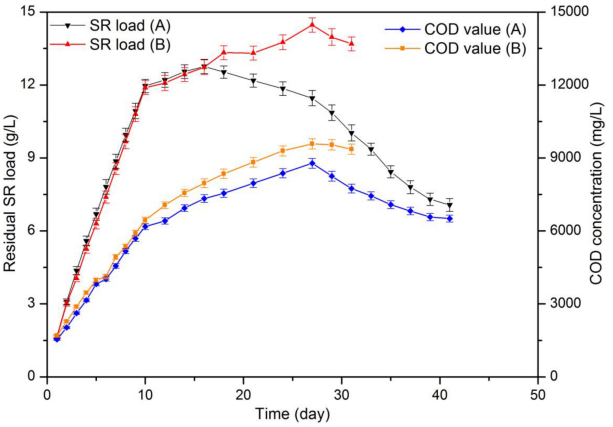

FIGURE 5 | Substrate load and chemical oxygen demand (COD) values during CSTR digestion of pork products after HTP.

Continuous Stirred Tank Reactors Digestion of Pork Products After HTP With Hydrochar Addition

Impact of Hydrochar Addition on Biogas Production

Figure 5 displays the results for biogas yield and **Figure 6** those for residual SR load and COD concentration of fermentation liquor. Both reactors displayed a rapid increase in daily biogas yield during the first 9 days of digestion. In addition, with an OLR of 4.2 g-VS (L d)$^{-1}$, the substrate load increased to 10.8 g/L. Maximum daily biogas yield values were 0.820 and 0.805 L L^{-1}d^{-1} for each reactor. A drop on biogas production occurred in the two reactors after day 9, maybe as a result of the high protein content in SR, indicating that the reactors were overloaded. Therefore, during digestion, the two reactors were fed on days 1–10, 12, 14, 16, 18, 21, 24, and 27. The corresponding OLR were 2.1 g-VS (L d)$^{-1}$ between days 11–17 and 1.4 g-VS (L d)$^{-1}$ between days 18 and 30. Prolonging feeding periods and decreasing OLR are common remediation strategies when better degradation rates of the accumulated substrate are intended. It has been reported that a decline in biogas production and an accumulation in VFA were observed at the OLR of 2.3 g (L d)$^{-1}$ during digestion of SW. Also, the OLR decreased to 1.5 g (L d)$^{-1}$ after a starvation period of 10 days (Eftaxias et al., 2018).

After day 9, both reactors showed fluctuations in daily biogas yield. The reason is that the added volume and COD amount of substrate in both reactors immediately increased and created a temporary inhibition. At day 22 and when the substrate load was up to 13.3 g/L, the daily biogas production was less than half that of the maximum value. Biogas production ended at day 31 and day 41, respectively. The total biogas yield of 309.2 L was achieved in the reactor with hydrochar addition, which represents a 28.62% higher than that (240.4 L) in control group.

In addition, the reactor with hydrochar addition displayed methane content between 71.6 and 77.9%, and that for control reactor was between 70.3 and 77.8%. The methane content first increased and later decreased as a consequence of a declined

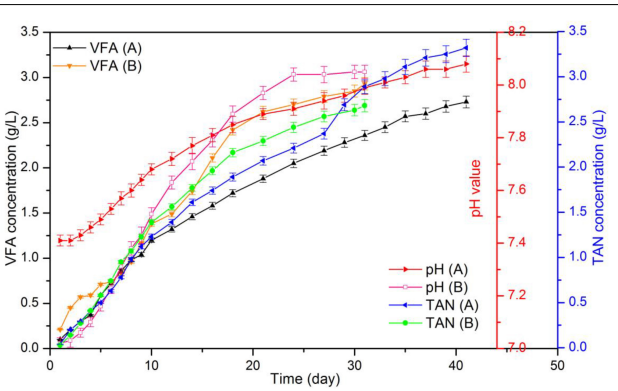

FIGURE 6 | pH and total ammonia nitrogen (TAN) concentration in VFA during CSTR digestion of pork products after HTP.

biogas production. Nearly 30% of CH_4 resulted from the reaction between CO_2 and H_2 (Yuan and Zhu, 2016).

After digestion, the control group showed a residual SR load and COD concentration of 13.69 and 9.36 g/L, respectively. In addition, the values in the reactor containing hydrochar were 7.07 and 6.51 g/L, correspondingly. Substrates containing 609.45 g-VS SR and 818.55 g-COD LP were added into each reactor during digestion. According to changes in volume load and COD, it was calculated that 294.52 g-VS SR and 414.55g-COD LP were decomposed in the control group during biogas production. On the other hand, the amounts were 406.59 g-VS SR and 558.15 g-COD LP in another reactor. The average specific biogas yields were 339.0 and 320.5 mL-g/VS in control and treatment, respectively. In the control reactor, the VS removal rates for SR and LP were 48.33 and 50.64%, respectively. After hydrochar addition, these values increased to 66.77 and 68.19%, respectively. In both reactors, SR removal rates were similar to those of LP. These results suggested that the degradation of proteins and lipids may occur in a synchronous way. In theory, the hydrolysis of lipids was slower than that of proteins. The

results suggested that the hydrolysis of lipids was promoted by HTP, which was able to increase the buffer capacity of the system through the synergistic effect of proteins and lipids. Moreover, at a inoculum/decomposed substrates ratio of 1.41, the specific biogas yield was 320.5 mL-g/VS. This value is similar to a yield of 315.3 mL-g/VS, which was obtained during the co-digestion of SR and LP at a I/S ratio of 1.40. Although with high theoretical biogas potential, the practical biogas yield from digestion of SW depends on operational parameter, such as the characteristics of the feedstock and inoculum, OLR and pretreatment method (Hu et al., 2018). The performance of mesothermal semi-continous digestion of SW in other studies were shown in **Table 5**, and the high methane yield of SW was obtained with a low OLR; it suggested that the low methane yield in this study was due to the overload of substrate.

In addition, the net energy was calculated by subtracting the energy consumed in HTC from the methane energy produced during hydrochar addition. The increase in methane energy (kJ) was evaluated by multiplying the lower heating value of methane (35.89 kJ/L) by the increased methane yield (L). Energy consumption for HTC was analyzed based on Mustafa et al. (2018) who reported a value of 1,092 kJ/kg at 260°C. It was determined that, after hydrochar addition, methane yield increased by 48.2 L which in total represents an energy yield of 1,728 kJ. It was also determined that 2,402 kJ were consumed during HTC of 200 g biomass and 2 L water. Even in the present experiments HTC displaced a high-energy consumption, a positive value for net energy can be obtained if the biogas inhibition is further ameliorated by hydrochar addition.

Process Stability

Figure 7 displays the results for pH, TAN and VFA during the digestion process. According to the data, in the control group the initial and final pH were 7.02 and 8.05, respectively. In addition, the final TAN and VFA concentrations were 2.68 and 2.93 g/L, respectively. Data also indicated that in the hydrochar treated reactor, pH increased from 7.41 to 8.08, and the concentrations of TAN and VFA were 3.38 and 2.73 g/L, respectively. Usually, ammonia and LCFA hinder the digestion of substrates with high protein and lipid content. High ammonia concentrations usually cause that the digesters operate within a neutral pH range, which is known as "inhibited steady state." This state results in a low biogas yield, VFA accumulation, and a drop in pH values (Shi et al., 2017). LCFA are readily adsorbed on the cell membrane, limiting the mass transfer between methanogens and substrate. LCFA inhibition also occurs along with acetate accumulation as hydrolysis product (Harris et al., 2018). **Figure 8** shows VFA composition. According to the data, no accumulation of acetate were observed in the reactors. Moreover, at day 16, TAN concentrations in both reactors occurred above the inhibition threshold of 1.7 g/L. These results may indicate that the decrease in biogas production occurred because of high ammonia concentrations.

Data also indicated a significant and positive relationship between acetate content and biogas production. At the beginning of the digestion process, the acetate content was more than

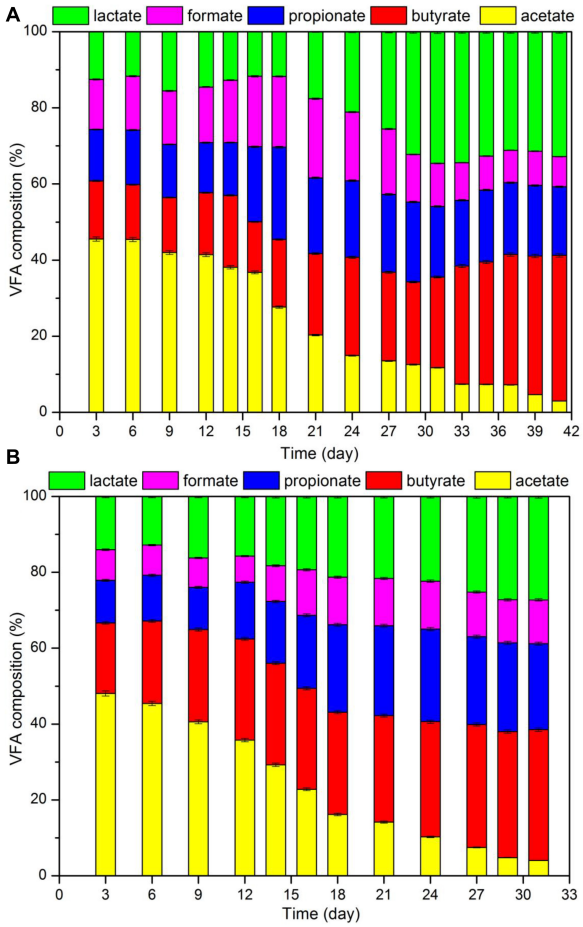

FIGURE 7 | Composition of VFA in the fermentation liquid during CSTR digestion of pork products after HTP: **(A)** reactor with hydrochar addition; **(B)** control group.

TABLE 5 | Performance of mesothermal semi-continous digestion of slaughterhouse waste (SW) in recent literatures.

Thermal treatment	Working volume (L)	Methane Yield (L/g-VS)	Organic loading rate [OLR, g·(L d)$^{-1}$]	Substrate	References
70°C, 2 h	8.0	0.640	1.3	SW	Escudero et al., 2014
Not treated	6.0	0.350	2.5–3.5	N-rich SW	Ortner et al., 2014
Not treated	11.0	0.291	1.1	lipid-rich SW	Rodríguez-Méndez et al., 2017
133°C, 3 bar, 20 min	42.0	0.408	1.5–10	SW + Ni, Co, Mo	Eftaxias et al., 2018
121°C, 30 min	1.8	0.588	0.85–1.00	High-fat SW	Harris et al., 2018
Not treated	14.8	0.574	NM	SW + sludge	Latifi et al., 2019

SW, slaughterhouse waste; NM, not mentioned.

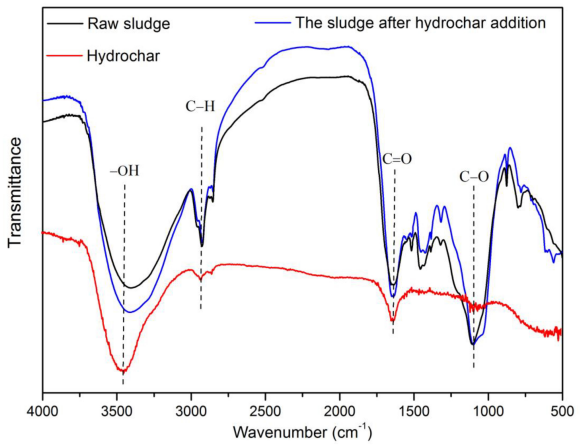

FIGURE 8 | The changes on the functional groups of inoculated sludge after hydrochar addition.

40%. When acetate content was decreased to 20%, daily biogas yield was reduced to half that of the peak value; in addition, methanogenesis nearly stopped when acetate content was below 5%. Since 72% methane was produced during acetate degradation, acetate was almost totally spent. On the other hand, during digestion, lactate, propionate, and butyrate accumulated (Yuan and Zhu, 2016). Thus, acetate content in VFA may be used as the index that reflects the degree of methanogenesis of a system.

The Role of Hydrochar on Improving Biogas Production

The increase of 28.62% in biogas yield was achieved when hydrochar was added in concentrations that reduced ammonium inhibition. In this case, ammonia tolerance increased from 2.68 to 3.38 g/L. Inhibition of ammonia on methanogens is mainly due to free ammonia (FA), since FA is able to permeate the cell membrane and limit electron transfer (Fajardo et al., 2014).

It has been reported that hydrochar addition enhances biogas production through different mechanisms. For example, hydrochar promotes electron transfer reactions because of the presence of surface functional groups, improves the buffer capacity of the system by providing an alkaline environment, and supports microbial proliferation through the porous structure (Fagbohungbe et al., 2017; Usman et al., 2020). Previous reports have indicated that biogas yield increased in 64 and 52% by hydrochar addition during the digestion of fish processing waste and hydrothermal liquefaction wastewater, respectively (Choe et al., 2019; Usman et al., 2020). As shown in **Figure 1**, the functional groups (–OH and C=O) present in the inoculated sludge increased after hydrochar addition. The porous properties of the hydrochar used in this study are presented in **Table 6**. According to the data, the porous structure of hydrochar, with the BET surface area of 19.4 m^2/g, was also beneficial for methanogens growth.

TABLE 6 | Pore properties of hydrochar.

	Value
BET surface area (m^2/g)	19.4 ± 0.1
Total pore volume (cm^3/g)	0.063 ± 0.002
Average pore size (nm)	13.0 ± 0.1

CONCLUSION AND PERSPECTIVE

This study demonstrated the feasibility of anaerobic digestion of pork products after HTP. According to the HTP results, most lipids broke down at 140°C, and protein decomposition was accelerated at temperatures above 160°C. The biogas yield of 320 mL/g-VS was achieved during CSTR digestion of pork products after HTP. It suggests that the ORL should not exceed 4.2 g-VS $(L\ d)^{-1}$ to prevent inhibition when pork waste was fed as substrate, a value similar to the case of food waste. Hydrochar addition offered a good option by reducing the ammonia inhibition. In the present work, hydrochar was added to the reactor only one time. However, hydrochar was gradually lost with the discharge of digestate. As remedy, the recycling of the digested effluents and continuous supplement of hydrochar to the reactors may be an option. Thus, a study about the optimal parameters and conditions for hydrochar addition during the continuous digestion process should be considered.

The results presented herein provide an option for a harmless utilization and treatment of animal carcass. Because of the advantage of biogas recovery, anaerobic digestion is the mainstream treatment for food waste in China. Since the increasing demand in environment protection and clean energy, the treatment of animal carcass by HTP and anaerobic digestion are encouraged. Assuming a centralized collection and sterilization for animal carcass, its co-digestion with hydrochar in large-scale digesters will be a promising way for the harmless treatment method.

DATA AVAILABILITY STATEMENT

The original contributions presented in the study are included in the article/supplementary material, further inquiries can be directed to the corresponding author.

AUTHOR CONTRIBUTIONS

All authors contributed equally to the article and approved the submitted version.

FUNDING

This work was financially supported by the Key Research and Development Projects of Zhejiang Province (No. 2019C02080) and the National Key R&D Program of China (No. 2016YFD0800804).

REFERENCES

Ahmad, F., Silva, E. L., and Amâncio Varesche, M. B. (2018). Hydrothermal processing of biomass for anaerobic digestion - A review. *Renew. Sustain. Energy Rev.* 98, 108–124. doi: 10.1016/j.rser.2018.09.008

Akindele, A. A., and Sartaj, M. (2018). The toxicity effects of ammonia on anaerobic digestion of organic fraction of municipal solid waste. *Waste Manage.* 71, 757–766. doi: 10.1016/j.wasman.2017.07.026

APHA (2006). *Standard Methods for the Examination of Water and Wastewater*, 20th Edn. Washington, DC: American Public Health Association.

Blome, S., Franzke, K., and Beer, M. (2020). African swine fever – A review of current knowledge. *Virus Res.* 287:198099. doi: 10.1016/j.virusres.2020.198099

Bono, C., Cornou, C., Lundbye-Christensen, S., and Kristensen, A. R. (2014). Dynamic production monitoring in pig herds III. Modeling and monitoring mortality rate at herd level. *Livestock Sci.* 168, 128–138. doi: 10.1016/j.livsci.2014.08.003

Choe, U. Y., Mustafa, A. M., Lin, H. J., Xu, J., and Sheng, K. C. (2019). Effect of bamboo hydrochar on anaerobic digestion of fish processing waste for biogas production. *Bioresour. Technol.* 283, 340–349. doi: 10.1016/j.biortech.2019.03.084

Dai, X., Chen, S., Xue, Y., Dai, L., Li, N., Takahashi, J., et al. (2015). Hygienic treatment and energy recovery of dead animals by high solid co-digestion with vinasse under mesophilic condition, feasibility study. *J. Hazard. Mater.* 297, 320–328. doi: 10.1016/j.jhazmat.2015.05.027

Ding, L. K., Cheng, J., Qiao, D., Yue, L. C., Li, Y. Y., Zhou, J. H., et al. (2017). Investigating hydrothermal pretreatment of food waste for two-stage fermentative hydrogen and methane co-production. *Bioresour. Technol.* 241, 491–499. doi: 10.1016/j.biortech.2017.05.114

Ding, Y. F., and Wang, Y. L. (2020). Big government: the fight against the African swine fever in China. *J. Biosaf. Biosecur.* 2, 44–49. doi: 10.1016/j.jobb.2020.04.001

Eftaxias, A., Diamantis, V., and Aivasidis, A. (2018). Anaerobic digestion of thermal pre-treated emulsified slaughterhouse wastes (TESW): effect of trace element limitation on process efficiency and sludge metabolic properties. *Waste Manage.* 76, 357–363. doi: 10.1016/j.wasman.2018.02.032

Escudero, A., Lacalle, A., Blanco, F., Pinto, M., Díaz, I., and Domínguez, A. (2014). Semi-continuous anaerobic digestion of solid slaughterhouse waste. *J. Environ. Chem. Eng.* 2, 819–825. doi: 10.1016/j.jece.2014.02.006

Fagbohungbe, M. O., Herbert, B. M., Hurst, L., Ibeto, C. N., Li, H., Usmani, S. Q., et al. (2017). The challenges of anaerobic digestion and the role of biochar in optimizing anaerobic digestion. *Waste Manage.* 61, 236–249. doi: 10.1016/j.wasman.2016.11.028

Fajardo, C., Mora, M., Fernández, I., Mosquera-Corral, A., Campos, J. L., and Méndez, R. (2014). Cross effect of temperature, pH and free ammonia on autotrophic denitrification process with sulphide as electron donor. *Chemosphere* 97, 10–15. doi: 10.1016/j.chemosphere.2013.10.028

Grause, G., Igarashi, M., Kameda, T., and Yoshioka, T. (2012). Lactic acid as a substrate for fermentative hydrogen production. *Int. J. Hydrogen Energy* 37, 16967–16973. doi: 10.1016/j.ijhydene.2012.08.096

Gwyther, C. L., Williams, A. P., Golyshin, P. N., Edwards-Jones, G., and Jones, D. L. (2011). The environmental and biosecurity characteristics of livestock carcase disposal methods. A review. *Waste Manage.* 31, 767–780. doi: 10.1016/j.wasman.2010.12.005

Harris, P. W., Schmidt, T., and McCabe, B. K. (2018). Impact of thermobaric pre-treatment on the continuous anaerobic digestion of high-fat cattle slaughterhouse waste. *Biochem. Eng. J.* 134, 108–113. doi: 10.1016/j.bej.2018.03.007

Hu, Y., Kobayashi, T., Qi, W., Oshibe, H., and Xu, K. Q. (2018). Effect of temperature and organic loading rate on siphon-driven self-agitated anaerobic digestion performance for food waste treatment. *Waste Manage.* 74, 150–157. doi: 10.1016/j.wasman.2017.12.016

Kong, X., Wei, Y. H., Xu, S., Liu, J. G., Li, H., Liu, Y. L., et al. (2016). Inhibiting excessive acidification using zero-valent iron in anaerobic digestion of food waste at high organic load rates. *Bioresour. Technol.* 211, 65–71. doi: 10.1016/j.biortech.2016.03.078

Kuruti, K., Begum, S., Ahuja, S., Anupoju, G. R., Juntupally, S., Gandu, B., et al. (2017). Exploitation of rapid acidification phenomena of food waste in reducing the hydraulic retention time (HRT) of high rate anaerobic digester without conceding on biogas yield. *Bioresour. Technol.* 226, 65–72. doi: 10.1016/j.biortech.2016.12.005

Latifi, P., Karrabi, M., and Danesh, S. (2019). Anaerobic co-digestion of poultry slaughterhouse wastes with sewage sludgein batch-mode bioreactors (effect of inoculum-substrate ratio and total solids). *Renew. Sustain. Energy Rev.* 107, 288–296. doi: 10.1016/j.rser.2019.03.015

Li, C. X., Wang, X. D., Zhang, G. Y., Yu, G. W., Lin, J. J., and Wang, Y. (2017). Hydrothermal and alkaline hydrothermal pretreatments plus anaerobic digestion of sewage sludge for dewatering and biogas production: bench-scale research and pilot-scale verification. *Water Res.* 117, 49–57. doi: 10.1016/j.watres.2017.03.047

Liu, X., Wang, W., Gao, X., Zhou, Y., and Shen, R. (2012). Effect of thermal pretreatment on the physical and chemical properties of municipal biomass waste. *Waste Manage.* 32, 249–255. doi: 10.1016/j.wasman.2011.09.027

Ministry of Agriculture and Rural Affairs of The People's Republic of China [MARF] (2017). Available online at: http://www.moa.gov.cn/nybgb/2017/dqq/201801/t20180103_6133924.htm (accessed July 20, 2017).

Munir, M. T., Mansouri, S. S., Udugama, I. A., Baroutian, S., Gernaey, K. V., and Young, B. R. (2018). Resource recovery from organic solid waste using hydrothermal processing: opportunities and challenges. *Renew. Sustain. Energy Rev.* 96, 64–75. doi: 10.1016/j.rser.2018.07.039

Mustafa, A. M., Li, H., Radwan, A. A., Sheng, K. C., and Chen, X. (2018). Effect of hydrothermal and Ca(OH)2 pretreatments on anaerobic digestion of sugarcane bagasse for biogas production. *Bioresour. Technol.* 259, 54–60. doi: 10.1016/j.biortech.2018.03.028

National Bureau of Statistics of China [NBSC] (2018). *Chinese Statistical Yearbook*. Beijing: China Statistics Press.

Ortner, M., Leitzinger, K., Skupien, S., Bochmann, G., and Fuchs, W. (2014). Efficient anaerobic mono-digestion of N-rich slaughterhouse waste: influence of ammonia, temperature and trace elements. *Bioresour. Technol.* 174, 222–232. doi: 10.1016/j.biortech.2014.10.023

Pavlovič, I., Knez, Ž., and Škerget, M. (2013). Hydrothermal reactions of agricultural and food processing wastes in sub- and supercritical water: a review of fundamentals, mechanisms, and state of research. *J. Agric. Food Chem.* 61, 8003–8025. doi: 10.1021/jf401008a

Rodríguez-Méndez, R., Bihan Le, Y., Béline, F., and Lessard, P. (2017). Long chain fatty acids (LCFA) evolution for inhibition forecasting during anaerobic treatment of lipid-rich wastes: case of milk-fed veal slaughterhouse waste. *Waste Manage.* 67, 51–58. doi: 10.1016/j.wasman.2017.05.028

Russo, V., and von Blottnitz, H. (2017). Potentialities of biogas installation in South African meat value chain for environmental impacts reduction. *J. Clean. Prod.* 153, 465–473. doi: 10.1016/j.jclepro.2016.11.133

Schmidt, T., McCabe, B. K., Harris, P. W., and Lee, S. (2018). Effect of trace element addition and increasing organic loading rates on the anaerobic digestion of cattle slaughterhouse wastewater. *Bioresour. Technol.* 264, 51–57. doi: 10.1016/j.biortech.2018.05.050

Shi, X., Lin, J., Zuo, J., Li, P., Li, X., and Guo, X. (2017). Effects of free ammonia on volatile fatty acid accumulation and process performance in the anaerobic digestion of two typical bio-wastes. *J. Environ. Sci.* 55, 49–57. doi: 10.1016/j.jes.2016.07.006

Spyridonidis, A., Skamagkis, T., Lambropoulos, L., and Stamatelatou, K. (2018). Modeling of anaerobic digestion of slaughterhouse wastes after thermal treatment using ADM1. *J. Environ. Manage.* 224, 49–57. doi: 10.1016/j.jenvman.2018.07.001

Usman, M., Shi, Z. J., Ren, S., Ngo, H. H., Luo, G., and Zhang, S. C. (2020). Hydrochar promoted anaerobic digestion of hydrothermal liquefaction wastewater: focusing on the organic degradation and microbial community. *Chem. Eng. J.* 399, 125766. doi: 10.1016/j.cej.2020.125766

Wei, X. J., Lin, W. L., and Hennessy, D. A. (2015). Biosecurity and disease management in China's animal agriculture sector. *Food Policy* 54, 52–64. doi: 10.1016/j.foodpol.2015.04.005

Wu, C. F., Wang, Q. H., Yu, M., Zhang, X., Song, N., Chang, Q., et al. (2015). Effect of ethanol pre-fermentation and inoculum-to-substrate ratio on methane yield from food waste and distillers' grains. *Appl. Energy* 155, 846–853. doi: 10.1016/j.apenergy.2015.04.081

Wu, G. X., Healy, M. G., and Zhan, X. M. (2009). Effect of the solid content on anaerobic digestion of meat and bone meal. *Bioresour. Technol.* 100, 4326–4331. doi: 10.1016/j.biortech.2009.04.007

Xu, J., Mustafa, A. M., Lin, H. J., Choe, U. Y., and Sheng, K. C. (2018). Effect of hydrochar addition on anaerobic digestion of dead pig carcass after hydrothermal pretreatment. *Waste Manage.* 78, 849–856. doi: 10.1016/j.wasman.2018.07.003

Xu, J., Mustafa, A. M., and Sheng, K. C. (2017). Effects of inoculum to substrate ratio and co-digestion with bagasse on biogas production of fish waste. *Environ. Technol.* 38, 2517–2522. doi: 10.1080/09593330.2016.1269837

Yan, W., Zhang, H. H., Sheng, K. C., Mustafa, A. M., and Yu, Y. F. (2018). Evaluation of engineered hydrochar from $KMnO_4$ treated bamboo residues: physicochemical properties, hygroscopic dynamics, and morphology. *Bioresour. Technol.* 250, 806–811. doi: 10.1016/j.biortech.2017.11.052

Yuan, H., and Zhu, N. (2016). Progress in inhibition mechanisms and process control of intermediates and by-products in sewage sludge anaerobic digestion. *Renew. Sustain. Energy Rev.* 58, 429–438. doi: 10.1016/j.rser.2015.12.261

Zhang, C. S., Su, H. J., and Tan, T. W. (2013). Batch and semi-continuous anaerobic digestion of food waste in a dual solid-liquid system. *Bioresour. Technol.* 145, 10–16. doi: 10.1016/j.biortech.2013.03.030

Zhang, G. Y., Ma, D. C., Peng, C. N., Liu, X. X., and Xu, G. W. (2014). Process characteristics of hydrothermal treatment of antibiotic residue for solid biofuel. *Chem. Eng. J.* 252, 230–238. doi: 10.1016/j.cej.2014.04.092

Conflict of Interest: The authors declare that the research was conducted in the absence of any commercial or financial relationships that could be construed as a potential conflict of interest.

frontiers in Microbiology

ORIGINAL RESEARCH
published: 09 June 2021
doi: 10.3389/fmicb.2021.671287

Effects of *Lactobacillus plantarum* on the Fermentation Profile and Microbiological Composition of Wheat Fermented Silage Under the Freezing and Thawing Low Temperatures

*Miao Zhang[1], Lei Wang[2], Guofang Wu[2], Xing Wang[1], Haoxin Lv[3], Jun Chen[1], Yuan Liu[1], Huili Pang[1] and Zhongfang Tan[1]**

[1] Henan Key Laboratory of Ion-Beam Bioengineering, College of Agricultural Sciences, Zhengzhou University, Zhengzhou, China, [2] Academy of Animal Science and Veterinary Medicine, Qinghai University, Xining, China, [3] College of Food Science and Engineering, Henan University of Technology, Zhengzhou, China

OPEN ACCESS

Edited by:
Panagiotis Tsapekos, Technical University of Denmark, Denmark

Reviewed by:
Xianjun Yuan, Nanjing Agricultural University, China
Assar Ali Shah, Jiangsu University, China

***Correspondence:**
Zhongfang Tan
tzhongfang@zzu.edu.cn

Specialty section:
This article was submitted to Microbiotechnology, a section of the journal Frontiers in Microbiology

Received: *23 February 2021*
Accepted: *06 May 2021*
Published: *09 June 2021*

Citation:
Zhang M, Wang L, Wu G, Wang X, Lv H, Chen J, Liu Y, Pang H and Tan Z (2021) Effects of Lactobacillus plantarum on the Fermentation Profile and Microbiological Composition of Wheat Fermented Silage Under the Freezing and Thawing Low Temperatures. Front. Microbiol. 12:671287. doi: 10.3389/fmicb.2021.671287

The corruption and/or poor quality of silages caused by low temperature and freeze-thaw conditions makes it imperative to identify effective starters and low temperature silage fermentation technology that can assist the animal feed industry and improve livestock productivity. The effect of *L. plantarum* QZ227 on the wheat silage quality was evaluated under conditions at constant low temperatures followed by repeated freezing and thawing at low temperatures. QZ227 became the predominant strain in 10 days and underwent a more intensive lactic acid bacteria fermentation than CK. QZ227 accumulated more lactic acid, but lower pH and ammonia nitrogen in the fermentation. During the repeated freezing and thawing process, the accumulated lactic acid in the silage fermented by QZ227 remained relatively stable. Relative to CK, QZ227 reduced the abundance of fungal pathogens in silage at a constant 5°C, including *Aspergillus*, *Sporidiobolaceae*, *Hypocreaceae*, *Pleosporales*, *Cutaneotrichosporon*, *Alternaria*, and *Cystobasidiomycetes.* Under varying low temperature conditions from days 40 to days 60, QZ227 reduced the pathogenic abundance of fungi such as *Pichia*, *Aspergillus*, *Agaricales*, and *Plectosphaerella*. QZ227 also reduced the pathogenic abundance of *Mucoromycota* after the silage had been exposed to oxygen. In conclusion, QZ227 can be used as a silage additive in the fermentation process at both constant and variable low temperatures to ensure fast and vigorous fermentation because it promotes the rapid accumulation of lactic acid, and reduces pH values and aerobic corruption compared to the CK.

Keywords: freezing and thawing temperatures, fermentation, lactic acid bacteria, silage, anti-bacteria

INTRODUCTION

The Qinghai-Tibet Plateau is the coldest region outside the poles, with an average elevation of more than 4,000 m (Qiu, 2008). Livestock production has always been the main economic activity in the alpine regions, but the alpine grassland on the plateau is very susceptible and vulnerable to climate change and human interference. Low and insufficient feed quantity are the main limiting constraints of livestock productivity and feed source utilization in alpine area (Alagawany et al., 2020). Natural pasture biomass reaches a maximum in early autumn and then gradually decreases during the cold season. This means that a large number of livestock are slaughtered before winter due to feed shortages. Therefore, the construction of a sustainable livestock production system for the continuous feeding of ruminants throughout the year is a particular requirement in alpine regions (Alonso et al., 2013).

Besides, the outer layer of the silage stacks is subject to temperature changes during fermentation, and oxygen touch caused by defective tightness. The risk of exposure to an aerobic environment may occur each time material is removed from the silo. This means that the outer layer of the silage stacks may be subject to corruption or the material is poor quality because of insufficient fermentation or secondary fermentation. When the silage silo is opened, the anaerobic environment becomes an aerobic environment and the microorganisms that hibernate during oxygen deficiency begin to proliferate, resulting in spoilage of the silage, commonly known as secondary fermentation. This process is characterized by rising temperatures and fungal growth, and leads to dry matter and nutrient losses.

Ensiling is an effective pretreatment technology for harvested crops. It creates an acidic environment that reduces the risk of feedstock decay and combustion under anaerobic conditions. However, the storage temperature is a critical parameter that significantly affects the silage quality by influencing the microbial community diversity in silages (Wang Y. et al., 2019; Ren et al., 2020). In addition, silage fermentation is limited by repeated freezing and thawing low temperatures because not enough lactic acid is produced to ensure the production of good quality silage (Cao et al., 2011; Zhou et al., 2016; Dong et al., 2019; Wang C. et al., 2019; Ren et al., 2020). One of the key solutions to silage corruption mentioned above in laboratory scale is to simulate the seasonal and outer-layer changing conditions of repeated freezing and thawing low temperatures.

The starter culture is another key to the fermentation quality of silage. Meanwhile, the hypoxia, reduced pressure, low temperatures, strong ultraviolet radiation, and other special climate conditions, along with the unique ecosystem environment of the Qinghai-Tibet Plateau, have led to unique resources of lactic acid bacteria (LAB) with strong stress tolerance abilities (Yang et al., 2014). In our previous study, more than 2,000 strains of LAB were isolated from plants, saline ± alkali soil, a brine lake, indigenous yogurt, and the intestines of *Gymnocypris przewalskii* from the Qinghai-Tibet Plateau at an altitude of 3,100 to 4,800 m (Li, 2013; Lv, 2014; Zhang et al., 2015; Zhang, 2018). Some of these samples showed excellent potential as silage inoculants (Roier et al., 2015; Zhang et al., 2017b, 2018b), and have considerable application potential in solving the silage corruption caused by insufficient fermentation or repeated freeze-thaw conditions. Freezing damage to forages represents a major economic loss to agriculture. Studies have shown that freeze-thaw treatment could promote the development of *Lactobacillus* during ensiling. Therefore, the control of aerobe revitalization needs to concentrate on silages made from freeze-damaged forages (Dong et al., 2019). In this study, we used a well proven strain, QZ227, to improve the fermentation quality of silage at low temperature and then evaluated the silage quality variations under low temperatures freezing and thawing. We simulated constant low temperature fermentation and then outer layer fermentation conditions under varying low temperatures. The QZ227 strain, isolated from the Qinghai-Tibet Plateau, was selected and the aim was to try and improve silage quality by first subjecting it to a low constant temperature of 5°C followed by repeated freezing and thawing at various low temperatures. We aimed to slow down the outer-layer silage losses and seasonal silage corruption caused by insufficient fermentation at low temperatures or secondary fermentation.

MATERIALS AND METHODS

Characteristics of the Inoculum

The sources of the QZ227 inoculates are shown in **Supplementary Table 1**. The QZ227 strains were isolated from a wheat landrace grown on the Qinghai-Tibet Plateau at 3,100 m above sea level. Permission to use the sampling location was issued by Zhengzhou University, China, and local farmers. The QZ227 isolates were identified as *Lactobacillus plantarum* using 16S rRNA-based phylogeny combined with an assessment of their typical morphophysiological characteristics. Absorbance values at 560 nm and the pH values of the bacteria solution were measured every 2 h to determine its growth curve and acid-producing ability. The abilities of the isolates to resist NaCl, bile, acid, alkali, and low and higher temperature stress were measured through culturing in de Man, Rogosa, and Sharpe (MRS) broth containing 3.0 and 6.5% (w/v) NaCl or 0.1 and 0.3% (w/v) bile, with pH values from 1 to 10, at temperatures of 5 – 50℃, severally (Zhang et al., 2018a). The bacterial growth rates were assayed using the turbidimetry method at 550 nm combined with visual turbidity. The antimicrobial characters of QZ227 were evaluated by the method of bidirectional diffusion method (Balouiri et al., 2016), and the standard bacterial strains including *Micrococcus luteus* (*M. luteus*), *Escherichia coli* (*E. coli*), *Staphylococcus aureus* (*S. aureus*), *Salmonella enterica* (*S. enterica*), *Listeria monocytogenes* (*L. monocytogenes*), *Pseudomonas aeruginosa* (*P. aeruginosa*), and *Bacillus subtilis* (*B. subtilis*) were bought from the China General Microbiological Culture Collection Center (CGMCC). The inhibition zone diameter was measured after anaerobic incubation at 30°C for 24 h.

Inoculates and Silage Preparation

The whole profile for silage making and fermentation is shown in **Supplementary Figure 1**. Revitalized QZ227 isolates were

inoculated into liquid MRS broth and cultured for 24 h. The viable cell concentration of QZ227 was 8 log CFU/mL.

Common hexaploid wheat plants grown in experimental field of Henan Provincial Key Laboratory of Ion Beam Bioengineering, Zhengzhou University, Xinxiang, China, was harvested on May 16, 2019 and sent to the silage laboratory within 2 h. The raw wheat materials were wilted for 10 h and then chopped into 2–3 cm lengths using a forage chopper. A total of 12 kg of chopped wheat and 800 mL of bacteria solution were thoroughly mixed, 800 g of the mixed material was placed in a plastic film bag (Dragon N-6; Asahi Kasei Co., Tokyo, Japan) degassed, and sealed by a vacuum sealer (SQ-203S Vacuum Sealer; Asahi Kasei Co., Tokyo, Japan). The packed silage bags were fermented in a refrigerator at 5℃ for 30 days, afterward the fermentation condition changed to a variational temperature of 10°C during the day and −10℃ during the night alternately. Three replicates of each treatment were opened every 10 days during the ensiling process. These were then used for the microbial and chemical analyses. The remaining samples were stored in a freezer at −80°C for further microbial genome sequencing.

Viable Microbial Community

The dilution separation method was used to isolate and count the microbial community. A total of 10 g of silage was shaken with 90 mL of sterilized deionized water using a vortex mixer (Ika Vortex 3, Staufen, Germany), and serial dilutions (10^{-1} to 10^{-5}) were prepared in sterilized filtered water. Then 20 μL 10^{-1}, 10^{-2}, and 10^{-3} dilutions were separately coated onto agar medium plates.

Different cultural media were used for various viable cell counts. Lactic acid bacteria were cultured in MRS medium at 30°C for 2 days anaerobically and then numerated. In the same way, NA culture was used for aerobic bacteria, the potato dextrose agar (PDA) contained a sterilized 10% dihydroxysuccinic acid solution (final concentration: 1.5%) was used for yeasts and molds. The *E. coli* were numbered using eosin methylene blue (EMB). The NA, PDA, and EMB agar media were purchased from QingDao Hope Bio-Technology Co., Ltd., Qingdao, China. The agar plates coated with the different dilutions were incubated at 30°C for 2 days. Then, the 10^{-1} and 10^{-2} dilutions were heated in a constant water bath at 75°C for 15 min and coated onto NA and *Clostridium difficile* agar so that the *B. subtilis* and *C. difficile* colonies, respectively, could be counted. All the colonies were counted and the logarithmic number of viable colony-forming units in fresh matter (l g CFU/g FM) was calculated.

Microbial Community Composition

A total of 10 g of refrigerated silage in 40 mL sterile deionized water was vibrated by an electron oscillator at 120 rpm for 2 h and then filtered using double gauze masks. A total of 40 mL sterile water was used to wash the microbial residues off the gauze. The filtrate was centrifuged for 15 min at 10,000 × *g*∼12,000 × *g* and 4°C, and the solids were collected and stored at −80℃ for further research.

The Metagenomics Sequencing was commissioned to Majorbio Bio-Pharm Technology Co., Ltd. (Shanghai, China). Follows the steps (Jiang et al., 2019; Yang et al., 2019): (i) DNA extraction and PCR amplification, The kit we selected is E.Z.N.A. Soil DNA Kit purchased from Omega Bio-tek (Norcross, GA, United States). (ii) Illumina MiSeq sequencing, amplicon sequencing was conducted using an Illumina MiSeqPE250 platform (Shanghai Majorbio162 Bio-pharm Technology Co., Ltd., China). (iii) Processing of the sequencing data, the original 16S rRNA sequencing reads were demultiplexed and quality-filtered by the software of Trimmomatic[1], and merged by FLASH based on the indexes below: (i) the 300 bp reads were truncated receiving an average quality score of < 20 over a 50 bp sliding window. (ii) Only overlapping sequences longer than 10 bp were assembled according to their overlapped sequence. The maximum mismatch ratio for the overlap region was 0.2. Reads that could not be assembled were discarded. (iii) Samples were distinguished according to their barcode and primers, and the sequence direction was adjusted based on exact barcode matching. A 2 nucleotide mismatch was allowed during primer matching. Operational taxonomic units (OTUs) with a 97% similarity cutoff (Liu et al., 2017) were clustered using UPARSE (version 7.1[2]), and chimeric sequences were identified and removed. The taxonomy of each OTU representative sequence was analyzed by RDP Classifier[3] against the 16S rRNA database (e.g., Silva SSU128) using a confidence threshold of 0.7.

Chemical Composition

A total of 10 g of silage materials were mixed with 90 mL of sterilized, purified water. About 50 mL of the liquid, after the organisms and visible solid matters had been filtered out with qualitative filter paper, was stored in a sterile container at −20°C for further NH_3-N and organic acid analyses (Shah et al., 2020a,b), while the remaining mixture was used to determine the pH. The dry matter, crude protein, and crude ash were assayed by the atmospheric pressure drying method (AOAC 934.01), the high temperature ashing method (AOAC 942.05), and the Kjeldahl method (AOAC 979.09), respectively.

Silage remained was further dried in an thermostatic blast furnace (Shanghai Shilu Instrument Co., Ltd., Shanghai, China) at 65°C for 2 days and then the percentage dry matter and free water contents were calculated according to the following formulas:

$$\text{Dry matter (\% FM)} = \frac{(M2-M0) * 100\%}{M1-M0}$$

Free water (% FM) 100%− DM%

M0, mass of the silage bag

M1, mass of silage prior to drying

M2, mass of the silage after it had been dried for 48 h.

The dried silage was ground using a high speed pulverizer (FW-100, Taisite Instrument Co., Ltd., Jinghai, Tianjin, China). The crude protein content of the silage powder was determined

[1]http://www.usadellab.org/cms/index.php?page=trimmomatic

[2]http://drive5.com/uparse/

[3]http://rdp.cme.msu.edu/

using automatic Kjeldahl apparatus (K1100, Jinan Hanon Instruments Co., Ltd., Jinan, China) with $CuSO_4$ and K_2SO_4 at a ratio of 1:15 as the catalyst. The standard concentration of the titrated H2SO4 solution was determined by color indicator titration method (Zhang et al., 2018b) with anhydrous sodium carbonate and bromocresol green ± methyl red as an color indicator. The crude ash content was calculated after incineration for 2 h at 550°C in a muffle furnace (REX-C900, RKC Instrument Inc., Osaka, Japan), followed by burning in an ashing furnace until no smoke was produced. The detergent fiber was determined by the Automatic Fiber Determination System (CXC-06, Zhejiang Top Instrument Ltd., Hangzhou, China). The organic acid content in silage were measured by high performance liquid chromatography, the chromatographic conditions and sample pretreatment methods were established according to the related literatures (Ni et al., 2017; Zhang et al., 2018b), the standard acids were purchased from Sigma-Aldrich Chemical Co. (St. Louis, MO, United States). The NH_3-N was measured using the indophenol blue method as described. A standard formula was created using an NH_4Cl solution as the reference. The absorbance of the sample was compared with the standard formula to determine the NH_4Cl content using the following equation:

$$\mathrm{NH_3{-}N\ (g/kg\ dry\ matter)} = \frac{\left(\mathrm{NH_4Cl\ concentration}\right) * 17}{53.5 * (\text{silage dry matter})}.$$

Statistical Analyses

Two-way analysis of variance was conducted with inoculation amount and fermentation time as the primary variables. Many variables interact significantly with each other, so the inoculation effect at each fermentation time was examined by one-way analysis of variance (ANOVA), followed by a multiple comparison by Tukey's test. The statistical significance of the antibacterial activity and the NH_3-N producing ability of pathogens were evaluated using ANOVA with Tukey's HSD test. These analyses were carried out using IBM SPSS Statistics 19 software[4], and the pH variations and microbial communities were plotted using Origin software Pro 8.5.1[5]. A P-value of < 0.05 was considered statistically significant and a P-value of < 0.01 was considered very significant. The bacterial and fungal sequencing data were analyzed using the free online Majorbio Cloud Platform[6].

[4]https://www.ibm.com/analytics/cn

[5]http://www.originlab.com/index.aspx?go=Products/Origin

[6]www.majorbio.com

RESULTS AND DISCUSSION

Characteristics of the Inoculum

The morphological characteristics, physiological and biochemical properties of QZ227 are shown in **Supplementary Table 1**. QZ227 cannot use glucose to produce gas, which means that it has a fermentation type called homofermentation. It is characterized as being low temperature resistant and has good high temperature tolerance because it can grow well at 5 and 50°C. Furthermore, it can grow well at 3.0 and 6.5% NaCl and under 0.1 and 0.3% bile conditions. Therefore, the QZ227 isolates were tolerant of bile and salt. In addition, QZ227 can live in extremely acid conditions of pH 2.0 and extremely alkaline conditions of pH 10.0.

The growth curve determination process showed that Q227 produced lactic acid and acetic acid (**Supplementary Figures 1**, **2**). After cultivation for 48 h, the lactic acid and acetic acid concentrations in QZ227 were 44.99 and 8.85 mg/mL, respectively.

Table 1 shows that QZ227 has broad-spectrum antibacterial activity and an antibacterial effect on gram-negative pathogens, including *Escherichia coli, Pseudomonas aeruginosa, Salmonella enterica*, and Gram-positive pathogens, including *Micrococcus luteus* and *Staphylococcus aureus*.

Silage Preparation

The chemical composition and microbial community composition of the raw materials prior to ensiling is shown in **Supplementary Table 2**. The pH of the raw materials was 6.57 and the moisture content was 63.48% FM. The crude protein and ether extract contents were 4.65 ± 0.12% DM and 12.51 ± 0.75% DM, respectively, and the neutral detergent fiber (NDF) and acid detergent fiber (ADF) contents were 50.37 ± 2.21% DM and 34.12 ± 1.55% DM, respectively. No organic acid was detected. The LAB counts for the raw materials were 2.69 ± 0.37 log CFU/g FM. *E. coli, F. fungi, S. cerevisiae*, and *B. subtilis* were detected, but aerobic bacteria and *S. marcescens* were not detected in the raw materials.

Treatment Effects on pH

As shown in **Figure 1**, the pH of the silage inoculated with QZ227 had decreased to 4.27 by day 40. Furthermore, the pH of the silage inoculated with LAB remained relatively low in the low temperature environment. However, the pH of the CK group without inoculates was undesirably above 6.17 during the whole variable low temperature process where the temperature varied from −10 to 10°C. As the fermentation temperature rose to 25°C

TABLE 1 | The pathogen inhibition of QZ227.

	Micrococcus luteus	*Staphylococcus aureus*	*Bacillus subtilis*	*Escherichia coli*	*Pseudomonas aeruginosa*	*Salmonella enterica*
CK	–	–	–	–	–	–
QZ227	+++	+++	–	++	+++	+++

The inhibition zone contains the external diameter of oxford cup (7.68 mm). Inhibition zone: Less than 8.00 mm, –; 8.00–12.00 mm,+; 12.00–16.00 mm,++; More than 16.00 mm,+++.

from day 60 to day 70, the pHs of all the silage groups decreased under both the anaerobic and aerobic conditions.

The pH is the main indicator of silage preservation quality and fermentation efficiency, and represents the final acidity of the fermentation product. The feeding intakes and rumen digestion stability of silage with low pH are poor, but a higher pH is often accompanied by a greater ammonia nitrogen content, which also leads to a poorer preservation quality and lower feed intake.

The dry weight contents should be combined when making a silage pH evaluation. A silage with a dry weight content of less than 28% has a higher quality when the pH is between 3.8 and 4.2, and silage with a dry weight greater than 28% can be better preserved with a pH greater than 4.5. Moist silage with a pH greater than 4.2 is difficult to preserve over long periods of time. In addition, when the pH exceeds 4.4 (except for low moisture silage), the activities of spoilage bacteria and butyric acid bacteria are generally more intense during the silage fermentation process. The dry matters of the silage in this study were above 33%, at the various low temperatures experienced from days 10 to 60. The pH of the CK group without inoculates indicated that it would be difficult to preserve the silage, whereas the pH of the inoculated silage suggested that QZ227 improved preservation.

During the silage process, lactic acid bacteria convert carbohydrates in raw materials into organic acids. The most important ingredient is lactic acid. The higher the lactic acid content, the better the aromatic flavor of the feed, the higher the feed intake, and the better the aerobic stability (Li et al., 2014). When the lactic acid content is 8–10% DM and it accounts for more than 75% of the total acid content, then the quality of the silage is good, but levels below 5% DM lead to poor quality silage. Many factors have been shown to affect the proportion of produced organic acids, including the microbial population, inoculum source, substrate complexity, nutrient availability, pH, and temperature (Bastidas-Oyanedel et al., 2015).

No lactic acid was detected in the CK group during the variant low temperature fermentation stage. During the continuous low temperature fermentation (5°C) stage, the lactic acid content of the silage inoculated with QZ227 continuously increased to 3.71 ± 1.31 mg/ml at day 30, but the lactic acid content of the fermented silage decreased to 2.04 ± 0.35 mg/ml when subjected to temperature variation. In this study, QZ227 promised a better aerobic stability than CK group.

The acetic acid contents of the QZ227 and the CK silages were not significantly different throughout the whole fermentation process. No propionic acid was detected during continuous low temperature fermentation and during the following variable temperatures stage. Propionic acid is produced in silage when the temperature rises to 25°C under both anaerobic and aerobic conditions. Heterofermentative lactic acid bacteria produce high concentrations of acetic or propionic acid. These acids inhibit the growth of spoilage yeasts and molds and improve the shelf life of the silage during feedout (Queiroz et al., 2013). However, they do not affect the relative abundances of predominant bacteria, such as *Lactobacillus*, *Weissella*, or *Pediococcus* (Ogunade et al., 2018). Propionic acid can be added as an antifungal agent to enhance the shelf life of silages during feedout (Kung et al., 2000). The propionic acid content of the QZ227 silage was higher than the CK group at 25°C although the increase was not significant ($P \geq 0.05$).

The dry matter contents of the CK group fermented at low temperature from days 10 to 60 was 33.77–34.12% and the dry matter of the silage fermented with QZ227 was from 33.30 to 34.22%. The psychrotrophic *L. plantarum* inoculates lowered the moisture content of silage at low temperature compared with raw materials, which promised less DM loss during conservation (Zhang et al., 2017a). The results of this study were consistent with the phenomena. In this study of a constant low temperature of 5°C, the dry matter content of control group reduced to $33.77 \pm 0.44\%$ from $34.45 \pm 0.14\%$, while the QZ227 group reduced to 33.30 ± 0.33 from $33.62 \pm 0.20\%$. QZ227 promised less DM loss at the constant low temperature of 5°C, which were consistent with the research before (Zhang et al., 2018b).

Cultural Microorganisms

During the natural silage process, the epiphytic lactic acid bacteria on the plant surface plays a decisive role in the quality of the final silage. **Figure 2** shows that *F. fungi* and *E. coli* were detected in the CK group after the silage had fermented for 30 days, but neither were found in the QZ227 silage. At day 60, *S. cerevisiae*, *F. fungi*, and *E. coli* were found in the CK group, whereas they were not detected in the QZ227 group. These results, combined with the antibacterial activity (**Supplementary Table 1**), demonstrated that QZ227 had broad-spectrum antibacterial activity and can effectively inhibit the pathogens found in silage.

When the temperature increased to 25°C and the conditions were anaerobic for 10 days, pathogens *S. cerevisiae*, *F. fungi*, and *E. coli* occurred in QZ227, but the *F. fungi* and *E. coli* numbers were lower than in the CK group. Similar pathogen trends to anaerobic fermentation were detected when the temperature increased to 25°C and the silage was exposed to an aerobic environment for 10 days (**Figure 3**).

QZ227 can inhibit viable *F. fungi* and *E. coli* in silage exposed to aerobic conditions and atmospheric temperatures. However, under anaerobic conditions and atmospheric temperatures, the QZ227 only inhibited *F. fungi*.

The main factors affecting fermentation are fermentation time and inoculates. The principal effect analysis showed that the chemical components of the silage were significantly affected by fermentation time and inoculates. However, the NH_3-N levels were significantly affected by the interactions between fermentation time and inoculates (**Table 2**).

The organic acid levels were significantly affected by fermentation time. Lactic acid was significantly affected by inoculates, but acetic acid and propionic acid were not. Lactic acid was also significantly affected by the interactions between time and inoculates.

The cultured microorganisms, except *S. cerevisiae* and *F. fungi*, were also significantly affected by fermentation time and inoculates. The principal factors at day 70 were oxygen and inoculates. **Table 2** shows that oxygen had a significant effect on NH_3-N and lactic acid, whereas inoculates had a significant effect on both pH and NH_3-N.

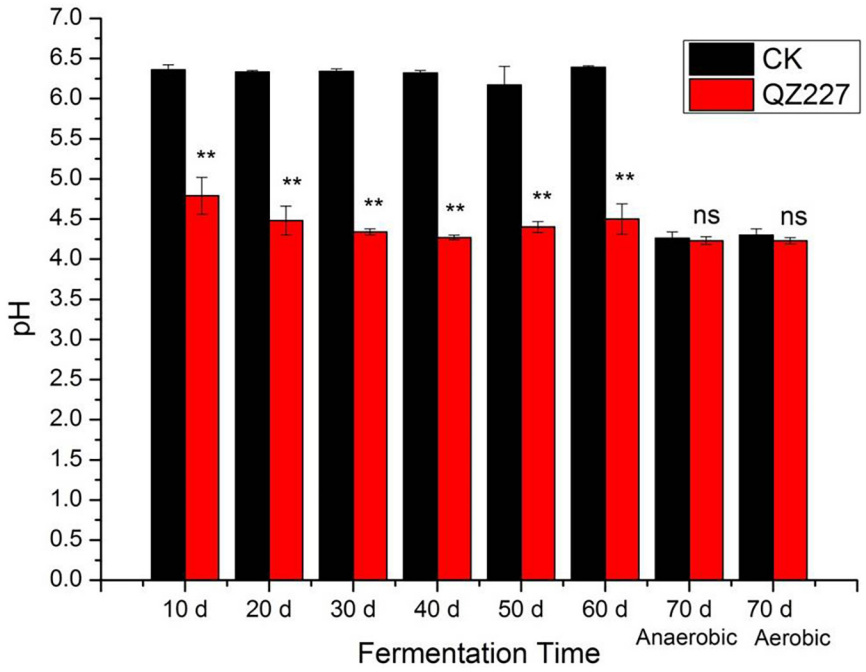

FIGURE 1 | The pH variations during the fermentation process. Ns, not significant, **, very significant, $0.001 < P \leq 0.01$.

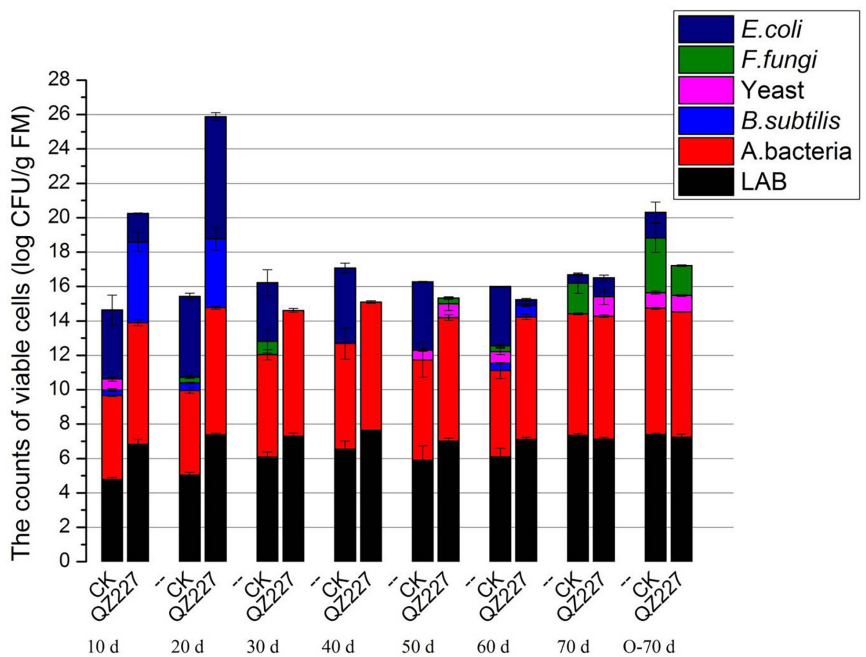

FIGURE 2 | The number of cultural microorganisms during the fermentation process.

Microbial Community Composition

The most abundant epiphytic bacteria in the raw wheat were *Pantoea*, followed by *Pseudomonas*. In the first 30 days of low temperature fermentation and the following repeated freeze-thaw stage, *Leuconostoc* was the predominant strain in CK while *Lactobacillus* was the predominant strain in silage inoculated with QZ227. The inoculants boosted the dominant fermentation flora and changed the bacterial composition. *Lactobacillus* abundance increased quickly in CK after 10 days of high temperature storage.

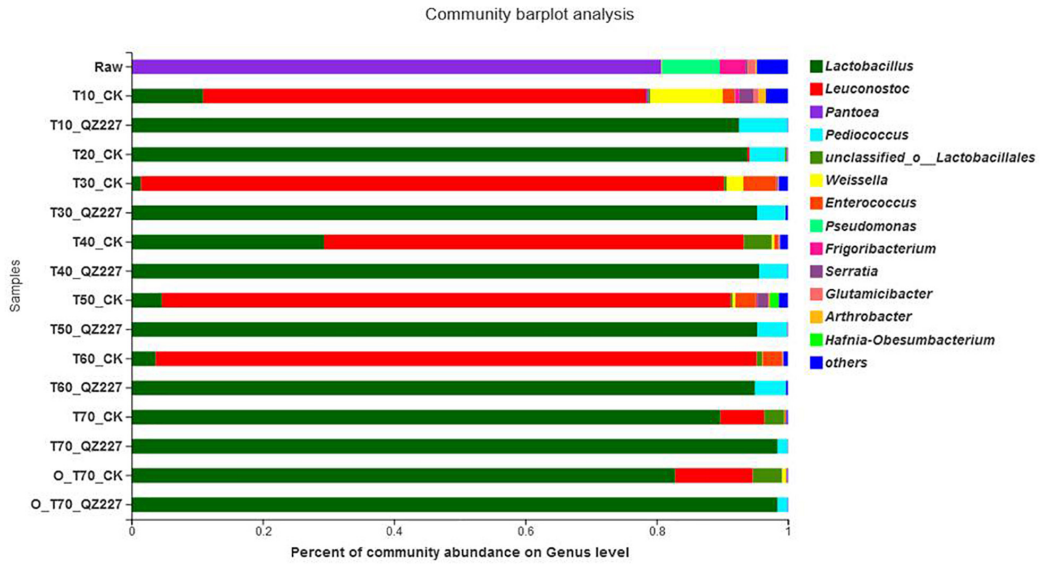

FIGURE 3 | Analysis of bacterial community composition.

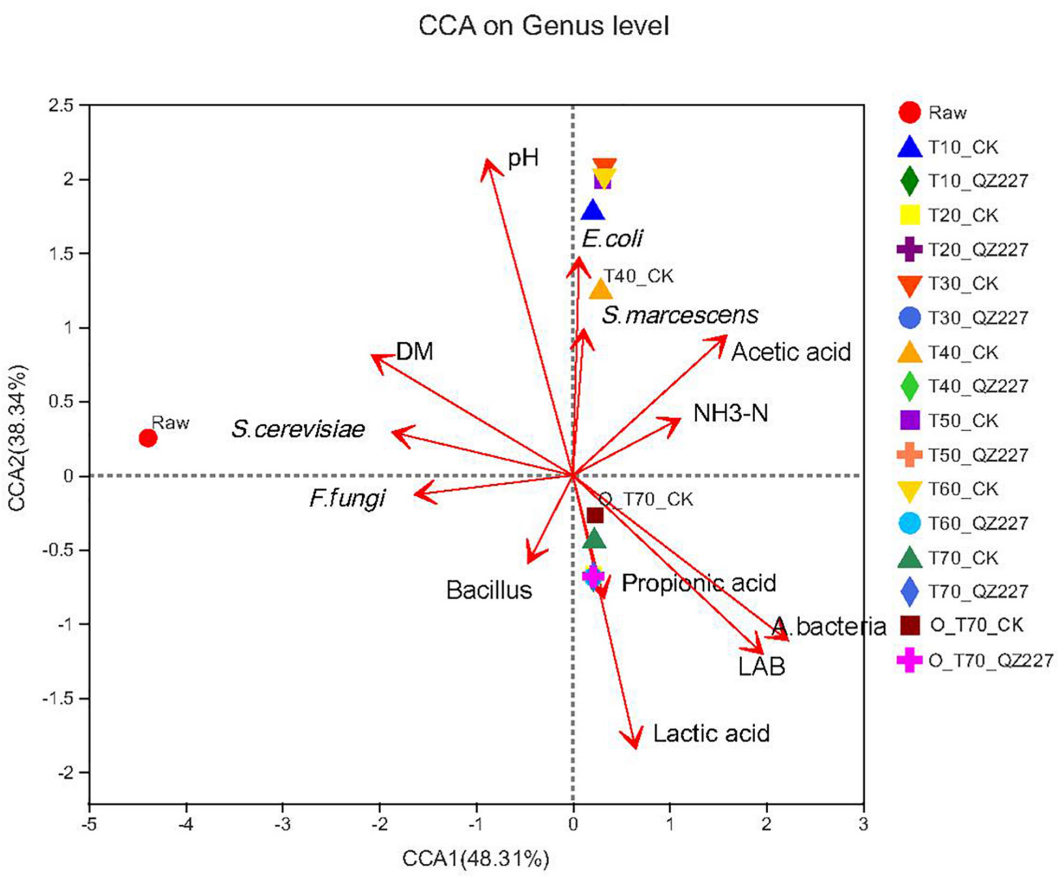

FIGURE 4 | Bacteria canonical correlation analysis (CCA) at the genus level. The dots in different colors or shapes represent the environment or condition sample groups. The red arrows represent quantitative environmental factors, and the length of the arrows for environmental factors can represent the degree of influence (explanatory volume) that an environmental factor has on the species data. The distance from the projection point of the samples to the origin represents the relative influence of the environmental factor on the distribution of the sample community.

TABLE 2 | Variations in chemical components (% FM) and principal effect analysis.

Items	Additives	Fermentation time						Sig.			Fermentation time		Sig. at days 70		
		10 d	20 d	30 d	40 d	50 d	60 d	T	I	T × I	70 d	O-70 d	O	I	O × I
Lactate	CK	0.00 ± 0.00^{A}	0.00 ± 0.00^{a}	0.00 ± 0.00^{A}	0.00 ± 0.00^{A}	0.00 ± 0.00^{a}	0.00 ± 0.00^{a}	**	**	**	5.62 ± 0.66	2.93 ± 0.41	**	ns	**
	QZ227	1.85 ± 0.42^{B}	3.00 ± 0.34^{b}	3.71 ± 1.31^{B}	3.85 ± 0.96^{B}	2.61 ± 0.85^{b}	2.04 ± 0.35^{b}				4.45 ± 0.91	3.36 ± 0.85			
Acetic acid	CK	1.16 ± 0.3	1.41 ± 0.52	1.72 ± 0.32	2.41 ± 0.37	1.66 ± 0.48	1.62 ± 1.12	**	ns	ns	1.05 ± 0.12	0.65 ± 0.46	ns	ns	ns
	QZ227	0.97 ± 0.17	1.42 ± 0.09	1.79 ± 0.61	1.64 ± 0.56	1.23 ± 0.38	0.95 ± 0.25				1.37 ± 1.03	1.22 ± 0.91			
Propionic acid	CK	nd	nd	nd	nd	nd	nd	**	ns	**	2.06 ± 013	0.91 ± 0.79	*	ns	*
	QZ227	nd	nd	nd	nd	nd	nd				2.17 ± 0.52	1.59 ± 0.16			
NH_3-N	CK	0.18 ± 0.03	0.16 ± 0.04	0.24 ± 0.01	0.34 ± 0.04	0.37 ± 0.06	0.33 ± 0.05^{a}	**	**	*	0.47 ± 0.05^{a}	0.35 ± 0.02	**	**	ns
	QZ227	0.21 ± 0.03	0.08 ± 0.08	0.16 ± 0.08	0.31 ± 0.07	0.29 ± 0.05	0.22 ± 0.05^{b}				0.34 ± 0.05^{b}	0.31 ± 0.03			
Dry matter	CK	34.45 ± 0.14^{A}	34.59 ± 0.21	33.77 ± 0.44	34.28 ± 0.41	34.12 ± 0.52	34.24 ± 0.12^{a}	**	**	ns	33.55 ± 0.34	33.36 ± 0.05	ns	ns	**
	QZ227	33.62 ± 0.20^{B}	34.09 ± 0.42	33.30 ± 0.33	34.03 ± 0.14	34.22 ± 0.98	33.72 ± 0.26^{b}				33.49 ± 0.01	33.03 ± 0.21			

*No butyric acid were detected. Sig. Significance, T Time, I Inoculates, O Oxygen. Ns, not significant, *0.01 < P ≤ 0.05, **P ≤ 0.01.*
^{ab} different letters indicate significantly differences at 0.01 < P < 0.05; ^{AB} different letters indicate significantly differences at P ≤ 0.01.

The bacterial community heatmap at the genus level is shown in **Supplementary Figure 4**. They showed that the bacterial community in the silage was affected by inoculates, and the different bacterial categories were differentially affected by the inoculates factors.

The results showed that pH had a negative correlation with lactic acid and viable lactic acid bacteria, but had a positive correlation with viable *E. coli, S. marcescens, S. cerevisiae, F. fungi*, and DM (**Figure 4**). Under aerobic conditions for 70 days, the lactic acid, propionic acid, lactic acid bacteria, and aerobic bacteria had greater impacts on the silage fermented with QZ227 than on the CK group. Similarly, under anaerobic conditions for 70 days, lactic acid, propionic acid, lactic acid bacteria, and aerobic bacteria also had greater impacts on QZ227 silage than on the CK silage.

The effects of different environmental factors on bacterial community composition in the silage are shown in the Spearman correlation heat map (**Figure 5**). The bacterial community compositions in the silage were affected by viable lactic acid bacteria, aerobic bacteria, *E. coli*, pH, DM, moisture, and lactic acid. The bacterial genera were differentially affected by the environmental factors. The lactobacillus genus was also significantly affected by propionic acid content ($0.01 < P \leq 0.05$).

According to **Figure 6**, *Filobasidium* was the most abundant fungal community in the raw materials and silage fermented for 10 days. At day 30, more fungal genera were detected in the CK group than in QZ227, and the percentages for pathogens in the CK group, such as *Aspergillus*, *Sporidiobolaceae*, *Hypocreaceae*, *Pleosporales*, *Cutaneotrichosporon*, *Alternaria,* and *Cystobasidiomycetes*, were larger than in QZ227. We concluded that QZ227 decreased the growth of these fungal pathogens in silage under low temperature (5°C).

From day 40 to day 60 of varying low temperature conditions, the main fungal genus in QZ227 was more obvious and uniform than in the CK group. The numbers and varieties of species from the main fungal genus in the CK group were not clear. QZ227 inhibited the growth of certain fungi genera from days 30 to 60. At day 40, the fungal pathogen percentages for *Pichia*, *Mucoromycota*, *Aspergillus*, *Hypocreaceae*, *Sordariales*, and *Agaricales* in CK were higher than in QZ227. At day 50, the fungal pathogen percentages for *Cladosporium*, *Saccharomycetaceae*, *Aspergillus*, *Mrakia*, *Sporidiobolaceae*, *Hypocreaceae*, *Pleosporales*, and *Sordariales* in CK were higher than in QZ227. At day 60, the *Pichia*, *Alternaria*, *Aspergillus*, *Agaricales*, *Plectosphaerella* percentages were higher than in QZ227. We concluded that QZ227 inhibited fungal growth under varying low temperature conditions.

Antifungal supplements are mostly used to hinder the growth of yeasts, fungi, and other undesirable microorganisms to improve fermentation of the silage (Shah et al., 2020b). Yeast has long been considered to be the main microorganism that causes aerobic deterioration in silage because the aerobic deterioration of silage is closely related to the metabolism of the main yeast strain (da Silva et al., 2020). The yeasts that cause aerobic deterioration in silage were divided into two groups. The first contained acid-using fungi, such as *Candida*, *Endomycopsis*, *Hansenula,* and *Pichia*. The other group used sugars, such as

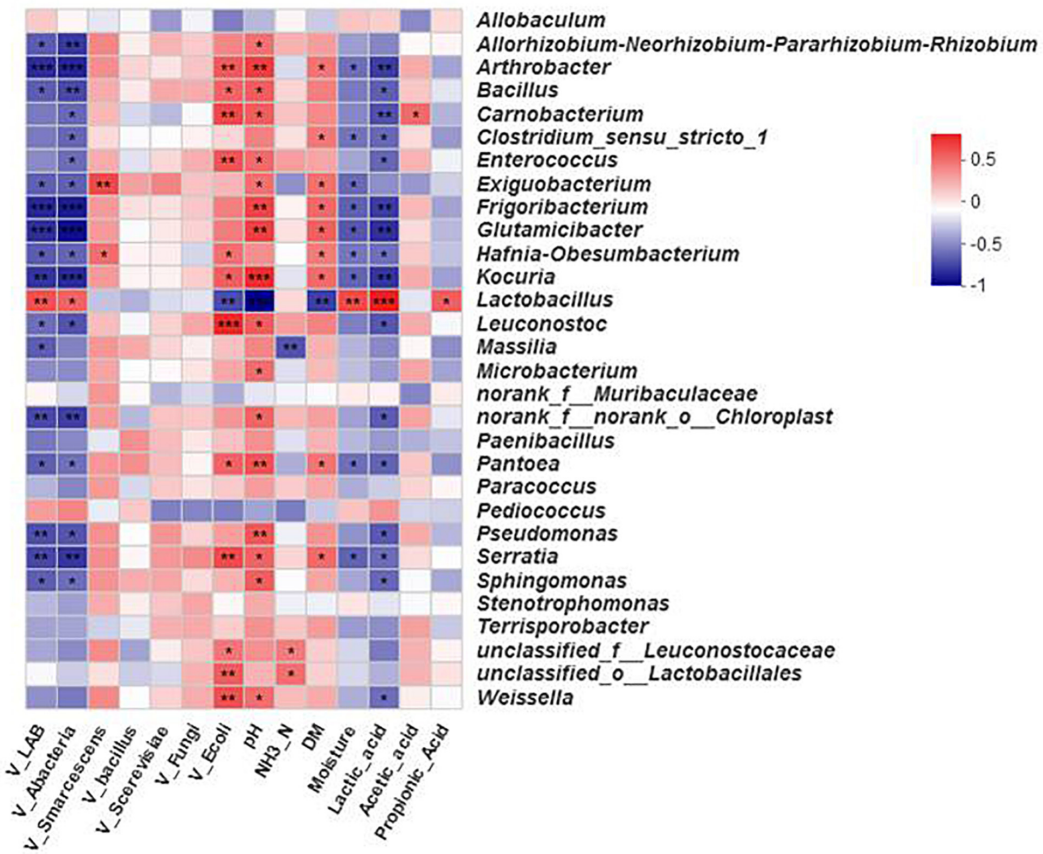

FIGURE 5 | Spearman's correlation heat map for bacteria at the genus level. *$0.01 < P \leq 0.05$, **$0.001 < P \leq 0.01$, ***$P \leq 0.001$. Microbial classification and environmental variables. The *x*-axis and *y*-axis are environmental factors and species, respectively. Different *R* values are shown in different colors.

the genus *Torulopsis*, *Pichia manshurica*, *Candida ethanolica,* and *Zygosaccharomyces bailii*, which meant that they were able to resist acetic acid and, therefore, had a greater effect on the aerobic metamorphism of silage during the early fermentation stage (Wang et al., 2018). At the later stage of silage production, *Zygosaccharomyces bailii* was the main yeast causing aerobic metamorphism in silage.

Figure 6 shows that at day 70, the dominant fungi in CK was *Pichia*, which meant that the CK group silage was in the initial stage of aerobic decay at day 70.

Mucoromycota, *Aspergillus bubble*, *Rhizopus oryzae*, *Penicillium acanthopanax*, and *Penicillium decumbens* were detected in moldy silage (Fu, 2012). In this study, after exposure to oxygen for 70 days, *Mucoromycota* were detected in the CK group, which meant that the CK group became moldy after exposure to oxygen for 70 days. *Pichia* were the dominant fungi while the *Mucoromycota* proportion was small in silage fermented with QZ227, which suggested that QZ227 inhibited the growth of *Mucoromycota*, and slowed down the speed and extent of corruption when the silage was exposed to oxygen.

Figure 7 shows that pH had a negative correlation with lactic acid, and viable lactic acid bacteria had a positive correlation with viable *E. coli*, *S. marcescens*, and DM, which was consistent with **Figure 4**. Under aerobic conditions for 70 days, the lactic acid and propionic acid had a greater impact on the silage fermented with QZ227 compared to the CK group, which was consistent with **Figure 4**. Similarly, under anaerobic conditions for 70 days, the lactic acid, propionic acid, lactic acid bacteria, and aerobic bacteria had a greater impact on QZ227 compared to CK, which was also consistent with **Figure 4**.

The fungal community composition in the silage was affected by all the environmental factors except DM and moisture, which had no effect on fungal community composition (**Figure 8**).

Intragroup Difference Analysis of Paralleled QZ227 at Day 60

The pHs of the three paralleled silages in the QZ227 group were 4.49, 4.70, and 4.32, respectively, and these differences were relatively large. The bacterial and fungal species in the paralleled QZ227 silages at day 60 were then analyzed.

Figure 9A shows that there were few or no differences between the number of bacterial genera among intro-groups QZ227①, QZ227②, and QZ227③. However, each of them

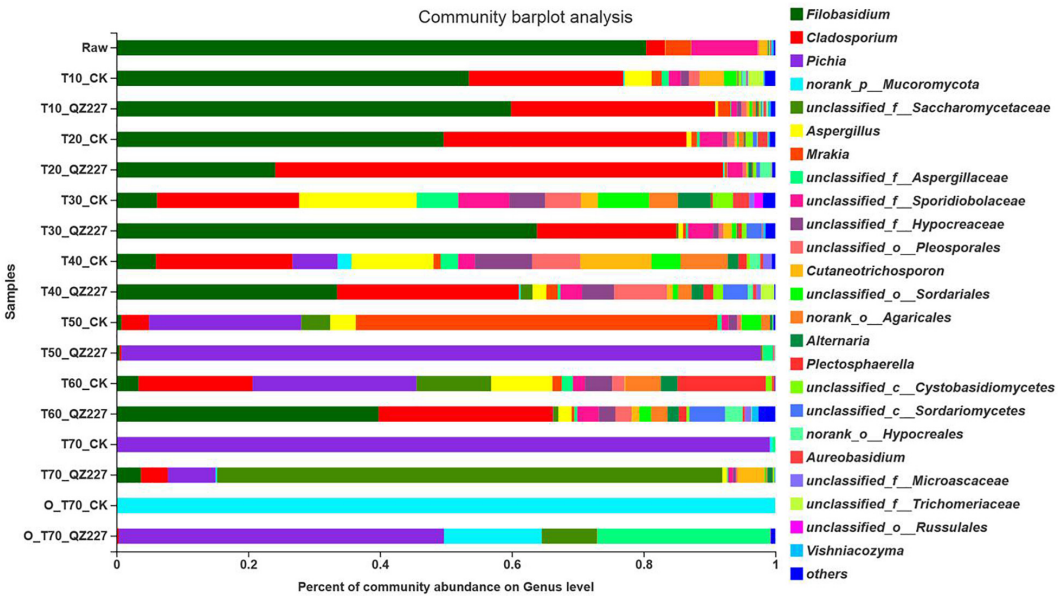

FIGURE 6 | Fungal community barplot analysis at the genus level. The *y* – axis is the name of the sample, the *x* – axis is the proportion of the species, Colored columns indicate different genera, and the length of the columns represents the proportion of the genera.

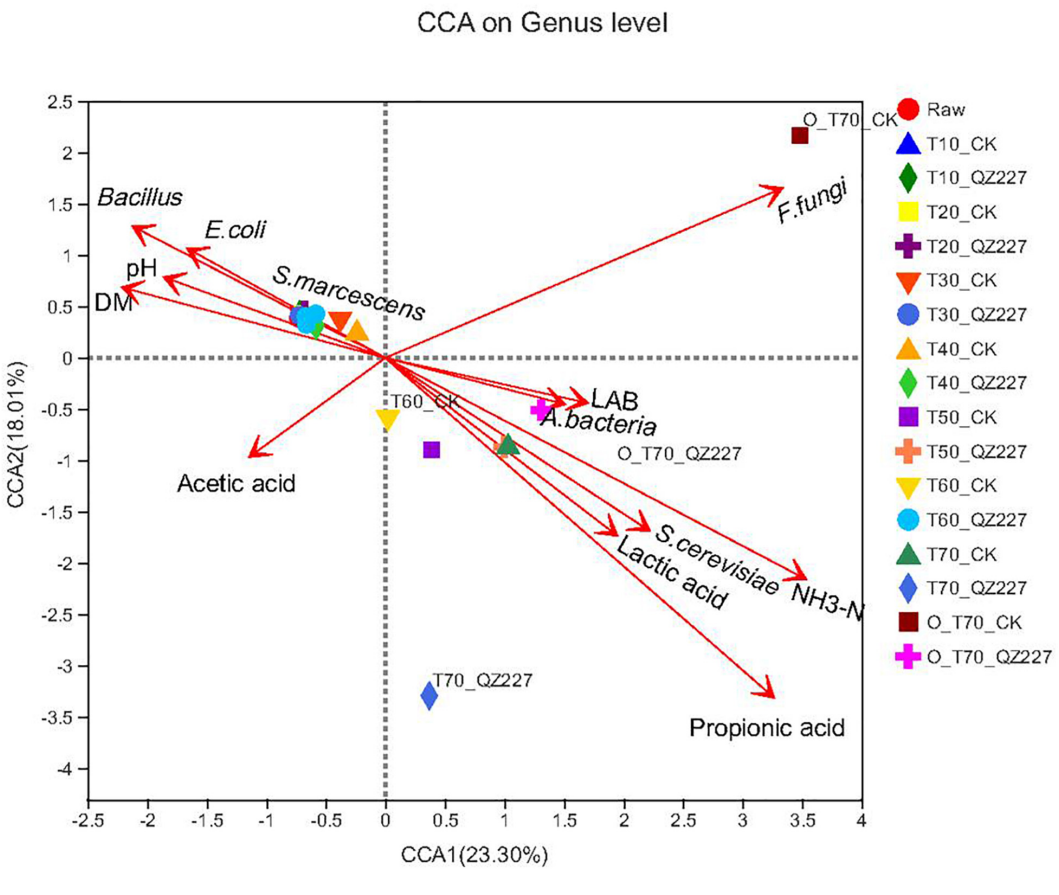

FIGURE 7 | Fungi CCA at the genus level. The dots in different colors or shapes represent the environment or condition sample groups.

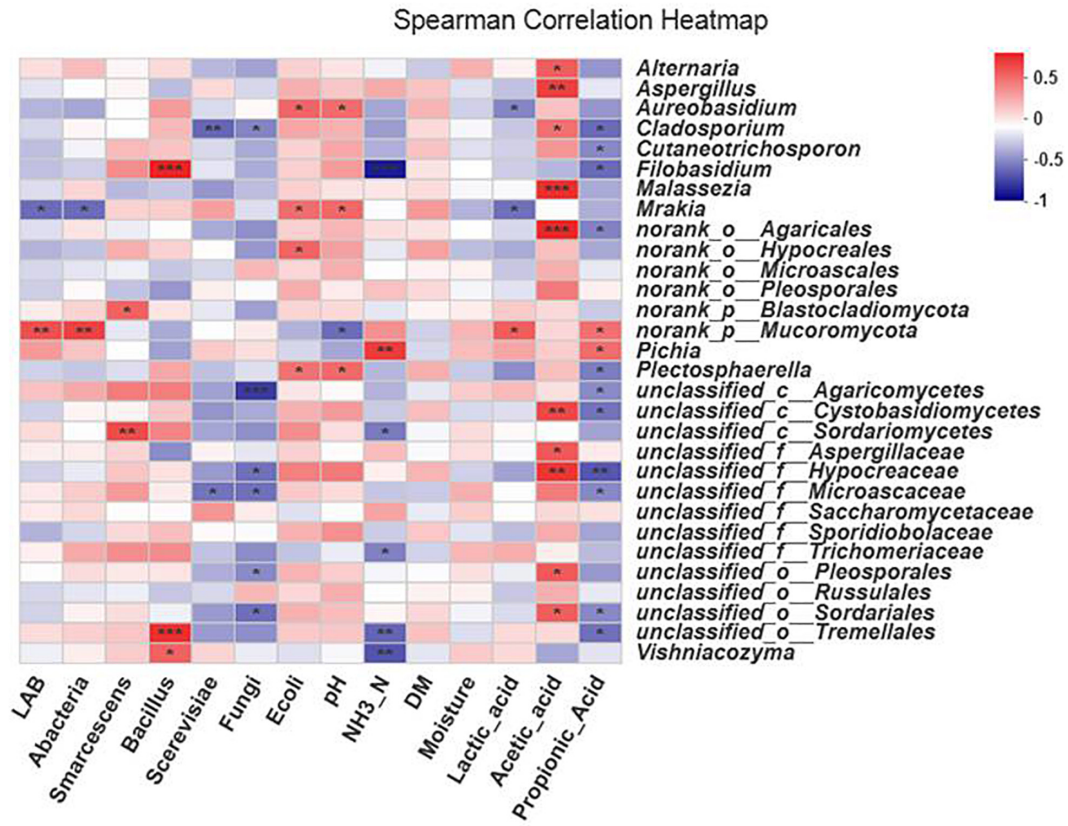

FIGURE 8 | Spearman's correlation heat map for fungi at the genus level. *$0.01 < P \leq 0.05$, **$0.001 < P \leq 0.01$, ***$P \leq 0.001$. The *x*-axis and *y*-axis are environmental factors and species, respectively. Different *R* values are shown in different colors.

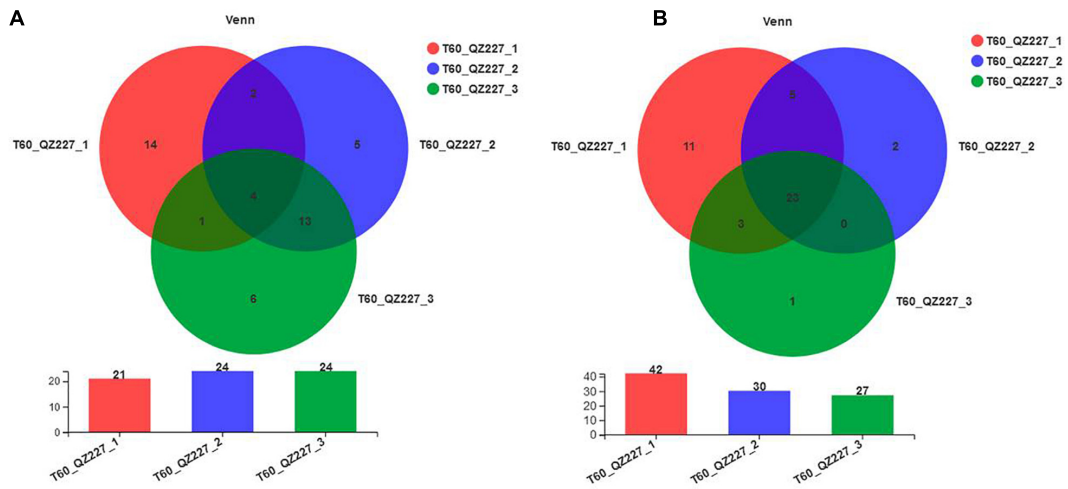

FIGURE 9 | Bacterial **(A)** and fungal **(B)** species in the paralleled QZ227 groups at day 60. The numbers in the overlapped areas represent the number of genera common to multiple groups and the numbers in the non-overlapped areas represent the number of genera unique to the corresponding group.

contained a unique genus of bacteria. The fungal genera among the QZ227 intro-groups were different (**Figure 9B**). The number and varieties of microorganisms probably affected the pH of the QZ227 intro-groups.

Figure 10 shows that *Lactobacillus* was the predominant stain. However, *Pediococcus* were also detected and *Pediococcus* abundance increased with pH in QZ227. The fungal community abundances were different among the QZ227 intro-groups.

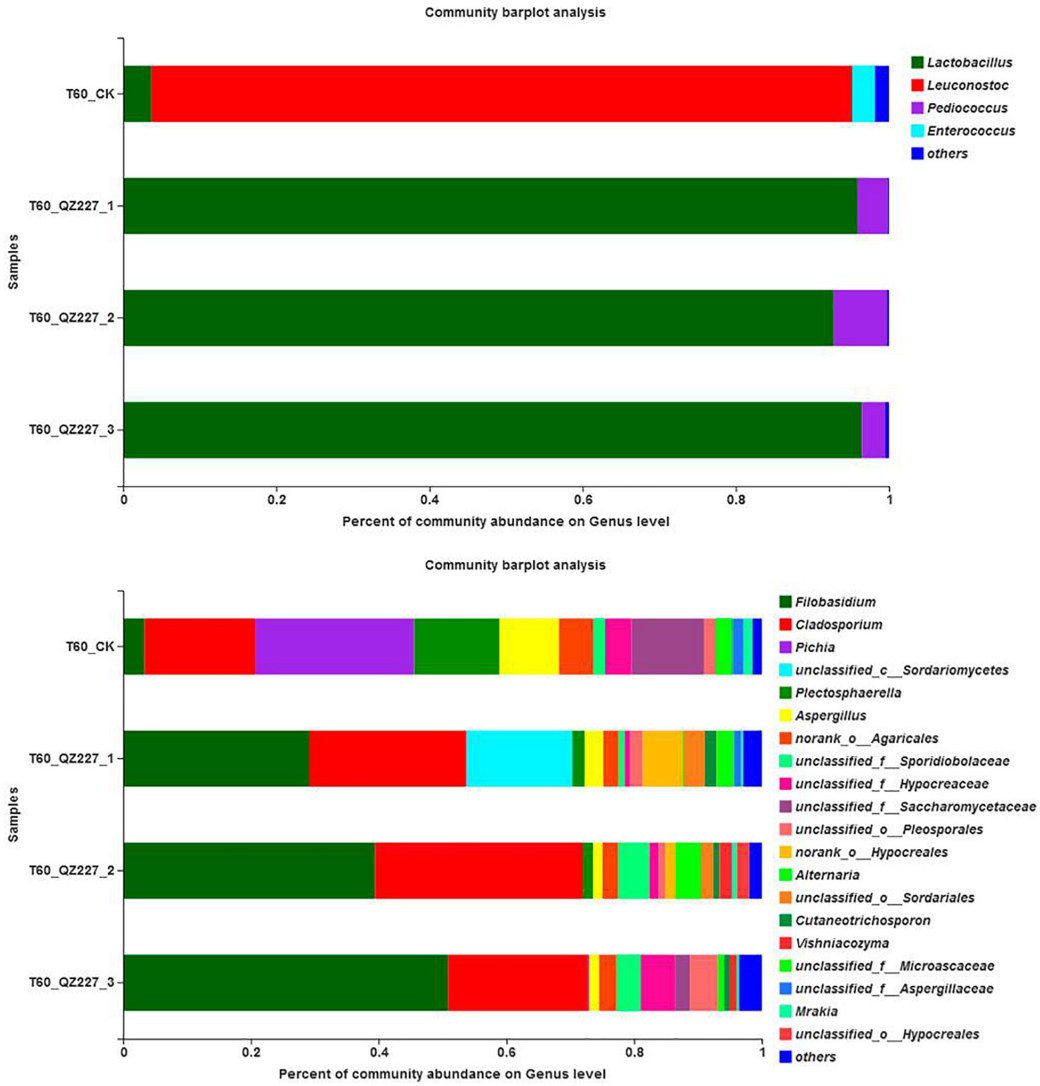

FIGURE 10 | Community abundances of the paralleled QZ227 groups at day 60.

Above all, the pHs of the QZ227 introgroups were significantly different. Possible reasons for these differences were the different number and varieties of microorganisms, and the different *Pediococcus* and fungal community abundances. The bacterial and fungal numbers, varieties, and abundances were different, even when they were treated with same inoculates and conditions. However, the pHs of the silage inoculated with QZ227 were lower and this would improve their storage potential compared to the CK group.

CONCLUSION

QZ227 has good stress tolerance of temperature, bile, salt, acid, and alkali. It has a strong acid-producing capacity and broad-spectrum antibacterial activity, and can effectively inhibit several pathogens that occur in silage. The inoculant boosted the dominant fermentation flora and changed the bacterial composition after 30 days. The pH of the silage inoculated with QZ227 decreased to 4.27 at day 40 and remained at a relatively low level in the subsequent variable low temperature stage, which will improve storage. In both the constant low temperature and variable low temperature fermentation stages, lactic acid was detected in silage inoculated with QZ227, but not in CK. The results for the high-throughput sequencing combined with viable cell culture counting method showed that QZ227 became the predominant strain and inhibited the fungal growth of *Aspergillus*, *Sporidiobolaceae*, *Hypocreaceae*, *Pleosporales*, *Cutaneotrichosporon*, *Alternaria*, and *Cystobasidiomycetes* at a constant low temperature of 5°C. Under the variable temperature conditions from days 30 to 60, QZ227 reduced the fungal pathogens percentages of *Pichia*, *Mucoromycota*, *Aspergillus*, *Hypocreaceae*, *Sordariales*, *Agaricales*, *Cladosporium*, *Saccharomycetaceae*, *Mrakia*, *Sporidiobolaceae*, *Pleosporales*,

Alternaria, and *Plectosphaerella*. QZ227 also inhibited the growth of *Mucoromycota* and slowed down the speed and extent of corruption when the silage was exposed to oxygen. The results showed that QZ227 has the potential to be used as a starter culture for wheat fermentation at low temperature and as a protective spray for the outside layers of silage stacks.

DATA AVAILABILITY STATEMENT

The raw data supporting the conclusions of this article will be made available by the authors, without undue reservation.

AUTHOR CONTRIBUTIONS

ZT: conceptualization. MZ: data curation, software, and writing – original draft. ZT and MZ: formal analysis, investigation, writing, review, and editing. ZT, LW, and GW: funding acquisition. XW, HL, JC, and YL: resources. HP and ZT: supervision. All authors contributed to the article and approved the submitted version.

FUNDING

This work was supported by the Scientific and Technological Cooperation Program for Assistance to Qinghai (Grant no. 2021-QY-204).

SUPPLEMENTARY MATERIAL

The Supplementary Material for this article can be found online at: https://www.frontiersin.org/articles/10.3389/fmicb.2021.671287/full#supplementary-material

REFERENCES

Alagawany, M., Farag, M. R., Sahfi, M. E., Elnesr, S. S., Alqaisi, O., El-Kassas, S., et al. (2020). Phytochemical characteristics of Paulownia trees wastes and its use as unconventional feedstuff in animal feed. *Anim. Biotechnol.* doi: 10.1080/10495398.2020.1806074 [Epub ahead of print],

Alonso, V. A., Pereyra, C. M., Keller, L. A. M., Dalcero, A. M., Rosa, C. A. R., Chiacchiera, S. M., et al. (2013). Fungi and mycotoxins in silage: an overview. *J. Appl. Microbiol.* 115, 637–643. doi: 10.1111/jam.12178

Balouiri, M., Sadiki, M., and Ibnsouda, S. K. (2016). Methods for in vitro evaluating antimicrobial activity: a review. *J. Pharm. Anal.* 6, 71–79. doi: 10.1016/j.jpha.2015.11.005

Bastidas-Oyanedel, J. R., Bonk, F., Thomsen, M. H., and Schmidt, J. E. (2015). Dark fermentation biorefinery in the present and future (bio)chemical industry. *Rev. Environ. Sci. Biotechnol.* 14, 473–498. doi: 10.1007/s11157-015-9369-3

Cao, Y., Cai, Y., Hirakubo, T., Fukui, H., and Matsuyama, H. (2011). Fermentation characteristics and microorganism composition of total mixed ration silage with local food by-products in different seasons. *Anim. Sci. J.* 82, 259–266. doi: 10.1111/j.1740-0929.2010.00840.x

da Silva, ÉB., Savage, R. M., Biddle, A. S., Polukis, S. A., Smith, M. L., and Kung, L. (2020). Effects of a chemical additive on the fermentation, microbial communities, and aerobic stability of corn silage with or without air stress during storage. *J. Anim. Sci.* 98:skaa246.

Dong, Z., Li, J., Chen, L., Wang, S., and Shao, T. (2019). Effects of Freeze–thaw event on microbial community dynamics during red clover ensiling. *Front. Microbiol.* 10:1559. doi: 10.3389/fmicb.2019.01559

Fu, C. (2012). *Study on the Law of Silage Mildew and Screening of Mildew Inhibito*. Zhengzhou: Henan Agricultural University.

Jiang, M., Zhou, Y., Wang, N., Xu, L., Zheng, Z., and Zhang, J. (2019). Allelopathic effects of harmful algal extracts and exudates on biofilms on leaves of *Vallisneria natans*. *Sci. Total Environ.* 655, 823–830. doi: 10.1016/j.scitotenv.2018.11.296

Kung, L. Jr., Robinson, J. R., Ranjit, N. K., Chen, J. H., Golt, C. M., and Pesek, J. D. (2000). Microbial populations, fermentation end-products, and aerobic stability of corn silage treated with ammonia or a propionic acid-based preservative. *J. Dairy Sci.* 83, 1479–1486. doi: 10.3168/jds.s0022-0302(00)75020-x

Li, J.-F., Sun, X. H., Yuan, X. J., Guo, G., Xiao, S. H., Sang, B. A., et al. (2014). Effect of adding acetic acid on fermentation quality and aerobic stability of mixed oat and alfalfa silage in Tibet. *Acta Pratacult. Sin.* 23, 271–278.

Li, Y. (2013). *Lactic Acid Bacteria Resource Screening From the Tibet Plateau and Preliminary Research of Application, Physical Engineering*. Zhengzhou: Zhengzhou University.

Liu, J. Z., Guo, P., Lu, W., Geng, Z., Levesque, C. L., Johnston, L. J., et al. (2017). Dietary corn bran fermented by Bacillus subtilis MA139 decreased gut cellulolytic bacteria and microbiota diversity in finishing pigs. *Front. Cell. Infect. Microbiol.* 7:526. doi: 10.3389/fcimb.2017.00526

Lv, H. (2014). *Isolation, Identification and Preliminary Application Research of Lactic Acid Bacteria Resource in Animal Faeces and the Intestine of Gymnocypris przewalskii from the Tibet Plateau, Henan Key Laboratory of Ion-Beam Bioengineering*. Zhengzhou: Zhengzhou University.

Ni, K., Wang, F., Zhu, B., Yang, J., Zhou, G., Pan, Y., et al. (2017). Effects of lactic acid bacteria and molasses additives on the microbial community and fermentation quality of soybean silage. *Bioresour. Technol.* 238:706. doi: 10.1016/j.biortech.2017.04.055

Ogunade, I. M., Jiang, Y., Cervantes, A. A. P., Kim, D. H., Oliveira, A. S., Vyas, D., et al. (2018). Bacterial diversity and composition of alfalfa silage as analyzed by Illumina MiSeq sequencing: effects of *Escherichia coli* O157:H7 and silage additives. *J. Dairy Sci.* 101, 2048–2059. doi: 10.3168/jds.2017-12876

Qiu, J. (2008). China: the third pole. *Nature* 454, 393–396. doi: 10.1038/454393a

Queiroz, O. C. M., Arriola, K. G., Daniel, J. L. P., and Adesogan, A. T. (2013). Effects of 8 chemical and bacterial additives on the quality of corn silage. *J. Dairy Sci.* 96, 5836–5843. doi: 10.3168/jds.2013-6691

Ren, H., Feng, Y., Liu, T., Li, J., Wang, Z., Fu, S., et al. (2020). Effects of different simulated seasonal temperatures on the fermentation characteristics and microbial community diversities of the maize straw and cabbage waste co-ensiling system. *Sci. Total Environ.* 708, 135113. doi: 10.1016/j.scitotenv.2019.135113

Roier, S., Blume, T., Klug, L., Wagner, G. E., Elhenawy, W., Zangger, K., et al. (2015). A basis for vaccine development: comparative characterization of *Haemophilus influenzae* outer membrane vesicles. *Int. J. Med. Microbiol.* 305, 298–309. doi: 10.1016/j.ijmm.2014.12.005

Shah, A. A., Qian, C., Wu, J., Liu, Z., Khan, S., Tao, Z., et al. (2020a). Effects of natamycin and Lactobacillus plantarum on the chemical composition, microbial community, and aerobic stability of Hybrid pennisetum at different temperatures. *RSC Adv.* 10, 8692–8702. doi: 10.1039/d0ra00028k

Shah, A. A., Wu, J., Qian, C., Liu, Z., Mobashar, M., Tao, Z., et al. (2020b). Ensiling of whole-plant hybrid pennisetum with natamycin and *Lactobacillus plantarum* impacts on fermentation characteristics and metagenomic microbial community at low temperature. *J. Sci. Food Agric.* 100, 3378–3385. doi: 10.1002/jsfa.10371

Wang, C., He, L., Xing, Y., Zhou, W., Yang, F., Chen, X., et al. (2019). Effects of mixing Neolamarckia cadamba leaves on fermentation quality, microbial community of high moisture alfalfa and stylo silage. *Microb. Biotechnol.* 12, 869–878. doi: 10.1111/1751-7915.13429

Wang, H., Hao, W., Ning, T., Zheng, M., and Xu, C. (2018). Characterization of culturable yeast species associating with whole crop corn and total mixed ration silage. *Asian-Australas. J. Anim. Sci.* 2, 198–207. doi: 10.5713/ajas.17.0183

Wang, Y., He, L., Xing, Y., Zhou, W., Pian, R., Yang, F., et al. (2019). Bacterial diversity and fermentation quality of *Moringa oleifera* leaves silage prepared with lactic acid bacteria inoculants and stored at different temperatures. *Bioresour. Technol.* 284, 349–358. doi: 10.1016/j.biortech.2019.03.139

Yang, L., Yuan, X., Li, J., Dong, Z., and Shao, T. (2019). Dynamics of microbial community and fermentation quality during ensiling of sterile and nonsterile alfalfa with or without *Lactobacillus plantarum* inoculant. *Bioresour. Technol.* 275, 280–287. doi: 10.1016/j.biortech.2018.12.067

Yang, Y., Gao, Y., Wang, S., Xu, D., Yu, H., Wu, L., et al. (2014). The microbial gene diversity along an elevation gradient of the Tibetan grassland. *ISME J.* 8:430. doi: 10.1038/ismej.2013.146

Zhang, B., Tan, Z., Wang, Y., Li, Z., Jiao, Z., and Huang, Q. (2015). Dynamic changes of the microbial communities during the preparation of traditional Tibetan Qula cheese. *Dairy Sci. Technol.* 95, 167–180. doi: 10.1007/s13594-014-0194-1

Zhang, M. (2018). *The Screening and Application of Phychrophilic Lactic Acid Bacteria and the Optimizing of the Low-Temperature-Ensiling System, Henan Key Laboratory of Ion-Beam Bioengineering*. Zhengzhou: Zhengzhou University.

Zhang, M., Lv, H., Tan, Z., Li, Y., Wang, Y., Pang, H., et al. (2017a). Improving the fermentation quality of wheat straw silage stored at low temperature by psychrotrophic lactic acid bacteria. *Anim. Sci. J.* 88, 277–285. doi: 10.1111/asj.12632

Zhang, M., Tan, Z., Wang, X., Cui, M., and Jiao, Z. (2018a). Impact inoculum dosage of lactic acid bacteria on oat and wheat silage fermentation at ambient and low temperatures. *Crop Past. Sci.* 69, 1225–1236. doi: 10.1071/cp17250

Zhang, M., Tan, Z. F., Wang, X. J., Cui, M. Y., Wang, Y. P., and Jiao, Z. (2018b). Impact inoculum dosage of lactic acid bacteria on oat and wheat silage fermentation at ambient and low temperatures. *Crop Past. Sci.* 69, 1225–1236. doi: 10.1071/cp17250

Zhang, M., Wang, Y., Tan, Z., Li, Z., Li, Y., Lv, H., et al. (2017b). Microorganism profile, fermentation quality and rumen digestibility in vitro of maize-stalk silages produced at different maturity stages. *Crop Past. Sci.* 68, 225–233. doi: 10.1071/cp16324

Zhou, Y., Drouin, P., and Lafrenière, C. (2016). Effect of temperature (5–25°C) on epiphytic lactic acid bacteria populations and fermentation of whole−plant corn silage. *J. Appl. Microbiol.* 121:657. doi: 10.1111/jam.13198

Conflict of Interest: The authors declare that the research was conducted in the absence of any commercial or financial relationships that could be construed as a potential conflict of interest.

frontiers in Microbiology

ORIGINAL RESEARCH
published: 16 June 2021
doi: 10.3389/fmicb.2021.675763

Directional Selection of Microbial Community Reduces Propionate Accumulation in Glycerol and Glucose Anaerobic Bioconversion Under Elevated pCO_2

Pamela Ceron-Chafla[1], Yu-ting Chang[1], Korneel Rabaey[2,3], Jules B. van Lier[1] and Ralph E. F. Lindeboom[1]*

[1] Sanitary Engineering Section, Department of Water Management, Delft University of Technology, Delft, Netherlands, [2] Center for Microbial Ecology and Technology, Ghent University, Ghent, Belgium, [3] Center for Advanced Process Technology for Urban Resource Recovery, Ghent, Belgium

OPEN ACCESS

Edited by:
Irini Angelidaki, Technical University of Denmark, Denmark

Reviewed by:
Bipro Ranjan Dhar, University of Alberta, Canada
Bo Svensson, Linköping University, Sweden

***Correspondence:**
Pamela Ceron-Chafla
p.s.ceronchafla@tudelft.nl

Specialty section:
This article was submitted to Microbiotechnology, a section of the journal Frontiers in Microbiology

Received: *03 March 2021*
Accepted: *24 May 2021*
Published: *16 June 2021*

Citation:
Ceron-Chafla P, Chang Y-t, Rabaey K, van Lier JB and Lindeboom REF (2021) Directional Selection of Microbial Community Reduces Propionate Accumulation in Glycerol and Glucose Anaerobic Bioconversion Under Elevated pCO_2. Front. Microbiol. 12:675763. doi: 10.3389/fmicb.2021.675763

Volatile fatty acid accumulation is a sign of digester perturbation. Previous work showed the thermodynamic limitations of hydrogen and CO_2 in syntrophic propionate oxidation under elevated partial pressure of CO_2 (pCO_2). Here we study the effect of directional selection under increasing substrate load as a strategy to restructure the microbial community and induce cross-protection mechanisms to improve glucose and glycerol conversion performance under elevated pCO_2. After an adaptive laboratory evolution (ALE) process, viable cell density increased and predominant microbial groups were modified: an increase in *Methanosaeta* and syntrophic propionate oxidizing bacteria (SPOB) associated with the *Smithella* genus was found with glycerol as the substrate. A modest increase in SPOB along with a shift in the predominance of *Methanobacterium* toward *Methanosaeta* was observed with glucose as the substrate. The evolved inoculum showed affected diversity within archaeal spp. under 5 bar initial pCO_2; however, higher CH_4 yield resulted from enhanced propionate conversion linked to the community shifts and biomass adaptation during the ALE process. Moreover, the evolved inoculum attained increased cell viability with glucose and a marginal decrease with glycerol as the substrate. Results showed differences in terms of carbon flux distribution using the evolved inoculum under elevated pCO_2: glucose conversion resulted in a higher cell density and viability, whereas glycerol conversion led to higher propionate production whose enabled conversion reflected in increased CH_4 yield. Our results highlight that limited propionate conversion at elevated pCO_2 resulted from decreased cell viability and low abundance of syntrophic partners. This limitation can be mitigated by promoting alternative and more resilient SPOB and building up biomass adaptation to environmental conditions via directional selection of microbial community.

Keywords: high-pressure anaerobic digestion, elevated CO_2 partial pressure, syntrophic propionate oxidation, *Smithella*, adaptive laboratory evolution

INTRODUCTION

Volatile fatty acids (VFA) are important chemical building blocks obtained by mixed culture fermentation in the carboxylate platform (Holtzapple and Granda, 2009; Agler et al., 2011). However, its accumulation is a symptom of reactor malfunctioning in anaerobic digestion (AD), attributed to dissimilarities between acidogenic, acetogenic, and methanogenic bio-conversion rates (Hickey and Switzenbaum, 1991). The identified causes leading to VFA accumulation are associated with substrate overload (Amorim et al., 2018), possible toxicity due to increasing concentrations of undissociated acids at low pH (Russell and Diez-Gonzalez, 1998), and disparities in the proportionality of acidogenic, syntrophic, and methanogenic microorganisms (McMahon et al., 2004; Li et al., 2016; Town and Dumonceaux, 2016). When VFA production is targeted under anaerobic conditions, the product spectrum selectivity is influenced by operational parameters such as temperature, substrate type, concentration, pH, solids retention time (SRT) and headspace composition (Arslan et al., 2016; Zhou et al., 2018; Wainaina et al., 2019).

Possible steering effects of headspace composition in AD could be magnified applying the auto-generative high-pressure AD technology, which was developed for simultaneous biogas production and upgrading (Lindeboom et al., 2011; Lemmer et al., 2015). Here, by applying a closed gastight vessel, the reactor pressure auto-generatively increases and a higher CH_4 content in the biogas is achieved due to enlarged differences in CO_2 and CH_4 solubility at high operational pressure. Lindeboom et al. (2013) observed a decline in the propionate oxidation rate at an increased total pressure with a concomitantly increased partial pressure of CO_2 (pCO_2). As part of the explanatory mechanism, an acidification process and reversible toxicity linked to carbamate formation were proposed. Both processes occur due to increased aqueous CO_2 concentration (H_2CO_3*) in the liquid medium resulting from enhanced CO_2 dissolution (Lindeboom et al., 2016). Recently, we investigated additional effects of elevated pCO_2 on syntrophic conversions occurring in AD (Ceron-Chafla et al., 2020). The observed limited propionate and butyrate conversion under elevated pCO_2 were explained by a more comprehensive mechanism that encompasses bioenergetics, kinetic and physiological effects.

The effects of elevated pCO_2 on the cell viability level can be attributed to the detrimental effect that increased H_2CO_3* concentrations have on cell membrane permeability. Leakage of internal components, structural modifications, and internal acidification are part of the explanatory mechanisms (Wu et al., 2007; Garcia-Gonzalez et al., 2010). In bioreactors with a pressurized headspace, the effects of elevated pCO_2 differ from inert gases, such as N_2, which does not severely compromise cell viability (Wu et al., 2007). Considerably higher hydrostatic pressures of N_2 are required to achieve the same inactivation levels as with elevated pCO_2 (Aertsen et al., 2009). Safeguarding cell viability is necessary since reduced cell density and increased percentage of permeable cells might result in impaired specific conversion rates, causing decreased productivity.

The extent of detrimental effects of increased dissolved CO_2 concentrations on cell membranes depends on localized conditions. Some microbial species have acid tolerance mechanisms involving enzymatic systems carrying out neutralization reactions, proton pumps and modifications in the cell membrane (Guan and Liu, 2020). In consequence, they can counteract ramping H^+ concentrations due to H_2CO_3* intracellular dissociation. Some authors observed during sterilization experiments that a reduction in water activity in the liquid medium decreases CO_2 dissolution thus diminishing its intracellular diffusion (Kumagai et al., 1997; Chen et al., 2017). In other cases, microorganisms induce the synthesis of compounds acting as compatible solutes, such as glutamate, which help to tackle changes in osmolarity and CO_2 toxicity (Oger and Jebbar, 2010; Park et al., 2020). Additionally, the presence of fats in the medium affects the porosity and structure of the cell wall or membranes, thus limiting CO_2 penetration (Lin et al., 1994).

Previous studies have shown that directional selection of microbial community through adaptive laboratory evolution (ALE) processes is highly effective to improve stress tolerance and selectively enhance product formation by activation of downregulated pathways (Portnoy et al., 2011; Dragosits and Mattanovich, 2013). However, in mixed culture fermentations changes in pathway predominance to enhance hydrogen production already have been observed after relatively short adaptive evolution processes (46 days) (Huang et al., 2016). In particular, ALE has shown to trigger the development of features such as acid resistance mechanisms (Kwon et al., 2011), as well as other physiological mechanisms to conserve cell membrane integrity. Such insights could act as cross-protection mechanisms against stressful pCO_2 levels and improve metabolic activity.

Elevated pCO_2 has also shown effects at the ecological level in anaerobic communities. In terms of structure and taxonomic diversity, the overall response to high CO_2 concentrations included a decrease in richness and lowering diversity, dependent on the actual prevailing pH (Gulliver et al., 2014; Fazi et al., 2019). Moreover, there is evidence of shifts in bacterial and archaeal predominant groups since CO_2 can be incorporated as a reactant to a different extent and consequently, enhances the metabolic pathways in a selective manner (Gulliver et al., 2014; Yu and Chen, 2019). Therefore, the modifying effect of elevated pCO_2 in highly redundant communities, such as the ones from anaerobic digesters, might redefine the metabolic activity output and overall process performance.

Elevated CO_2 concentrations could steer specific metabolic pathways in anaerobic conversion systems, particularly those reactions coupled to the phosphoenolpyruvate (PEP)–pyruvate–oxaloacetate (OAA) node in the biochemical conversions. In addition, high pCO_2 could promote carboxylation reactions, i.e., propionate formation is favored over acetate formation since the latter will require a decarboxylation reaction of acetyl-CoA (Baez et al., 2009). The enhancement of methane production at high CO_2 levels could occur due to the combination of homoacetogenic activity coupled with aceticlastic methanogenesis when an electron sink is required (Bajón Fernández et al., 2019). Otherwise, under the

stoichiometric provision of a suitable electron donor, such as hydrogen or formate, it will directly promote hydrogenotrophic methanogenesis (Zabranska and Pokorna, 2018).

Glucose and glycerol conversion, under anaerobic conditions, share the glycolytic pathway after glycerol has been converted to glyceraldehyde-3-phosphate and subsequently to PEP (Saint-Amans et al., 2001) (**Supplementary Figure 1**). These substrates differ in their degree of reduction: for glycerol, this value corresponds to –0.67 electron equivalents/C-mol, whereas for glucose this value is 0. Due to this, glycerol fermentation leads to the formation of reduced compounds and less acetate and CO_2 as in the case of *Propionibacterium acidipropionici* (Zhang et al., 2016). With the formation of more reduced fermentation products, the redox balance is maintained and biomass growth and overall productivity are sustained (Himmi et al., 2000). In terms of biomass yields, the substrates also have contrasting differences: the theoretical values are higher for glucose than for glycerol being 0.239 vs. 0.145 C-mol biomass/C-mol electron donor, respectively (Heijnen and Kleerebezem, 2010). Moreover, the enzymatic activity associated with CO_2 fixation also differs in cells grown in glycerol due to the expression of pyruvate carboxylase, which has not been observed with glucose (Parizzi et al., 2012).

These fundamental differences between glucose and glycerol fermentation make a comparative study highly relevant to elucidate the potential of elevated pCO_2 as a steering parameter in anaerobic conversions when performance limitations need to be overcome. Therefore, in this work, we applied a directional selection process based on increasing substrate load to restructure the microbial community and activate cross-protection mechanisms to enhance the anaerobic conversion of glucose and glycerol under elevated pCO_2. As a negative control, we investigated the effect of elevated pCO_2 on the original inoculum. We expected differences in the product spectrum as a result of the dissimilar substrate oxidation state and increased pCO_2 favoring propionate production. Nonetheless, further propionate oxidation (Pr-Ox) would be limited due to thermodynamic constraints on syntrophic Pr-Ox in relation to interspecies hydrogen transfer (Stams et al., 1998). Further constraints will be established due to the negative effects of elevated pCO_2 on cell viability and relative abundance of methanogens and syntrophic propionate oxidation bacteria (SPOB) in the original inoculum. The evolved inoculum would feature enhanced cell viability, a higher proportion of fermenters and more resilient SPOB and methanogenic groups. These factors could help to circumvent thermodynamic and performance limitations present in the original inoculum, thereby enabling propionate conversion under elevated pCO_2.

MATERIALS AND METHODS

Inoculum

Flocculent anaerobic sludge from an anaerobic membrane bioreactor (AnMBR) treating wastewater from a chocolate and pet food industry was used as the starting inoculum. Measured physicochemical parameters are presented in **Table 1**.

TABLE 1 | Physicochemical characterization of the original anaerobic inoculum used for the experiments of glucose and glycerol conversion under elevated pCO_2 and evolved inoculum after adaptive laboratory evolution (ALE) using glucose and glycerol (1 g COD L^{-1}) at T = 35°C, initial pCO_2 = 0.3 bar and initial pH in the range 7.5–8.0.

Parameter	Unit	Original inoculum	Glucose-evolved inoculum	Glycerol-evolved inoculum
		Mean ± SD (n = 3)	Mean ± SD (n = 3)	Mean ± SD (n = 3)
TCOD	mg/L	22,200 ± 1000	3,500 ± 550	6,800 ± 650
SCOD	mg/L	1,900 ± 400	678 ± 65	162 ± 4
TOC	mg/L	7,700 ± 800	681 ± 6	705 ± 3
TSS	g/L	15.9 ± 0.5	3.5 ± 0.1	6.0 ± 0.1
VSS	g/L	13.6 ± 0.1	2.9 ± 0.3	4.9 ± 0.1
VSS/TSS	%	86	81	82
NH_4-N	mg/L	107 ± 2	269 ± 22	281 ± 7
TP	mg/L	112 ± 1	17 ± 2	28 ± 1
pH	–	7.3	7.2	7.2

Reactor Set-Up and Operation

Batch experiments with original inoculum were conducted at four different pCO_2, namely 0.3, 3, 5, and 8 bar initial pressures. Schott bottles with a working volume of 250 mL, air-tight sealed with rubber stoppers were used for the experiments at atmospheric conditions, i.e., 0.3 bar pCO_2. The employed gas to liquid ratio was 2:3. Stainless steel reactors working in a pressure range of 1–600 bar (Nantong Vasia, China) were used for the experiments at moderately elevated pressure, i.e., 3, 5, and 8 bar. These reactors are fitted with gas and liquid sampling ports in the head, as well as a glycerin manometer. The working liquid volume, in this case, was 120 mL, and the same gas to liquid ratio as before was kept. Reactors were inoculated with 2 g VSS L^{-1}. The liquid medium added to each reactor contained 1 g glucose or glycerol as COD L^{-1}, macronutrients, micronutrients both prepared according to García Rea et al. (2020) and buffer solution (100 mM as HCO_3^-). The initial pH of all the reactors was not adjusted and values were in the range 7.5–8.0.

After filling and closure, atmospheric reactors were flushed for 2 min with 100% N_2 and sequentially with N_2:CO_2, 70:30%. Pressure reactors were initially flushed with the same gas mixture as the atmospheric reactors and afterward, consecutive pressurization-release cycles with >99% CO_2 were applied to ensure initial headspace composition. Reactors were operated for approximately 10 days, kept at 35°C and continuously shaken at 110 rpm. All the experimental treatments were conducted in triplicates. Pressurized controls with only nitrogen in the headspace were additionally included. To diminish sampling interference during the experiment, we applied the same sampling strategy as previously described (Ceron-Chafla et al., 2020). A graphical description of the experimental design is presented in **Figure 1**.

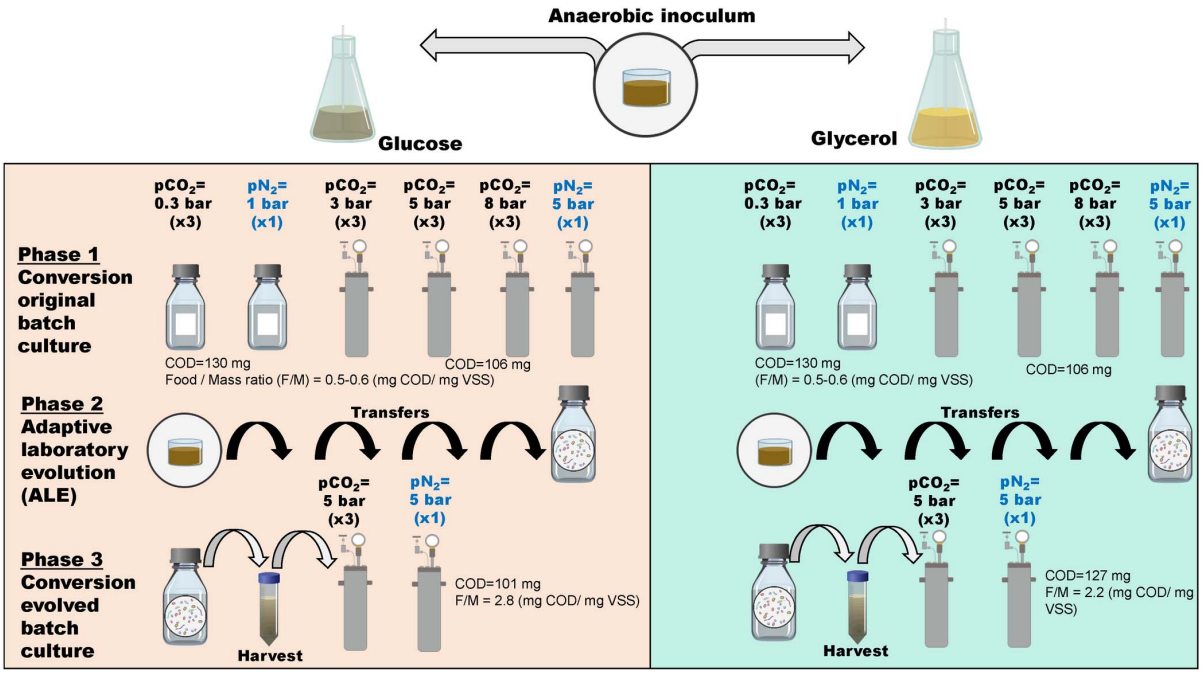

FIGURE 1 | Graphical summary of experimental conditions for the anaerobic conversion experiments at elevated pCO_2 using glucose and glycerol as substrates. Experiments are organized according to substrate and inoculum conditions.

Directional Selection of Microbial Community via Adaptive Laboratory Evolution With Increased Glucose and Glycerol Load

The total length of the atmospheric ALE process was 61 days divided into four cycles with duration as follows: the two first cycles lasted 7 days, which corresponded to complete substrate conversion for initial atmospheric experiments at 0.3 bar pCO_2. However, due to the limited growth and conversion of intermediates identified after the second cycle, it was decided to perform the third and fourth cycles at 0.3 bar pCO_2 for 21 and 26 days, respectively, to achieve complete conversion. Schott bottles with a working volume of 2,000 mL were used for the ALE incubation. After every cycle, 240 mL were removed, replaced by fresh medium and the bottles were flushed with N_2:CO_2, 70:30%. The substrate concentration in the medium refreshing solution was fixed for all the cycles at 1 g COD L^{-1} glucose or glycerol. It should be noted that owing to the serial dilution procedure, biomass was exposed to a deliberately increased substrate load per cycle. The evolved inoculum was harvested after the fourth cycle, employing low-speed centrifugation and resuspension with macro and micronutrient solution. After this, the obtained biomass was characterized in terms of physicochemical parameters (**Table 1**) and used to inoculate pressure reactors at 5 bar pCO_2 and controls at 5 bar pN_2 to evaluate anaerobic conversion performance of evolved microbial biomass at a higher Food to Mass ratio (F:M ratio) (phase 3; **Figure 1**). The pressurized experiments with evolved inoculum lasted approximately 10 days.

Microbial Community Analysis

Biomass samples stored at −80°C from the endpoint of the batch experiments were used to evaluate Microbial community dynamics. After thawing, DNA was extracted according to the instructions included in the DNeasy UltraClean Microbial Kit (Qiagen, Germany). The quality and quantity of the obtained DNA were checked through Qubit® 3.0 DNA detection (Qubit dsDNA HS Assay Kit, Life Technologies, United States). Library construction and sequencing by the Illumina platform were conducted by Novogene (Hong Kong). A summary of the internal protocol is presented in **Supplementary Information**.

Analyses

Secondary metabolites in the liquid medium (acetate, propionate, butyrate, and valerate) were measured by gas chromatography (7890A GC; Agilent Technologies, United States) according to the method described by Muñoz Sierra et al. (2020). The gas composition of samples stabilized at atmospheric conditions was determined via gas chromatography (7890A GC; Agilent Technologies, United States) using a thermal conductivity detector operated at 200°C and oven temperature ramping from 40 to 100°C. The system operated with two columns: an HP-PLOT Molesieve GC Column 30 m × 0.53 mm × 25.00 μm and an HP-PLOT U GC Column, 30 m, 0.53 mm, and 20.00 μm (Agilent Technologies, United States). The carrier gas was helium at a constant flow rate of 10 mL min^{-1}.

Total cell numbers and live/dead cells were assessed by flow cytometry (BD Accuri® C6, BD Biosciences, Belgium) using

Milli-Q as sheath fluid. Before measurement, samples were pre-treated as follows: First, samples were diluted (×500) with 0.22-μm filtered phosphate-buffered-saline (PBS) solution. Diluted samples were sonicated in three cycles of 45 s at 100 W and the amplitude at 50%. Subsequently, samples were diluted (×500) and filtered at 22 μm. Immediately after the pre-treatment, the samples were stained with 5% SYBR® Green I or SYBR® Green I combined with propidium iodide (Invitrogen) and incubated at 37°C for 10 min.

pH, total and soluble COD, TSS, and VSS, ammonium and total phosphorus were measured according to standard methods (American Public Health Association, 2005).

Statistical Analyses

Statistical analyses were carried out in the R software (R Core Team, 2019). After processing the amplicon sequencing data, a table was generated with relative abundances of the different OTUs and their taxonomic assignment of each sample. Normalization of the samples was carried out based on the flow cytometry data (Props et al., 2017). The R packages vegan (Oksanen et al., 2016) and phyloseq (McMurdie and Holmes, 2013) were used for community analysis. Significant differences ($p < 0.05$) in microbial community composition were identified employing pair-wise Permutational ANOVA (PERMANOVA) with Bonferroni correction using the *adonis* function included in the vegan package.

The order-based Hill's numbers were used to evaluate the alpha diversity in terms of richness (number of OTUs, H_0), the exponential of the Shannon diversity index (H_1) and the Inverse Simpson index (H_2) (Hill, 1973). Beta diversity was evaluated via the Bray–Curtis distance measure (Bray and Curtis, 1957). Spearman's correlation analysis was performed using the function *cor.test* ().

RESULTS

The main results of the glucose and glycerol conversion experiments at elevated pCO_2 using the evolved and original inoculum are summarized in **Table 2**. Observations are categorized in terms of cell viability, microbial community, and product spectrum and explained in detail in the following sections.

Effect of ALE Strategy on Glucose Conversion Under Elevated pCO_2

Cell Viability

Original inoculum

The total and viable cell density of the starting inoculum is presented in **Figure 2A**. During the experiments of glucose conversion at pCO_2 of 0.3 bar using this inoculum, there was a negligible reduction in the final viable cell density, expressed as percentage change, after 10 days (**Figure 2B**). However, at moderately high pressures, i.e., 3, 5, and 8 bar initial pCO_2, the treatments showed a more substantial decrease of approximately 66% in viable cell density for the same period (**Figure 2B**). It should be noted that nitrogen controls at 5 bar showed a comparable decrease of 73% in viable cell density.

Evolved inoculum

Total and viable cell density increased in comparison to the original inoculum after the ALE cycle using glucose as a substrate. In particular, there was a 2.2-fold increase in viable cell density in comparison to the original inoculum (**Figure 2A**). After the exposure to 5 bar pCO_2, the viable cell density of the evolved inoculum showed an increase of 163% compared to the original inoculum. Nitrogen controls at 5 bar presented a smaller increase of 67% in viable cell density after 10 days (**Figure 2B**).

Microbial Community

Original inoculum

The proportion of bacteria and archaea, based on the total number of processed reads, corresponded to 79 and 21%, respectively, in the original inoculum. The bacterial community of the original inoculum was majorly composed of the phyla Chloroflexi (52%), Actinobacteriota (22%), Firmicutes (10%), and Proteobacteria (5%). In terms of the relative abundance of the bacterial community at the genus level, there were a representative proportion of *SJA-15_ge* (35%) and *unclassified Micrococcales* (19%) (**Figure 3A**). The proportion of genera associated with syntrophic Pr-Ox namely *Smithella* was low (<1%). The archaeal community was mainly composed of members of the aceticlastic genus *Methanosaeta* (68%) and the hydrogenotrophic genus *Methanobacterium* (31%) (**Figure 3B**).

In the experiments at 3, 5, and 8 bar initial pCO_2, bacterial genera from the class Anaerolineae: *SJA-15_ge* (38–45%), *unclassified Micrococcales* (11–16%) were predominant (**Figure 3A**). The relative abundance of syntrophic groups remained low (<1%). The proportion of total archaea was below 45% in all treatments. Additionally, **Figure 3B** suggests a contrasting relationship in the relative abundance of *Methanobacterium* and *Methanosaeta* in the treatments when compared to the original inoculum.

Evolved inoculum

After the ALE cycles, the proportion of bacteria and archaea was 70 and 30%, respectively. The directional selection of microbial community favored the relative abundance of bacterial phyla Actinobacteria, increasing its abundance to 48% and decreased the proportion of Chloroflexi to 20% of total bacterial reads for this inoculum. At the genus level, the relative abundance of *unclassified Micrococcales* and *SJA-15_ge* corresponded to 44 and 12%, respectively (**Figure 3A**). *Smithella* increased to 4% of the total bacterial reads. At the archaeal level, the proportions of the two methanogenic genera *Methanosaeta* and *Methanobacterium* corresponded to 68 and 31% of the archaeal reads, respectively (**Figure 3B**).

For the experiments at 5 bars initial pCO_2 with evolved inoculum, at the genus level, *unclassified Micrococcales* remained predominant (28%), as well as *SJA-15_ge* (15%) (**Figure 3A**). Under the imposed experimental conditions, the abundance of syntrophic groups, e.g., *Smithella* (**Figure 3A**) and *Syntrophobacter*, cumulatively increased to 8% of the total bacterial reads. The proportion of total archaea after exposure to pCO_2 corresponded to 39% of the total reads. The

TABLE 2 | Summary of the observed effects of the Adaptive Laboratory Evolution (ALE) strategy in the performance of anaerobic conversion of glucose and glycerol under 5 bar pCO_2.

	5 bar initial pCO_2			
	Glucose		**Glycerol**	
	Original	**Evolved**	**Original**	**Evolved**
Cell density	Decrease in final total and viable cell density	Increase in final total and viable cell density	Increase in final total and viable cell density	Moderate decrease in final cell density and comparable viable cell density between start and endpoint
Microbial community	Low relative abundance (RA) (<1%) of syntrophic groups. Higher RA of *Methanosaeta* compared to *Methanobacterium*	Increased RA of *Smithella* and *Syntrophobacter* (8%). Slight increase in RA of *Methanosaeta* compared to *Methanobacterium*	Higher RA of *Methanosaeta* compared to *Methanobacterium* than in glucose treatments	Highest RA of *Smithella* and *Syntrophobacter* (18%). RA of *Methanosaeta* and *Methanobacterium* comparable to upper limit in original inoculum treatments
Product spectrum and productivity	Propionate accumulation. Higher acetate and butyrate concentration than under atmospheric conditions Low CH_4 production	Propionate conversion. Higher CH_4 production than using original inoculum	Propionate accumulation, despicable butyrate production Lower CH_4 production compared to glucose	Propionate conversion. Higher CH_4 production than original inoculum and glucose treatment

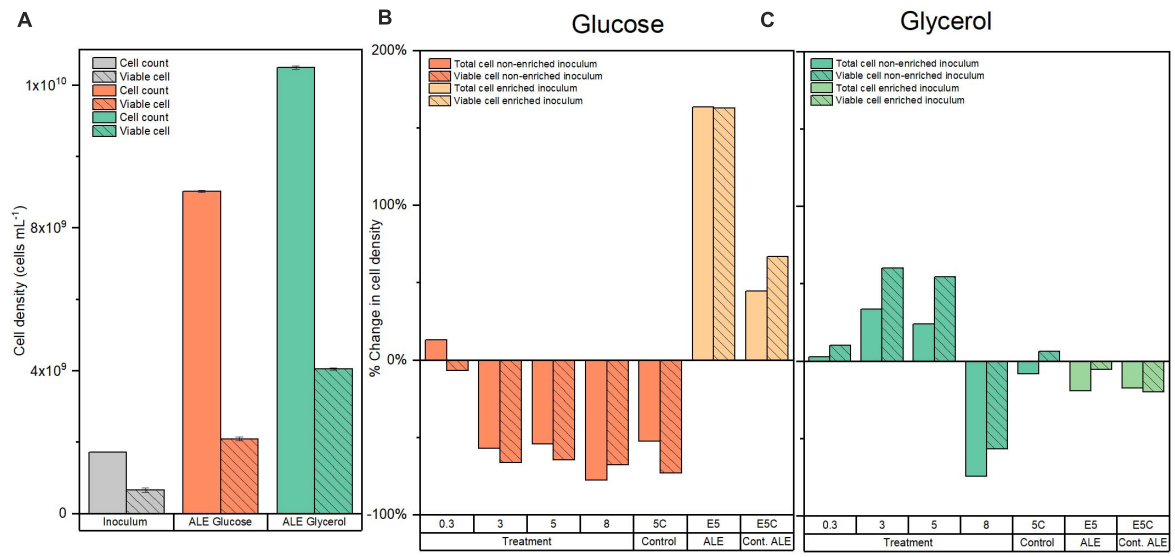

FIGURE 2 | (A) Total and viable cell density for the original and evolved inoculum with glucose and glycerol. Percentage of change of total and viable cell density for the **(B)** glucose and **(C)** glycerol conversion experiments at different initial pCO_2 in the headspace (0.3, 3, 5, and 8 bar) using original inoculum and at 5 bar initial pCO_2 using evolved inoculum. Pressure controls with N_2 headspace for the original and evolved inoculum at 5 bar (5C and E5C in the graphs) are included for reference.

relative abundance of *Methanosaeta* increased to 77%, whereas *Methanobacterium* remained around 22% of total processed archaeal reads (**Figure 3B**).

Product Spectrum During Glucose Consumption

Original inoculum

The product spectrum of the anaerobic conversion of glucose under different initial pCO_2 levels was mainly composed of propionate, acetate, butyrate and CH_4. Propionate production was predominant under initial pCO_2 of 0.3 bar, reaching 399 mg COD–Pr L^{-1}, which in terms of the mass balance corresponded to 44% of the initial COD (**Figure 4A**). In the experiments at 3, 5, and 8 bar pCO_2, propionate production peaked at approximately 407 ± 32 mg COD–Pr L^{-1}, which accounted for 38% of the initial COD. Small discrepancies in the total amount being fed to atmospheric and pressure reactors were experienced since the effective volume differed among reactors to keep the liquid to gas ratio comparable. Acetate and butyrate amounts were higher at initial pCO_2 of 8 bar compared to atmospheric conditions, whereas at 3 and 5 bar a noteworthy accumulation of these metabolites was not detected (**Figures 4B–D**). Propionate conversion was hindered by elevated pCO_2 and in consequence, decreased CH_4 production was observed in the treatments

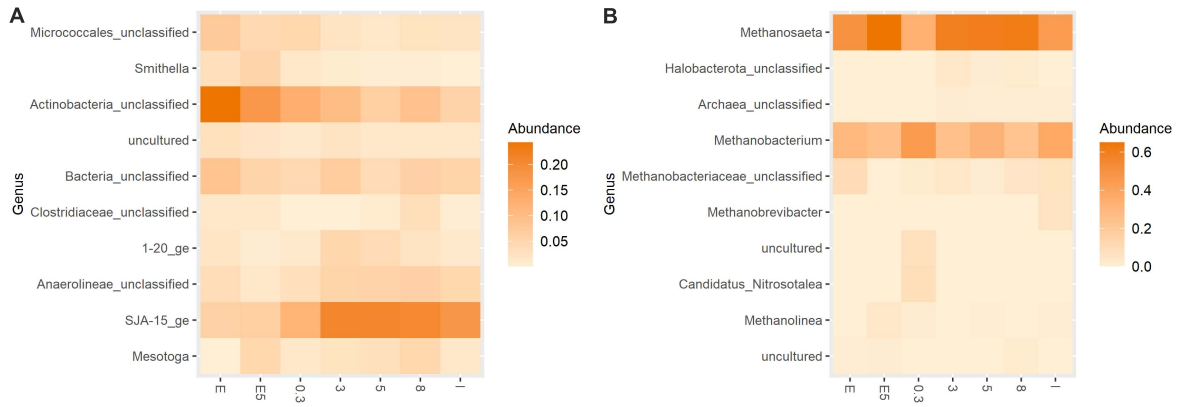

FIGURE 3 | Heatmap presenting the relative abundance of **(A)** Bacterial community and **(B)** Archaeal community at the genus level. Experimental treatments correspond to glucose conversion at elevated pCO_2 using original (0.3, 3, 5, and 8 bar) and evolved inoculum (5 bar–E5). I corresponds to the original inoculum and E to the evolved inoculum. Pressure corresponds to initial values before equilibrium.

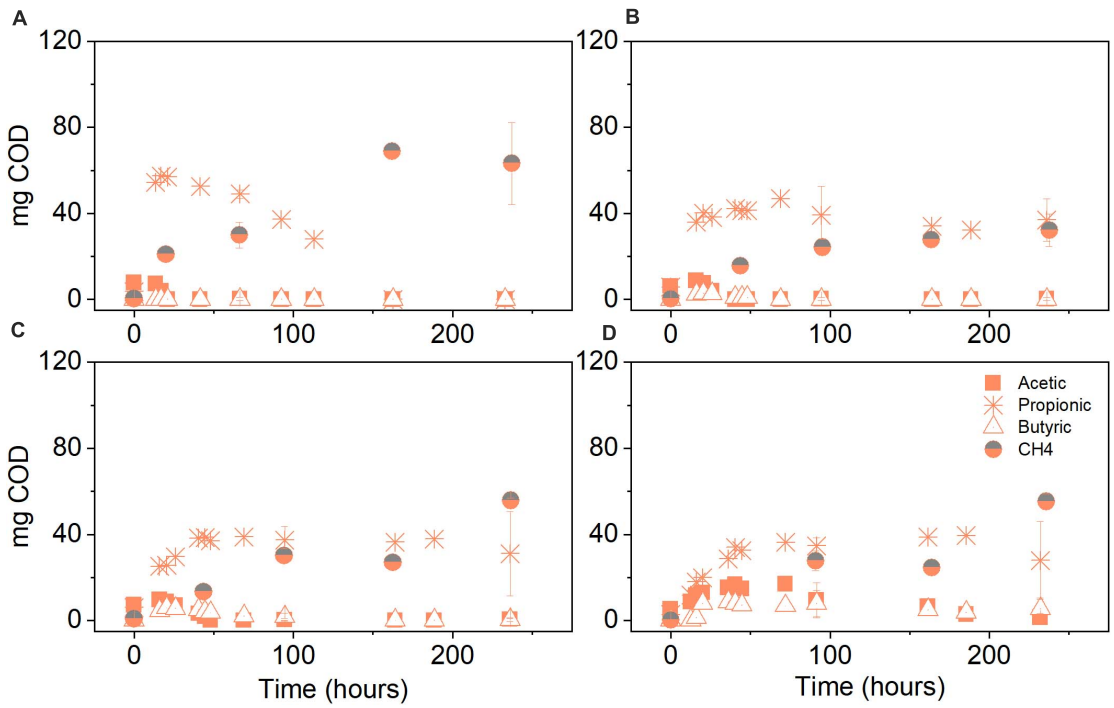

FIGURE 4 | Volatile fatty acid (VFA) and CH_4 production (mg COD) over time for the glucose conversion experiments using original inoculum at initial pCO_2 of **(A)** 0.3 bar, **(B)** 3 bar, **(C)** 5 bar, and **(D)** 8 bar. Pressure corresponds to initial values before equilibrium. Data points represent experimental data. Bars represent the standard deviation of three biological replicates measured at the beginning, middle, and end of the experiment.

at high initial pCO_2. The experiments at 3, 5, and 8 bar pCO_2 resulted in an average 30% decrease in the final amount of COD–CH_4 produced in comparison to the atmospheric control at 0.3 bar pCO_2 evaluated after 10 days (**Figures 4A–D**).

Evolved inoculum

Figure 5A shows the composition of the product spectrum in the experiments with evolved inoculum which remained similar to the experiments with original inoculum; however, less accumulation of intermediates, particularly propionate, was detected. Propionate production peaked after 92 h (**Supplementary Figure 6**) and it was no longer detected at significant amounts at the end of the experiment (**Supplementary Table 1**). A preliminary 33% decrease in the final COD–CH_4 was calculated when comparing to the treatment at the same pCO_2, i.e., 5 bar, using the original inoculum (**Figure 4C**).

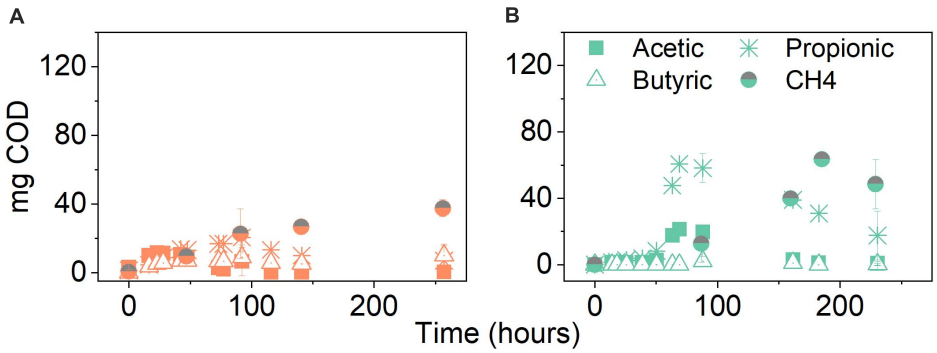

FIGURE 5 | Volatile fatty acid and CH_4 production (mg COD) over time for **(A)** glucose and **(B)** glycerol conversion experiments at elevated pCO_2 using evolved inoculum at 5 bar initial pCO_2. Pressure corresponds to initial values before equilibrium. Data points represent experimental data. Bars represent the standard deviation of three biological replicates measured at the beginning, middle, and end of the experiment.

Effect of ALE Strategy on Glycerol Conversion Under Elevated pCO_2

Cell Viability

Original inoculum

In the experiments of glycerol conversion at elevated pCO_2 using the starting inoculum at 0.3 bar pCO_2, there was a negligible 10% increase in final viable cell density compared to initial conditions. However, at initial pCO_2 of 3, 5, and 8 bar there was an increase of approximately 50% for the two lowest pressures and a comparable percentage decrease for the highest pCO_2. Nitrogen controls at 5 bar did not present a considerable change in viable cell density, just accounting for a 6% increase (**Figure 2C**).

Evolved inoculum

After the ALE process with increasing glycerol load, there was a 5.2-fold increase in viable cell density in comparison to the original inoculum and a 0.9-fold increase compared to the ALE with glucose as substrate (**Figures 2A,B**). After exposure to 5 bar pCO_2, the evolved inoculum showed a negligible 5% decrease in viable cell density. Nitrogen controls at 5 bar showed a 20% decrease compared to the initial conditions after 10 days (**Figure 2C**).

Microbial Community

Original inoculum

In the experiments with the original inoculum at 3, 5, and 8 bar initial pCO_2, results showed a predominance of bacterial genus *SJA-15_ge*, whose relative abundance calculated based on processed reads varied between 34 and 42%, and other genera, such as *Clostridium_sensu_stricto_12* (8–12%), as well as *unclassified Micrococcales* and *Mesotoga* with relative abundances <14% (**Figure 6A**). The relative abundance of SPOB remained low (<1%) in all cases. There was a descending trend regarding the changes in the proportion of total archaea for the high pCO_2 experiments using the original inoculum: for experiments at 3, 5, and 8 bar pCO_2, the archaeal presence corresponded to 35, 22, and 18% of the total number of processed reads, respectively. *Methanosaeta* had the highest relative abundance at the genus level, varying between 58 and 82%, while *Methanobacterium* ranged between 17 and 41% of total processed archaeal reads (**Figure 6B**).

Evolved inoculum

After ALE with glycerol, the proportion of Bacteria and Archaea corresponded to 81 and 19% of processed reads, respectively. The bacterial community composition was dominated by phyla Chloroflexi (35%), Actinobacteriota (19%), Desulfobacterota (14%), and Synergistota (14%). At the genus level, *SJA-15* (27%), *unclassified Micrococcales* (17%), *Smithella* (13%), and *Thermovirga* (11%) showed the highest relative abundances (**Figure 6A**). The archaeal community was majorly composed of genera *Methanosaeta* and *Methanobacterium* at a corresponding relative abundance of 76 and 22% (**Figure 6B**).

For the experiments at 5 bar pCO_2 with evolved inoculum, the relative abundance of *SJA-15_ge* decreased to 19% and *Clostridium_sensu_stricto_12* (21%) was predominant. At this condition, the relative abundance of syntrophic groups, e.g., *Smithella* (**Figure 6A**) and *Syntrophobacter,* cumulatively increased to 18%. The proportion of total archaea, in this case, showed an increase to 35% of total processed reads. In terms of community composition, it differed from the glucose experiments: a slightly higher proportion of *Methanosaeta* (89%) was observed, whereas *Methanobacterium* represented 10% of processed archaeal reads (**Figure 6B**).

Changes in Microbial Community Structure Due to Exposure to Glycerol and Glucose and Elevated pCO_2

A basic analysis of alpha diversity via calculation of the Hill numbers showed an overall decrease in the richness (H_0) of the bacterial community associated with the directional selection process at increasing substrate concentrations, which seemed to be more noticeable in the case of glycerol compared to glucose (**Supplementary Figure 2**). The inoculum condition (original vs. evolved) only exposed significant differences in terms of the bacterial community structure for the case of richness, H_0 ($p = 0.032$) when all treatments were analyzed together. In the case of Pielou's evenness, significant differences were explained by the type of substrate ($p = 0.044$) and not by elevated pCO_2.

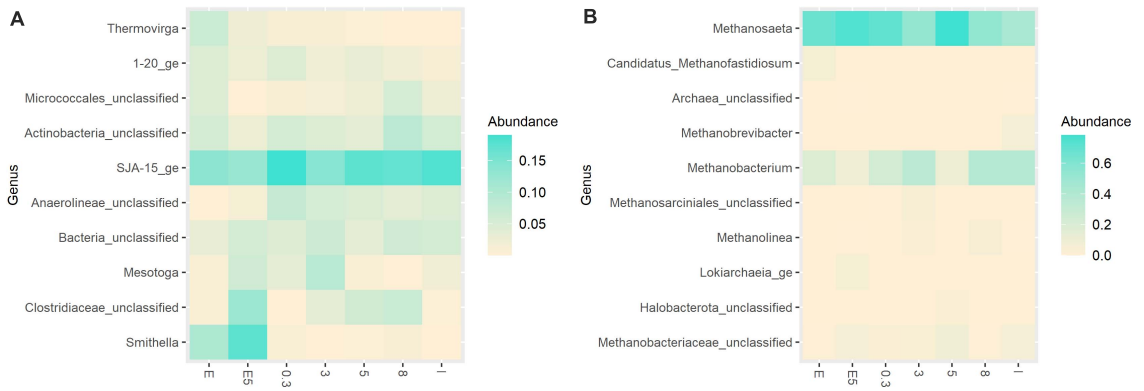

FIGURE 6 | Heatmap presenting the relative abundance of **(A)** Bacterial community and **(B)** Archaeal community at the genus level. Experimental treatments correspond to glycerol conversion at elevated pCO_2 using original (0.3, 3, 5, and 8 bar) and evolved inoculum (5 bar–E5). I corresponds to the original inoculum and E to the evolved inoculum. Pressure corresponds to initial values before equilibrium.

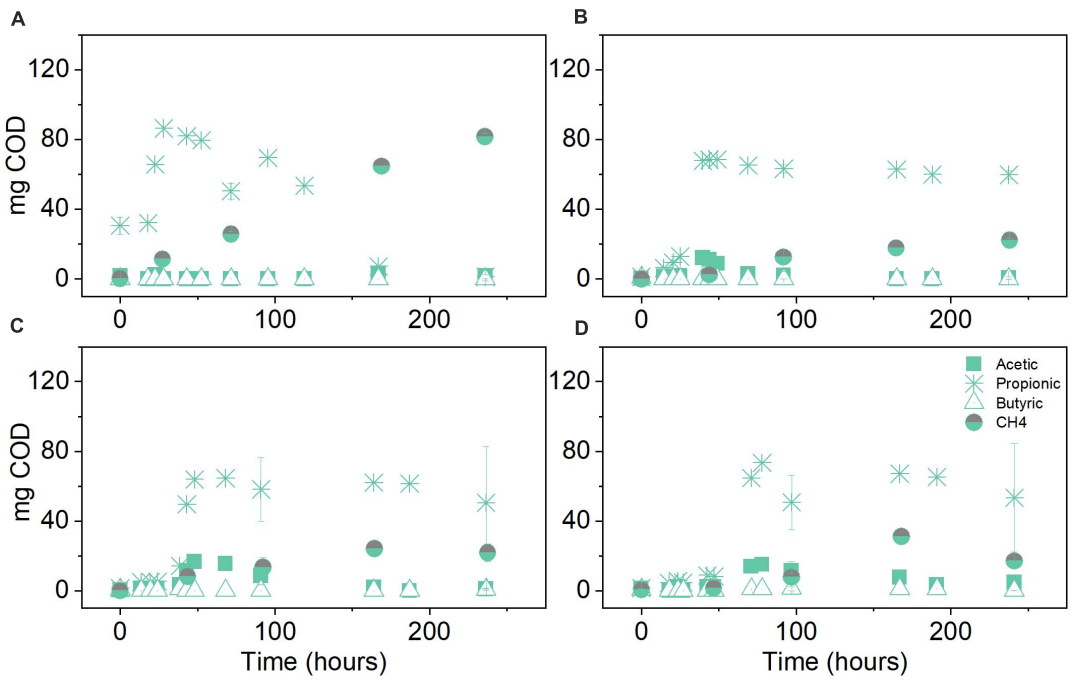

FIGURE 7 | Volatile fatty acid and CH_4 production (mg COD) over time for the glycerol conversion experiments using original inoculum at initial pCO_2 of **(A)** 0.3 bar, **(B)** 3 bar, **(C)** 5 bar, and **(D)** 8 bar. Pressure corresponds to initial values before equilibrium. Data points represent experimental data. Bars represent the standard deviation of three biological replicates measured at the beginning, middle and end of the experiment.

Beta diversity analysis via calculation of the Bray Curtis distance measures revealed significant differences in the community at the highest taxonomic level (Kingdom) because of exposure to elevated pCO_2 ($p = 0.01$ and $p = 0.04$, respectively). The inoculum condition was significant only to explain the variability of the bacterial community ($p = 0.07$) among all experimental treatments.

Product Spectrum

Original inoculum

The glycerol anaerobic conversion experiments showed a similar final product spectrum to glucose in terms of VFA. The difference was observed in the overall production: propionate in each condition of glycerol fermentation was around two times higher than during glucose fermentation and butyrate production was, on average, four times lower. Under atmospheric conditions, propionate production reached 600 mg COD–Pr L^{-1} at 0.3 bar pCO_2. In terms of the mass balance, this accounts for 67% of the initial COD (**Figure 7A**). In the elevated pCO_2 experiments, the propionate concentration reached its plateau around 647 ± 41 mg COD–Pr L^{-1}, corresponding in mass to 57–66% of the initial COD input. Similar to the glucose experiments, propionate conversion was seemingly affected by elevated pCO_2 leading to its accumulation after approximately 70 h and until the

end of the experimental period (**Figures 7B–D**). Consequently, CH_4 production was majorly impacted in the glycerol treatments at elevated pCO_2. On average, methane production was lowered by 69%, compared to the atmospheric control at 0.3 bar pCO_2. CH_4 production in the pressurized treatments was, on average, 48% lower in the case of glycerol compared to glucose.

Evolved inoculum

In the case of glycerol conversion at 5 bar pCO_2 using evolved inoculum, propionate peaked after 69 h (**Supplementary Figure 6**) and decreased until complete conversion was observed by the end of the experiment (**Figure 5B**). An increment of 55% in final CH_4 production was achieved when compared to the treatments at the same pCO_2 using the original inoculum (**Figure 7C**). Contrary to what was observed with the original inoculum experiments, CH_4 production from glycerol with evolved inoculum was 23% higher than from glucose at 5 bar pCO_2.

Evaluation of CH_4 Yield of Glucose and Glycerol Conversion Under Elevated pCO_2 Using Evolved Inoculum

The processed sequencing data were used to estimate the proportions of bacteria and archaea in the incubations at atmospheric and pressurized conditions with glucose and glycerol. These proportions together with the results of FCM analysis were used to estimate the theoretical CH_4 yield in ng of COD per viable archaeal cell for the experimental treatments (**Figure 8**). Based on these results, we calculated that in the 5 bar pCO_2 experiment using evolved inoculum, the CH_4 yield per viable archaeal cell was approximately 2.6 and 4.4 times higher compared to the same condition using the original inoculum for glucose and glycerol, respectively. When comparing glucose and glycerol incubations with evolved inoculum and 5 bar pCO_2, the CH_4 yield per cell in the incubation with glycerol was slightly higher than with glucose (1.3 times), which contrasts with the results of the original inoculum. In all cases, elevated pCO_2 treatments evidenced lower CH_4 yield than pN_2 controls. The increased CH_4 production is likely associated with changes in total archaeal proportion, resulting from the directional microbial community selection process. Furthermore, enhanced product formation is remarkable, since an elevated pCO_2 of 5 bar seemed to constrain cell growth in the case of the glycerol evolved inoculum (**Figure 2C**), but not for glucose (**Figure 2B**). This might suggest the development of different stress-response strategies to elevated pCO_2 depending on the type of substrate and selected microbial community. Moreover, the relative abundance of *Smithella* + *Syntrophobacter* is 2.3 times higher in glycerol than glucose evolved inoculum (**Figures 3A**, **6A**), which in turn might help to explain higher CH_4 production due to community and pathway selection despite limited growth. It is postulated that due to the ALE process, a higher F:M ratio employed during the elevated pCO_2 experiments with evolved inoculum did not constrained bioconversion activity. The F:M ratio was 4–5 times higher in elevated pCO_2 experiments with evolved inoculum (phase 3, **Figure 1**) compared to original inoculum (phase 1, **Figure 1**). However, due to the differences in viable cell concentration, the substrate loads (calculated as mg COD per viable cell), were actually 10 and three times higher compared to the ones using original inoculum for glucose and glycerol, respectively. These differences at the "biomass" and "cell" level could have caused additional inhibition of the biochemical activity of the evolved inoculum, however, results indicate that the ALE process selected for more resilient microorganisms able to cope with the imposed conditions.

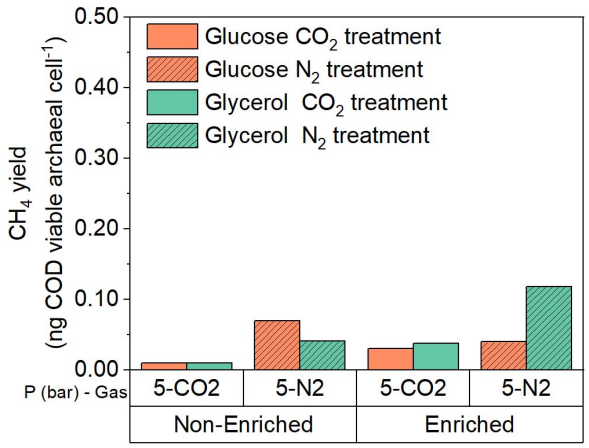

FIGURE 8 | CH_4 yield normalized by the viable archaeal cell density at the end of the experiment for the glucose and glycerol conversion experiments at elevated pCO_2 using original inoculum and evolved inoculum at 5 bar. Pressure corresponds to initial values before equilibrium. Nitrogen controls (5 bar) are included as a reference.

DISCUSSION

From the directional selection of microbial community via ALE, the three main achievements were: (i) an increase in the overall total and viable cell density, (ii) a higher proportion of archaea compared to the original inoculum for glucose and (iii) a larger proportion of SPOB for both substrates (**Table 2**). These achievements provide a reasonable explanation for enabling propionate conversion and consequently improving CH_4 production under elevated pCO_2.

The ALE process could have contributed to the development of protective mechanisms associated with the conservation of cell membrane integrity. It is known that changes in environmental conditions, such as temperature and osmotic pressure, trigger modifications in the structure and fluidity of cell membranes (Beney and Gervais, 2001). Bacteria and archaea differ in the chemical composition of their membrane lipids (Albers and Meyer, 2011), which confers them a distinctive degree of protection toward changes in total pressure and pCO_2. If membrane fluidity and permeability are being compromised, both groups of microorganisms are capable of adjusting their lipid composition to control ion leakage (Van De Vossenberg et al., 2000). However, previous works suggest that the lipid core of bacterial membranes can adjust itself better to regulate membrane fluidity (Siliakus et al., 2017). This adaptation might

confer a survival advantage to bacterial spp. under conditions compromising membrane fluidity and in turn intracellular fluxes, such as the exposure to elevated pCO_2.

According to Wu et al. (2007), the application of high-pressure CO_2, i.e., >20 bar, has shown a strong bactericidal effect in cultures of the model organism *E. coli*. The mechanisms contributing to the bactericidal effect included: (i) compromised membrane integrity due to facilitated intracellular diffusion of increased H_2CO_3* concentrations, (ii) drainage of internal cell components such as DNA, and cations as K^+, Na^+ that are linked to a more permeable membrane, and (iii) possible internal acidification jeopardizing enzymatic activity as a consequence of a surpassed cytoplasmic buffering capacity (Yao et al., 2014). In our experiments, final pH measurements after decompression (**Supplementary Table 1**) did not show dramatic differences at the studied pCO_2 levels because of elevated buffer concentration. It should be realized that the external pH only partly determines cytoplasmic pH, which depends on the physiological features of each microorganism and the internal buffer capacity of the cell. The latter could be compromised by additional neutralization requirements to keep pH homeostasis when H_2CO_3* dissociation occurs in the cytoplasm (Slonczewski et al., 2009). Thus, some degree of cytoplasmic acidification cannot be discarded compromising cell growth in the case of glucose experiments with original inoculum (**Figure 2B**) and inhibition of microbial activity leading to intermediate propionate accumulation at elevated pCO_2 for both substrates with the inoculum before the ALE process (**Figures 4**, **7**).

It can be hypothesized that the increased load of an acidifying substrate, such as glucose, in every ALE cycle will lead to the development of protective measures against accumulating acidity, which could help to minimize effects on cell membrane integrity by elevated pCO_2 (Sun et al., 2005) and could help to explain the increase in cell viability after ALE with glucose (**Figure 2B**). The noticeable positive effects of using glycerol as the substrate on cell viability (**Figure 2C**) could be attributed to several factors. Firstly, changes in the medium viscosity can affect the diffusion rate of CO_2 and could lead to lower microbial inactivation rates by high-pressure CO_2. A similar observation previously has been reported for a growth medium with increased fat content (Lin et al., 1994). Secondly, researchers recently described that compatible solutes can also act as piezolytes to increase tolerance to pressure exposure (Martin et al., 2002; Scoma and Boon, 2016). Since glycerol can also act as a compatible solute, it might as well confer a temporary piezotolerance depending on its specific uptake and conversion rate. Thirdly, because of its non-ionic nature, glycerol may reduce water activity (a_w) in the medium, which in turn could contribute to lower microbial inactivation rates by high-pressure CO_2 as a result of decreased H_2CO_3* formation and a stabilization effect on membrane proteins (Wu et al., 2007; Kish et al., 2012). Regarding the effects of substrate concentration on the a_w in the experimental treatments, theoretical calculations performed in the hydrogeochemical software Phreeqc® indeed showed that glycerol lowered the water activity compared to glucose but at elevated substrate concentrations (**Supplementary Table 3**). At the applied low substrate concentrations of 5 and 9 mM for glycerol and glucose, respectively, it is questionable whether changes in a_w would have significantly impacted cell viability in our experiments. Nonetheless, the observed differences in cell viability between glycerol and glucose treatments with the original inoculum (**Figure 2**), where a higher biomass concentration was applied, might suggest the occurrence of CO_2 diffusion limitation associated with the presence of glycerol in the medium.

The detrimental effects of high pCO_2 cannot be solely attributed to a pressure effect. A comparable loss of viability as the one observed at elevated pCO_2 has up till now only been achieved at hydrostatic pressures higher than 100 MPa (Pagán and Mackey, 2000). When using a non-reactive gas such as N_2, strong biocidal effects have not been observed even if the pH is significantly lowered to emulate pH levels due to CO_2 dissolution (Wu et al., 2007). However, we observed a detrimental effect of pressurized N_2 on the cell viability of evolved inoculum with glycerol (**Figure 2C**) which suggests a negative effect of headspace pressure at low biomass concentration. Moreover, an increased amount of non-viable cells following pressurized conditions can also be explained by reactor depressurization. It has been shown that pressure release, even if performed gradually, can increase the amount of permeabilized cells (Park and Clark, 2002), and thus, compromising their viability. Further investigations are needed to thoroughly quantify possible decompression effects on cell viability and metabolic activity when using reactive and inert gases such as CO_2 and N_2.

At high propionate concentrations and low pH, a microbial community shift toward increased proportions of hydrogenotrophic methanogens has been evidenced, which contributes to maintaining a low partial pressure of hydrogen (pH_2) to enable Pr-Ox under syntrophic conditions (Li et al., 2018; Han et al., 2020). Apparently, low pH_2 conditions favor the production of H_2 instead of NADH from the oxidation of reduced ferredoxin (Fd_{red}) (Lee et al., 2008). Furthermore, at low pH_2, hydrogenotrophic methanogenesis has been described as kinetically (Liu et al., 2016) and thermodynamically more feasible than homoacetogenesis at increasing pCO_2 (**Supplementary Figure 4**). This would imply that, in principle, we should have observed an increased proportion of hydrogenotrophic methanogens in the glucose experiments. However, this occurred only in the treatment with the original inoculum at the lowest pCO_2 of 0.3 bar (**Figure 3B**). Zhang et al. (2011) described a possible detrimental effect of elevated CO_2 concentration on the transcription levels of functional [FeFe] hydrogenases of the moderate thermophile *Thermoanaerobacterium thermosaccharolyticum W16*. The reduction in the ratio mRNA expression to 16S DNA gene depended on the type of substrate employed, glucose or xylose, and varied between 66 and 98% (Zhang et al., 2011). Considering this as a plausible hypothesis, H_2 production might have been hindered in our elevated pCO_2 experiments, leaving the production of reduced compounds as the main route for NADH consumption.

The biochemical pathways of anaerobic conversion of glucose and glycerol share PEP and pyruvate as central intermediates (Zhang et al., 2015). Pathway steering toward particular electron sinks such as propionate will depend on

the environmental conditions and type of microorganism (**Supplementary Figure 1**). Under the assumption of CO_2 fixation, the carboxylation from PEP or pyruvate to OAA, which is subsequently further reduced to fumarate, is favored at the reductive branch of the PEP-pyruvate-OAA node (Sauer and Eikmanns, 2005; Stams and Plugge, 2009). Without the presence of sufficient reducing equivalents, a presumed CO_2 fixation will have a more limited impact on the production of more reduced compounds during glucose fermentation. It should be realized that, compared to glucose, the metabolism of glycerol requires balancing double the amount of reducing equivalents per mole of pyruvate or PEP produced. Under limited hydrogen production, NADH will act as electron carrier, channeling the reducing equivalents toward products such as propionate, whose formation stoichiometrically consumes the NADH from glycerol conversion (Zhang et al., 2015). Concomitantly, acetate production from the acetyl-CoA pathway is downregulated to limit reductive stress due to presence of excess NADH (Doi and Ikegami, 2014). Propionate production from pyruvate in glucose metabolism requires an additional electron donor or extra NADH input. Thus, the simultaneous production of a more oxidized compound, namely acetate, helps to satisfy the redox balance. However, this will occur at the expense of a decreased propionate yield, due to diverged carbon flux (Zhang et al., 2015), helping to explain the differences in propionate levels between the used substrates (**Figures 4**, **5**, **7**). Increased propionate production could also be attributed to enhanced enzymatic activities as a result of the substrate choice for the ALE cycles. The activity of pyruvate carboxylase and succinyl CoA: propionyl CoA transferase, both enzymes with a significant role in propionate production, has been enhanced in cultures of *Propionibacterium acidipropionici* using glycerol as the substrate (Zhang et al., 2016). Conversely, this was not observed by these authors when the culture was grown using glucose as the sole carbon and energy source.

The premise of compromised hydrogenase activity because of elevated CO_2 concentrations could help to explain the decreased proportions of hydrogenotrophic methanogens, particularly in the treatments with glucose. Moreover, the initially high proportion of *Methanosaeta* in the original inoculum (**Figure 6B**), the reduced H_2 production when using glycerol as the substrate according to stoichiometry, and a plausible detrimental effect of pCO_2 on hydrogenase activity, support the idea of the enhancement of a Pr-Ox pathway where thermodynamic limitations associated with interspecies H_2 transfer plays a less significant role, i.e., the dismutation pathway of *Smithella*, whose relative abundance considerably increased following the ALE process (**Figures 3A**, **6A**). Members of the genus *Smithella* are metabolically active in a broader range of propionate concentrations (Ariesyady et al., 2007), low HRT (Ban et al., 2015) and acidic pH (Li et al., 2018) than members of the genus *Syntrophobacter*. The conditions imposed during the directional selection, i.e., serial transfers to fresh medium, exposed the microorganisms to increased substrate loadings per cell. This possibly contributed to the enrichment of this genus, particularly in the glycerol experiments at 5 bar pCO_2 using evolved inoculum (**Figure 6A**). Additionally, if thermodynamic feasibility is considered, the dismutation pathway, i.e., propionate conversion to butyrate and acetate, is less sensitive to the effects of increasing pH_2 and pCO_2 than the methyl malonyl-CoA pathway, where propionate is converted to acetate and H_2, which undergo further conversion by methanogenic archaea (Dolfing, 2013) (**Supplementary Figure 5**). For further reference, we have summarized the stoichiometries of possible metabolic pathways for the anaerobic conversion of glucose and glycerol including either the dismutation or the methyl malonyl-CoA pathways (**Supplementary Table 2**).

It is postulated that the occurrence of the *Smithella* pathway in the incubation with both substrates relates well with enhanced CH_4 yield and might ameliorate end-product inhibition due to elevated pCO_2 in the case of glucose (**Supplementary Table 2**). Moreover, less CO_2 is being produced in the glycerol treatments either by methyl malonyl-CoA pathway or by the dismutation pathway from *Smithella* (**Supplementary Table 2**). Theoretically, this could enable a substantial CO_2 fixation via the OAA route (**Supplementary Figure 1**) and enhanced propionate production if enough reducing equivalents are available. Regulation of the redox balance could be achieved in this pathway by the consumption of reducing equivalents in the intermediate steps, forming malate and succinate. Due to these two reasons, moderately high pCO_2 levels have likely affected glycerol conversion to a lesser extent.

The here presented higher CH_4 yields at 5 bar pCO_2 using evolved inoculum have to be interpreted with caution since significant differences were found in the initial viable cell density of treatments with evolved and original inoculum ($p = 0.004$), as a consequence of the higher microbial F:M ratio imposed to keep the experimental liquid volume comparable in all treatments. The observed lower initial cell density in the experiments with evolved inoculum is attributed to the followed harvesting and resuspension procedure for biomass recovery. These initial differences did not necessarily lead to statistically significant higher proportions of viable biomass ($p = 0.43$) at the end of the experiments using original inoculum, thus comparisons in terms of active biomass are fairly reasonable. The CH_4-yield calculated per viable cell showed that the methanogenic activity under elevated pCO_2 was moderately enhanced due to the directional selection process and might be indicative of microbial community resilience to elevated pCO_2. It was not possible to extrapolate these yields in terms of VSS concentration since this parameter only showed a moderate positive correlation with the log-transformed viable cell density data ($r_s = 0.65$, $p = 0.005$) (**Supplementary Figure 3**) and did not constitute a good proxy for microbial biomass in the experiments here presented. We would not have been able to evidence subtle changes in total cell density and cell viability compromising overall metabolic activity by only relying on this measurement, since it includes dead/non-viable cells and extracellular compounds besides the active biomass (Foladori et al., 2010).

At the microbial ecology level, high CO_2 concentrations shift the community structure and reduce the taxonomic diversity in different environmental systems (Yu and Chen, 2019), with effects beyond acidification (Gulliver et al., 2014). In our experiments, the directional selection process, prior exposure

to elevated pCO_2, proved to be preponderant for changes in community structure (Hill number H_0–Richness **Supplementary Figure 2A**) and overall diversity (**Figures 3**, **6**), which can benefit reactor start-up. Changes in alpha diversity could be linked to a community reorganization as a consequence of the selection pressure (increased substrate load) or an applied disturbance, namely the elevated pCO_2 (Werner et al., 2011). In our experiments, as expected, microbial community richness decreased due to the ALE process, but VFA production was not compromised. Fermentative activity tends to be conserved even if decreased richness is observed, most likely due to the resilience of this process to stress conditions (Mota et al., 2017). However, conservation of functionality features of the evolved community and its prevalence as the core microbiome in long-term AD-operation will depend on process operation and control (Tonanzi et al., 2018). Concerning the archaeal community structure, CO_2 enrichment in anaerobic digesters at atmospheric conditions can modify the ratio aceticlastic: hydrogenotrophic methanogens favoring the abundance of *Methanosaeta* (Bajón Fernández et al., 2019). This finding is in alignment with the observations here described and the study by Lindeboom et al. (2016), where a high relative abundance of *Methanosaeta* is reported at increased pCO_2 levels during high-pressure AD.

Our observations associated with changes in structure and diversity are only indicative of the effects of elevated CO_2 in fermentative and methanogenic communities and their syntrophic interactions at the bioreactor level, because of the short duration of our experiments. Further support for these conclusions needs to come from longer incubations under pressurized CO_2 conditions with different types of inocula. Longer incubations leading to increased growth of adapted biomass could enable a more accurate quantification with standard methods (VSS). If a more thorough characterization of the biomass at cell level in terms of average cell dimension and biovolume would be performed, it could permit a better correlation between VSS and FCM results. Similar to previous work, a correlation between protein measurements following the Lowry method and VSS could also provide additional characterization (Lindeboom et al., 2018). Moreover, if these incubations are monitored with online pH, pressure measurements and intensive sampling for microbial community dynamics, a clearer correlation could be obtained between changes in the community and operational variables modified by the pressurized operation. But, even then, the accounted effects might depend on specific system characteristics and operational strategy. Observations of natural soil communities exposed to elevated atmospheric pCO_2 show that there is not a common agreement over the effects on the microbial ecology. Recent studies have reported either no significant changes (Bruce et al., 2000; Ahrendt et al., 2014) or major shifts in the microbial community (Xu et al., 2013; Šibanc et al., 2014). These shifts include, for example, the predominance of acid-resistant groups such as Chloroflexi and Firmicutes or acetogenic spore-forming Clostridia (Conrad, 2020), which agrees with the results here reported (**Figures 3**, **6**). From these investigations, it can be deduced that other environmental factors such as temperature, pH, nutrient availability as well as CO_2 final concentration and exposure time will determine the overall fate of the microbial community after exposure to elevated pCO_2.

CONCLUSION

A microbial community directional selection strategy was employed in this study to overcome limited syntrophic Pr-Ox in glucose and glycerol anaerobic conversions under elevated pCO_2. The pressurized incubations using evolved inoculum showed a dissimilarly enhanced final cell viability, with a stronger positive effect of the ALE in cell viability of glucose incubations. Our results suggest that directional selection of microbial community with increased substrate load per cell triggered mechanisms to preserve cell viability. Moreover, it increased the proportions and enhanced the metabolic activity of microorganisms resilient to increasing propionate concentrations such as SPOB and the interrelated methanogenic community. The increased abundance of the genus *Smithella* accompanied by higher proportions of *Methanosaeta* after incubation with glycerol proved to be beneficial for propionate conversion at elevated pCO_2. The highest CH_4 yield per cell at conditions elevated pCO_2 was observed in the glycerol experiments, which was attributed to enhanced propionate formation, as a way to incorporate CO_2 and maintain the redox balance via metabolic regulation. Overall, using an evolved inoculum with higher viable cell density and restructured community with a predominance of key microbial groups proved to be a right course of action into surmounting reduced metabolic performance associated with elevated pCO_2.

DATA AVAILABILITY STATEMENT

The raw fastq files used to create the OTU table for the microbial community analysis, have been deposited in the National Center for Biotechnology Information (NCBI) database (Accession number PRJNA704575).

AUTHOR CONTRIBUTIONS

PC-C designed the experiment, supervised the experiment execution, and wrote the manuscript in its majority. Y-tC performed the experiments, analytical measurements, and contributed to the manuscript writing and editing process. PC-C and Y-tC analyzed the data. JL provided feedback to the experimental design and critically revised the final version of the manuscript. KR constructively revised the final version of the manuscript. RL helped to design, supervised the development of the experiment, and provided constructive feedback to the manuscript. All authors contributed to the article and approved the submitted version.

FUNDING

This research was funded by the European Union's Horizon 2020 Research and Innovation Program under the Marie

Skłodowska-Curie grant agreement no. 676070 (SuPER-W). This communication reflects only the author's view, and the Research Executive Agency of the EU is not responsible for any use that may be made of the information it contains.

ACKNOWLEDGMENTS

The authors kindly acknowledge Lais Soares for her technical assistance during the experiments and Ingrid Pinel for her technical assistance with the flow cytometry measurements. Tim Lacoere and Jo de Vrieze are acknowledged for their contribution to the Illumina sequencing data processing and statistical analysis.

SUPPLEMENTARY MATERIAL

The Supplementary Material for this article can be found online at: https://www.frontiersin.org/articles/10.3389/fmicb.2021.675763/full#supplementary-material

REFERENCES

Aertsen, A., Meersman, F., Hendrickx, M. E. G., Vogel, R. F., and Michiels, C. W. (2009). Biotechnology under high pressure: applications and implications. *Trends Biotechnol.* 27, 434–441. doi: 10.1016/j.tibtech.2009.04.001

Agler, M. T., Wrenn, B. A., Zinder, S. H., and Angenent, L. T. (2011). Waste to bioproduct conversion with undefined mixed cultures: the carboxylate platform. *Trends Biotechnol.* 29, 70–78. doi: 10.1016/j.tibtech.2010.11.006

Ahrendt, S. R., Mobberley, J. M., Visscher, P. T., Koss, L. L., and Foster, J. S. (2014). Effects of elevated carbon dioxide and salinity on the microbial diversity in lithifying microbial mats. *Minerals* 4, 145–169. doi: 10.3390/min4010145

Albers, S. V., and Meyer, B. H. (2011). The archaeal cell envelope. *Nat. Rev. Microbiol.* 9, 414–426. doi: 10.1038/nrmicro2576

American Public Health Association. (2005). *Standard Methods for the Examination of Water and Wastewater*. 21st Edn. Washington, D.C: American Public Health Association.

Amorim, N. C. S., Amorim, E. L. C., Kato, M. T., Florencio, L., and Gavazza, S. (2018). The effect of methanogenesis inhibition, inoculum and substrate concentration on hydrogen and carboxylic acids production from cassava wastewater. *Biodegradation* 29, 41–58. doi: 10.1007/s10532-017-9812-y

Ariesyady, H. D., Ito, T., Yoshiguchi, K., and Okabe, S. (2007). Phylogenetic and functional diversity of propionate-oxidizing bacteria in an anaerobic digester sludge. *Appl. Microbiol. Biotechnol.* 75, 673–683. doi: 10.1007/s00253-007-0842-y

Arslan, D., Steinbusch, K. J. J., Diels, L., Hamelers, H. V. M., Strik, D. P. B. T. B., Buisman, C. J. N., et al. (2016). Selective short-chain carboxylates production: a review of control mechanisms to direct mixed culture fermentations. *Crit. Rev. Environ. Sci. Technol.* 46, 592–634. doi: 10.1080/10643389.2016.1145959

Baez, A., Flores, N., Bolívar, F., and Ramírez, O. T. (2009). Metabolic and transcriptional response of recombinant *Escherichia coli* to elevated dissolved carbon dioxide concentrations. *Biotechnol. Bioeng.* 104, 102–110. doi: 10.1002/bit.22379

Bajón Fernández, Y., Soares, A., Vale, P., Koch, K., Masse, A. L., and Cartmell, E. (2019). Enhancing the anaerobic digestion process through carbon dioxide enrichment: initial insights into mechanisms of utilization. *Environ. Technol.* 40, 1744–1755. doi: 10.1080/09593330.2019.1597173

Ban, Q., Zhang, L., and Li, J. (2015). Shift of propionate-oxidizing bacteria with HRT decrease in an UASB reactor containing propionate as a sole carbon source. *Appl. Biochem. Biotechnol.* 175, 274–286. doi: 10.1007/s12010-014-1265-8

Beney, L., and Gervais, P. (2001). Influence of the fluidity of the membrane on the response of microorganisms to environmental stresses. *Appl. Microbiol. Biotechnol.* 57, 34–42. doi: 10.1007/s002530100754

Bray, J. R., and Curtis, J. T. (1957). An ordination of the upland forest communities of southern Wisconsin. *Ecol. Monogr.* 27, 325–349. doi: 10.2307/1942268

Bruce, K. D., Jones, T. H., Bezemer, T. M., Thompson, L. J., and Ritchie, D. A. (2000). The effect of elevated atmospheric carbon dioxide levels on soil bacterial communities. *Glob. Change Biol.* 6, 427–434. doi: 10.1046/j.1365-2486.2000.00320.x

Ceron-Chafla, P., Kleerebezem, R., Rabaey, K., van Lier, J. B., and Lindeboom, R. E. F. (2020). Direct and Indirect Effects of increased CO2 partial pressure on the bioenergetics of syntrophic propionate and butyrate conversion. *Environ. Sci. Technol.* 54, 12583–12592. doi: 10.1021/acs.est.0c02022

Chen, Y. Y., Temelli, F., and Gänzle, M. G. (2017). Mechanisms of inactivation of dry *Escherichia coli* by high-pressure carbon dioxide. *Appl. Environ. Microbiol.* 83:e00062. doi: 10.1128/AEM.00062-17

Conrad, R. (2020). Importance of hydrogenotrophic, aceticlastic and methylotrophic methanogenesis for methane production in terrestrial, aquatic and other anoxic environments: a mini review. *Pedosphere* 30, 25–39. doi: 10.1016/S1002-0160(18)60052-9

Doi, Y., and Ikegami, Y. (2014). Pyruvate formate-lyase is essential for fumarate-independent anaerobic glycerol utilization in the *Enterococcus faecalis* strain W11. *J. Bacteriol.* 196, 2472–2480. doi: 10.1128/JB.01512-14

Dolfing, J. (2013). Syntrophic propionate oxidation via butyrate: a novel window of opportunity under methanogenic conditions. *Appl. Environ. Microbiol.* 79, 4515–4516. doi: 10.1128/AEM.00111-13

Dragosits, M., and Mattanovich, D. (2013). Adaptive laboratory evolution – principles and applications for biotechnology. *Microb. Cell Fact.* 12:64. doi: 10.1186/1475-2859-12-64

Fazi, S., Ungaro, F., Venturi, S., Vimercati, L., Cruz Viggi, C., Baronti, S., et al. (2019). Microbiomes in soils exposed to naturally high concentrations of CO2 (Bossoleto Mofette Tuscany, Italy). *Front. Microbiol.* 10:2238. doi: 10.3389/fmicb.2019.02238

Foladori, P., Bruni, L., Tamburini, S., and Ziglio, G. (2010). Direct quantification of bacterial biomass in influent, effluent and activated sludge of wastewater treatment plants by using flow cytometry. *Water Res.* 44, 3807–3818. doi: 10.1016/j.watres.2010.04.027

García Rea, V. S., Muñoz Sierra, J. D., Fonseca Aponte, L. M., Cerqueda-Garcia, D., Quchani, K. M., Spanjers, H., et al. (2020). Enhancing phenol conversion rates in saline anaerobic membrane bioreactor using acetate and butyrate as additional carbon and energy sources. *Front. Microbiol.* 11:604173. doi: 10.3389/fmicb.2020.604173

Garcia-Gonzalez, L., Geeraerd, A. H., Mast, J., Briers, Y., Elst, K., Van Ginneken, L., et al. (2010). Membrane permeabilization and cellular death of *Escherichia coli*, Listeria monocytogenes and Saccharomyces cerevisiae as induced by high pressure carbon dioxide treatment. *Food Microbiol.* 27, 541–549. doi: 10.1016/j.fm.2009.12.004

Guan, N., and Liu, L. (2020). Microbial response to acid stress: mechanisms and applications. *Appl. Microbiol. Biotechnol.* 104, 51–65. doi: 10.1007/s00253-019-10226-1

Gulliver, D. M., Lowry, G. V., and Gregory, K. B. (2014). CO2 concentration and pH alters subsurface microbial ecology at reservoir temperature and pressure. *RSC Adv.* 4, 17443–17453. doi: 10.1039/C4RA02139H

Han, Y., Green, H., and Tao, W. (2020). Reversibility of propionic acid inhibition to anaerobic digestion: inhibition kinetics and microbial mechanism. *Chemosphere* 255:126840. doi: 10.1016/j.chemosphere.2020.126840

Heijnen, J. J., and Kleerebezem, R. R. (2010). "Bioenergetics of Microbial Growth," in *Encyclopedia of Industrial Biotechnology*, ed. M. C. Flickinger (Hoboken, NJ: John Wiley & Sons, Inc.), 1–66.

Hickey, R. F., and Switzenbaum, M. S. (1991). Thermodynamics of volatile fatty acid accumulation in anaerobic digesters subject to increases in hydraulic and organic loading. *Res. J. Water Pollut. Control Fed.* 63, 141–144.

Hill, M. O. (1973). Diversity and evenness: a unifying notation and its consequences. *Ecology* 54, 427–432. doi: 10.2307/1934352

Himmi, E. H., Bories, A., Boussaid, A., and Hassani, L. (2000). Propionic acid fermentation of glycerol and glucose by Propionibacterium acidipropionici and Propionibacterium freudenreichii ssp. shermanii. *Appl. Microbiol. Biotechnol.* 53, 435–440. doi: 10.1007/s002530051638

Holtzapple, M. T., and Granda, C. B. (2009). Carboxylate platform: the MixAlco process part 1: comparison of three biomass conversion platforms. *Appl. Biochem. Biotechnol.* 156, 95–106. doi: 10.1007/s12010-008-8466-y

Huang, Z., Yu, J., Xiao, X., Miao, H., Ren, H., Zhao, M., et al. (2016). Directional regulation of the metabolic heterogeneity in anaerobic mixed culture to enhance fermentative hydrogen production by adaptive laboratory evolution. *Int. J. Hydrogen Energy* 41, 10145–10151. doi: 10.1016/j.ijhydene.2016.05.012

Kish, A., Griffin, P. L., Rogers, K. L., Fogel, M. L., Hemley, R. J., and Steele, A. (2012). High-pressure tolerance in Halobacterium salinarum NRC-1 and other non-piezophilic prokaryotes. *Extremophiles* 16, 355–361. doi: 10.1007/s00792-011-0418-8

Kumagai, H., Hata, C., and Nakamura, K. (1997). CO2 sorption by microbial cells and sterilization by high-pressure CO2. *Biosci. Biotechnol. Biochem.* 61, 931–935. doi: 10.1271/bbb.61.931

Kwon, Y. D., Kim, S., Lee, S. Y., and Kim, P. (2011). Long-term continuous adaptation of *Escherichia coli* to high succinate stress and transcriptome analysis of the tolerant strain. *J. Biosci. Bioeng.* 111, 26–30. doi: 10.1016/j.jbiosc.2010.08.007

Lee, H.-S., Salerno, M. B., and Rittmann, B. E. (2008). Thermodynamic evaluation on H $_2$ production in glucose fermentation. *Environ. Sci. Technol.* 42, 2401–2407. doi: 10.1021/es702610v

Lemmer, A., Chen, Y., Lindner, J., Wonneberger, A. M., Zielonka, S., Oechsner, H., et al. (2015). Influence of different substrates on the performance of a two-stage high pressure anaerobic digestion system. *Bioresour. Technol.* 178, 313–318. doi: 10.1016/j.biortech.2014.09.118

Li, L., He, Q., Ma, Y., Wang, X., and Peng, X. (2016). A mesophilic anaerobic digester for treating food waste: process stability and microbial community analysis using pyrosequencing. *Microb. Cell Fact.* 15:65. doi: 10.1186/s12934-016-0466-y

Li, Y., Sun, Y., Li, L., and Yuan, Z. (2018). Acclimation of acid-tolerant methanogenic propionate-utilizing culture and microbial community dissecting. *Bioresour. Technol.* 250, 117–123. doi: 10.1016/j.biortech.2017.11.034

Lin, H., Cao, N., and Chen, L.-F. (1994). Antimicrobial effect of pressurized carbon dioxide on listeria monocytogenes. *J. Food Sci.* 59, 657–659. doi: 10.1111/j.1365-2621.1994.tb05587.x

Lindeboom, R. E. F., Fermoso, F. G., Weijma, J., Zagt, K., and van Lier, J. B. (2011). Autogenerative high pressure digestion: anaerobic digestion and biogas upgrading in a single step reactor system. *Water Sci. Technol.* 64, 647–653. doi: 10.2166/wst.2011.664

Lindeboom, R. E. F., Ferrer, I., Weijma, J., and van Lier, J. B. (2013). Effect of substrate and cation requirement on anaerobic volatile fatty acid conversion rates at elevated biogas pressure. *Bioresour. Technol.* 150, 60–66. doi: 10.1016/j.biortech.2013.09.100

Lindeboom, R. E. F., Ilgrande, C., Carvajal-Arroyo, J. M., Coninx, I., Van Hoey, O., Roume, H., et al. (2018). Nitrogen cycle microorganisms can be reactivated after space exposure. *Sci. Rep.* 8, 8–14. doi: 10.1038/s41598-018-32055-4

Lindeboom, R. E. F., Shin, S. G., Weijma, J., van Lier, J. B., and Plugge, C. M. (2016). Piezo-tolerant natural gas-producing microbes under accumulating pCO2. *Biotechnol. Biofuels* 9, 98–127. doi: 10.1186/s13068-016-0634-7

Liu, R., Hao, X., and Wei, J. (2016). Function of homoacetogenesis on the heterotrophic methane production with exogenous H2/CO2 involved. *Chem. Eng. J.* 284, 1196–1203. doi: 10.1016/j.cej.2015.09.081

Martin, D. D., Bartlett, D. H., and Roberts, M. F. (2002). Solute accumulation in the deep-sea bacterium *Photobacterium profundum*. *Extremophiles* 6, 507–514. doi: 10.1007/s00792-002-0288-1

McMahon, K. D., Zheng, D., Stams, A. J. M., Mackie, R. I., and Raskin, L. (2004). Microbial population dynamics during start-up and overload conditions of anaerobic digesters treating municipal solid waste and sewage sludge. *Biotechnol. Bioeng.* 87, 823–834. doi: 10.1002/bit.20192

McMurdie, P. J., and Holmes, S. (2013). Phyloseq: an R package for reproducible interactive analysis and graphics of microbiome census data. *PLoS One* 8:e61217. doi: 10.1371/journal.pone.0061217

Mota, M. J., Lopes, R. P., Koubaa, M., Roohinejad, S., Barba, F. J., Delgadillo, I., et al. (2017). Fermentation at non-conventional conditions in food- and bio-sciences by application of advanced processing technologies. *Crit. Rev. Biotechnol.* 38, 122–140. doi: 10.1080/07388551.2017.1312272

Muñoz Sierra, J. D., García Rea, V. S., Cerqueda-García, D., Spanjers, H., and van Lier, J. B. (2020). Anaerobic conversion of saline phenol-containing wastewater under thermophilic conditions in a membrane bioreactor. *Front. Bioeng. Biotechnol.* 8:565311. doi: 10.3389/fbioe.2020.565311

Oger, P. M., and Jebbar, M. (2010). The many ways of coping with pressure. *Res. Microbiol.* 161, 799–809. doi: 10.1016/j.resmic.2010.09.017

Oksanen, J., Blanchet, F. G., Kindt, R., Legendre, P., Minchin, P. R., O'Hara, B., et al. (2016). *Vegan: Community Ecology Package. R Package Version 2.3-4*. (Vienna, Austria: R Foundation for Statistical Computing).

Pagán, R., and Mackey, B. (2000). Relationship between membrane damage and cell death in pressure-treated *Escherichia coli* cells: differences between exponential- and stationary-phase cells and variation among strains. *Appl. Environ. Microbiol.* 66, 2829–2834. doi: 10.1128/AEM.66.7.2829-2834.2000

Parizzi, L. P., Grassi, M. C. B., Llerena, L. A., Carazzolle, M. F., Queiroz, V. L., Lunardi, I., et al. (2012). The genome sequence of propionibacterium acidipropionici provides insights into its biotechnological and industrial potential. *BMC Genom.* 13:562. doi: 10.1186/1471-2164-13-562

Park, C. B., and Clark, D. S. (2002). Rupture of the cell envelope by decompression of the deep-sea methanogen methanococcus jannaschii. *Appl. Environ. Microbiol.* 68, 1458–1463. doi: 10.1128/AEM.68.3.1458-1463.2002

Park, S., Kwon, H. S., Lee, C. H., and Ahn, I. S. (2020). Correlation between fixation of high-concentration CO2 and glutamate accumulation in sulfurovum lithotrophicum 42BKTT. *J. Ind. Eng. Chem.* 92, 56–61. doi: 10.1016/j.jiec.2020.08.015

Portnoy, V. A., Bezdan, D., and Zengler, K. (2011). Adaptive laboratory evolution-harnessing the power of biology for metabolic engineering. *Curr. Opin. Biotechnol.* 22, 590–594. doi: 10.1016/j.copbio.2011.03.007

Props, R., Kerckhof, F. M., Rubbens, P., De Vrieze, J., Hernandez Sanabria, E., Waegeman, W., et al. (2017). Absolute quantification of microbial taxon abundances. *ISME J.* 11, 584–587. doi: 10.1038/ismej.2016.117

R Core Team. (2019). *R: A language and Environment for Statistical Computing*. Available online at: https://www.r-project.org/ (accessed January 15, 2020).

Russell, J. B., and Diez-Gonzalez, F. (1998). The effects of fermentation acids on bacterial growth. *Adv. Microb. Physiol.* 39, 228–234. doi: 10.1016/s0065-2911(08)60017-x

Saint-Amans, S., Girbal, L., Andrade, J., Ahrens, K., and Soucaille, P. (2001). Regulation of carbon and electron flow in *Clostridium butyricum* VPI 3266 grown on glucose-glycerol mixtures. *J. Bacteriol.* 183, 1748–1754. doi: 10.1128/JB.183.5.1748

Sauer, U., and Eikmanns, B. J. (2005). The PEP-pyruvate-oxaloacetate node as the switch point for carbon flux distribution in bacteria. *FEMS Microbiol. Rev.* 29, 765–794. doi: 10.1016/j.femsre.2004.11.002

Scoma, A., and Boon, N. (2016). Osmotic stress confers enhanced cell integrity to hydrostatic pressure but impairs growth in *Alcanivorax borkumensis* SK2. *Front. Microbiol.* 7:729. doi: 10.3389/fmicb.2016.00729

Šibanc, N., Dumbrell, A. J., Mandič-Mulec, I., and Maćek, I. (2014). Impacts of naturally elevated soil CO2 concentrations on communities of soil archaea and bacteria. *Soil Biol. Biochem.* 68, 348–356. doi: 10.1016/j.soilbio.2013.10.018

Siliakus, M. F., van der Oost, J., and Kengen, S. W. M. (2017). Adaptations of archaeal and bacterial membranes to variations in temperature, pH and pressure. *Extremophiles* 21, 651–670. doi: 10.1007/s00792-017-0939-x

Slonczewski, J. L., Fujisawa, M., Dopson, M., and Krulwich, T. A. (2009). Cytoplasmic pH measurement and homeostasis in bacteria and archaea. *Adv. Microb. Physiol.* 55:317. doi: 10.1016/S0065-2911(09)05501-5

Stams, A. J. M., Dijkema, C., Plugge, C. M., and Lens, P. (1998). Contribution of 13C-NMR spectroscopy to the elucidation of pathways of propionate formation and degradation in methanogenic environments. *Biodegradation* 9, 463–473. doi: 10.1023/A:1008342130938

Stams, A. J. M., and Plugge, C. M. (2009). Electron transfer in syntrophic communities of anaerobic bacteria and archaea. *Nat. Rev. Microbiol.* 7, 568–577. doi: 10.1038/nrmicro2166

Sun, L., Fukamachi, T., Saito, H., and Kobayashi, H. (2005). Carbon dioxide increases acid resistance in *Escherichia coli*. *Lett. Appl. Microbiol.* 40, 397–400. doi: 10.1111/j.1472-765X.2005.01714.x

Tonanzi, B., Gallipoli, A., Gianico, A., Montecchio, D., Pagliaccia, P., Di Carlo, M., et al. (2018). Long-term anaerobic digestion of food waste at semi-pilot scale: relationship between microbial community structure and process performances. *Biomass Bioenergy* 118, 55–64. doi: 10.1016/j.biombioe.2018.08.001

Town, J. R., and Dumonceaux, T. J. (2016). Laboratory-scale bioaugmentation relieves acetate accumulation and stimulates methane production in stalled anaerobic digesters. *Appl. Microbiol. Biotechnol.* 100, 1009–1017. doi: 10.1007/s00253-015-7058-3

Van De Vossenberg, J. L. C. M., Driessen, A. J. M., and Konings, W. N. (2000). "Adaptations of the cell membrane for life in extreme environments," in *Environmental Stressors and Gene Responses*, eds K. B. Storey and J. M. Storey (Netherlands: University of Groningen), 71–88.

Wainaina, S., Lukitawesa, L., Kumar Awasthi, M., and Taherzadeh, M. J. (2019). Bioengineering of anaerobic digestion for volatile fatty acids, hydrogen or methane production: a critical review. *Bioengineered* 10, 437–458. doi: 10.1080/21655979.2019.1673937

Werner, J. J., Knights, D., Garcia, M. L., Scalfone, N. B., Smith, S., Yarasheski, K., et al. (2011). Bacterial community structures are unique and resilient in full-scale bioenergy systems. *Proc. Natl. Acad. Sci. U.S.A.* 108, 4158–4163. doi: 10.1073/pnas.1015676108

Wu, Y., Yao, S.-J., and Guan, Y.-X. (2007). Inactivation of microorganisms in carbon dioxide at elevated pressure and ambient temperature. *Ind. Eng. Chem. Res.* 46, 6345–6352. doi: 10.1021/ie0702330

Xu, M., He, Z., Deng, Y., Wu, L., Van Nostrand, J. D., Hobbie, S. E., et al. (2013). Elevated CO2 influences microbial carbon and nitrogen cycling. *BMC Microbiol* 13:124. doi: 10.1186/1471-2180-13-124

Yao, C., Li, X., Bi, W., and Jiang, C. (2014). Relationship between membrane damage, leakage of intracellular compounds, and inactivation of *Escherichia coli* treated by pressurized CO_2. *J. Basic Microbiol.* 54, 858–865. doi: 10.1002/jobm.201200640

Yu, T., and Chen, Y. (2019). Effects of elevated carbon dioxide on environmental microbes and its mechanisms: a review. *Sci. Total Environ.* 655, 865–879. doi: 10.1016/j.scitotenv.2018.11.301

Zabranska, J., and Pokorna, D. (2018). Bioconversion of carbon dioxide to methane using hydrogen and hydrogenotrophic methanogens. *Biotechnol. Adv.* 36, 707–720. doi: 10.1016/j.biotechadv.2017.12.003

Zhang, A., Sun, J., Wang, Z., Yang, S.-T., and Zhou, H. (2015). Effects of carbon dioxide on cell growth and propionic acid production from glycerol and glucose by *Propionibacterium acidipropionici* - sciencedirect. *Bioresour. Technol.* 175, 374–381. doi: 10.1016/J.BIORTECH.2014.10.046

Zhang, K., Ren, N. Q., Cao, G. L., and Wang, A. J. (2011). Biohydrogen production behavior of moderately thermophile Thermoanaerobacterium thermosaccharolyticum W16 under different gas-phase conditions. *Int. J. Hydrogen Energy* 36, 14041–14048. doi: 10.1016/j.ijhydene.2011.04.056

Zhang, L., Zhu, K., and Li, A. (2016). Differentiated effects of osmoprotectants on anaerobic syntrophic microbial populations at saline conditions and its engineering aspects. *Chem. Eng. J.* 288, 116–125. doi: 10.1016/j.cej.2015.11.100

Zhou, M., Yan, B., Wong, J. W. C., and Zhang, Y. (2018). Enhanced volatile fatty acids production from anaerobic fermentation of food waste: a mini-review focusing on acidogenic metabolic pathways. *Bioresour. Technol.* 248, 68–78. doi: 10.1016/J.BIORTECH.2017.06.121

Conflict of Interest: The authors declare that the research was conducted in the absence of any commercial or financial relationships that could be construed as a potential conflict of interest.

frontiers in Microbiology

ORIGINAL RESEARCH
published: 06 July 2021
doi: 10.3389/fmicb.2021.688290

Anaerobic and Microaerobic Pretreatment for Improving Methane Production From Paper Waste in Anaerobic Digestion

Chao Song[1†], Wanwu Li[1,2†], Fanfan Cai[1], Guangqing Liu[1] and Chang Chen[1]*

[1] College of Chemical Engineering, Beijing University of Chemical Technology, Beijing, China, [2] TEDA Institute of Biological Sciences and Biotechnology, Nankai University, Tianjin, China

Having been generated with a tremendous amount annually, paper waste (PW) represents a large proportion in municipal solid waste (MSW) and also a potential source of renewable energy production through the application of anaerobic digestion (AD). However, the recalcitrant lignocellulosic structure poses obstacles to efficient utilization in this way. Recently, anaerobic and microaerobic pretreatment have attracted attention as approaches to overcome the obstacles of biogas production. This study was set out to present a systematic comparison and assessment of anaerobic and microaerobic pretreatment of PW with different oxygen loadings by five microbial agents: composting inoculum (CI), straw-decomposing inoculum (SI), cow manure (CM), sheep manure (SM), and digestate effluent (DE). The hints of microbial community evolution during the pretreatment and AD were tracked by 16S rRNA high-throughput sequencing. The results demonstrated that PW pretreated by DE with an oxygen loading of 15 ml/gVS showed the highest cumulative methane yield (CMY) of 343.2 ml/gVS, with a BD of 79.3%. In addition to DE, SI and SM were also regarded as outstanding microbial agents for pretreatment because of the acceleration of methane production at the early stage of AD. The microbial community analysis showed that *Clostridium sensu stricto 1* and *Clostridium sensu stricto 10* possessed high relative abundance after anaerobic pretreatment by SI, while *Bacteroides* and *Macellibacteroides* were enriched after microaerobic pretreatment by SM, which were all contributable to the cellulose degradation. Besides, aerobic *Bacillus* in SI and *Acinetobacter* in SM and DE probably promoted lignin degradation only under microaerobic conditions. During AD, *VadinBC27*, *Ruminococcaceae Incertae Sedis*, *Clostridium sensu stricto 1*, *Fastidiosipila*, and *Caldicoprobacter* were the crucial bacteria that facilitated the biodegradation of PW. By comparing the groups with same microbial agent, it could be found that changing the oxygen loading might result in the alternation between hydrogenotrophic and acetoclastic methanogens, which possibly affected the methanogenesis stage. This study not only devised a promising tactic for making full use of PW but also provided a greater understanding of the evolution of microbial community in the pretreatment and AD processes, targeting the efficient utilization of lignocellulosic biomass in full-scale applications.

Keywords: paper waste, anaerobic pretreatment, microaerobic pretreatment, microbial community analysis, anaerobic digestion

OPEN ACCESS

Edited by:
Yi Zheng,
Kansas State University, United States

Reviewed by:
Sanjay Kumar Singh Patel,
Konkuk University, South Korea
Vivekanand Vivekanand,
Malaviya National Institute of Technology, India

****Correspondence:***
Chang Chen
chenchang@mail.buct.edu.cn

† These authors have contributed equally to this work

Specialty section:
This article was submitted to Microbiotechnology, a section of the journal Frontiers in Microbiology

Received: *30 March 2021*
Accepted: *18 May 2021*
Published: *06 July 2021*

Citation:
Song C, Li W, Cai F, Liu G and Chen C (2021) Anaerobic and Microaerobic Pretreatment for Improving Methane Production From Paper Waste in Anaerobic Digestion. Front. Microbiol. 12:688290. doi: 10.3389/fmicb.2021.688290

INTRODUCTION

In modern society, paper materials have become indispensable consumer products with a wide variety of civil and industrial uses (Bajpai, 2014). With the unprecedented economic growth and social improvement in the past 20 years, China has become one of the largest paper-producing and paper-consuming countries (NationMaster, 2021), resulting in tremendous production of paper waste (PW) annually. In 2016, the production of PW in China was over 18 million tons, accounting for 9.15% of total municipal solid waste (MSW) (Zhu et al., 2020). At present, the pathway for the environmentally friendly utilization of PW focuses on the recycling and reproduction for new paper products. However, only for limited cycles can the PW be reused due to the decreased fiber strength, whiteness, and quality in the reproduction (Li et al., 2020). Besides, the PW tainted with glue, paint, food wastes, and other residues cannot be recycled, much of which is simply discarded as MSW (Ma et al., 2020; Zhao et al., 2020). Although other treatment methods, such as incineration, landfilling, and composting, have been gradually developed, the environmental impacts and low energy recovery place a heavy burden on their broader popularization (Manfredi et al., 2011; Sanscartier et al., 2012). Therefore, it is of high significance to develop alternative approaches to make the utmost utilization of PW.

For decades, anaerobic digestion (AD) has been emerging as an efficient and viable solution for biowastes to alleviate environmental pollution and produce renewable energy (Wang et al., 2021). Originated from wood, grass, and other plants, PW is mainly composed of lignocellulosic matter and can be applied in AD (Li et al., 2020), whereas, similar to other feedstocks, the intrinsic lignocellulosic structure retards the decomposition of organic matter and negatively affects the biodegradation process (Abraham et al., 2020). Therefore, many pretreatment strategies have been proposed to break the ceiling of their digestibility. Microbial pretreatment, as a means of biological pretreatment, has recently aroused great interest. The various microbes inoculated into the biowaste produce functional enzymes and metabolites, causing the destruction of the lignocellulosic structure. As a result, enzymatic hydrolysis and biomethanation efficiency could be enhanced (Zhao et al., 2019; Lee et al., 2020). Compared with physical and chemical-based pretreatment methods, microbial pretreatment possesses advantages of low cost, safety, and non-pollution along with the absence of intensive heating or chemicals (Carrere et al., 2016; Amin et al., 2017). Up to now, diverse fungi, bacteria, and microbial consortia have been introduced for pretreatment to assist in the bioconversion of biowaste. Kainthola et al. reported that the methane yield of rice straw was significantly increased by microbial pretreatment using *Phanerochaete chrysosporium* (Kainthola et al., 2019). It was reported by Ali et al. that the methane yield of sawdust pretreated by bacterial consortium increased by 92.2% compared with the control (Ali et al., 2019). The constructed microbial consortia described by Patel et al. led to a 3.7-fold polyhydroxybutyrate yield improvement during the dark fermentation of pea-shell slurry (Patel et al., 2015). However, there are still drawbacks undermining the feasibility of microbial pretreatment in large-scale applications. The mild biochemical reactions by microbes make the degradation rate to be slower than that of physical and chemical solutions (Den et al., 2018). Besides, the hydraulic retention time of microbial pretreatment is naturally extended due to microbial growth and propagation, especially for fungi (Amin et al., 2017). Such disadvantages will consequently increase the equipment scale, energy consumption, and capital investment to an extent.

Recently, microaerobic pretreatment, that is, supplying a small amount of oxygen during microbial pretreatment, has been given much attention. Previous studies have shown that under the microaerobic condition, the stimulated microbes showed higher hydrolysis and acidogenesis activity (Lim and Wang, 2013). Therefore, the shorter pretreatment period and lower energy costs can be realized (He et al., 2017; Xu et al., 2018; Wang et al., 2020). However, the microbes for pretreatment were not adaptive to every substrate to improve methane production, nor was it under every oxygen content. For instance, Zhen et al. (2020) stated that cumulative methane yield (CMY) of kitchen wastes did not show any improvement after the microaerobic pretreatment. It was reported by Fu et al. that microaerobic pretreatment with excessive oxygen resulted in decreased methane production of corn straw (Fu et al., 2016). During the microbial pretreatment, there existed a complicated microbial relationship created by a variety of microbes with distinct functions, some of which possibly exhibited different response to the oxygen loading and therefore affected the AD process. Zhen et al. stated that after the microaerobic pretreatment, the *Firmicute* and *Bacteroidetes* were the predominant phyla during the AD of rice straw (Zhen et al., 2021). However, Ruan et al. (2019) found that the digestate from the anaerobic sludge digestion possessed higher abundances of *Proteobacteria* and *Chloroflexi*. It can be deduced that the substrate, microbial consortia, and oxygen loadings are crucial factors that contribute to this difference. However, the systematic comparison in terms of these factors was still insufficient due to the various experimental conditions. In this work, five different microbial agents enriched with various microbes, namely, composting inoculum (CI), straw-decomposing inoculum (SI), cow manure (CM), sheep manure (SM), and digestate effluent (DE), were introduced to achieve the following aims:

1. Construct an optimal microbial pretreatment tactic that combines the microbial agent with suitable oxygen loading to attain improved methane production performance of PW.
2. Explore the evolution of the microbial community in anaerobic pretreatment, microaerobic pretreatment, and AD.
3. Propose the functional microbes that synergistically facilitate the biodegradation of lignocellulosic materials during the pretreatment and AD.

TABLE 1 | Characteristics of substrates and microbial agents.

Parameters	CB	TP	CI	SI	CM	SM	DE
TS (%)[a]	95.54 ± 0.09	97.92 ± 0.02	1.55 ± 0.02	86.39 ± 0.06	28.56 ± 1.10	15.93 ± 0.30	17.03 ± 0.03
VS (%)[a]	93.44 ± 0.08	97.46 ± 0.05	1.20 ± 0.03	22.20 ± 0.60	11.77 ± 0.27	13.89 ± 0.42	9.30 ± 0.04
VS/TS (%)	97.76	99.53	77.43	25.69	41.20	87.16	54.61
pH	NA	NA	6.77 ± 0.04	NA	8.26 ± 0.20	7.83 ± 0.14	8.45 ± 0.09
Cellulose (%)[b]	51.84 ± 0.13	90.92 ± 0.39	NA	NA	9.44 ± 0.81	18.98 ± 0.86	NA
Hemicellulose (%)[b]	8.65 ± 0.71	4.66 ± 0.96	NA	NA	8.94 ± 0.14	27.12 ± 0.73	NA
Lignin (%)[b]	20.71 ± 0.69	1.11 ± 1.46	NA	NA	10.71 ± 0.75	6.63 ± 0.18	NA
C (%)[b]	45.49 ± 0.14	42.90 ± 0.06	NA	8.86 ± 0.45	19.82 ± 0.89	35.83 ± 0.94	28.82 ± 0.13
H (%)[b]	5.96 ± 0.11	5.99 ± 0.08	NA	1.04 ± 0.07	2.46 ± 0.21	5.50 ± 0.19	4.38 ± 0.49
O (%)[b]	43.92 ± 0.65	48.46 ± 0.27	NA	9.84 ± 1.03	20.53 ± 0.29	38.67 ± 0.37	26.95 ± 1.07
N (%)[b]	0.13 ± 0.02	0.15 ± 0.03	NA	0.73 ± 0.08	0.93 ± 0.01	2.05 ± 0.41	2.90 ± 0.06
S (%)[b]	0.76 ± 0.02	0.44 ± 0.22	NA	0.25 ± 0.01	0.28 ± 0.06	0.36 ± 0.08	0.93 ± 0.01
C/N	349.90	295.86	NA	12.14	21.31	17.48	9.94
TMY (ml/gVS)	457.54	407.81	NA	356.59	403.36	415.32	443.94

[a]*Calculated based on total weight (%).* [b]*Calculated based on TS (%). NA: not analyzed.*

MATERIALS AND METHODS

Substrates, Microbial Agents, and Inoculum

The corrugated board (CB) and tissue paper (TP) bought in a supermarket were cut into pieces about 5 mm in length. The CI and SI were liquid and solid microbial consortia commercially designed for composting crop residues. The CM and SM were directly delivered from a farm in Shunyi District, Beijing. DE and inoculum for AD were the activated anaerobic sludge obtained from a biogas plant in Shunyi District, Beijing, which was naturally degassed for 20 days to eliminate the residual biogas. The characteristics of the substrates and microbial agents are shown in **Table 1**.

Anaerobic and Microaerobic Pretreatment

The pretreatment was conducted in 20 digesters, which were split into four groups. In each group, the five digesters were filled with each 5 g (based on total solids, TS) of corrugated board and tissue paper and then assigned to the five microbial agents, respectively. Five milliliters of CI and 2 g (based on volatile solids, VS) of SI, CM, SM, and DE were added into assigned digesters. A proper amount of deionized water was also filled into all digesters to reach a TS of 15% and then shaken well to homogenize the mixture. The digesters were purged with high-purity nitrogen (99.99%) for 3 min before a specific amount of pure oxygen was injected into the digesters of each group, that is, 0, 5, 15, and 30 ml/gVS, respectively. All digesters were labeled as "microbial agent—oxygen loading" and placed in a 37°C thermostatic incubator, and the concentrations of oxygen and carbon dioxide were measured every 12 h. The experiments were conducted in triplicate.

Anaerobic Digestion

The preparation of AD started when the oxygen in all digesters was almost exhausted. The substrate-to-inoculum ratio was set to 1:1 (based on VS), and the anaerobic inoculum was added to each digester. Besides, some water was also added into the digester to keep the TS at 15% (organic loading at 47.7 gVS/L). The digesters were purged with pure nitrogen to eliminate other gases, carefully sealed, and placed in a 37°C incubator to start the AD process. Simultaneously, the untreated group (labeled as UN) and blank group for the AD experiment were set up. In the untreated group, PW was directly mixed with inoculum and each microbial agent in five digesters, whose dosages were consistent with what we used for the pretreatment. The blank group was established using five digesters containing inoculum and each microbial agent to calculate the net methane production without the substrates. The untreated and blank groups were also flushed with nitrogen gas and placed in the incubator. Before the biogas pressure test, all digesters were made to shake for 1 min at a low speed. A flowsheet of the experimental setup is shown in **Figure 1**.

Analytical Methods

Basic Characteristics

The TS and VS for substrates and inoculum could be calculated by Eqs. (1) and (2), based on the standard test methods from APHA (APHA, 2005):

$$\mathrm{TS} = \frac{m_3 - m_1}{m_2 - m_1} \times 100\% \quad (1)$$

$$\mathrm{VS} = \frac{m_3 - m_4}{m_2 - m_1} \times 100\% \quad (2)$$

where m_1 represents the weight of dish (mg), m_2 is equal to the weight of fresh sample and dish (mg), m_3 is the weight of dried residue and dish (mg), and m_4 is assigned to the weight of residue and dish after ignition (mg). A fiber analyzer (ANKOM, New York) was installed to calculate the cellulose, hemicellulose,

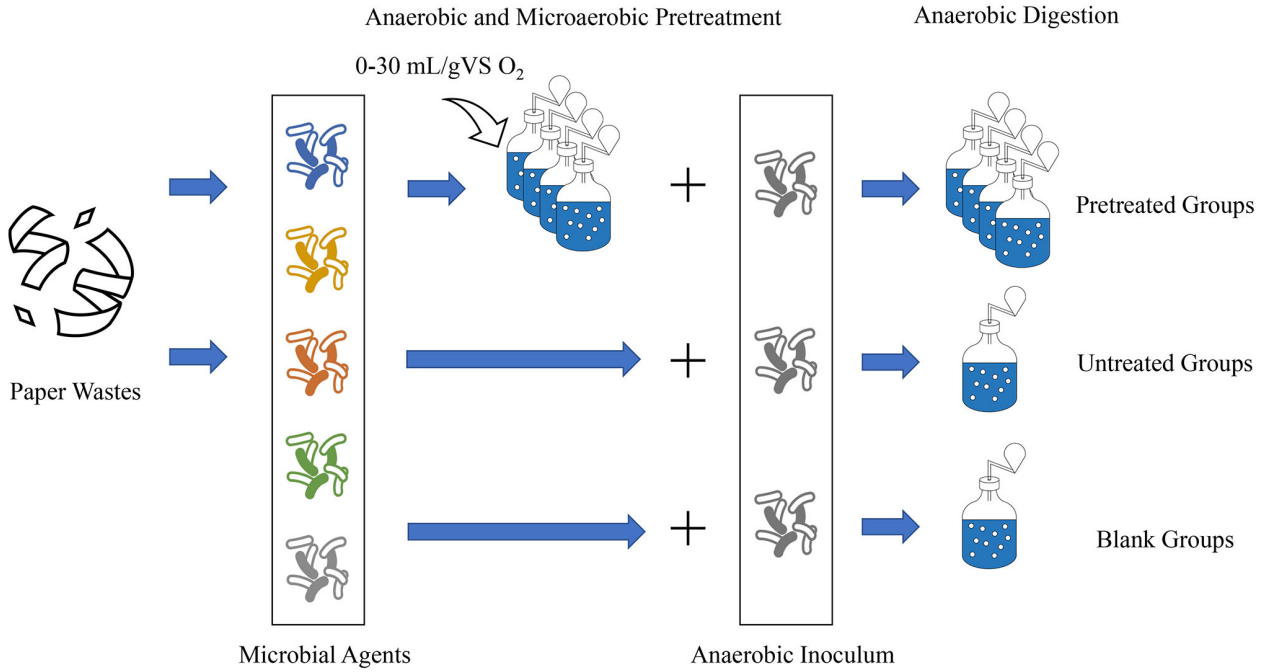

FIGURE 1 | Schematic diagram of the experimental setup.

and lignin contents according to the conventional method (Van Soest et al., 1991; Zhao et al., 2017). The determination of organic elements, including carbon (C), nitrogen (N), hydrogen (H), and sulfur (S), relied on an elemental analyzer (Vario EL cube, Elementar, Germany) (Ning et al., 2018). The mass balance equation supported the calculation of O content, that is, C + H + O + N = 99.5% (based on VS) (Rincón et al., 2012). Since then, it was reasonable to compute the theoretical maximum methane yield (TMY, ml/gVS) of substrates and microbial agents using Buswell's formula (Li et al., 2018), as shown in Eqs. (3) and (4).

$$\begin{aligned} C_aH_bO_cN_d + \left(a - \frac{b}{4} - \frac{c}{2} + \frac{3d}{4}\right) H_2O \\ \rightarrow \left(\frac{a}{2} + \frac{b}{8} - \frac{c}{4} - \frac{3d}{8}\right) CH_4 \\ + \left(\frac{a}{2} - \frac{b}{8} + \frac{c}{4} + \frac{3d}{8}\right) CO_2 + dNH_3 \end{aligned} \quad (3)$$

$$TMY = \frac{22.4 \times 1000 \times \left(\frac{a}{2} + \frac{b}{8} - \frac{c}{4} - \frac{3d}{8}\right)}{12a + b + 16c + 14d} \quad (4)$$

Production of Methane and Volatile Fatty Acids

The daily biogas yield was calculated following the ideal gas law as shown in Eq. (5) and modified into the standard conditions (0°C, 101 kPa):

$$V_{biogas} = \frac{P \times V_{headspace} \times C}{R \times T} \quad (5)$$

where V_{biogas} stands for the daily biogas yield (L), P refers to the pressure difference (kPa) before and after discharging biogas, $V_{headspace}$ is defined as the headspace volume of the digester (L), and T is the absolute temperature (K). C and R are physical constants referring to the molar volume (22.41 L/mol) and universal gas constant (8.314 L kPa/K/mol), respectively.

The biogas compositions and volatile fatty acids (VFAs) contents were measured daily by a gas chromatograph (GC) system (7890B, Agilent, USA), and the detailed instruments were reported elsewhere (Li et al., 2020). The biodegradability (BD) was defined as the ratio of the experimental methane yield (EMY), namely, the highest CMY, divided by the TMY, as shown in Eq. (6):

$$BD = \frac{EMY}{TMY} \times 100\% \quad (6)$$

Microbial Community Analysis

To identify the functional microbes and evolution of the microbial community during pretreatment and AD, the groups that possessed relatively higher methane yield after AD were selected to conduct the 16S rRNA high-throughput sequencing for the microbial agents, pretreated PW, and digestates after AD. The PCR reaction mixture (30 μl) consisted of 10 ng of extracted DNA, 0.5 μl of Taq DNA polymerase (5 U/μl), 5 μl of deoxyribonucleotide triphosphate (10 mM), and 10 pmol of each primer. 805R (5′-GACTACHVGGGTATCTAATCC-3′) and 341F (5′-15CTACGGGNGGCWGCAG-3′) were considered as the primer pair of amplification for the analysis of total bacteria (Wu et al., 2020). The identification of archaea contained two rounds. 340F (5′-15CCTAYGGGGYGCASCAG-3′) and 1000R (5′-GGCCATGCACYWCYTCTC-3′) were used for the first round of amplification, and 349F

(5′-GYGCASCAGKCGMGAAW-3′) and 806R (5′-GGACTACVSGGGTATCTAAT-3′) were used for the second round (Wang et al., 2018).

The Cutadapt software was adopted for the amplicon sequences from the original sequenced fragments. The PEAR program with default settings was adopted for merging the high-quality paired-end reads. The reads abandoned from the raw sequencing data were shorter than 200 bp and contained ambiguous nucleotides, incorrect barcodes, or primers. The UCHIME program was introduced to remove the potential chimera and then cluster the remaining reads into operational taxonomic units (OTUs) with a minimum identity of 97%. The taxonomic assignment of OTUs was supported by the RDP Resource, SILVA rRNA database, and NCBI taxonomy database. The species diversity was estimated by Shannon index, while the species richness was reflected by Chao1 and ACE indexes, which were all calculated using MOTHUR. The relative abundance (RA) was defined as the ratio of the number of sequences affiliated with a taxonomic category to the total number of sequences per sample.

Statistical Analysis

The results are shown with the average value ± standard deviation and organized by Origin pro 2021 Learning Edition. Circos graphs of microbial community structure were generated by Circos Online[1].

RESULTS AND DISCUSSION

Variation in O_2 and CO_2 Concentrations During Pretreatment

Figure 2 exhibits the variation in O_2 and CO_2 concentrations in the digesters during the pretreatment with five microbial agents. The trends showed that regardless of the microbial agent used, CO_2 concentration steadily increased at the beginning of pretreatment along with the consumption of O_2. CO_2 and O_2 concentrations finally reached a stable state within 5 days. Besides, the greater amounts of O_2 injected into digesters corresponded to higher CO_2 production. Thus, it could be inferred that all of these agents contained various aerobic or facultative microbes that converted O_2 into CO_2 for their growth. More interestingly, at the same oxygen loading, the rates of O_2 consumption and CO_2 production in SI, SM, and DE groups were faster than those of CI and CM groups, and the time to exhaust O_2 was 2 days, even for the highest oxygen loading groups (30 ml/gVS). The results indicated that the aerobic or facultative microbes in SI, SM, and DE groups were more active or abundant, which might possibly contribute to the higher hydrolysis rate.

Effect of Microbial Pretreatment on Daily Methane Yield

The trends in daily methane yield (DMY) of PW pretreated by different microbial agents are shown in **Figure 3**. The DMY of PW pretreated by CI exhibited an outstanding peak between the 5th and 10th day. Then, there was a swift decrease until another small peak appeared around the 35th day. However, the trends of DMY of PW pretreated by SI, CM, SM, and DE were quite different. There are two peaks observed: one was around the 5th day, and another was between the 10th and 20th days. This phenomenon was related to the accumulation of intermediate products (e.g., VFAs), which has already been reported by Li et al. (2020). The maximum DMY of untreated PW mixed with CI, SI, CM, SM, and DE were 15.1, 16.9, 22.0, 18.9, and 13.5 ml/gVS, respectively. The maximum DMY of PW pretreated by different microbial agents were observed in the groups of CI-0 (21.7 ml/gVS), SI-5 (26.8 ml/gVS), CM-15 (28.2 ml/gVS), SM-15 (26.0 ml/gVS), and DE-15 (39.4 ml/gVS), respectively, with the increase of 43.7, 58.6, 28.2, 37.6, and 191.9% compared with untreated, respectively. The noticeable improvement might be

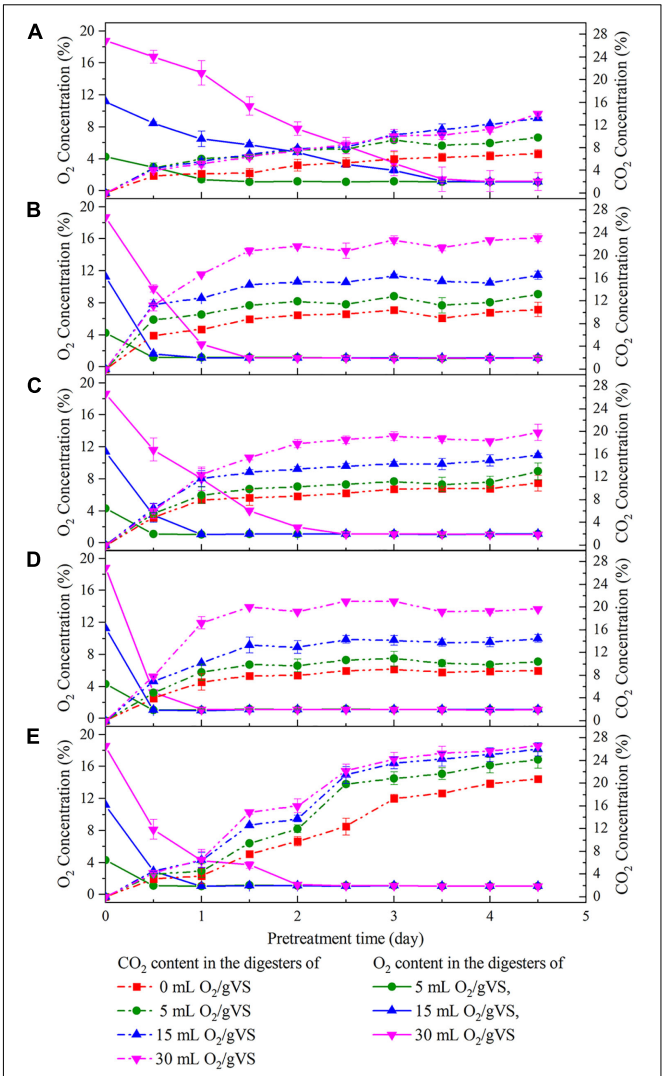

FIGURE 2 | Changes of O_2 and CO_2 concentration in the digesters during the pretreatment by CI **(A)**, SI **(B)**, CM **(C)**, SM **(D)**, and DE **(E)**.

[1]http://circos.ca/intro/tabular_visualization/

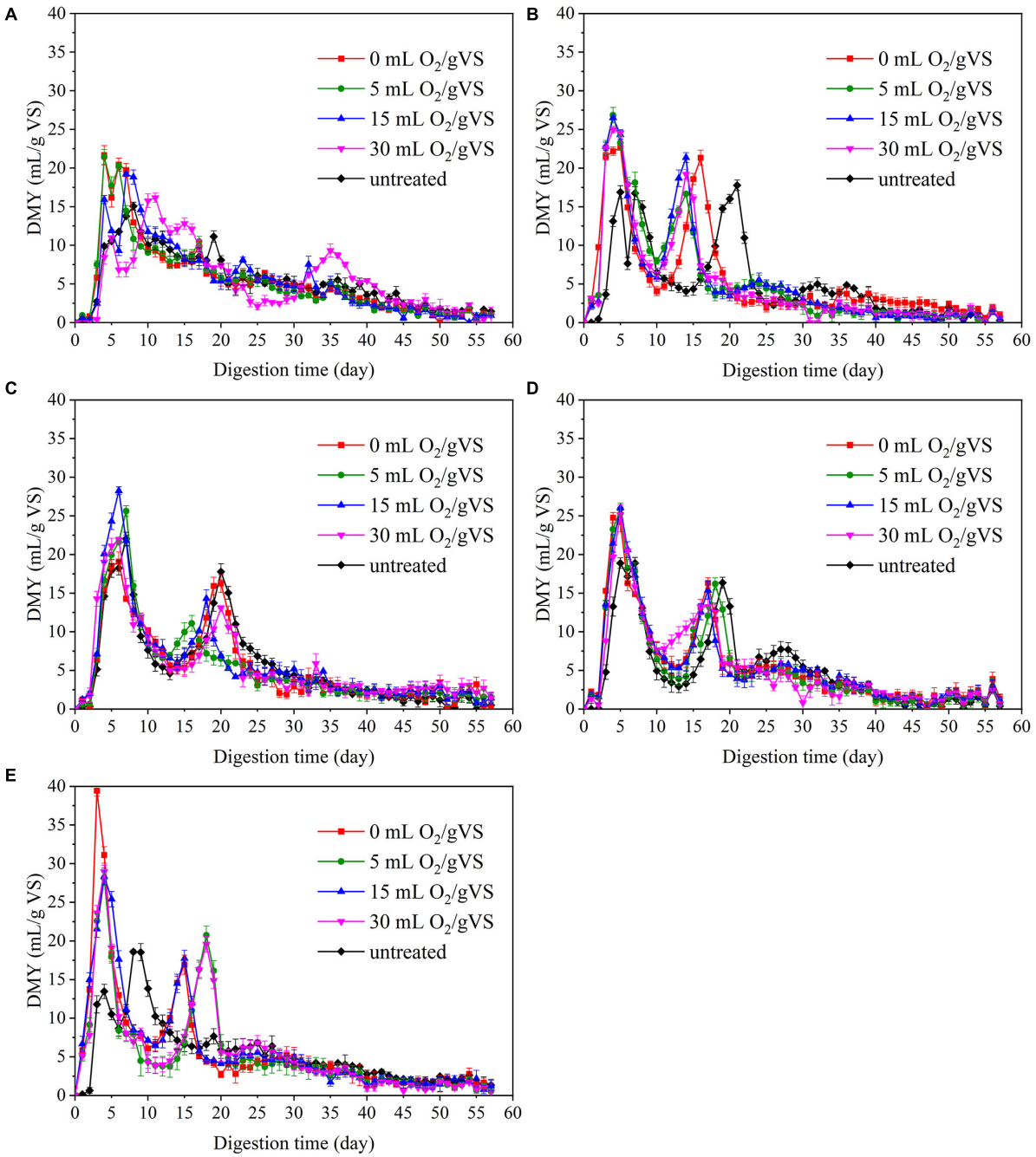

FIGURE 3 | The daily methane yield (DMY) untreated and pretreated PW by CI **(A)**, SI **(B)**, CM **(C)**, SM **(D)**, and DE **(E)**.

related to diverse microbes that degrade the organic matter to small molecules such as VFAs during the pretreatment.

Effect of Microbial Pretreatment on Cumulative Methane Yield and Biodegradability

Figure 4 and **Table 2** present the cumulative methane production of untreated and pretreated PW by microbial agents. Generally, the AD experiment can be divided into two stages by taking the 20th day as the dividing line. During the first 20 days of AD, when DMY remained relatively high, the increase of CMY of all groups was faster than those in the next 40 days. The CMY in the first 20 days (CMY_{20}) of CI-UN, SI-UN, CM-UN, SM-UN, and DE-UN were 177.5, 168.1, 194.7, 173.0, and 181.1 ml/gVS, respectively. The enhanced CMY_{20} was achieved after microbial pretreatment. The CMY_{20} of PW in CI-0 was 195.3 ml/gVS, with the highest increase of 10.0% compared with

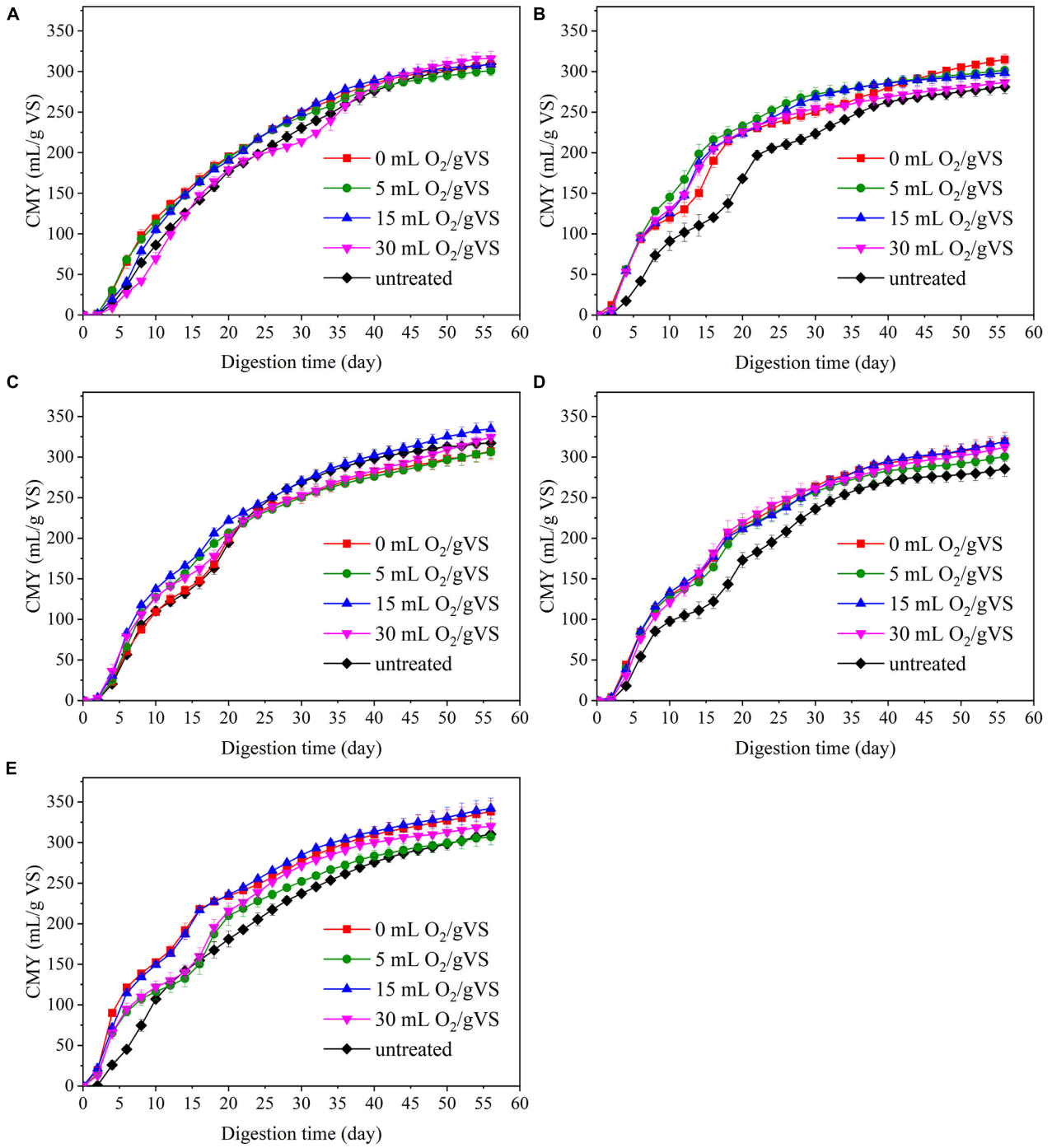

FIGURE 4 | The cumulative methane yield (CMY) of untreated and pretreated PW by CI **(A)**, SI **(B)**, CM **(C)**, SM **(D)**, and DE **(E)**.

the untreated. The maximum CMY_{20} of PW pretreated by CM was 222.0 ml/gVS in CM-15, with an increase of 14.0% compared with the untreated. However, when the oxygen loading increased to 30 ml/gVS, the CMY_{20} of PW pretreated by CI and CM gradually fell, with an increase of only 0.9 and 3.5%, respectively. Compared with CI and CM, the microbial pretreatments by SI, SM, and DE were more effective in enhancing methane yield at the early stage of AD. The maximum CMY_{20} of PW pretreated by SI, SM, and DE were 232.7 ml/gVS in SI-5, 219.6 ml/gVS in SM-30, and 235.8 ml/gVS in DE-15, with an increase of 38.4, 26.9, and 30.2% compared with untreated. Besides, it is found that changes in oxygen loading during the pretreatment of SI, SM, and DE had a slight influence on the improvement of CMY_{20}.

TABLE 2 | Digestion performance of untreated and pretreated PW.

Group	CMY_{20}	CMY_{20} improvement (%)	BD_{20} (%)	EMY	EMY improvement (%)	BD (%)
CI-0	195.3 ± 4.0	10.0	45.1	309.7 ± 3.6	−0.3	71.6
CI-5	194.2 ± 4.6	9.4	44.9	302.0 ± 6.3	−2.8	69.8
CI-15	190.2 ± 3.0	7.1	44.0	309.5 ± 1.4	−0.4	71.5
CI-30	179.0 ± 7.4	0.9	41.4	316.9 ± 8.1	2.0	73.2
CI-UN	177.5 ± 8.1	–	41.0	310.7 ± 3.9	–	71.8
SI-0	224.6 ± 2.7	33.6	51.9	315.6 ± 7.0	12.3	72.9
SI-5	232.7 ± 5.7	38.4	53.8	301.6 ± 3.8	7.3	69.7
SI-15	223.7 ± 5.4	33.0	51.7	298.8 ± 5.3	6.3	69.1
SI-30	226.1 ± 7.5	34.5	52.3	286.9 ± 3.7	2.0	66.3
SI-UN	168.1 ± 2.1	–	38.9	281.2 ± 8.3	–	65.0
CM-0	200.2 ± 7.4	2.8	46.3	307.2 ± 10.2	−3.3	71.0
CM-5	206.6 ± 3.6	6.1	47.8	307.7 ± 7.2	−3.1	71.1
CM-15	222.0 ± 4.5	14.0	51.3	336.0 ± 9.0	5.8	77.7
CM-30	201.5 ± 7.3	3.5	46.6	325.9 ± 10.6	2.6	75.3
CM-UN	194.7 ± 5.7	–	45.0	317.7 ± 5.5	–	73.4
SM-0	215.2 ± 10.1	24.4	49.7	320.6 ± 11.5	12.2	74.1
SM-5	212.1 ± 7.2	22.6	49.0	301.4 ± 6.0	5.5	69.6
SM-15	211.4 ± 2.6	22.2	48.9	320.2 ± 6.9	12.0	74.0
SM-30	219.6 ± 10.7	26.9	50.7	312.7 ± 6.9	9.4	72.3
SM-UN	173.0 ± 9.4	–	40.0	285.7 ± 9.5	–	66.0
DE-0	234.3 ± 0.3	29.3	54.1	339.1 ± 13.8	8.8	78.4
DE-5	209.9 ± 11.9	15.9	48.5	307.6 ± 10.1	−1.3	71.1
DE-15	235.8 ± 1.2	30.2	54.5	343.2 ± 13.3	10.1	79.3
DE-30	216.0 ± 9.0	19.2	49.9	320.6 ± 3.0	2.9	74.1
DE-UN	181.1 ± 9.8	–	41.9	311.6 ± 3.6	–	72.0

CMY_{20}, cumulative methane yield in the first 20 days; BD_{20}, BD of the PW in the first 20 days; EMY, experimental methane yield; BD, final BD of the PW; UN, untreated.

TABLE 3 | Comparison of highest methane production of various paper wastes from reported literature and this study.

Substrate	Pretreatment method	Organic loading (gVS/L)	Methane production (ml/gVS)	Reference
Waste paper	Microaerobic pretreatment	47.7	343.2	This study
Corrugated paper	None	2.0	272.0	Krause et al., 2018
Paperboard	None	2.0	273.0	Krause et al., 2018
Office paper	None	2.0	375.0	Krause et al., 2018
Toilet paper	None	6.25	348.0	Kim et al., 2019
Office paper	Microbial pretreatment	25.0	221.0	Yuan et al., 2014
Waste paper	Mechanic pretreatment	Not mentioned	253.6	Rodriguez et al., 2017
Corrugated board	None	15.0	243.9	Li et al., 2020
Office paper	None	15.0	284.5	Li et al., 2020
Tissue paper	None	15.0	358.8	Li et al., 2020
Magazine paper	None	10.0	316.4	Li et al., 2020

When the AD process came to an end, the EMY of each group could be attained. The highest EMY of pretreated PW was 343.2 ml/gVS in DE-15, with an increase of 10.1% compared with the untreated. The maximum BD of 79.3% was also from this group. **Table 3** provides a literature summary regarding the methane production of PW. It is clear that the organic loading in this study was the highest (47.7 gVS/L), followed by 25 gVS/L in the study of Yuan et al. (2014) and 15 gVS/L in that of Li et al. (2020). On the other hand, the methane yield of 343.2 ml/gVS in this study was higher than the estimated methane yield (315.4 ml/gVS) of untreated PW, which was the weighted sum of maximum methane yield of untreated corrugated paper (Krause et al., 2018) and tissue paper (Li et al., 2020) at a ratio of 1 to 1. These findings indicated that with the help of microaerobic pretreatment by DE, the AD of PW might be conducted at a smaller reactor with high organic loading and achieve satisfactory biomethanation efficiency. In addition, the maximum EMY of PW pretreated by other microbial agents were 316.9 ml/gVS in CI-30, 315.6 ml/gVS in SI-0, 336.0 ml/gVS in CM-15, and 320.6 ml/gVS in SM-0, increasing by 2.0, 12.3, 5.8, and 12.2% compared with

TABLE 4 | VFA composition and concentration of PW after microbial pretreatment of SI, SM, and DE*.

Group	Acetic acid	Propionic acid	Isobutyric acid	n-Butyric acid	Isovaleric acid	Total acid
SI-0	2846.7 ± 181.2	37.7 ± 2.8	54.2 ± 1.0	441.9 ± 9.9	23.8 ± 0.9	3404.3 ± 52.6
SI-15	2522.8 ± 211.6	22.0 ± 6.4	12.4 ± 4.3	1344.4 ± 36.8	4.0 ± 1.3	3905.6 ± 54.1
SM-0	2040.4 ± 129.6	514.9 ± 28.5	59.0 ± 2.1	487.9 ± 20.2	85.1 ± 5.2	3187.3 ± 98.7
SM-15	2175.5 ± 136.3	309.4 ± 16.7	46.9 ± 6.5	1149.4 ± 27.4	43.9 ± 2.6	3725.0 ± 278.6
DE-0	2206.5 ± 146.9	398.0 ± 18.6	41.5 ± 19.1	1.5 ± 0.0	0.0 ± 0.0	2647.5 ± 261.4
DE-15	2456.6 ± 102.5	580.3 ± 24.2	15.1 ± 1.3	0.4 ± 0.0	0.0 ± 0.0	3052.5 ± 68.0

*Unit: mg/L.

untreated, respectively. It was noteworthy that the improvement in EMY was not as great compared with that of CMY_{20} for all groups except CI-30, demonstrating that microbial pretreatment tended to accelerate the methane production rate at the early stage of AD. Taken into account the amount or improvement of DMY, $CMY_{20,}$ and EMY, the anaerobic pretreatment or microaerobic pretreatment by SI, SM, and DE were attractive schemes for attaining better methane production performance of PW and deserved deeper investigation in the next sections.

VFA Compositions After Microbial Pretreatment by SI, SM, and DE

VFAs represent a series of intermediate products generated from digestible substances and are precursors for methane production. The VFA compositions and concentrations in the anaerobic and microaerobic pretreatment groups by SI, SM, and DE are shown in **Table 4**. Evidently, the total acid concentration after the microaerobic pretreatment was higher than those of anaerobic pretreatment, indicating that a small amount of oxygen during the pretreatment could help microbes degrade PW into VFAs. At the same oxygen loading level, the pretreated groups by SI possessed the highest total acid concentration in comparison with the SM and DE, implying that SI might harbor more microbes that were efficient in the acidogenesis of PW. The composition of VFAs included various short-chain fatty acids, among which acetic acid took the highest percentage of total acids in all groups. The highest acetic acid concentration was 2846.7 mg/L in SI-0, followed by 2522.8 mg/L in SI-15 and 2456.6 mg/L in DE-15. Since acetic acid could be efficiently converted into methane by acetotrophic methanogens, its production during the pretreatment had positive effects on the AD performance of PW. By comparison, the groups with SM and DE possessed a relatively higher concentration of propionic acid, while n-butyric acid and isovaleric acid were abundant in SI and SM groups. The findings suggested that there existed many microbes in SI, SM, and DE capable of converting the substrates into different VFAs.

Microbial Community Analysis During Pretreatment and AD

Evolution of Microbial Community During Microbial Pretreatment by SI, SM, and DE

The overview of RA of predominant bacteria in SI, SM, DE, and pretreated PW is provided in **Figure 5** and **Supplementary Table S1**. *Staphylococcus* and *Bacillus* were the predominant genera in SI, whose RAs were 51.42 and 9.07%, respectively. After the anaerobic pretreatment, the RA of *Bacillus* decreased slightly to 6.82%, while that of *Staphylococcus* decreased significantly to 31.52%. Besides, *Clostridium sensu stricto 1* and *Clostridium sensu stricto 10* appeared in SI-0 with the RAs of 25.10 and 15.27%, respectively. Members of *Bacillus* are aerobes or facultative anaerobes that produce cellulase, hemicellulase, ligninase, amylase, protease, and pectinase (Dastager et al., 2015; Yang et al., 2017; Xu et al., 2018). Therefore, this genus might result in the rapid consumption of oxygen during the pretreatment (as shown in **Figure 2B**) and induce cellulose and lignin degradation. *Staphylococcus* was regarded as a facultative anaerobic organism that could convert various sugars to organic acids (Supré et al., 2010; De Bel et al., 2013) and was possibly the main contributor to anaerobic pretreatment by SI. *Clostridium sensu stricto 1* and *Clostridium sensu stricto 10* accounted for a large proportion in SI-0. *Clostridium* included a variety of bacteria that specialized in utilizing multiple sugars as carbon and energy sources to generate methanogenic precursors such as acetic acid, butyric acid, H_2, and CO_2 (Lanjekar et al., 2015; Amin et al., 2021). Compared with SI-UN, the higher RA of *Clostridium* in SI-0 might contribute to the acceleration of methane production at the early stage, as shown in **Figure 4B**. The SM and DE also contained various hydrolysis and acidogenesis bacteria. The RAs of *Bacteroides* and *Macellibacteroides* in SM were 0.63 and 0.15%, respectively, but increased by dozens and hundreds of times in SM-15, respectively. Many bacteria in these genera could convert cellulose into various VFAs (Jabari et al., 2012; Sakamoto and Ohkuma, 2013; Hatamoto et al., 2014). The RAs of *Proteiniphilum* in SM and DE were 0.08 and 1.24%, respectively, but significantly increased after microbial pretreatment. It was reported that *Proteiniphilum* functioned by converting the proteins and pyruvate into acetate and propionate (Chen and Dong, 2005). Noticeably, *Acinetobacter* was abundant in SM (15.87%) and SM-15 (31.16%). Most bacteria from this genus were aerobic, and some were associated with lignin degradation (Radolfova-Krizova et al., 2016; Yang et al., 2017), contributing to the rapid oxygen consumption (shown in **Figure 2D**) and higher methane production of pretreated PW.

Changes of Microbial Community After AD

Table 5 provides information regarding the species diversity and richness of bacteria and archaea in selected groups after AD, including sequence number, OTU number, ACE, Chao1,

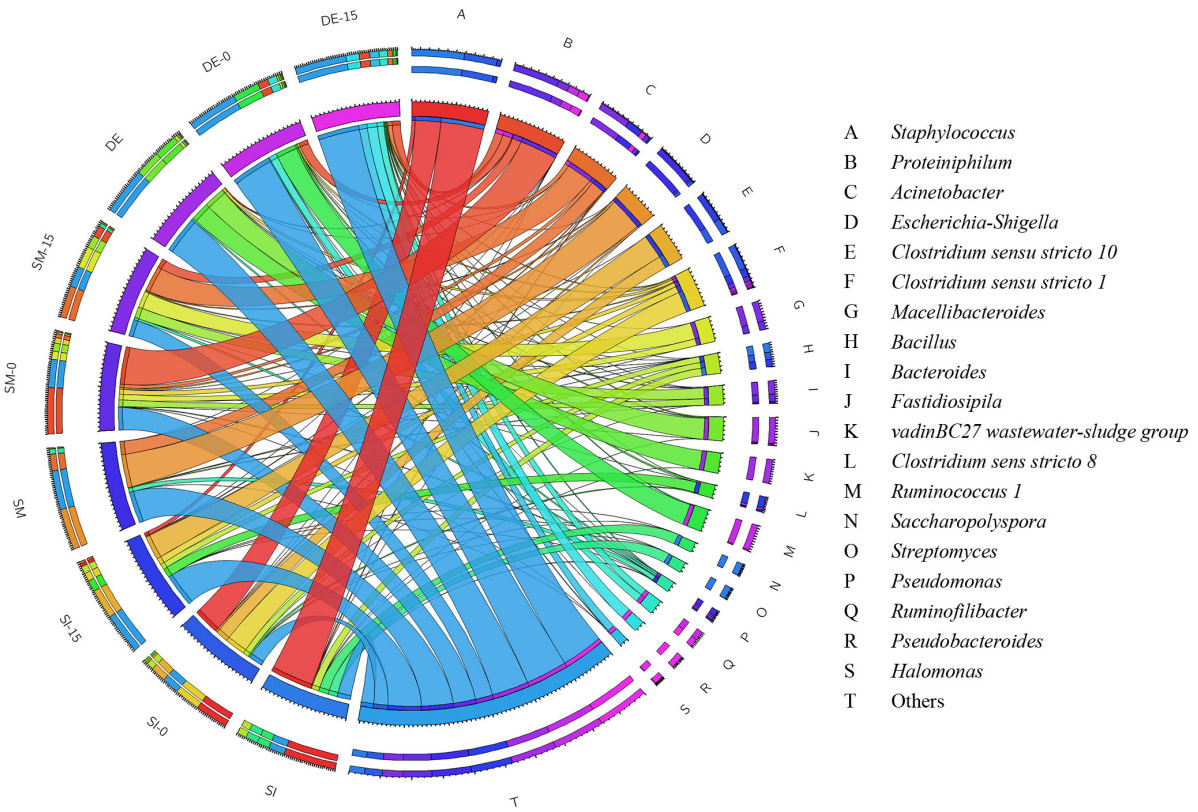

FIGURE 5 | The relative abundance of bacteria in the SI, SM, DE, and pretreated PW at the genus level.

TABLE 5 | Ecological indexes of bacteria and archaea in selected groups after AD.

	Group	Sequence number	OTU number	Shannon	ACE	Chao1	Coverage	Simpson
Bacteria	SI-0	43202	1144	4.25	2007.24	1591.66	0.99	0.05
	SI-15	73884	1522	4.59	2571.82	2182.26	0.99	0.03
	SI-UN	64742	1354	4.59	2425.33	2006.00	0.99	0.03
	SM-0	64964	1658	4.75	2444.58	2424.27	0.99	0.02
	SM-15	61462	1392	4.54	2440.20	2338.35	0.99	0.03
	SM-UN	75071	1742	5.00	2906.55	2509.54	0.99	0.02
	DE-0	57959	1783	4.66	2568.92	2424.17	0.99	0.03
	DE-15	52705	1558	4.75	2894.59	2358.81	0.99	0.03
	DE-UN	56081	1446	4.65	2483.26	2029.88	0.99	0.02
Archaea	SI-0	64353	471	1.93	1250.39	805.60	1.00	0.27
	SI-15	57131	400	1.69	906.49	680.73	1.00	0.32
	SI-UN	58345	424	1.81	771.91	732.37	1.00	0.27
	SM-0	64300	548	1.54	1242.33	970.27	1.00	0.46
	SM-15	47132	369	1.80	1323.66	872.52	1.00	0.32
	SM-UN	65814	473	2.24	1298.76	881.37	1.00	0.16
	DE-0	69012	520	1.21	1346.49	956.11	1.00	0.59
	DE-15	60695	457	2.15	961.04	707.87	1.00	0.20
	DE-UN	61481	373	1.73	1427.72	803.18	1.00	0.29

Shannon, and Simpson indexes. After the pretreatment by SI, the highest sequence number, OTU number, Shannon, ACE, and Chao1 indexes of bacteria in bacteria were achieved in SI-15, followed by SI-UN and SI-0. However, the observed outcomes in the groups of SM were quite different. These indexes of bacteria in SM-UN were the highest, followed by SM-0 and SM-15.

A possible explanation for this result might be that the vulnerable bacteria in SM gradually disappeared due to the changes in the environment in the digester. The Shannon, ACE, and Chao1 indexes of bacteria in DE-0 and DE-15 showed a minor difference with those of DE-UN, indicating that many bacteria in the digestate were not susceptible to interference during the pretreatment and AD. The variations of species diversity and richness of archaea were quite different from those of bacteria. For SI and DE, the sequence number of archaea in the groups of anaerobic pretreatments higher than the untreated group and microaerobic pretreatment group. Besides, the sequence number and OTU number of archaea in SM-0 was higher than that in SM-15. It could be inferred that the anaerobic pretreatment was beneficial for methanogens to keep their activity during the AD.

Figure 6 and **Supplementary Table S2** exhibit the overview of abundant bacteria in selected groups after AD. Evidently, the microbial community in each digester was significantly changed. Some remarkable bacteria for pretreatment, like *Proteiniphilum*, *Bacillus*, and *Staphylococcus*, were nearly absent, while *VadinBC27* and *Ruminococcaceae Incertae Sedis* appeared as the predominant bacteria in all digesters. From previous studies, *VadinBC27* was recognized as degrading amino acids in syntrophic association with hydrogenotrophic methanogens (Li et al., 2015). *Ruminococcaceae Incertae Sedis* was previously identified as a functional bacterium associated with cellulose and hemicellulose degradation (Ecem Öner et al., 2018). Therefore, the microbial community containing these bacteria enabled the enhancement of methane production. *Clostridium sensu stricto 1* was another primary bacterium in the digesters with SI. The RA of *Clostridium sensu stricto 1* in SI-0 was 16.23%, with an increase of 58.6% compared with SI-UN. Noticeably, *Clostridium sensu stricto 1* took up a large part after the pretreatment and possessed high abundance after AD. These results suggested that it was adaptive to the environment in digesters and might play critical roles in both microbial pretreatment and AD. Besides, *Fastidiosipila* and *Caldicoprobacter* were also observed in the digesters with SM and DE after AD. The former was able to produce acetate and butyrate from carbohydrates and protein (Falsen et al., 2005), and the latter could metabolize cellulose and hemicellulose into oligosaccharides or monosaccharides (Zhou et al., 2018). Aside from the predominant bacteria mentioned above, others detected in these digestates include *Sedimentibacter*, *Syntrophomonas*, *Owenweeksia*, and *Petrimonas*. The RAs of *Sedimentibacter* in SI-0 and SI-15 were 3.70 and 3.89%, respectively, with an increase of 30.0 and 36.9% compared with the untreated (2.84%). It has been reported that *Sedimentibacter* was identified as a strict anaerobe that could degrade amino acids into ethanol and organic acids (Lechner, 2015; Imachi et al., 2016). *Syntrophomonas* facilitates the conversion of butyric acid into acetate, propionate, and H_2 under methanogenic conditions

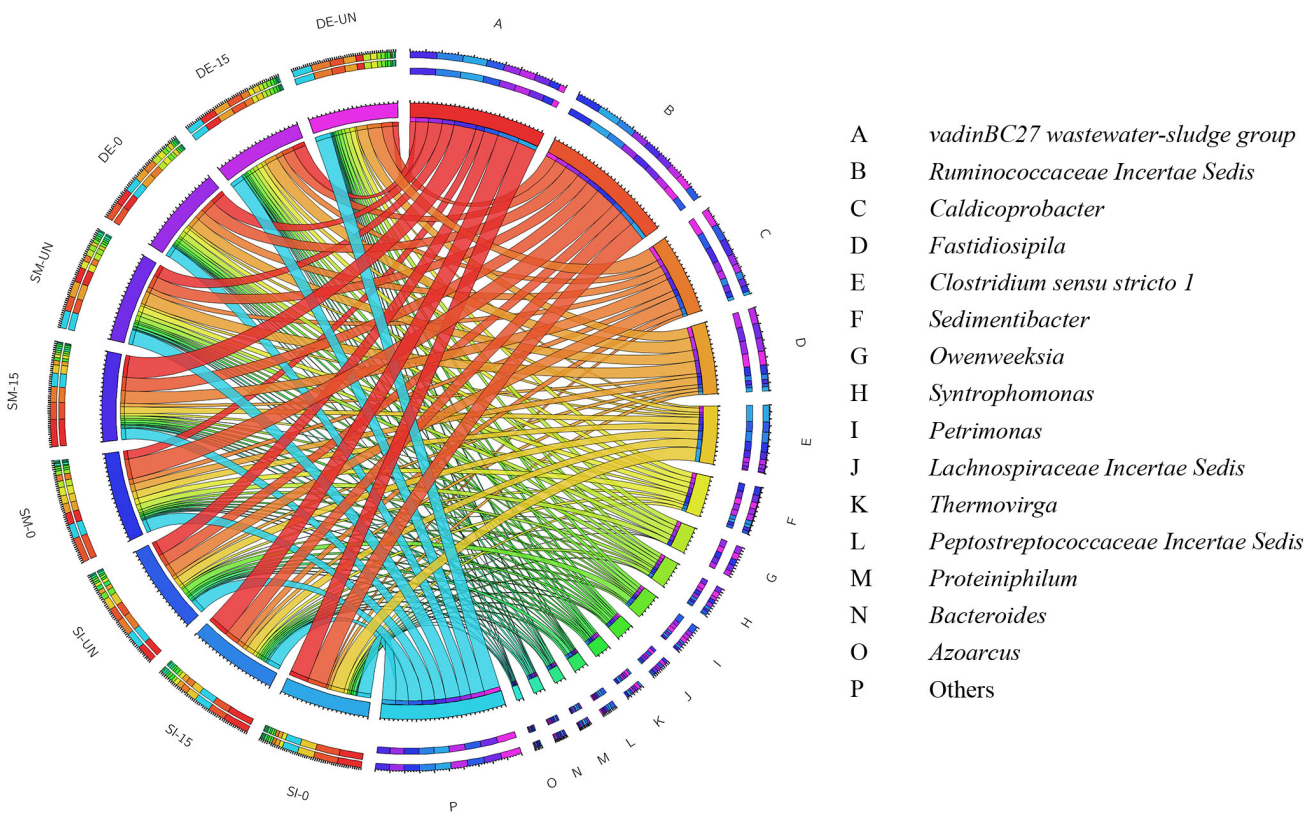

FIGURE 6 | The relative abundance of bacteria in the selected digestates after AD at the genus level.

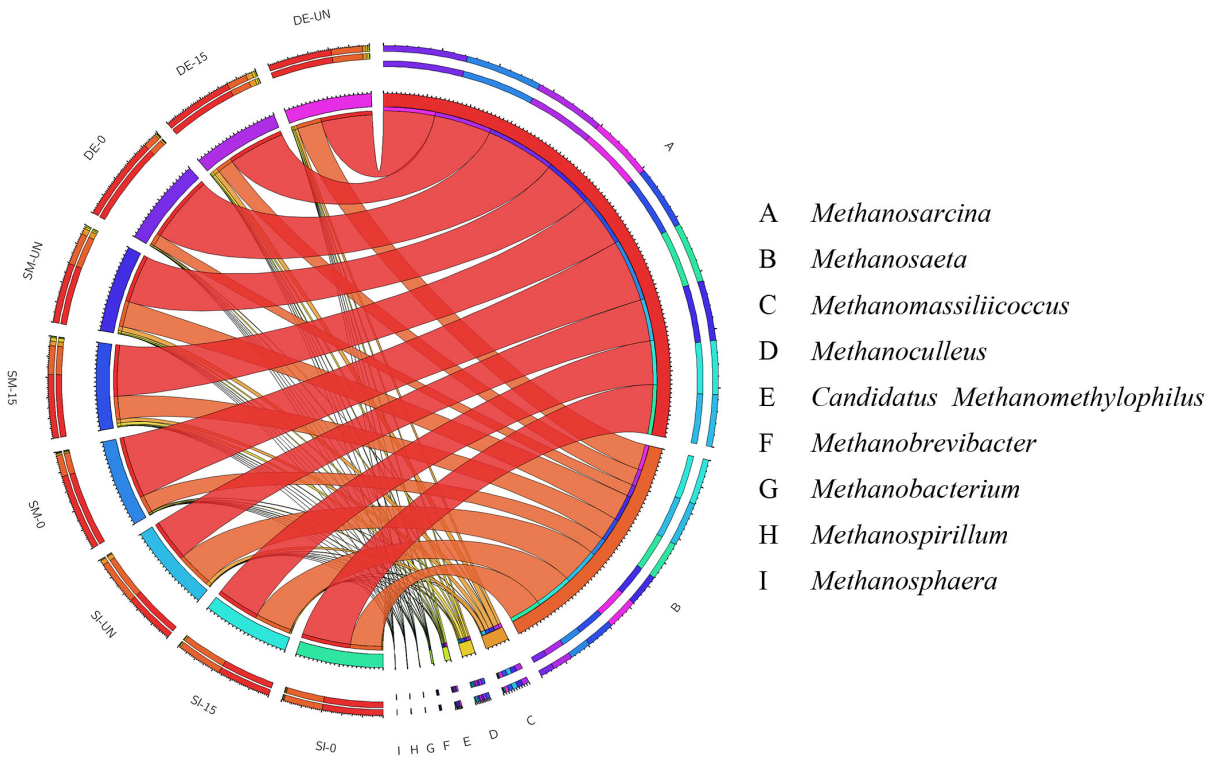

FIGURE 7 | The relative abundance of archaea in the selected digestates after AD at the genus level.

(Sekiguchi, 2015), and its RA ranged between 1.54 and 5.41% in the digestates we collected. The RA of *Petrimonas* experienced a minor difference in the groups of SM (1.67–2.47%) and DE (3.69–4.23%). This genus was an important participant during AD as it could ferment many sugars and organic acids into methane production precursors like acetate, H_2, and CO_2 (Grabowski et al., 2005).

The community structures of archaea in selected groups after AD are presented in **Figure 7** and **Supplementary Table S3**. Obviously, *Methanosarcina,* and *Methanosaeta* were the main methanogens in all groups regardless of microbial agents and oxygen loading for pretreatment. By comparing these two genera in the same microbial agent groups, it could be found that the groups with anaerobic pretreatment possessed the highest RA of *Methanosarcina*, followed by those with microaerobic pretreatment and without pretreatment, while the RA of *Methanosaeta* showed opposite trends. For example, the RAs of *Methanosarcina* and *Methanosaeta* in SM-UN were 59.13 and 31.60%, respectively. *Methanosarcina* significantly increased to 62.51 and 75.53% in SM-15 and SM-0, respectively, while the *Methanosaeta* decreased to 28.27 and 21.33%. *Methanosarcina* is known as the only methanogen compatible with the acetoclastic and hydrogenotrophic methanogenesis routes, while *Methanosaeta* has the ability to follow the acetoclastic pathway only (Zakaria and Dhar, 2019). The shift between *Methanosarcina* and *Methanosaeta* might probably result from the changes of precursors produced by the pretreatment with different microbial agents and oxygen loading and consequently bring about better performance of methane production of PW.

CONCLUSION

This study was designed to investigate the methane production performance of PW subjected to anaerobic and microaerobic pretreatments by five microbial agents, namely, CI, SI, CM, SM, and DE. Results showed the diverse efficacy of these microbial agents and oxygen loadings on the methane production performance of PW. The EMY of pretreated PW was enhanced by the pretreatments of SI, SM, and DE under an optimal oxygen loading. The microbial community analysis revealed that microbial agents provided functional bacteria for enhancing the hydrolytic and acidogenic process, which exhibited a different response to the oxygen loading during the anaerobic and microaerobic pretreatment. Besides, the anaerobic and microaerobic pretreatment had a profound effect on the microbial community in AD digesters, leading to the enhanced methane production performance. The work not only provided a promising technique to make full use of PW but also gave a reference for further studies on biodegradation mechanisms of lignocellulosic biowastes during the microbial pretreatment at various oxygen concentrations and AD processes.

DATA AVAILABILITY STATEMENT

The raw data supporting the conclusions of this article will be made available by the authors, without undue reservation.

AUTHOR CONTRIBUTIONS

CS and WL conducted the experiment and wrote the original draft. FC performed the statistical analysis. GL provided the resources for this experiment. CC contributed to the conception and supervision of this study. All authors contributed to manuscript revision, read, and approved the submitted version.

SUPPLEMENTARY MATERIAL

The Supplementary Material for this article can be found online at: https://www.frontiersin.org/articles/10.3389/fmicb.2021.688290/full#supplementary-material

REFERENCES

Abraham, A., Mathew, A. K., Park, H., Choi, O., Sindhu, R., Parameswaran, B., et al. (2020). Pretreatment strategies for enhanced biogas production from lignocellulosic biomass. *Bioresour. Technol.* 301:122725. doi: 10.1016/j.biortech.2019.122725

Ali, S. S., Al-Tohamy, R., Manni, A., Luz, F. C., Elsamahy, T., and Sun, J. (2019). Enhanced digestion of bio-pretreated sawdust using a novel bacterial consortium: microbial community structure and methane-producing pathways. *Fuel* 254:115604. doi: 10.1016/j.fuel.2019.06.012

Amin, F. R., Khalid, H., El-Mashad, H. M., Chen, C., Liu, G., and Zhang, R. (2021). Functions of bacteria and archaea participating in the bioconversion of organic waste for methane production. *Sci. Total Environ.* 763:143007. doi: 10.1016/j.scitotenv.2020.143007

Amin, F. R., Khalid, H., Zhang, H., Rahman, S., Zhang, R., Liu, G., et al. (2017). Pretreatment methods of lignocellulosic biomass for anaerobic digestion. *AMB Exp.* 7:72. doi: 10.1186/s13568-017-0375-4

APHA (2005). *Standard Methods for the Examination of Water and Wastewater*, 21 Edn. Washington, DC: American Public Health Association.

Bajpai, P. (2014). "Uses of recovered paper other than papermaking," in *Recycling and Deinking of Recovered Paper*, ed. P. Bajpai (Oxford: Elsevier), 283–295. doi: 10.1016/b978-0-12-416998-2.00016-7

Carrere, H., Antonopoulou, G., Affes, R., Passos, F., Battimelli, A., Lyberatos, G., et al. (2016). Review of feedstock pretreatment strategies for improved anaerobic digestion: From lab-scale research to full-scale application. *Bioresour. Technol.* 199, 386–397. doi: 10.1016/j.biortech.2015.09.007

Chen, S., and Dong, X. (2005). *Proteiniphilum acetatigenes* gen. nov., sp. nov., from a UASB reactor treating brewery wastewater. *Int. J. Syst. Evol. Microbiol.* 55, 2257–2261. doi: 10.1099/ijs.0.63807-0

Dastager, S. G., Mawlankar, R., Mual, P., Verma, A., Krishnamurthi, S., Joseph, N., et al. (2015). *Bacillus encimensis* sp. nov. isolated from marine sediment. *Int. J. Syst. Evol. Microbiol.* 65, 1421–1425. doi: 10.1099/ijs.0.000114

De Bel, A., Van Hoorde, K., Wybo, I., Vandoorslaer, K., Echahidi, F., De Brandt, E., et al. (2013). *Staphylococcus jettensis* sp. nov., a coagulasenegative staphylococcal species isolated from human clinical specimens. *Int. J. Syst. Evol. Microbiol.* 63, 3250–3256. doi: 10.1099/ijs.0.044438-0

Den, W., Sharma, V. K., Lee, M., Nadadur, G., and Varma, R. S. (2018). Lignocellulosic biomass transformations via greener oxidative pretreatment processes: access to energy and value added chemicals. *Front. Chem.* 6:141. doi: 10.3389/fchem.2018.00141

Ecem Öner, B., Akyol, Ç, Bozan, M., Ince, O., Aydin, S., and Ince, B. (2018). Bioaugmentation with *Clostridium thermocellum* to enhance the anaerobic biodegradation of lignocellulosic agricultural residues. *Bioresour. Technol.* 249, 620–625. doi: 10.1016/j.biortech.2017.10.040

Falsen, E., Collins, M. D., Welinder-Olsson, C., Song, Y., Finegold, S. M., and Lawson, P. A. (2005). *Fastidiosipila sanguinis* gen. nov., sp. nov., a new Gram-positive, coccus-shaped organism from human blood. *Int. J. Syst. Evol. Microbiol.* 55, 853–858. doi: 10.1099/ijs.0.63327-0

Fu, S., Wang, F., Shi, X., and Guo, R. (2016). Impacts of microaeration on the anaerobic digestion of corn straw and the microbial community structure. *Chem. Eng. J.* 287, 523–528. doi: 10.1016/j.cej.2015.11.070

Grabowski, A., Tindall, B. J., Bardin, V., Blanchet, D., and Jeanthon, C. (2005). *Petrimonas sulfuriphila* gen. nov., sp. nov., a mesophilic fermentative bacterium isolated from a biodegraded oil reservoir. *Int. J. Syst. Evol. Microbiol.* 55, 1113–1121. doi: 10.1099/ijs.0.63426-0

Hatamoto, M., Kaneshige, M., Nakamura, A., and Yamaguchi, T. (2014). *Bacteroides luti* sp. nov., an anaerobic, cellulolytic and xylanolytic bacterium isolated from methanogenic sludge. *Int. J. Syst. Evol. Microbiol.* 64, 1770–1774. doi: 10.1099/ijs.0.056630-0

He, S., Fan, X., Luo, S., Katukuri, N. R., and Guo, R. (2017). Enhanced the energy outcomes from microalgal biomass by the novel biopretreatment. *Energy Convers. Manag.* 135, 291–296. doi: 10.1016/j.enconman.2016.12.049

Imachi, H., Sakai, S., Kubota, T., Miyazaki, M., Saito, Y., and Takai, K. (2016). *Sedimentibacter acidaminivorans* sp. nov., an anaerobic, amino-acid-utilizing bacterium isolated from marine subsurface sediment. *Int. J. Syst. Evol. Microbiol.* 66, 1293–1300. doi: 10.1099/ijsem.0.000878

Jabari, L., Gannoun, H., Cayol, J. L., Hedi, A., Sakamoto, M., Falsen, E., et al. (2012). *Macellibacteroides fermentans* gen. nov., sp. nov., a member of the family *Porphyromonadaceae* isolated from an upflow anaerobic filter treating abattoir wastewaters. *Int. J. Syst. Evol. Microbiol.* 62, 2522–2527. doi: 10.1099/ijs.0.032508-0

Kainthola, J., Kalamdhad, A. S., Goud, V. V., and Goel, R. (2019). Fungal pretreatment and associated kinetics of rice straw hydrolysis to accelerate methane yield from anaerobic digestion. *Bioresour. Technol.* 286:121368. doi: 10.1016/j.biortech.2019.121368

Kim, J., Kim, J., and Lee, C. (2019). Anaerobic co-digestion of food waste, human feces, and toilet paper: methane potential and synergistic effect. *Fuel* 248, 189–195. doi: 10.1016/j.fuel.2019.03.081

Krause, M. J., Chickering, G. W., Townsend, T. G., and Pullammanappallil, P. (2018). Effects of temperature and particle size on the biochemical methane potential of municipal solid waste components. *Waste Manag.* 71, 25–30. doi: 10.1016/j.wasman.2017.11.015

Lanjekar, V. B., Marathe, N. P., Shouche, Y. S., and Ranade, D. R. (2015). *Clostridium punense* sp. Nov., an obligate anaerobe isolated from healthy human faeces. *Int. J. Syst. Evol. Microbiol.* 65, 4749–4756. doi: 10.1099/ijsem.0.000644

Lechner, U. (2015). "*Sedimentibacter*," in *Bergey's Manual of Systematics of Archaea and Bacteria*, ed. W. B. Whitman (New York, NY: John Wiley & Sons, Ltd.), 1–7. doi: 10.1002/9781118960608.gbm00718

Lee, J. K., Patel, S. K. S., Sung, B. H., and Kalia, V. C. (2020). Biomolecules from municipal and food industry wastes: an overview. *Bioresour. Technol.* 298:122346. doi: 10.1016/j.biortech.2019.122346

Li, L., He, Q., Ma, Y., Wang, X., and Peng, X. (2015). Dynamics of microbial community in a mesophilic anaerobic digester treating food waste: relationship between community structure and process stability. *Bioresour. Technol.* 189, 113–120. doi: 10.1016/j.biortech.2015.04.015

Li, W., Khalid, H., Amin, F. R., Zhang, H., Dai, Z., Chen, C., et al. (2020). Biomethane production characteristics, kinetic analysis, and energy potential of different paper wastes in anaerobic digestion. *Renew. Energy* 157, 1081–1088. doi: 10.1016/j.renene.2020.04.035

Li, W., Khalid, H., Zhu, Z., Zhang, R., Liu, G., Chen, C., et al. (2018). Methane production through anaerobic digestion: participation and digestion characteristics of cellulose, hemicellulose and lignin. *Appl. Energy* 226, 1219-1228. doi: 10.1016/j.apenergy.2018.05.055

Lim, J. W., and Wang, J.-Y. (2013). Enhanced hydrolysis and methane yield by applying microaeration pretreatment to the anaerobic co-digestion of brown

water and food waste. *Waste Manag.* 33, 813–819. doi: 10.1016/j.wasman.2012.11.013

Ma, S., Zhou, C., Chi, C., Liu, Y., and Yang, G. (2020). Estimating physical composition of municipal solid waste in China by applying artificial neural network method. *Environ. Sci. Technol.* 54, 9609–9617. doi: 10.1021/acs.est.0c01802

Manfredi, S., Tonini, D., and Christensen, T. H. (2011). Environmental assessment of different management options for individual waste fractions by means of life-cycle assessment modelling. *Resour. Conserv. Recycl.* 55, 995–1004. doi: 10.1016/j.resconrec.2011.05.009

NationMaster (2021). *Top Countries for Paperboard and Packaging Paper Production. NationMaster*. Available online at: https://www.nationmaster.com/nmx/ranking/paperboard-and-packaging-paper-production (accessed May 3, 2021).

Ning, Z., Zhang, H., Li, W., Zhang, R., Liu, G., and Chen, C. (2018). Anaerobic digestion of lipid-rich swine slaughterhouse waste: methane production performance, long-chain fatty acids profile and predominant microorganisms. *Bioresour. Technol.* 269, 426–433. doi: 10.1016/j.biortech.2018.08.001

Patel, S. K. S., Kumar, P., Singh, M., Lee, J. K., and Kalia, V. C. (2015). Integrative approach to produce hydrogen and polyhydroxybutyrate from biowaste using defined bacterial cultures. *Bioresour. Technol.* 176, 136–141. doi: 10.1016/j.biortech.2014.11.029

Radolfova-Krizova, L., Maixnerova, M., and Nemec, A. (2016). *Acinetobacter pragensis* sp. nov., found in soil and water ecosystems. *Int. J. Syst. Evol. Microbiol.* 66, 3897–3903. doi: 10.1099/ijsem.0.001285

Rincón, B., Heaven, S., Banks, C. J., and Zhang, Y. (2012). Anaerobic digestion of whole-crop winter wheat silage for renewable energy production. *Energy Fuels* 26, 2357–2364. doi: 10.1021/ef201985x

Rodriguez, C., Alaswad, A., El-Hassan, Z., and Olabi, A. G. (2017). Mechanical pretreatment of waste paper for biogas production. *Waste Manag.* 68, 157–164. doi: 10.1016/j.wasman.2017.06.040

Ruan, D., Zhou, Z., Pang, H., Yao, J., Chen, G., and Qiu, Z. (2019). Enhancing methane production of anaerobic sludge digestion by microaeration: enzyme activity stimulation, semi-continuous reactor validation and microbial community analysis. *Bioresour. Technol.* 289:121643. doi: 10.1016/j.biortech.2019.121643

Sakamoto, M., and Ohkuma, M. (2013). *Bacteroides reticulotermitis* sp. nov., isolated from the gut of a subterranean termite (*Reticulitermes speratus*). *Int. J. Syst. Evol. Microbiol.* 63, 691–695. doi: 10.1099/ijs.0.040931-0

Sanscartier, D., MacLean, H. L., and Saville, B. (2012). Electricity production from anaerobic digestion of household organic waste in Ontario: techno-economic and GHG emission analyses. *Environ. Sci. Technol.* 46, 1233–1242. doi: 10.1021/es2016268

Sekiguchi, Y. (2015). "*Syntrophomonas*," in *Bergey's Manual of Systematics of Archaea and Bacteria*, ed. W. B. Whitman (New York, NY: John Wiley & Sons, Ltd.), 1–11. doi: 10.1002/9781118960608.gbm00682

Supré, K., De Vliegher, S., Cleenwerck, I., Engelbeen, K., Van Trappen, S., Piepers, S., et al. (2010). *Staphylococcus devriesei* sp. nov., isolated from teat apices and milk of dairy cows. *Int. J. Syst. Evol. Microbiol.* 60, 2739–2744. doi: 10.1099/ijs.0.015982-0

Van Soest, P. J., Robertson, J. B., and Lewis, B. A. (1991). Methods for dietary fiber, neutral detergent fiber, and nonstarch polysaccharides in relation to animal nutrition. *J. Dairy Sci.* 74, 3583–3597. doi: 10.3168/jds.S0022-0302(91)78551-2

Wang, C., Zhang, J., Hu, F., Zhang, S., Lu, J., and Liu, S. (2020). Bio-pretreatment promote hydrolysis and acidification of oilseed rape straw: roles of fermentation broth and micro-oxygen. *Bioresour. Technol.* 308:123272. doi: 10.1016/j.biortech.2020.123272

Wang, G., Li, Q., Gao, X., and Wang, X. C. (2018). Synergetic promotion of syntrophic methane production from anaerobic digestion of complex organic wastes by biochar: performance and associated mechanisms. *Bioresour. Technol.* 250, 812–820. doi: 10.1016/j.biortech.2017.12.004

Wang, L., Zhang, H., Dai, Z., Liu, Y., Chen, C., and Liu, G. (2021). Effect of nicotine inhibition on anaerobic digestion and the co-digestion performance of tobacco stalks with different animal manures. *Process Saf. Environ. Prot.* 146, 377–382. doi: 10.1016/j.psep.2020.09.005

Wu, Y., Wang, L., Jin, M., and Zhang, K. (2020). Simultaneous copper removal and electricity production and microbial community in microbial fuel cells with different cathode catalysts. *Bioresour. Technol.* 305:123166. doi: 10.1016/j.biortech.2020.123166

Xu, W., Fu, S., Yang, Z., Lu, J., and Guo, R. (2018). Improved methane production from corn straw by microaerobic pretreatment with a pure bacteria system. *Bioresour. Technol.* 259, 18–23. doi: 10.1016/j.biortech.2018.02.046

Yang, C. X., Wang, T., Gao, L. N., Yin, H. J., and Lü, X. (2017). Isolation, identification and characterization of lignin-degrading bacteria from Qinling. *China. J. Appl. Microbiol.* 123, 1447–1460. doi: 10.1111/jam.13562

Yuan, X., Wen, B., Ma, X., Zhu, W., Wang, X., Chen, S., et al. (2014). Enhancing the anaerobic digestion of lignocellulose of municipal solid waste using a microbial pretreatment method. *Bioresour. Technol.* 154, 1–9. doi: 10.1016/j.biortech.2013.11.090

Zakaria, B. S., and Dhar, B. R. (2019). Progress towards catalyzing electromethanogenesis in anaerobic digestion process: fundamentals, process optimization, design and scale-up considerations. *Bioresour. Technol.* 289:121738. doi: 10.1016/j.biortech.2019.121738

Zhao, C., Zhang, R., He, Y., Wang, W., Chen, C., Liu, G., et al. (2017). Maximization of the methane production from durian shell during anaerobic digestion. *Bioresour. Technol.* 238, 433–438. doi: 10.1016/j.biortech.2017.03.184

Zhao, H. L., Liu, F., Liu, H. Q., Wang, L., Zhang, R., and Hao, Y. (2020). Comparative life cycle assessment of two ceramsite production technologies for reusing municipal solid waste incinerator fly ash in China. *Waste Manag* 113, 447–455. doi: 10.1016/j.wasman.2020.06.016

Zhao, Y., Xu, C., Ai, S., Wang, H., Gao, Y., Yan, L., et al. (2019). Biological pretreatment enhances the activity of functional microorganisms and the ability of methanogenesis during anaerobic digestion. *Bioresour. Technol.* 290:121660. doi: 10.1016/j.biortech.2019.121660

Zhen, F., Luo, X., Xing, T., Sun, Y., Kong, X., and Li, W. (2021). Performance evaluation and microbial community analysis of microaerobic pretreatment on thermophilic dry anaerobic digestion. *Biochem. Eng. J.* 167, 107873. doi: 10.1016/j.bej.2020.107873

Zhen, X., Zhang, X., Li, S., Li, M., and Kang, J. (2020). Effect of micro-oxygen pretreatment on gas production characteristics of anaerobic digestion of kitchen waste. *J. Mater. Cycles Waste Manag.* 22, 1852–1858. doi: 10.1007/s10163-020-01072-9

Zhou, Y., Xu, Z., Zhao, M., Shi, W., Huang, Z., He, D., et al. (2018). Construction and evaluation of efficient solid-state anaerobic digestion system via vinegar residue. *Int. Biodeterior. Biodegrad.* 133, 142–150. doi: 10.1016/j.ibiod.2018.06.020

Zhu, Y., Zhang, Y., Luo, D., Chong, Z., Li, E., and Kong, X. (2020). A review of municipal solid waste in China: characteristics, compositions, influential factors and treatment technologies. *Environ. Dev. Sustain.* 23, 6603–6622. doi: 10.1007/s10668-020-00959-9

Conflict of Interest: The authors declare that the research was conducted in the absence of any commercial or financial relationships that could be construed as a potential conflict of interest.

frontiers in Microbiology

ORIGINAL RESEARCH
published: 16 August 2021
doi: 10.3389/fmicb.2021.700256

Microbiological Surveillance of Biogas Plants: Targeting Acetogenic Community

*Abhijeet Singh[1], Jan Moestedt[2], Andreas Berg[3] and Anna Schnürer[1]**

[1]Anaerobic Microbiology and Biotechnology Group, Department of Molecular Sciences, Swedish University of Agricultural Sciences, Uppsala, Sweden, [2]Tekniska Verken i Linköping AB, Department R&D, Linköping, Sweden, [3]Gasum, Linköping, Sweden

Acetogens play a very important role in anaerobic digestion and are essential in ensuring process stability. Despite this, targeted studies of the acetogenic community in biogas processes remain limited. Some efforts have been made to identify and understand this community, but the lack of a reliable molecular analysis strategy makes the detection of acetogenic bacteria tedious. Recent studies suggest that screening of bacterial genetic material for formyltetrahydrofolate synthetase (FTHFS), a key marker enzyme in the Wood-Ljungdahl pathway, can give a strong indication of the presence of putative acetogens in biogas environments. In this study, we applied an acetogen-targeted analyses strategy developed previously by our research group for microbiological surveillance of commercial biogas plants. The surveillance comprised high-throughput sequencing of FTHFS gene amplicons and unsupervised data analysis with the AcetoScan pipeline. The results showed differences in the acetogenic community structure related to feed substrate and operating parameters. They also indicated that our surveillance method can be helpful in the detection of community changes before observed changes in physico-chemical profiles, and that frequent high-throughput surveillance can assist in management towards stable process operation, thus improving the economic viability of biogas plants. To our knowledge, this is the first study to apply a high-throughput microbiological surveillance approach to visualise the potential acetogenic population in commercial biogas digesters.

Keywords: anaerobic digestion, acetogens, formyltetrahydrofolate synthetase, high-throughput sequencing, community profile

OPEN ACCESS

Edited by:
Shanfei Fu,
Jiangnan University, China

Reviewed by:
Vivekanand Vivekanand,
Malaviya National Institute of Technology, India
Gang Luo,
Fudan University, China

***Correspondence:**
Anna Schnürer
anna.schnurer@slu.se

Specialty section:
This article was submitted to Microbiotechnology, a section of the journal Frontiers in Microbiology

Received: *25 April 2021*
Accepted: *21 July 2021*
Published: *16 August 2021*

Citation:
Singh A, Moestedt J, Berg A and Schnürer A (2021) Microbiological Surveillance of Biogas Plants: Targeting Acetogenic Community. Front. Microbiol. 12:700256. doi: 10.3389/fmicb.2021.700256

INTRODUCTION

Biogas generation is a very versatile process, in which almost any biodegradable material can be used to produce biogas and biofertiliser (Schnürer, 2016; Schnürer and Jarvis, 2017). It involves a complex and interdependent anaerobic microbiological consortium working in synergy to carry out hydrolysis, acidogenesis, anaerobic/syntrophic oxidation and methanogenesis (Schnürer, 2016; Borja and Rincón, 2017; Robles et al., 2018; Kleinsteuber, 2019; Theuerl et al., 2019). Thousands of known and unknown microbial species cooperate and coordinate in the biogas process, making it very different from other industrial fermentation processes (Wolf et al., 2009; Madsen et al., 2011; Drosg, 2013; Ferguson et al., 2014; Maus et al., 2016;

Treu et al., 2016; Campanaro et al., 2020; Yoshida and Shimizu, 2020). This microbiological complexity lowers the scope for automatic control and optimisation, making the process prone to unintended changes in performance and stability (Ward et al., 2008; Wolf et al., 2009; Madsen et al., 2011). For adequate use of the resources invested in commercial biogas production, process optimisation and constant monitoring of the process are extremely important (Madsen et al., 2011; Drosg, 2013; Schnürer, 2016). Various physical and chemical analysis technologies are available for monitoring the biogas process, but they are based on consequential parameters and are not completely reliable in predicting disturbances in microbial communities (Ward et al., 2008; Ferguson et al., 2018; Yoshida and Shimizu, 2020). Therefore, new methods are needed for constant monitoring of microbiological community structure and dynamics in biogas reactors (Fernández et al., 1999; Drosg, 2013; Ferguson et al., 2014).

The whole microbial aggregation is important in the synergistic coordination required for the biogas process (Schnürer, 2016; Kleinsteuber, 2019). Among the microbial communities involved, the acetogenic community is critical in synchronising and balancing the biogas process and acts as a connecting link between hydrolysing/fermenting bacteria and methanogens (Kovács et al., 2004). Despite their importance and versatility in biogas generation, the acetogens remain neglected in microbiome-oriented studies on the anaerobic digestion process (Theuerl et al., 2019). Studies using advanced technologies, such as metagenomics, metatranscriptomics, metaproteomics, etc., have demonstrated that biogas microbiomes are highly diverse and that each biogas reactor develops its specific microbial community based on the substrate/s and operating parameters (Schlüter et al., 2008; Hanreich et al., 2012; Heyer et al., 2013, 2016; Kohrs et al., 2014; Campanaro et al., 2016; Güllert et al., 2016; Luo et al., 2016; Maus et al., 2016; Ortseifen et al., 2016; Treu et al., 2016). Large-scale omics studies have been paramount in unravelling microbial dark matter, but none to date has focused on the structure or diversity of specifically acetogenic communities or examined the importance or functional role of this vital group in biogas reactors.

Some targeted amplicon-based studies have examined the acetogenic communities in biogas reactors and other environments (Leaphart and Lovell, 2001; Pester and Brune, 2006; Ohashi et al., 2007; Gagen et al., 2010, 2014; Henderson et al., 2010; Akuzawa et al., 2011; Hori et al., 2011; Westerholm et al., 2011a, 2018; Moestedt et al., 2016; Müller et al., 2016; Li et al., 2017; Saheb-Alam et al., 2017). These studies employed the formyltetrahydrofolate synthetase (FTHFS) gene, which is a marker for acetogenic bacteria but were performed using techniques, such as clone library or T-RFLP profiling, yielding limited information about acetogenic community structure and diversity, taxonomic identities, temporal changes, etc. This was due to the lack of tools and methods that could be used efficiently and reliably to gain a deeper understanding of acetogenic communities and their characteristics. Recent developments, such as the creation of the acetogen-specific database AcetoBase (Singh et al., 2019) and the high-throughput data analysis pipeline AcetoScan (Singh et al., 2020), have helped significantly in facilitating the in-depth analysis of potential acetogenic communities. Moreover, a recent comparative study demonstrated the superiority of a FTHFS gene-based sequencing method over FTHFS gene-based T-RFLP or 16S rRNA gene sequencing in targeting acetogenic community structure and community dynamics (Singh et al., 2021a).

The aim of the present study was to use a FTHFS gene-based high-throughput sequencing method for microbiological surveillance of potential acetogenic communities in commercial biogas plants in Sweden. For this, long time series of weekly samples from full-scale biogas reactors operating with different feed substrates (food waste, sludge, manure, green waste, etc.) and operating conditions were used. To our knowledge, no previous study has successfully devised and applied an acetogenic community-oriented microbiological surveillance strategy for biogas plants.

MATERIALS AND METHODS

Sample Collection and Processing

Samples were collected weekly for several years from six Swedish biogas plants with different operating conditions [continuous stirred-tank reactor (CSTR) or plug flow, organic loading rate (OLR), hydraulic retention time (HRT), temperature, etc.] and different substrates (e.g., food waste, food waste with sludge, agricultural waste, manure, sludge, etc.; **Table 1**). Volatile fatty acid (VFA) analysis, including C2–C6 acids, was performed by the respective biogas plant operator and process metadata (OLR, HRT, temperature, gas yield, methane content, ammonium-nitrogen, pH, VFA, etc.) were provided. The VFA and ammonium-nitrogen analyses were mainly performed using methods described by Moestedt et al. (2016). The period with no VFA accumulation was defined as the stable phase, the period with VFA accumulation as the disturbance phase, and the subsequent phase, where the accumulated VFA were degraded, as the recovery phase. Disturbance was characterised by varying levels of volatile acid accumulation (2–17 g/L). Samples for microbiological surveillance were selected using a disturbance-centred strategy, with samples collected from the stable phase preceding disturbance, during the disturbance phase and in the recovery phase. For DNA extraction and library preparation, single replicates from the stable phase and two or three replicates from the disturbed phase over an extended time series were selected. The genomic DNA and sequencing library were prepared as previously described (Singh, 2020; Singh et al., 2021a). All samples were pooled, with an equal amount from each (20 ng), and paired-end sequencing was carried out on Illumina MiSeq with v3 chemistry at the sequencing facility of the SNP&SEQ technology platform in Uppsala (UGC, 2018). For multiplexed high-throughput sequencing, a total of 391 samples were used in two separate sequencing runs, from which the data were combined for analysis.

Sequence Data Analysis

Unsupervised FTHFS gene sequence data analysis was performed using the AcetoScan pipeline (1.0; Singh et al., 2020). Before the

TABLE 1 | Characteristics of the six Swedish commercial and industrial-scale biogas reactors sampled for microbiological surveillance in this study.

No.	Reactor code	Reactor type	Substrate	Avg. biogas ($Nm^3\ d^{-1}$)	Total VFA ($g\ L^{-1}$)	pH	$N\text{-}NH_4^+$ ($g\ L^{-1}$)	Temp. (°C)	OLR ($gVS\ L^{-1}\ d^{-1}$)	HRT (Days)
1*	C1-DD1	Plug-flow	Food waste	1,683	0.4–17	7.4–8.0	4.0–6.6	38–40	5.7–9.3	30–49
2†	C2-VX1/2	CSTR	Food waste + sewage sludge	2,102	0.0–3.2	7.5–7.9	1.2–2.3	39–41	3.2–3.4	18–29
3†	C3-K1/2	CSTR	Cow/pig manure, cereals, silage and fats	7,375	0.0–0.3	7.5–8.0	2.6–4.2	36–38	1.1–4.9	30–68
4†	C4-VS1/2	CSTR	Horse/chicken/pig manure and cereal husks	4,543	0.0–1.2	7.6–7.9	2.6–7.9	36–38	0.8–3.8	23–103
5†	C5-A1/3	CSTR	Food/slaughterhouse waste	11,937	0.0–0.2	7.5–8.2	2.2–3.4	38–42	0.2–3.9	27–50
6†	C6-O1/2	CSTR	Stillage, grass silage and plant residues	10,255	0–3.3	7.3–7.9	2.9–3.7	36–40	3.4–7.7	45–111

*Values included in the table are metadata provided by respective biogas plant operator. *Plug-flow dry digestion type biogas reactor. †Parallel biogas reactor. Average values/range of each parameter are provided here, for exact values see **supplementary material**.*

analysis, a single file was created by concatenating the raw forward and reverse read files for each sample. The parameters used for the AcetoScan analysis were −m 300, −n 150, −q 20, −c 5 and −e 1e−30, while for other parameters default settings were used (AcetoScan users' manual). Customised visualisation of the AcetoScan results was done using the packages *phyloseq* (1.30.0; McMurdie and Holmes, 2013) and *vegan* (2.5.7; Oksanen et al., 2019) in R (3.6.3; R Core Team, 2013) and RStudio (1.3.1073; RStudio Team, 2020). All data processing and visual analyses were performed on a Debian Linux-based system with x86_64 architecture and 3.4 Ghz Intel® Core™ i7-6700 processor.

RESULTS

Reactor Characteristics

The biogas reactors that supplied samples for the analysis differed in their operating strategies and feed substrates (see **Table 1**). Except for reactor C1-DD1, all reactors were parallel reactors at the specific plant (C2–C5). During the sampling period, some fluctuations in feed ratio, temperature and OLR and in associated consequential parameters, such as methane and carbon dioxide content (%), pH, etc., were observed (**Table 1**). Reactor C1-DD1, a food waste plug flow reactor, reached a very high level of VFA accumulation (~17 g/L), but only minor VFA accumulation (2–3 g/L) was observed for the CSTR reactors C2-VX1/2, C3-K1/2, C4-VS1/2 and C6-O1/2, and no accumulation of VFA was observed in C5-A1/3.

High-Throughput Sequencing

The size (compressed) of combined forward and reverse reads from two separate runs was ~6.5 and ~7.1 Gb, respectively. Since the forward and reverse reads cannot be paired, the forward and reverse read fastq files for individual samples were merged in a single file. The overall final size of the merged fastq data files was ~14 Gb and ~61 M sequences. After quality filtering ~35 M sequences were used for clustering at 100% identity, which resulted in 1897 OTUs.

Potential Acetogenic Community Structure

The total number of taxa detected in community-level analysis for the classification levels from phylum to species was 11, 23, 32, 52, 106 and 152, respectively. It should be noted that for C1-DD1, the initial samples (1–4) were taken from a stable period longer than 1 year (with low VFA levels), whereas the following samplings were in the VFA accumulation phase (**Figure 1**). However, community structure was similar in the phases before and after VFA accumulation.

Phylum-Level Community Structure

The top three most abundant phyla detected in all the reactors were Firmicutes, Candidatus Clocimonetes and Actinobacteria (**Figure 1**). At phylum level, the changes in community structure during VFA accumulation were most distinct for C1-DD1. Candidatus Clocimonetes was the most abundant phylum in

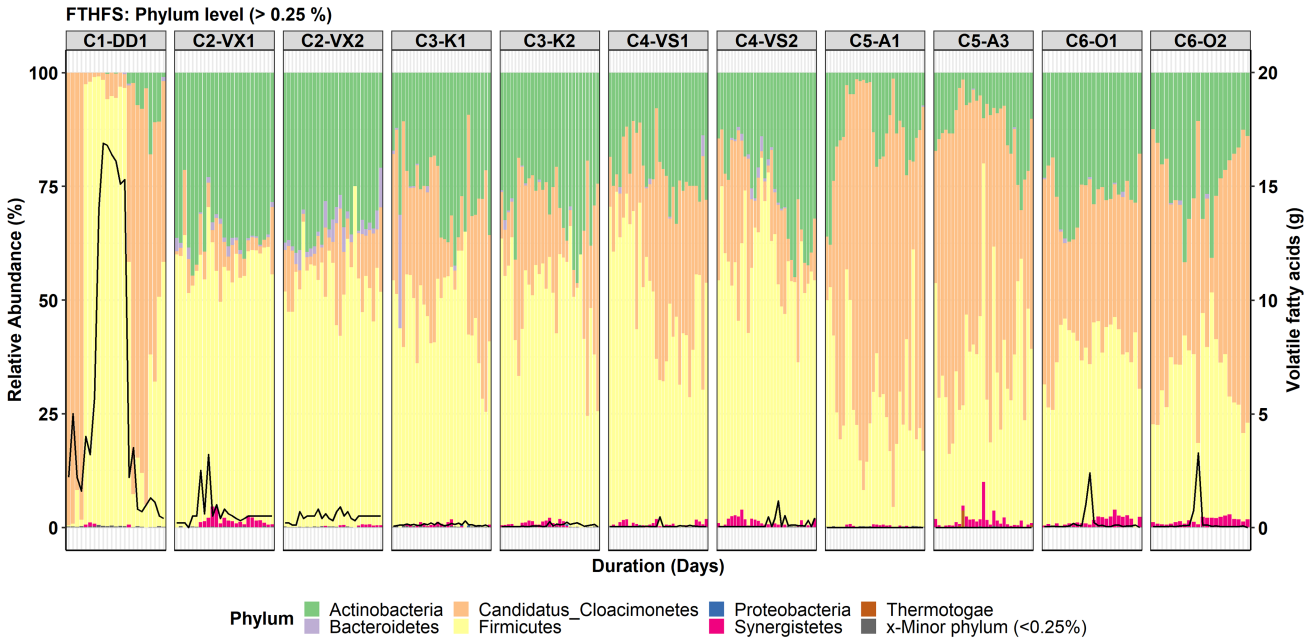

FIGURE 1 | Phylum-level community structure in the six reactors (C1–C6) visualised with formyltetrahydrofolate synthetase (FTHFS) amplicon sequencing. The black line represents the concentration (g/L) of total volatile fatty acids.

the stable and recovery phases, but during the period with VFA increase the community structure drastically changed and Firmicutes was instead the dominant phylum, representing >90% of total relative abundance (RA; **Figure 1**). The phylum-level community structure for C2-VX1/2 showed the highest abundance of Firmicutes (RA ~50–60%) and Actinobacteria (RA ~25–35%), followed by Candidatus Clocimonetes (RA ~1–20%), Bacteroidetes and Synergistetes. The phylum-level community structure in C3-K1/2 and C4-VS1/2 was found to be similar with respect to the top three phyla, *viz*. Firmicutes (RA ~40–50%), Actinobacteria (RA ~20–40%) and Candidatus Clocimonetes (RA ~5–20%). High abundance of Candidatus Clocimonetes (RA ~10–90%) compared with Firmicutes (RA ~8–40%) and Actinobacteria (RA ~2–35%) was also observed in C5-A1/3. In reactor C6-O1/2, the top three phyla were Firmicutes, Candidatus Clocimonetes and Actinobacteria, which showed similar RA.

Genus- and Species-Level Community Structure

A total of 106 genera were observed in the genus-level community analysis, but in low abundance, with only 39 and 32 genera having RA >3 and >5%, respectively. At species level, 152 species we observed, of which 48 and 37 species had RA >3 and >5%, respectively. Overall, Candidatus Cloacimonetes bacterium was the most abundant genus detected (**Figure 2**). It was also the most abundant genus in C1-DD1, before and after VFA accumulation, and in C5-A1/3 and C6-O1/2. However, in reactor C2-VX1/2, *Enteroscipio* and *Oscillibacter* were instead the most abundant genera, except in the first period of surveillance, where this reactor was enriched with uncultured Firmicutes bacterium. Other genera identified at relatively high abundance (RA >3%) were *Lagierella* and *Varibaculum* in C6-O1/2 and *Tepidanaerobacter*, most significantly (RA >3%) in C4-VS1/2 (**Figure 2**).

For the species-level community analysis, the threshold used for visualisation was 3% RA. The results showed that the Candidatus Cloacimonetes bacterium in the different reactors was represented by three different species (**Figure 3**). In reactor C1-DD1, Cloacimonetes bacterium HGW_Cloacimonetes_3 (Cloacimonetes_HGW3) was the only species detected within the phylum Candidatus Clocimonetes. With the increase in VFA levels in reactor C1-DD1, the RA of this genus fell below the 3% threshold, in parallel with appearance and increasing RA of the species *Romboutsia weinsteinii* and *Oxobacter pfennigii*. In C5-A1/3, the species Cloacimonetes_HGW1 was instead detected (RA >3%). The species Cloacimonetes_HGW2 was detected (RA >3%) in all reactors except for C1-DD1 and C2-VX1/2. Other species detected were *Mahella australiensis*, observed in C5-A1/3, *Lactobacillus antri*, detected in C3-K1/2 and C4-VS1/2, and *Thermoanaerobacter kivui*, detected in reactors C1-DD1 and C5-A1/3. *Clostridium beijerinckii* was most significantly observed during the high VFA levels in reactor C1-DD1 (**Figure 3**).

Non-metric multidimensional scaling (NMDS) diversity analysis with Bray distances helped to visualise differences in microbial diversity in samples from the different biogas reactors under the influence of different operating parameters (**Figure 4**). The most influential driving parameters for microbial community structure in reactor C1-DD1 were ammonium and VFA level. The temperature was the most influential environment variable for microbial community structure in reactor C2-VX1/2. Reactors C3-K1/2 and

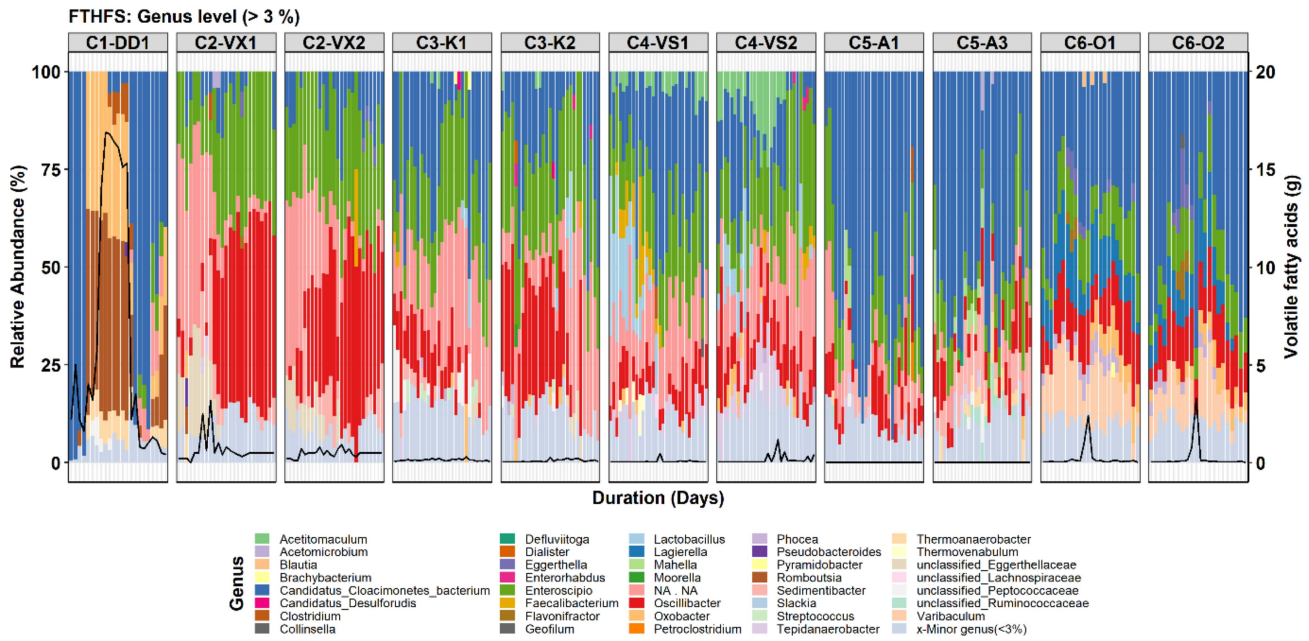

FIGURE 2 | Genus-level community structure in the six reactors (C1–C6) visualised with FTHFS amplicon sequencing. The black line represents the concentration (g/L) of total volatile fatty acids.

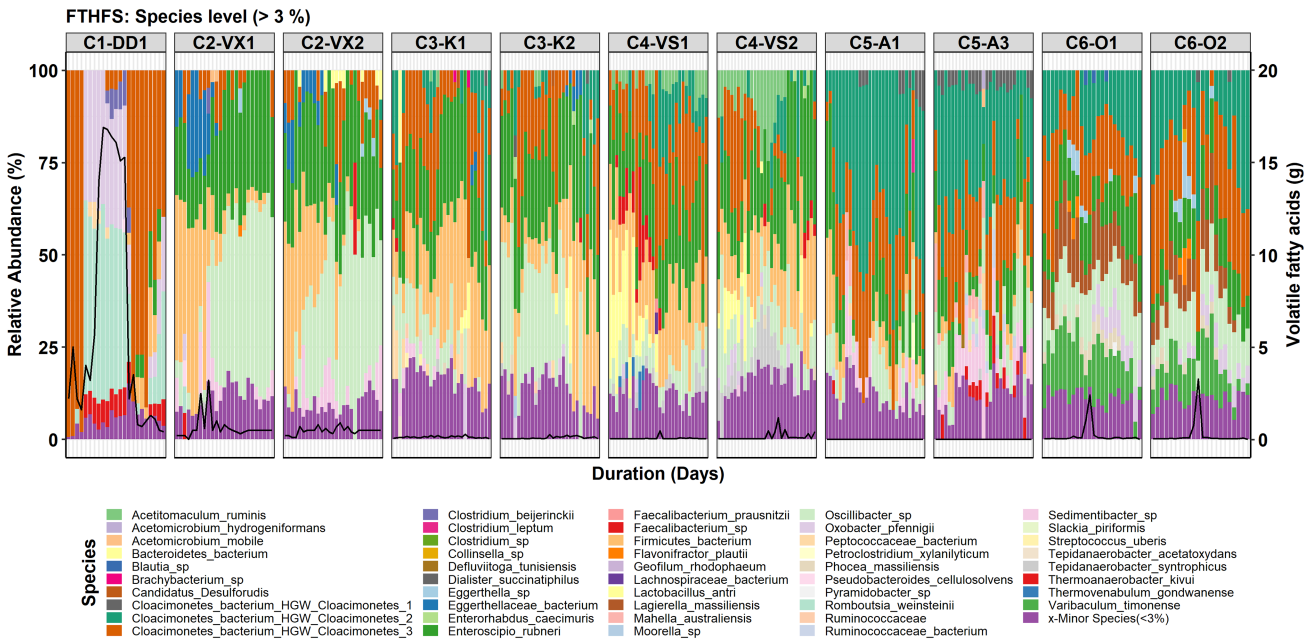

FIGURE 3 | Species-level community structure in the six reactors (C1–C6) visualised with FTHFS amplicon sequencing. The black line represents the concentration (g/L) of total volatile fatty acids.

C4-VS/2 did not show any specific significant sample dispersal under any environment variable. The samples from reactor C5-A1/3 were observed to be influenced by OLR and HRT, while those from reactor C6-O1/2 were influenced by the combined effect of HRT and temperature.

Based on NMDS analysis with Bray distances on samples from the different reactors, the top 15 species from the top three phyla showed relationships with physico-chemical changes (**Figure 5**). The species *Romboutsia weinsteinii* and *Oxobacter pfennigii* were found to be positively related to ammonium and VFA levels in

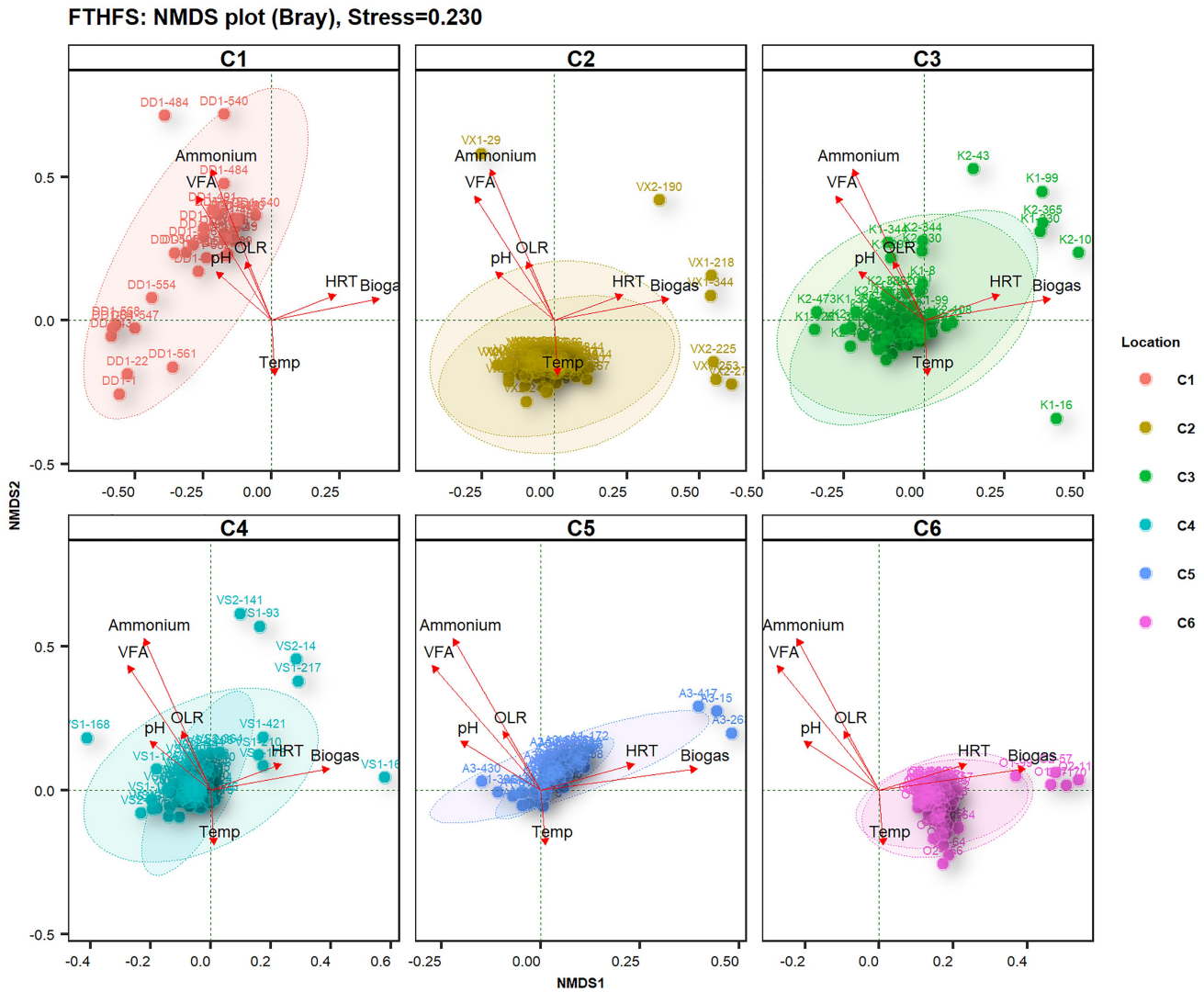

FIGURE 4 | Beta-diversity of samples from the six reactors (where C2–C6 are parallel reactors) operated with different substrates visualised with FTHFS amplicon sequencing and non-metric multidimensional scaling (NMDS) analysis with Bray distances.

the reactor, whereas Cloacimonetes_HGW3 appeared to be most sensitive to changes in physico-chemical parameters, particularly OLR, VFA and ammonium. *Lagierella massiliensis* and *Varibaculum timonense* were positively influenced by temperature and HRT. Uncultured Eggerthellaceae bacterium and Firmicutes bacterium showed negative relationships with VFA levels.

DISCUSSION

Community profiling analyses using FTHFS gene amplicon sequencing revealed potential acetogenic community structure, temporal dynamics and the influence of environmental variables on the microbial diversity in biogas reactors. Different reactors were operated with different feed substrates and operating conditions (**Table 1**), which resulted in differences and some similarities in overall community profile and dynamics. However, the similarities and difference in community structure could not be directly associated to the substrate type. The reactors used in this study were operated with mixed waste, which might explain why a clear substrate-specific clustering of samples or taxa were not observed (**Figures 4, 5**). The main driver of the community structure appeared instead to be the ammonium levels in different reactors. This result is in concordance with the previous studies of the biogas microbiome targeting 16S rRNA, suggesting that ammonia is a strong driver for clustering the community (De Vrieze et al., 2015). The most distinct features of the microbial communities in the individual reactors, in association with the environmental parameters, are further discussed below.

Reactor C1-DD1, a high solid plug flow system operating at high loads using food waste as substrate showed drastic changes in community structure during the sampling period. This could have been partly due to the large sampling gap

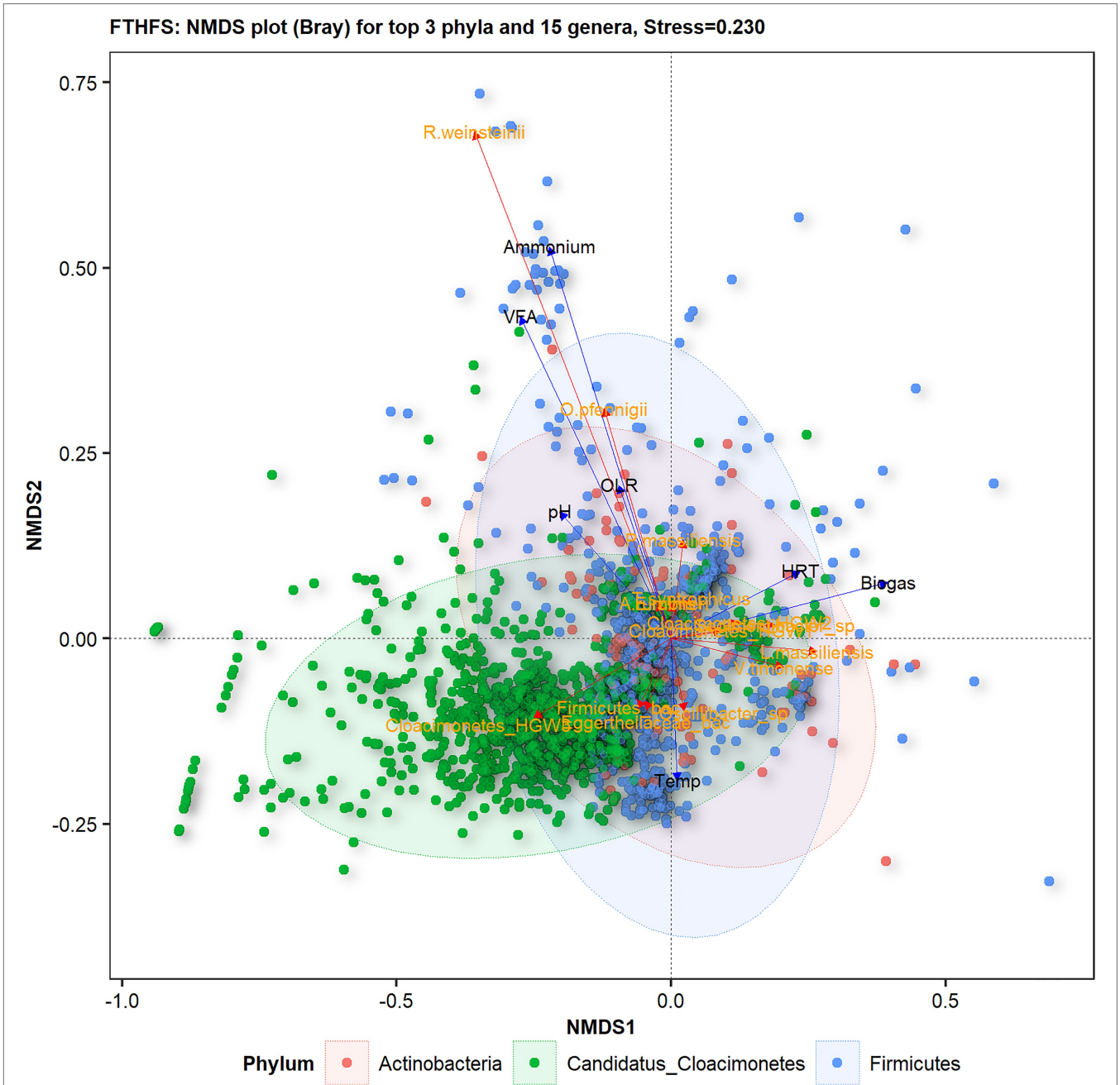

FIGURE 5 | Beta-diversity of the top 15 genera belonging to the top three phyla from in reactors (C1–C6) operated with different substrates, visualised with FTHFS amplicon sequencing and NMDS analysis with Bray distances.

(385 days) between samples 4 and 5, but was more likely caused by an increase in VFA level around sampling point 7, caused by an increase in ammonium-nitrogen level (to above 6 g/L). Ammonium-nitrogen concentrations of this level have previously been shown to cause a significant inhibition of the biogas process and VFA consumption (Moestedt et al., 2016; Schnürer and Jarvis, 2017). Moreover a shift in the potential acetogenic community in response to increasing ammonia level and a shift to syntrophic acetate oxidation have been observed before targeting FTHFS gene in TRFLP analyses (Müller et al., 2016). The species *Romboutsia weinsteinii*, *Thermoanaerobacter kivui* and *Oxobacter pfennigii* were the most prominent species in C1-DD1 when the VFA levels were high, and with the appearance of *Clostridium beijerinckii*, a drop in VFA levels was seen. It should be noted that *Thermoanaerobacter kivui* and *Clostridium beijerinckii* are known acetogens (Drake et al., 2008; Singh et al., 2019), while *Romboutsia weinsteinii* and *Oxobacter pfennigii* are suggested to be acetogens

(Collins et al., 1994; Nierychlo et al., 2020). *Romboutsia* was previously observed to be a misclassification of *Acetobacterium woodii* in AcetoScan mock-community analyses by Singh et al. (2020). *Acetobacterium woodii* is a known acetogen and, if it were misclassified as *Romboutsia*, the involvement of acetogens in VFA metabolism is further supported. *Clostridium beijerinckii* is a versatile acetogenic species since, in addition to acetate, it can produce ethanol, butyrate, etc. (Patakova et al., 2019).

Peptococcaceae bacterium was also observed (RA ~3–8%) while the VFA levels were high in reactors C1-DD1. This OTU, also found in C3-K1/2 and in the stable phase in C5-A1/3, were 84–92% similar to Peptococcaceae bacterium 1109, previously proposed to be a syntrophic organic acid-oxidising bacterium (Town et al., 2014; Town and Dumonceaux, 2016; Buettner et al., 2019; Wirth et al., 2019; Singh et al., 2021a). The OTU could also be related to the recently discovered and uncultured syntrophic propionate oxidising bacteria *Candidatus* Syntrophopropionicum ammoniitolerans isolated from propionate oxidising enrichments (Singh et al., 2021b). As this OTU was observed during the high levels of VFA (3–17 g/L) including propionate (2–10 g/L), its involvement in propionate degradation is further supported. Overall, the results obtained for C1-DD1 indicate a role of syntrophic organic-acid oxidising communities, which have been shown previously for reactors operating at high ammonia and VFA levels (Schnürer et al., 1994, 1996; Schnürer and Nordberg, 2008; Müller et al., 2016). During the VFA accumulation phase in C1-DD1, a decrease in RA of phylum Candidatus Clocimonetes was also observed. Disappearance of this phylum is suggested to be an indicator of disturbance (Calusinska et al., 2018; Klang et al., 2019; Poirier et al., 2020; Singh et al., 2021a), which is further supported by the results in this study. In the present analysis, it was observed that not all species belonging to this phylum were present in all types of reactors. Thus, the connection to process imbalance might need to be validated for each species within the phylum Candidatus Clocimonetes.

Reactor C2-VX1/2, which was operated with food waste and sewage sludge, showed somewhat different community structure from the other reactors. A community shift was also observed in this reactor around day 185, possibly due to a change in feed ratio of food waste and sewage sludge around that time. Among the dominant species, *Enteroscipio rubneri* was most abundant in C2-VX1/2, unlike in the other reactors. The OTU sequences represented by this species were observed to be ~80–86% similar to *Enteroscipio rubneri*. However, further analysis of the OTUs revealed that they were also associated with novel uncultured Clostridiaceae bacterium found by Campanaro et al. (2020), which is not yet validated. Since the reference database AcetoBase mostly contains sequences from validated bacterial species and AcetoScan identifies taxonomic relationships with the best-blast-hit strategy, the annotation for this species must be interpreted with caution.

The species *Acetitomaculum ruminis* was only observed (RA >3%) in the manure-supplemented reactors C3-K1/2 and C4-VS1/2. It is a known acetogen present in the rumen and performs reductive acetogenesis (Greening and Leedle, 1989; Le Van et al., 1998; Yang et al., 2015). An increase in RA of this species and decrease in RA of Cloacimonetes_HGW3 was observed prior to VFA accumulation (~day 175–217) in reactor C4-VS2, indicating a role in acetogenesis and syntrophic acid oxidation, respectively. *Lactobacillus antri*, observed in the same reactors, is a lactic acid-producing bacterium (Roos et al., 2005). Interestingly a decrease in its RA appeared to be related to an increase in RA of *Tepidanaerobacter syntrophicus*, followed by accumulation of VFA. *Tepidanaerobacter syntrophicus* is a syntrophic lactate/ethanol-degrading bacterium that produces acetate and is suggested to be an acetogen (Sekiguchi et al., 2006). These related events strongly indicate a role of the species in reductive acetogenesis in VFA metabolism in manure-based reactors.

Reactor C5-A1/3 was operated at 40–42°C with food waste and moderate to high ammonium-nitrogen conditions. Characteristic for this reactor was the presence of *Mahella australiensis*. This is a saccharolytic, (moderately) thermophilic bacterium producing not only acetate but also lactate, ethanol and H_2/CO_2 as end products (Bonilla Salinas et al., 2004). It is commonly reported in reactors operated with high protein substrates contents and an increase in ammonium-nitrogen might cause a decrease in relative abundance of this species (Niu et al., 2013; Zhang et al., 2021). Moreover, in this reactor the species *Thermoanaerobacter kivui* was detected. This is also a thermophilic acetogen (Leigh and Wolfe, 1983; Basen et al., 2018) generally not present in mesophilic reactors, but OTUs corresponding to this species (in C1-DD1 and C5-A1/3) were 80–93% similar to *Thermoanaerobacter kivui*. Potentially, this species could be the new uncultured bacteria also detected before in 16S rRNA gene amplicon analysis (Navarro et al., 2020) and recently identified in metagenomics analysis as a member of family Thermoanaerobacteraceae (Taxonomy ID: 2100788; Campanaro et al., 2020). The reactor operated with green waste (reactor C6-O1/2) specifically showed high RA (>3%) abundance of *Lagierella massiliensis* and *Varibaculum timonense* (renamed as *Urmitella timonensis*; GTDB, 2020), which were not detected in any other reactor. These bacteria belong to the poorly characterised order Tissierellales and might be involved in VFA metabolism, since other members of this order are known syntrophic organic acid-oxidising bacteria such as *Clostridium ultunense* (renamed as *Schnuerera ultunensis*; Schnürer et al., 1996; Oren and Garrity, 2020).

Surveillance of Industrial Biogas Plants

In microbiological surveillance in this study, a disturbance-oriented long time series sampling strategy was adopted. Time series sampling was preferred over sampling with replicates because the sequential samples obtained in time series are as good as replicates in visualising changes in the community over time (Faust et al., 2015; Singh et al., 2021a). This was supported by the similar community composition and dynamics found in parallel reactors. Time series sampling also enabled simultaneous long-term surveillance of multiple reactors. The overall strategy adopted in the study helped overcome the low throughput barrier of FTHFS-based analytical methods (FTHFS gene T-RFLP, clone library or qPCR analysis), resolved the

long duration dynamics of potential acetogenic and syntrophic communities and revealed changes in community structure before and during VFA accumulation. If community changes are closely followed in future studies, they can be used as an indicator of possible disturbance, which could help in the modification of operating parameters to avoid or minimise the impact of disturbance. Thus, the approach adequately meets the criteria for microbiological surveillance in biogas plants.

Further, the results from this study indicates that the applied method is able to target not only the potential acetogenic community but also syntrophic organic-acid oxidising bacterial communities *viz*. syntrophic acetate-oxidising bacteria (SAOB; phylum Cloacimonetes, *Tepidanaerobacter*, Peptococcaceae bacterium 1109; Sekiguchi et al., 2006; Westerholm et al., 2011b; Town et al., 2014; Town and Dumonceaux, 2016; Buettner et al., 2019; Wirth et al., 2019), syntrophic-propionate oxidising bacteria (phylum Cloacimonetes, family Peptococcaceae; Pelletier et al., 2008; Dyksma and Gallert, 2019; Singh et al., 2021b), syntrophic fatty-acid degraders (*Syntrophomonas*, *Syntrophothermus*; Sekiguchi et al., 2000; Zhang et al., 2004; Sousa et al., 2007) and syntrophic benzene degrading bacteria (family Peptococcaceae; van der Zaan et al., 2012; Gieg et al., 2014; Zhuang et al., 2015). Syntrophic organic-acid oxidising bacteria play a key role in the biogas process and even though not all being acetogens they can be detected due to the presence of FTHFS gene (Singh et al., 2019; Singh, 2021). The importance of both acetogenic and syntrophic bacterial communities in biogas process is well established and documented. Thus, combined visualization of these two communities makes our strategy a very strong tool for surveillance of biogas plants.

CONCLUSION

Microbiological surveillance of biogas reactors was carried out by using FTHFS gene amplicon sequencing in an analysis of long time-series of weekly samples from commercial biogas plants operating with different substrates. The results obtained clearly visualised the diversity of the potential acetogenic community as well as several groups of syntrophic bacteria in biogas reactors based on different feed substrate/s and operating parameters and related to VFA metabolism. This targeted community may be involved in VFA metabolism, reductive acetogenesis and/or syntrophic acid oxidisation. The surveillance strategy also revealed changes in microbial communities before any significant changes were detectable in the physico-chemical profiles. These findings highlight the role of the targeted community in microbiological surveillance of biogas plants. Some potential indicators related to process disturbances were identified, findings which require validation. Overall, our FTHFS gene amplicon-based microbiological surveillance strategy demonstrated strong potential for use as a tool for monitoring the acetogenic and syntrophic community in biogas plants.

DATA AVAILABILITY STATEMENT

The datasets presented in this study can be found in online repositories. The names of the repository/repositories and accession number(s) can be found at: https://www.ncbi.nlm.nih.gov/, PRJNA723176.

AUTHOR CONTRIBUTIONS

ASc conceived the idea of the present study and was responsible for funding acquisition. ASi performed experiment and data analysis and wrote the manuscript with valuable help from all co-authors. JM and AB were responsible for collection of samples from the biogas plants and compiled corresponding metadata. All authors have read and agreed to the published version of the manuscript.

FUNDING

This work was funded and supported by the Swedish Energy Agency (project no. 2014-000725), Västra Götaland Region (project no. MN 2016-00077) and Interreg Europe (project Biogas2020).

ACKNOWLEDGMENTS

We thank the participating biogas plants for collecting samples and assisting with metadata collection.

SUPPLEMENTARY MATERIAL

The Supplementary Material for this article can be found online at: https://www.frontiersin.org/articles/10.3389/fmicb.2021.700256/full#supplementary-material

REFERENCES

Akuzawa, M., Hori, T., Haruta, S., Ueno, Y., Ishii, M., and Igarashi, Y. (2011). Distinctive responses of metabolically active microbiota to acidification in a thermophilic anaerobic digester. *Microb. Ecol.* 61, 595–605. doi: 10.1007/s00248-010-9788-1

Basen, M., Geiger, I., Henke, L., and Müller, V. (2018). A genetic system for the thermophilic acetogenic bacterium thermoanaerobacter kivui. *Appl. Environ. Microbiol.* 84, e02210–e02217. doi: 10.1128/AEM.02210-17

Bonilla Salinas, M., Fardeau, M.-L., Thomas, P., Cayol, J.-L., Patel, B. K. C., and Ollivier, B. (2004). Mahella australiensis gen. Nov., sp. nov., a moderately thermophilic anaerobic bacterium isolated from an Australian oil well. *Int. J. Syst. Evol. Microbiol.* 54, 2169–2173. doi: 10.1099/ijs.0.02926-0

Borja, R., and Rincón, B. (eds.) (2017). "Biogas production," in *Reference Module in Life Sciences* (Elsevier), 785–798. doi: 10.1016/B978-0-12-809633-8.09105-6

Buettner, C., von Bergen, M., Jehmlich, N., and Noll, M. (2019). Pseudomonas spp. are key players in agricultural biogas substrate degradation. *Sci. Rep.* 9:12871. doi: 10.1038/s41598-019-49313-8

Calusinska, M., Goux, X., Fossépré, M., Muller, E. E. L., Wilmes, P., and Delfosse, P. (2018). A year of monitoring 20 mesophilic full-scale bioreactors reveals the existence of stable but different core microbiomes in bio-waste and wastewater anaerobic digestion systems. *Biotechnol. Biofuels* 11, 1–19. doi: 10.1186/s13068-018-1195-8

Campanaro, S., Treu, L., Kougias, P. G., De Francisci, D., Valle, G., and Angelidaki, I. (2016). Metagenomic analysis and functional characterization of the biogas microbiome using high throughput shotgun sequencing and a novel binning strategy. *Biotechnol. Biofuels* 9:26. doi: 10.1186/s13068-016-0441-1

Campanaro, S., Treu, L., Rodriguez-R, L. M., Kovalovszki, A., Ziels, R. M., Maus, I., et al. (2020). New insights from the biogas microbiome by comprehensive genome-resolved metagenomics of nearly 1600 species originating from multiple anaerobic digesters. *Biotechnol. Biofuels* 13:25. doi: 10.1186/s13068-020-01679-y

Collins, M. D., Lawson, P. A., Willems, A., Cordoba, J. J., Fernandez-Garayzabal, J., Garcia, P., et al. (1994). The phylogeny of the genus *Clostridium*: proposal of five new genera and eleven new species combinations. *Int. J. Syst. Bacteriol.* 44, 812–826. doi: 10.1099/00207713-44-4-812

De Vrieze, J., Saunders, A. M., He, Y., Fang, J., Nielsen, P. H., Verstraete, W., et al. (2015). Ammonia and temperature determine potential clustering in the anaerobic digestion microbiome. *Water Res.* 75, 312–323. doi: 10.1016/j.watres.2015.02.025

Drake, H. L., Gößner, A. S., and Daniel, S. L. (2008). Old acetogens, new light. *Ann. N. Y. Acad. Sci.* 1125, 100–128. doi: 10.1196/annals.1419.016

Drosg, B. (2013). Process Monitoring in Biogas Plants. IEA Bioenergy. Available at: https://www.ieabioenergy.com/publications/process-monitoring-in-biogas-plants (Accessed November 16, 2020).

Dyksma, S., and Gallert, C. (2019). Candidatus Syntrophosphaera thermopropionivorans: a novel player in syntrophic propionate oxidation during anaerobic digestion. *Environ. Microbiol. Rep.* 11, 558–570. doi: 10.1111/1758-2229.12759

Faust, K., Lahti, L., Gonze, D., de Vos, W. M., and Raes, J. (2015). Metagenomics meets time series analysis: unraveling microbial community dynamics. *Curr. Opin. Microbiol.* 25, 56–66. doi: 10.1016/j.mib.2015.04.004

Ferguson, R. M. W., Coulon, F., and Villa, R. (2018). Understanding microbial ecology can help improve biogas production in AD. *Sci. Total Environ.* 642, 754–763. doi: 10.1016/j.scitotenv.2018.06.007

Ferguson, R. M. W., Villa, R., and Coulon, F. (2014). Bioengineering options and strategies for the optimization of anaerobic digestion processes. *Environ. Technol. Rev.* 3, 1–14. doi: 10.1080/09593330.2014.907362

Fernández, A., Huang, S., Seston, S., Xing, J., Hickey, R., Criddle, C., et al. (1999). How stable is stable? Function versus community composition. *Appl. Environ. Microbiol.* 65, 3697–3704. doi: 10.1128/AEM.65.8.3697-3704.1999

Gagen, E. J., Denman, S. E., Padmanabha, J., Zadbuke, S., Al Jassim, R., Morrison, M., et al. (2010). Functional gene analysis suggests different acetogen populations in the bovine rumen and tammar wallaby forestomach. *Appl. Environ. Microbiol.* 76, 7785–7795. doi: 10.1128/AEM.01679-10

Gagen, E. J., Wang, J., Padmanabha, J., Liu, J., de Carvalho, I. P. C., Liu, J., et al. (2014). Investigation of a new acetogen isolated from an enrichment of the tammar wallaby forestomach. *BMC Microbiol.* 14:314. doi: 10.1186/s12866-014-0314-3

Gieg, L. M., Fowler, S. J., and Berdugo-Clavijo, C. (2014). Syntrophic biodegradation of hydrocarbon contaminants. *Curr. Opin. Biotechnol.* 27, 21–29. doi: 10.1016/j.copbio.2013.09.002

Greening, R. C., and Leedle, J. A. Z. (1989). Enrichment and isolation of Acetitomaculum ruminis, gen. Nov., sp. nov.: acetogenic bacteria from the bovine rumen. *Arch. Microbiol.* 151, 399–406. doi: 10.1007/BF00416597

GTDB (2020). Varibaculum timonense (Actinomycetaceae) reclassified to Urmitella timonensis (Tissierellaceae). GTDB. Available at: https://gtdb.ecogenomic.org/genomes?gid=GCF_900169515.1 (Accessed December 18, 2020).

Güllert, S., Fischer, M. A., Turaev, D., Noebauer, B., Ilmberger, N., Wemheuer, B., et al. (2016). Deep metagenome and metatranscriptome analyses of microbial communities affiliated with an industrial biogas fermenter, a cow rumen, and elephant feces reveal major differences in carbohydrate hydrolysis strategies. *Biotechnol. Biofuels* 9, 1–20. doi: 10.1186/s13068-016-0534-x

Hanreich, A., Heyer, R., Benndorf, D., Rapp, E., Pioch, M., Reichl, U., et al. (2012). Metaproteome analysis to determine the metabolically active part of a thermophilic microbial community producing biogas from agricultural biomass. *Can. J. Microbiol.* 58, 917–922. doi: 10.1139/w2012-058

Henderson, G., Leahy, S. C., and Janssen, P. H. (2010). Presence of novel, potentially homoacetogenic bacteria in the rumen as determined by analysis of formyltetrahydrofolate synthetase sequences from ruminants. *Appl. Environ. Microbiol.* 76, 2058–2066. doi: 10.1128/AEM.02580-09

Heyer, R., Benndorf, D., Kohrs, F., De Vrieze, J., Boon, N., Hoffmann, M., et al. (2016). Proteotyping of biogas plant microbiomes separates biogas plants according to process temperature and reactor type. *Biotechnol. Biofuels* 9:155. doi: 10.1186/s13068-016-0572-4

Heyer, R., Kohrs, F., Benndorf, D., Rapp, E., Kausmann, R., Heiermann, M., et al. (2013). Metaproteome analysis of the microbial communities in agricultural biogas plants. *New Biotechnol.* 30, 614–622. doi: 10.1016/j.nbt.2013.01.002

Hori, T., Sasaki, D., Haruta, S., Shigematsu, T., Ueno, Y., Ishii, M., et al. (2011). Detection of active, potentially acetate-oxidizing syntrophs in an anaerobic digester by flux measurement and formyltetrahydrofolate synthetase (FTHFS) expression profiling. *Microbiology* 157, 1980–1989. doi: 10.1099/mic.0.049189-0

Klang, J., Szewzyk, U., Bock, D., and Theuerl, S. (2019). Nexus between the microbial diversity level and the stress tolerance within the biogas process. *Anaerobe* 56, 8–16. doi: 10.1016/j.anaerobe.2019.01.003

Kleinsteuber, S. (2019). "Metagenomics of methanogenic communities in anaerobic digesters," in *Biogenesis of Hydrocarbons*. eds. A. J. M. Stams and D. Z. Sousa (Cham: Springer International Publishing), 337–359.

Kohrs, F., Heyer, R., Magnussen, A., Benndorf, D., Muth, T., Behne, A., et al. (2014). Sample prefractionation with liquid isoelectric focusing enables in depth microbial metaproteome analysis of mesophilic and thermophilic biogas plants. *Anaerobe* 29, 59–67. doi: 10.1016/j.anaerobe.2013.11.009

Kovács, K. L., Kovács, Á. T., Maróti, G., Bagi, Z., Csanádi, G., Perei, K., et al. (2004). Improvement of biohydrogen production and intensification of biogas formation. *Rev. Environ. Sci. Biotechnol.* 3, 321–330. doi: 10.1007/s11157-004-7460-2

Le Van, T. D., Robinson, J. A., Ralph, J., Greening, R. C., Smolenski, W. J., Leedle, J. A. Z., et al. (1998). Assessment of reductive acetogenesis with indigenous ruminal bacterium populations and Acetitomaculum ruminis. *Appl. Environ. Microbiol.* 64, 3429–3436. doi: 10.1128/AEM.64.9.3429-3436.1998

Leaphart, A. B., and Lovell, C. R. (2001). Recovery and analysis of formyltetrahydrofolate synthetase gene sequences from natural populations of acetogenic bacteria. *Appl. Environ. Microbiol.* 67, 1392–1395. doi: 10.1128/AEM.67.3.1392-1395.2001

Leigh, J. A., and Wolfe, R. S. (1983). Acetogenium kivui gen. Nov., sp. nov., a thermophilic acetogenic bacterium. *Int. J. Syst. Bacteriol.* 33:886. doi: 10.1099/00207713-33-4-886

Li, Z., Henderson, G., Yang, Y., and Li, G. (2017). Diversity of formyltetrahydrofolate synthetase genes in the rumens of roe deer (*Capreolus pygargus*) and sika deer (*Cervus nippon*) fed different diets. *Can. J. Microbiol.* 63, 11–19. doi: 10.1139/cjm-2016-0424

Luo, G., Fotidis, I. A., and Angelidaki, I. (2016). Comparative analysis of taxonomic, functional, and metabolic patterns of microbiomes from 14 full-scale biogas reactors by metagenomic sequencing and radioisotopic analysis. *Biotechnol. Biofuels* 9:51. doi: 10.1186/s13068-016-0465-6

Madsen, M., Holm-Nielsen, J. B., and Esbensen, K. H. (2011). Monitoring of anaerobic digestion processes: a review perspective. *Renew. Sust. Energ. Rev.* 15, 3141–3155. doi: 10.1016/j.rser.2011.04.026

Maus, I., Koeck, D. E., Cibis, K. G., Hahnke, S., Kim, Y. S., Langer, T., et al. (2016). Unraveling the microbiome of a thermophilic biogas plant by metagenome and metatranscriptome analysis complemented by characterization of bacterial and archaeal isolates. *Biotechnol. Biofuels* 9:171. doi: 10.1186/s13068-016-0581-3

McMurdie, P. J., and Holmes, S. (2013). Phyloseq: an R package for reproducible interactive analysis and graphics of microbiome census data. *PLoS One* 8:e61217. doi: 10.1371/journal.pone.0061217

Moestedt, J., Müller, B., Westerholm, M., and Schnürer, A. (2016). Ammonia threshold for inhibition of anaerobic digestion of thin stillage and the importance of organic loading rate. *Microb. Biotechnol.* 9, 180–194. doi: 10.1111/1751-7915.12330

Müller, B., Sun, L., Westerholm, M., and Schnürer, A. (2016). Bacterial community composition and fhs profiles of low- and high-ammonia biogas digesters reveal novel syntrophic acetate-oxidising bacteria. *Biotechnol. Biofuels* 9, 1–18. doi: 10.1186/s13068-016-0454-9

Navarro, R. R., Otsuka, Y., Matsuo, K., Sasaki, K., Sasaki, K., Hori, T., et al. (2020). Combined simultaneous enzymatic saccharification and

comminution (SESC) and anaerobic digestion for sustainable biomethane generation from wood lignocellulose and the biochemical characterization of residual sludge solid. *Bioresour. Technol.* 300:122622. doi: 10.1016/j.biortech.2019.122622

Nierychlo, M., Andersen, K. S., Xu, Y., Green, N., Jiang, C., Albertsen, M., et al. (2020). MiDAS 3: an ecosystem-specific reference database, taxonomy and knowledge platform for activated sludge and anaerobic digesters reveals species-level microbiome composition of activated sludge. *Water Res.* 182:115955. doi: 10.1016/j.watres.2020.115955

Niu, Q., Qiao, W., Qiang, H., and Li, Y.-Y. (2013). Microbial community shifts and biogas conversion computation during steady, inhibited and recovered stages of thermophilic methane fermentation on chicken manure with a wide variation of ammonia. *Bioresour. Technol.* 146, 223–233. doi: 10.1016/j.biortech.2013.07.038

Ohashi, Y., Igarashi, T., Kumazawa, F., and Fujisawa, T. (2007). Analysis of acetogenic bacteria in human feces with formyltetrahydrofolate synthetase sequences. *Biosci. Microflora* 26, 37–40. doi: 10.12938/bifidus.26.37

Oksanen, J., Blanchet, F. G., Friendly, M., Kindt, R., Legendre, P., McGlinn, D., et al. (2019). *Vegan*: Community Ecology Package. Version 2.5–6; Comprehensive R Archive Network (CRAN). Available at: https://cran.r-project.org/package=vegan

Oren, A., and Garrity, G. (2020). List of new names and new combinations previously effectively, but not validly, published. *Int. J. Syst. Evol. Microbiol.* 70, 4043–4049. doi: 10.1099/ijsem.0.004244

Ortseifen, V., Stolze, Y., Maus, I., Sczyrba, A., Bremges, A., Albaum, S. P., et al. (2016). An integrated metagenome and -proteome analysis of the microbial community residing in a biogas production plant. *J. Biotechnol.* 231, 268–279. doi: 10.1016/j.jbiotec.2016.06.014

Patakova, P., Branska, B., Sedlar, K., Vasylkivska, M., Jureckova, K., Kolek, J., et al. (2019). Acidogenesis, solventogenesis, metabolic stress response and life cycle changes in Clostridium beijerinckii NRRL B-598 at the transcriptomic level. *Sci. Rep.* 9:1371. doi: 10.1038/s41598-018-37679-0

Pelletier, E., Kreimeyer, A., Bocs, S., Rouy, Z., Gyapay, G., Chouari, R., et al. (2008). "*Candidatus* Cloacamonas acidaminovorans": genome sequence reconstruction provides a first glimpse of a new bacterial division. *J. Bacteriol.* 190, 2572–2579. doi: 10.1128/JB.01248-07

Pester, M., and Brune, A. (2006). Expression profiles of *fhs* (FTHFS) genes support the hypothesis that spirochaetes dominate reductive acetogenesis in the hindgut of lower termites. *Environ. Microbiol.* 8, 1261–1270. doi: 10.1111/j.1462-2920.2006.01020.x

Poirier, S., Déjean, S., Midoux, C., Lê Cao, K.-A., and Chapleur, O. (2020). Integrating independent microbial studies to build predictive models of anaerobic digestion inhibition by ammonia and phenol. *Bioresour. Technol.* 316:123952. doi: 10.1016/j.biortech.2020.123952

R Core Team (2013). R: A Language and Environment for Statistical Computing. R Foundation for Statistical Computing; Vienna, Austria. Available at: http://www.r-project.org

Robles, G., Nair, R. B., Kleinsteuber, S., Nikolausz, M., and Sárvári Horváth, I. (2018). "Biogas production: microbiological aspects," in *Biogas: Fundamentals, Process, and Operation*. eds. M. Tabatabaei and H. Ghanavati (Cham: Springer International Publishing), 163–198.

Roos, S., Engstrand, L., and Jonsson, H. (2005). Lactobacillus gastricus sp. nov., lactobacillus antri sp. nov., lactobacillus kalixensis sp. nov. and lactobacillus ultunensis sp. nov., isolated from human stomach mucosa. *Int. J. Syst. Evol. Microbiol.* 55, 77–82. doi: 10.1099/ijs.0.63083-0

RStudio Team (2020). RStudio: Integrated Development Environment for R. Boston, MA: RStudio, PBC. Available at: http://www.rstudio.com/

Saheb-Alam, S., Singh, A., Hermansson, M., Persson, F., Schnürer, A., Wilén, B.-M., et al. (2017). Effect of start-up strategies and electrode materials on carbon dioxide reduction on biocathodes. *Appl. Environ. Microbiol.* 84, e02242–e02317. doi: 10.1128/AEM.02242-17

Schlüter, A., Bekel, T., Diaz, N. N., Dondrup, M., Eichenlaub, R., Gartemann, K.-H., et al. (2008). The metagenome of a biogas-producing microbial community of a production-scale biogas plant fermenter analysed by the 454-pyrosequencing technology. *J. Biotechnol.* 136, 77–90. doi: 10.1016/j.jbiotec.2008.05.008

Schnürer, A. (2016). "Biogas production: microbiology and technology," in *Advances in Biochemical Engineering/Biotechnology*. eds. R. Hatti-Kaul, G. Mamo and B. Mattiasson (Cham: Springer International Publishing), 195–234.

Schnürer, A., Houwen, F. P., and Svensson, B. H. (1994). Mesophilic syntrophic acetate oxidation during methane formation by a triculture at high ammonium concentration. *Arch. Microbiol.* 162, 70–74. doi: 10.1007/BF00264375

Schnürer, A., and Jarvis, Å. (2017). Microbiology of the Biogas Process. Swedish University of Agricultural Sciences. Available at: https://www.researchgate.net/publication/327388476_Microbiology_of_the_biogas_process

Schnürer, A., and Nordberg, Å. (2008). Ammonia, a selective agent for methane production by syntrophic acetate oxidation at mesophilic temperature. *Water Sci. Technol.* 57, 735–740. doi: 10.2166/wst.2008.097

Schnürer, A., Schink, B., and Svensson, B. H. (1996). *Clostridium ultunense* sp. nov., a mesophilic bacterium oxidizing acetate in syntrophic association with a hydrogenotrophic methanogenic bacterium. *Int. J. Syst. Bacteriol.* 46, 1145–1152. doi: 10.1099/00207713-46-4-1145

Sekiguchi, Y., Imachi, H., Susilorukmi, A., Muramatsu, M., Ohashi, A., Harada, H., et al. (2006). Tepidanaerobacter syntrophicus gen. Nov., sp. nov., an anaerobic, moderately thermophilic, syntrophic alcohol- and lactate-degrading bacterium isolated from thermophilic digested sludges. *Int. J. Syst. Evol. Microbiol.* 56, 1621–1629. doi: 10.1099/ijs.0.64112-0

Sekiguchi, Y., Kamagata, Y., Nakamura, K., Ohashi, A., and Harada, H. (2000). Syntrophothermus lipocalidus gen. Nov., sp. nov., a novel thermophilic, syntrophic, fatty-acid-oxidizing anaerobe which utilizes isobutyrate. *Int. J. Syst. Evol. Microbiol.* 50, 771–779. doi: 10.1099/00207713-50-2-771

Singh, A. (2020). Genomic DNA Extraction From Anaerobic Digester Samples. protocols.io. doi: 10.17504/protocols.io.bgxkjxkw.

Singh, A. (2021). Microbiological Surveillance of Biogas Plants: Focusing on the Acetogenic Community. Available at: https://pub.epsilon.slu.se/22699/

Singh, A., Müller, B., Fuxelius, H.-H., and Schnürer, A. (2019). AcetoBase: a functional gene repository and database for formyltetrahydrofolate synthetase sequences. *Database* 2019:baz142. doi: 10.1093/database/baz142

Singh, A., Müller, B., and Schnürer, A. (2021a). Profiling temporal dynamics of acetogenic communities in anaerobic digesters using next-generation sequencing and T-RFLP. *Sci. Rep.* 11:13298. doi: 10.1038/s41598-021-92658-2

Singh, A., Nylander, J. A. A., Schnürer, A., Bongcam-Rudloff, E., and Müller, B. (2020). High-throughput sequencing and unsupervised analysis of formyltetrahydrofolate synthetase (FTHFS) gene amplicons to estimate acetogenic community structure. *Front. Microbiol.* 11:2066. doi: 10.3389/fmicb.2020.02066

Singh, A., Schnürer, A., and Westerholm, M. (2021b). Enrichment and description of novel bacteria performing syntrophic propionate oxidation at high ammonia level. *Environ. Microbiol.* 23, 1620–1637. doi: 10.1111/1462-2920.15388

Sousa, D. Z., Smidt, H., Madalena Alves, M., and Stams, A. J. M. (2007). Syntrophomonas zehnderi sp. nov., an anaerobe that degrades long-chain fatty acids in co-culture with Methanobacterium formicicum. *Int. J. Syst. Evol. Microbiol.* 57, 609–615. doi: 10.1099/ijs.0.64734-0

Theuerl, S., Klang, J., and Prochnow, A. (2019). Process disturbances in agricultural biogas production—causes, mechanisms and effects on the biogas microbiome: a review. *Energies* 12:365. doi: 10.3390/en12030365

Town, J. R., and Dumonceaux, T. J. (2016). Laboratory-scale bioaugmentation relieves acetate accumulation and stimulates methane production in stalled anaerobic digesters. *Appl. Microbiol. Biotechnol.* 100, 1009–1017. doi: 10.1007/s00253-015-7058-3

Town, J. R., Links, M. G., Fonstad, T. A., and Dumonceaux, T. J. (2014). Molecular characterization of anaerobic digester microbial communities identifies microorganisms that correlate to reactor performance. *Bioresour. Technol.* 151, 249–257. doi: 10.1016/j.biortech.2013.10.070

Treu, L., Kougias, P. G., Campanaro, S., Bassani, I., and Angelidaki, I. (2016). Deeper insight into the structure of the anaerobic digestion microbial community; the biogas microbiome database is expanded with 157 new genomes. *Bioresour. Technol.* 216, 260–266. doi: 10.1016/j.biortech.2016.05.081

UGC (2018). Next Generation Sequencing at Uppsala Genome Center (UGC). Uppsala: Uppsala Genome Center, Science for Life Lab; Sweden. Available at: https://www.scilifelab.se

van der Zaan, B. M., Saia, F. T., Stams, A. J. M., Plugge, C. M., de Vos, W. M., Smidt, H., et al. (2012). Anaerobic benzene degradation under denitrifying conditions: peptococcaceae as dominant benzene degraders and evidence for a syntrophic process. *Environ. Microbiol.* 14, 1171–1181. doi: 10.1111/j.1462-2920.2012.02697.x

Ward, A. J., Hobbs, P. J., Holliman, P. J., and Jones, D. L. (2008). Optimisation of the anaerobic digestion of agricultural resources. *Bioresour. Technol.* 99, 7928–7940. doi: 10.1016/j.biortech.2008.02.044

Westerholm, M., Müller, B., Arthurson, V., and Schnürer, A. (2011a). Changes in the acetogenic population in a mesophilic anaerobic digester in response to increasing ammonia concentration. *Microbes Environ.* 26, 347–353. doi: 10.1264/jsme2.ME11123

Westerholm, M., Müller, B., Singh, A., Karlsson Lindsjö, O., and Schnürer, A. (2018). Detection of novel syntrophic acetate-oxidizing bacteria from biogas processes by continuous acetate enrichment approaches. *Microb. Biotechnol.* 11, 680–693. doi: 10.1111/1751-7915.13035

Westerholm, M., Roos, S., and Schnürer, A. (2011b). *Tepidanaerobacter acetatoxydans* sp. nov., an anaerobic, syntrophic acetate-oxidizing bacterium isolated from two ammonium-enriched mesophilic methanogenic processes. *Syst. Appl. Microbiol.* 34, 260–266. doi: 10.1016/j.syapm.2010.11.018

Wirth, R., Böjti, T., Lakatos, G., Maróti, G., Bagi, Z., Rákhely, G., et al. (2019). Characterization of core microbiomes and functional profiles of mesophilic anaerobic digesters fed with *Chlorella vulgaris* green microalgae and maize silage. *Front. Energy Res.* 7:111. doi: 10.3389/fenrg.2019.00111

Wolf, C., McLoone, S., and Bongards, M. (2009). Biogas plant control and optimization using computational intelligence methods (biogasanlagenregelung und -optimierung mit computational intelligence methoden). *Automatisierungstechnik* 57, 638–649. doi: 10.1524/auto.2009.0809

Yang, C.-L., Guan, L.-L., Liu, J.-X., and Wang, J.-K. (2015). Rumen fermentation and acetogen population changes in response to an exogenous acetogen TWA4 strain and *Saccharomyces cerevisiae* fermentation product. *J Zhejiang Univ Sci B* 16, 709–719. doi: 10.1631/jzus.B1500013

Yoshida, K., and Shimizu, N. (2020). Biogas production management systems with model predictive control of anaerobic digestion processes. *Bioprocess Biosyst. Eng.* 43, 2189–2200. doi: 10.1007/s00449-020-02404-7

Zhang, C., Liu, X., and Dong, X. (2004). Syntrophomonas curvata sp. nov., an anaerobe that degrades fatty acids in co-culture with methanogens. *Int. J. Syst. Evol. Microbiol.* 54, 969–973. doi: 10.1099/ijs.0.02903-0

Zhang, L., Mou, A., Guo, B., Sun, H., Anwar, M. N., and Liu, Y. (2021). Simultaneous phosphorus recovery in energy generation reactor (SPRING): high rate thermophilic Blackwater treatment. *Resour. Conserv. Recycl.* 164:10516. doi: 10.1016/j.resconrec.2020.105163

Zhuang, L., Tang, J., Wang, Y., Hu, M., and Zhou, S. (2015). Conductive iron oxide minerals accelerate syntrophic cooperation in methanogenic benzoate degradation. *J. Hazard. Mater.* 293, 37–45. doi: 10.1016/j.jhazmat.2015.03.039

Conflict of Interest: The authors declare that the research was conducted in the absence of any commercial or financial relationships that could be construed as a potential conflict of interest.

Publisher's Note: All claims expressed in this article are solely those of the authors and do not necessarily represent those of their affiliated organizations, or those of the publisher, the editors and the reviewers. Any product that may be evaluated in this article, or claim that may be made by its manufacturer, is not guaranteed or endorsed by the publisher.

frontiers in Microbiology

ORIGINAL RESEARCH
published: 03 September 2021
doi: 10.3389/fmicb.2021.658494

Bioaugmented Mixed Culture by *Clostridium aceticum* to Manipulate Volatile Fatty Acids Composition From the Fermentation of Cheese Production Wastewater

Merve Atasoy and Zeynep Cetecioglu*

Department of Chemical Engineering, KTH Royal Institute of Technology, Stockholm, Sweden

Production of targeted volatile fatty acid (VFA) composition by fermentation is a promising approach for upstream and post-stream VFA applications. In the current study, the bioaugmented mixed microbial culture by *Clostridium aceticum* was used to produce an acetic acid dominant VFA mixture. For this purpose, anaerobic sequencing batch reactors (bioaugmented and control) were operated under pH 10 and fed by cheese processing wastewater. The efficiency and stability of the bioaugmentation strategy were monitored using the production and composition of VFA, the quantity of *C. aceticum* (by qPCR), and bacterial community profile (16S rRNA Illumina Sequencing). The bioaugmented mixed culture significantly increased acetic acid concentration in the VFA mixture (from 1170 ± 18 to 122 ± 9 mgCOD/L) compared to the control reactor. Furthermore, the total VFA production (from 1254 ± 11 to 5493 ± 36 mgCOD/L) was also enhanced. Nevertheless, the bioaugmentation could not shift the propionic acid dominancy in the VFA mixture. The most significant effect of bioaugmentation on the bacterial community profile was seen in the relative abundance of the *Thermoanaerobacterales Family III*. *Incertae sedis,* its relative abundance increased simultaneously with the gene copy number of *C. aceticum* during bioaugmentation. These results suggest that there might be a syntropy between species of *Thermoanaerobacterales Family III*. *Incertae sedis* and *C. aceticum.* The cycle analysis showed that 6 h (instead of 24 h) was adequate retention time to achieve the same acetic acid and total VFA production efficiency. Biobased acetic acid production is widely applicable and economically competitive with petroleum-based production, and this study has the potential to enable a new approach as produced acetic acid dominant VFA can replace external carbon sources for different processes (such as denitrification) in WWTPs. In this way, the higher treatment efficiency for WWTPs can be obtained by recovered substrate from the waste streams that promote a circular economy approach.

Keywords: volatile fatty acid, acetic acid, *Clostridium aceticum*, bioaugmentation, bacterial community profile, qPCR, cheese production wastewater, fermentation

OPEN ACCESS

Edited by:
Hyung-Sool Lee,
University of Waterloo, Canada

Reviewed by:
Yi Wang,
Auburn University, United States
Po-Heng Lee,
Imperial College London,
United Kingdom

****Correspondence:***
Merve Atasoy
mervea@kth.se

Specialty section:
This article was submitted to Microbiotechnology, a section of the journal Frontiers in Microbiology

Received: *08 February 2021*
Accepted: *30 June 2021*
Published: *03 September 2021*

Citation:
Atasoy M and Cetecioglu Z (2021) Bioaugmented Mixed Culture by Clostridium aceticum to Manipulate Volatile Fatty Acids Composition From the Fermentation of Cheese Production Wastewater. Front. Microbiol. 12:658494. doi: 10.3389/fmicb.2021.658494

INTRODUCTION

The current size of global chemical production is unknown. In Europe, it was 330 million tons in 2007 (Eurostat, 2020), and is increasing by a 7% compound annual growth rate (UNEP, 2013) to meet the demands for industrial, agricultural, pharmaceutical applications. On the other hand, the adverse environmental effects of petroleum based production have resulted in an increase of CO_2 emissions from two billion tons to over 36 billion tons in the last 115 years (Ritchie and Roser, 2019). Therefore, sustainable, environmentally friendly, and economically competitive bioproduction is a vital method in achieving Sustainable Development Goals (United Nations, 2018) and the targets of the Paris Agreement, (UNFCCC, 2015). One of the crucial methods of attaining sustainable bioproduction is transforming traditional wastewater treatment plants into biorefineries, that use waste streams as feedstock (Dietrich et al., 2017; Mussatto, 2017).

Several studies for biobased chemical production from waste streams have been conducted in recent years (Lu et al., 2019; Xie et al., 2019). Foremost among them, volatile fatty acid (VFA) is one of the most promising products because of its versatile usage area in post stream and upstream applications (Khan et al., 2016b; Atasoy et al., 2018). Nevertheless, low production efficiency, unstable VFA composition for upstream and post stream applications, complications in purification, and separation of the end products, post-process requirements, and high substrate cost, etc., limit the industrialisation of biobased VFA production. Various studies have been carried out to enhance biobased VFA production efficiency by optimizing operational and environmental conditions (Khan et al., 2016a; Bhatia and Yang, 2017; Atasoy et al., 2018; Fang et al., 2020). These studies showed that different parameters such as pH, temperature, retention time, loading rate, reactor type, and mixing, etc., must be taken into account for efficient biobased VFA production.

The end product spectrum of VFA is another crucial factor in post stream and upstream applications. For example, acetic acid dominant VFA as a carbon source achieved the highest polyhydroxyalkanoates (PHA) production yield (Ciesielski and Przybylek, 2014; Kedia et al., 2014) and acetic acid has been used as an efficient carbon source for denitrification processes (Du et al., 2019). Furthermore, every industry has different feedstock requirements, for example, acetic acid has been extensively used in the polymer industry for the production of vinyl acetate monomer (Gunjan and Haresh, 2020). Thus, enhancement of specific acid concentration in the VFA mixture is preferred for easier separation/purification of the end product. For these reasons, the efficient and sustainable production of the desired acid composition is one of the primary research problems that need to be addressed in the commercialization of biobased VFA production. Therefore, the current study aimed to develop acetic acid dominant VFA mixture production.

Acetic acid comprises a large part of the VFAs market (Bhatia and Yang, 2017) and has been used as a vinyl acetate monomer, purified terephthalic acid, acetate esters, acetic anhydride in several industries such as chemical, food and beverage, inks, paints, and coatings, etc., (Vidra and Németh, 2018; Allied Market Research, 2020). The global acetic acid market is estimated to reach 20.3 million tons by 2024 (Expert Market Research, 2019). Nevertheless, more than 90% of acetic acid is produced synthetically (Atasoy et al., 2018). In several wastewater treatment plants, acetic acid has been used as a carbon source in the denitrification process (Mielcarek et al., 2018; Du et al., 2019). However, this acetic acid is mostly bought externally, which is obtained by petroleum-based methods. Furthermore, biobased acetic acid is approved and generally recognized as safe (GRAS) by the United States Food and Drug Administration (FDA, 1989) and has been preferred as a food additive (Younes et al., 2020). In this sense, biobased acetic acid production is essential to achieve sustainable and environmentally friendly chemical production. Accordingly, the current study aimed to produce an acetic acid dominant VFA mixture by the application of a bioaugmentation strategy.

Recent studies suggested that bioaugmentation is a successful strategy to not only enhance microbial community performance for obtaining desired products (Tang et al., 2019; Atasoy and Cetecioglu, 2020; Li et al., 2020; Wu et al., 2020) but also improve the microbial community and their interactions for better adaptations to various environmental conditions (Tabatabaei et al., 2020). Bioaugmentation is a promising approach by adding microorganisms externally to the existing microbial community for improving the degradation rate of the contaminants (Cirne et al., 2006), enhancing the production efficiency of specific products (Chi et al., 2018; Tabatabaei et al., 2020), reducing the inhibition effects of some substances in the process (Yang et al., 2019), which has been used to find a solution for several practical issues in wastewater treatment plants (Herrero and Stuckey, 2015; Hong et al., 2020). Yang et al. (2019) investigated the effects of bioaugmentation with several pure cultures on anaerobic digestion to improve biogas production *via* preventing ammonia inhibition (Yang et al., 2019). In anaerobic digestion, the microbial community is comprised of undefined mixed culture, which is robust and easy for operation; nevertheless, monoculture produces a specific product. Therefore, bioaugmentation is a promising strategy for developing a new microbial consortium for strong, higher productivity and open for manipulation to produce targeted product profiles.

Clostridium aceticum is the first isolated acetogen from soil, found by Wieringa in 1936 (Küsel and Drake, 2011). It is a well-known acetic acid producer bacteria (Braun et al., 1981). *C. aceticum* is strictly anaerobic and can grow both autotrophically and heterotopically (Poehlein et al., 2015). Because of its versatile growth ability, *C. aceticum* has been widely used for acetic acid production (Sim et al., 2007; Arslan et al., 2019; Riegler et al., 2019). In our previous study, we used *C. aceticum* for acetic acid production from semi-synthetic milk processing wastewater fermentation under alkali pH (Atasoy et al., 2020a). Therefore, *C. aceticum* is selected as pure culture in the current study to bioaugment mixed microbial culture for acetic acid dominant VFA mixture.

Although different types of waste streams have been used for acetic acid production *via* fermentation, one of the most promising waste streams comes from dairy industry, which

has a massive wastewater production volume (Hansen, 1974) with a rich carbohydrate, protein, and fat content (Britz and van Schalkwyk, 2006). Lagoa-Costa et al. (2020) showed that cheese whey has great potential for VFA production as a substrate because it includes more than 90% of easily degradable compounds. Their results stated that acetic acid concentration in VFA mixture from cheese whey fermentation at acidogenic pH was almost similar under different retention times, food/microorganism (F/M) ratios, and sludge retention times (SRTs), despite the degree of acidification and the acidification yield was changed under different conditions. On the other hand, Jankowska et al. (2017) showed the effects of various pH on VFA composition from cheese whey fermentation: acetic acid production was around 20% under acidic pH and approximately 40% without pH adjustment (neutral pH), whereas, it was more than 91% under alkali pH (Jankowska et al., 2017). Atasoy et al. (2019a) stated that higher acetic acid concentration was obtained from the monoculture (*C. aceticum*) (743 mg COD/L) than mixed culture (541 mg COD/L) from milk processing wastewater fermentation under alkali pH (Atasoy et al., 2019a). As previously stated, various waste streams as substrate provide an excellent opportunity for acetic acid and VFA production *via* fermentation. Nevertheless, further studies are required to increase the production yield for economically competitive and sustainable VFA production from waste streams.

In the current study, enhancement of acetic acid in VFA mixture was aimed by bioaugmentation. With this approach, the produced acetic acid dominant VFA mixture could be used in different processes (such as denitrification) as a carbon source to achieve a circular economy approach in WWTPs. In this regard, the mixed culture is bioaugmented by *C. aceticum*. Cheese production wastewater was used as a substrate to integrate the bioaugmentation strategy into industrial waste streams. The long term ASBR was operated under alkali pH to investigate the effects of the bioaugmentation. The bacterial community profile was analyzed by 16S rRNA sequencing and *C. aceticum* was quantified by quantitative real-time polymerase chain reaction (qPCR). Cycle analysis was also conducted to investigate the effects of bioaugmentation on acid composition.

MATERIALS AND METHODS

Substrate and Inoculum

Cheese production wastewater was used as a substrate in all reactors. The wastewater was taken from the cheese production industry, which is located in Sweden. The wastewater included 20000 ± 60 mg COD/L, 200 mg/L total nitrogen, 18 mg/L total phosphate, and 11 mg/L orthophosphate. The wastewater contained 14.26 ± 6 mg COD/L VFA and 0.22 ± 0.08 mg COD/L lactic acid. The medium, vitamin, and trace element solutions were prepared according to the OECD 311 (OECD, 2003) and used for pure culture incubation. The medium and trace element solution was autoclaved separately for 30 min at 121°C. The vitamin solution was also filtered through a membrane filter with a 0.22 μm pore size filter for sterilization.

Mixed Culture

The granular seed sludge (≈3.5 mm with 43% total solids (TS) and volatile solids (VS) 30%) were used as a mixed culture, which was collected from the UASB reactor at Hammarby Sjöstadsverk Pilot Plant, Stockholm, Sweden. It was stored at +4°C until the experiments were set up. The detailed characterization of granular seed sludge was described by Atasoy et al. (2019b).

Monoculture

The bioaugmentation of mixed culture was applied by *C. aceticum* (No. 1496, DSMZ, Germany) to enhance acetic acid production in mixed culture fermentation. The monoculture was grown in YPD Liquid Media (VWR Life Science, Sweden) at 32.5°C in an incubator with 120 rpm mixing for 36 h under anaerobic conditions. Before bioaugmentation, the monoculture was cultivated with the substrate to observe and evaluate their growth and interactions. The growth of monoculture was observed by using OD600. The pure culture from the actively growing culture (the OD600 was 2.0) was used for bioaugmentation. In addition, approximately 50 mL (aliquoted 5 mL) of pure culture was stored in glycerol (50% as volume) at −80°C for further usage.

Reactor Design and Operation

The AMPTS II System (Bioprocess Control, Sweden) was used for an anaerobic sequencing batch reactor which had 1400 mL active volume, 2000 mL total volume. The reactors were operated by cycling through a sequence of four phases in a single reaction vessel, the detailed operation of the reactors was presented in **Figure 1**. The system was mixed continuously at 120 rpm under 35°C and pH 10 ± 0.5, which was adjusted using 2 M NaOH.

The reactors were fed in a stepwise manner with different organic loading rates (OLR) which are explained in detail in Atasoy et al. (2020a). In steady-state conditions (based on influent and effluent chemical oxygen demand (COD) concentrations), the bioaugmentation was applied with a 0.6 F/M ratio. The SRT was 35 days, calculated according to the VS loss during decanting. The hydraulic retention time (HRT) was 3.5 days.

Cycle Analysis

The cycle analysis was conducted to observe the bioaugmentation effects on VFA composition shift during a cycle, which was carried out after 7 days the bioaugmentation was completed in each reactor. The samples were taken in each hour during one cycle (24 h) as well as before (−1st hour) and after feeding (0th hour).

Bioaugmentation Strategy

The bioaugmentation strategy was applied as explained by Atasoy and Cetecioglu (2020). It included three main phases; Phase A: before bioaugmentation (steady-state conditions based on COD concentration), Phase B: during bioaugmentation (the monoculture was added to the bioaugmented reactor in each cycle for 7 days as 10% of the reactor volume), and Phase C: after bioaugmentation (the reactors were operated for two sludge ages to observe the growth of monoculture in mixed culture).

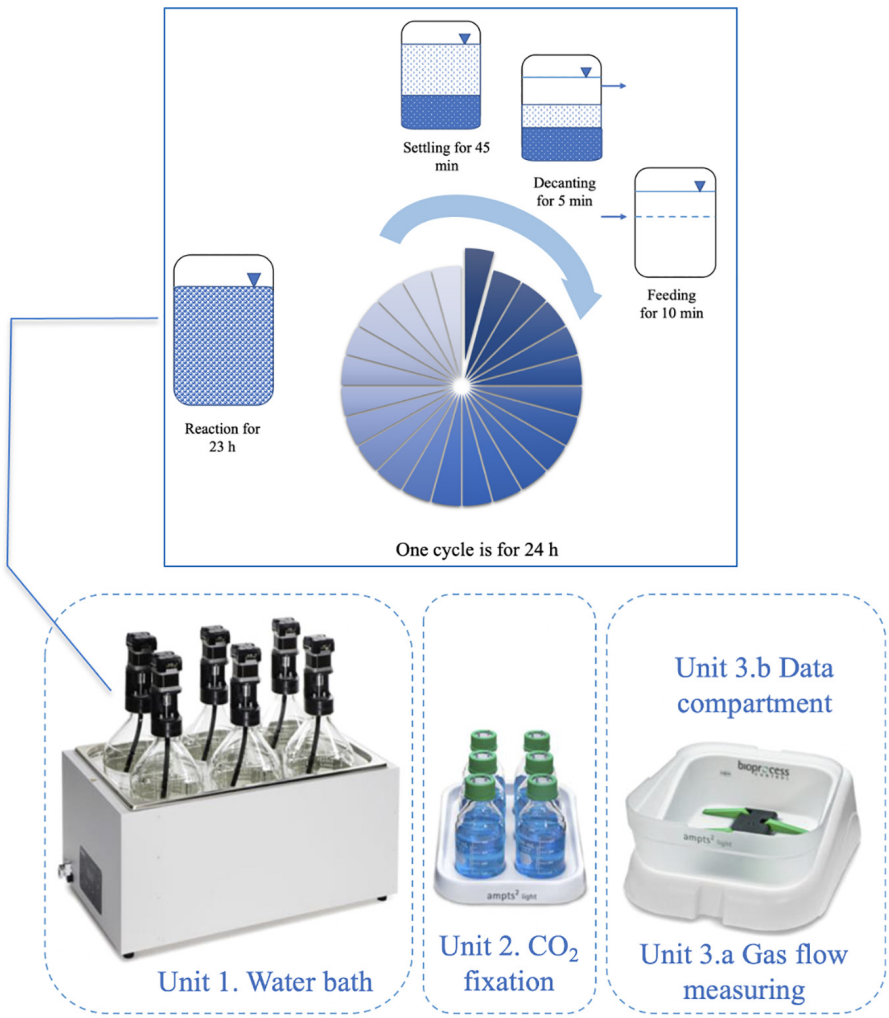

FIGURE 1 | The AMPTS II System (Bioprocess Control, Sweden) for anaerobic sequencing batch reactors and detailed operation regime.

Analytical Methods

During the whole operation, Total COD (TCOD), soluble COD (SCOD), organic acids, VFA compositions, and pH were monitored in both influent and effluent of the reactor. The COD equivalent of each VFA was calculated to validate the mass balances derived. The SCOD/TCOD, organic acids, total Nitrogen, and Phosphorus were measured using LCK 514 COD (100–2000 mg/L), organic acids LCK 365 Organic Acids (50–2500 mg/L), LCK 238 total Nitrogen (5–40 mg/L TN), and LCK 348 Phosphate (Orto + total) (0.5–5 mg /LPO4 – P) (Hach Lange, United States) cuvette tests by Hach Lange DR 3900 spectrophotometer. Also, TS and VS of the sludge were measured according to the Standard Methods (APHA et al., 2012). The concentration and composition of VFA (formic, acetic, butyric, propionic, valeric, isovaleric, hexanoic, and heptanoic acids) in the effluents were analyzed by gas chromatography (GC 6890, Agilent) with a flame ionization detector, as described in the previous study (Atasoy et al., 2019b). Biomethane production (BMP) was monitored during operation, nevertheless, a negligible amount of biomethane was produced because of alkali pH. Therefore, the biomethane data did not present in the results. During and after the feeding of the reactors, the reactors flushed with nitrogen gas to enable anaerobic conditions.

Bacterial Community Analysis

The bacterial community profile was analyzed by 16S rRNA gene sequencing. Total genomic DNA from 0.5 g samples with three replicates were isolated using NucleoSpin Soil Kit, (Macherey-Nagel, Germany) following the manufacturer's instructions. The bacterial 16S rRNA gene was amplified using primers 516F (5′ to 3′: TGC CAG CAG CCG CGG TAA) and 806R (5′ to 3′: GGA CTA CHV GGG TWT CTA AAT) (Caporaso et al., 2011; Klindworth et al., 2013). The PCR amplification conditions, purification and quantification of the PCR products, and preparation of the sequencing libraries were followed by Atasoy et al. (2019b). The samples were sequenced using the Illumina MiSeq platform by Science for Life Laboratory, the

National Genomics Infrastructure, NGI (Sweden). Biophyton 1.78 was used to merge and quality filter the sequence data as well as to assign taxonomies at 97% similarity cut-off value (Cock et al., 2009). Raw sequence data is available at NCBI (project no. of PRJNA667606).

Quantification of *Clostridium aceticum*

The *C. aceticum* was quantified by using quantitative real-time polymerase chain reaction (qPCR) by using total genomic DNA. For the DNA extraction, 0.5 g samples as triplicate were isolated by using NucleoSpin Soil Kit, (Macherey-Nagel, Germany). The concentration of the extracted DNA was measured by fluorimetry using Qubit dsDNA HS Assay Kit (Invitrogen, Thermo Fisher Scientific, North America).

Quantitative real-time polymerase chain reaction was performed by using Applied Biosystems® QuantStudio® 3 Real-Time PCR System Thermo Fisher Scientific (United States). For each PCR run with PowerUp SYBR Green Master Mix, Applied Biosystems (Thermo Fisher Scientific Co., United States) detection, a melting curve analysis was performed to confirm the specificity in each reaction tube by the absence of primer-dimers and other nonspecific products. Reactions for all samples were shown to have only one melting peak, which indicated a specific amplification, making it suitable for accurate quantification. Controls were included for each PCR run during the analyses. At the end of the reactions, melting curve analyses were applied to confirm the absence of primer dimers and nonspecific products.

The primer for the quantification of *C. aceticum* sets targeting formyltetrahydrofolate synthetase gene (fhs) fhs1 (GTW TGG GCW AAR GGY GGM GAA GG) and fhs2 (GAR GAY GGW TTT GAY ATY AC) (Xu et al., 2009). Although fhs gene encoding 10-formylte- tetrahydrofolate synthetase is used for quantification of authentic acetogenic bacteria (De Vrieze and Verstraete, 2016), it was used to quantify *C. aceticum* in the current study, since the bioaugmentation was applied by using a specific strain. Standard curves were obtained for QPCR constructed from PCR products of *C. aceticum* by using a 10-fold dilution series, separately. Standard curves were constructed in each PCR run, and the copy numbers of the genes in each sample were interpolated using these standard curves.

Calculation of Products Yield

Acetic acid production yield (Y_{acetic}) (Eq. 1) and total VFA production yield (Y_{VFA}) (Eq. 2) were calculated as the ratio of acid concentration to the consumed COD concentration (Jankowska et al., 2017; Atasoy et al., 2020a).

$$Y_{acetic} = \frac{C_{acetic}}{C_{CODconsumed}} \quad (1)$$

$$Y_{VFA} = \frac{C_{VFA}}{C_{CODconsumed}} \quad (2)$$

where, C_{acetic} is the acetic acid concentration (g COD/L) in the effluent, C_{VFA} is the total VFA concentration (g COD/L) in the effluent and $C_{COD\,consumed}$ is the consumed COD concentration (g COD/L).

Statistical Analysis

All experiments were conducted in triplicate, the standard deviation of the average results was calculated. Additionally, Pearson's correlation analysis was conducted to identify the relationship between the quantification of monocultures and each acid type production. All statistical analysis was performed using IBM SPSS Statistics, Version 25.0.

RESULTS AND DISCUSSION

The effects of bioaugmentation on both the acetic acid production efficiency and total VFA production and acid composition were evaluated, separately. The assessment of acetic acid production efficiency was performed based on acetic acid concentration and quantification of *C. aceticum,* before, during and after the bioaugmentation. Additionally, the quantification of *C. aceticum* was correlated with the concentration of each acid type to investigate the effects of bioaugmentation regarding VFA composition from the mixed culture fermentation. Also, the cycle analysis to observe the shift of acids type during a cycle (24-h) was conducted.

Acetic Acid Dominant VFA Production

The acetic acid concentration in the bioaugmented and the control reactor with the gene copy number of the *C. aceticum* is represented in **Figure 2**, regarding before bioaugmentation (Phase A), during bioaugmentation (Phase B), and after bioaugmentation (Phase C). The average acetic acid concentration before bioaugmentation (Phase A) was 88 ± 23 mg COD/L in the bioaugmented reactor, while it was 96 ± 29 mg COD/L in the control reactor. During bioaugmentation (Phase B), the concentration was 287 ± 102 mg COD/L in the bioaugmented reactor, 156 ± 43 mg COD/L in the control reactor. After bioaugmentation was completed, the acetic acid concentration increased to 836 ± 261 mg COD/L in the bioaugmented reactor, while it was 200 ± 87 mg COD/L in the control reactor. The results showed that the average acetic acid production was increased almost four times by bioaugmentation of *C. aceticum.* The maximum acetic acid production was 1170 ± 18 mg COD/L at day 63 in the bioaugmented reactor; it was 122 ± 9 mg COD/L in the control reactor. Based on the maximum acetic acid production, the concentration increased by almost 10 times in the bioaugmented reactor than in the control reactor.

The effects of bioaugmentation on acetic acid production were evaluated based on the literature studies as summarized in **Table 1**. For instance, Lagoa-Costa et al. (2020) used cheese whey for VFA production from acidogenic fermentation under different retention times and F/M ratios. In their study, the highest acetic acid concentration was obtained as 3580 mg COD/L from 55000 mg COD/L substrate concentration, regardless of operational parameters (Lagoa-Costa et al., 2020). In another study, the highest acetic acid concentration (5500 ± 70 mg COD/L) was obtained by lettuce fermentation (SCOD content of substrate was 35700 mg COD/L) under acidic pH (6 ± 0.4) from the evaluation of VFA production

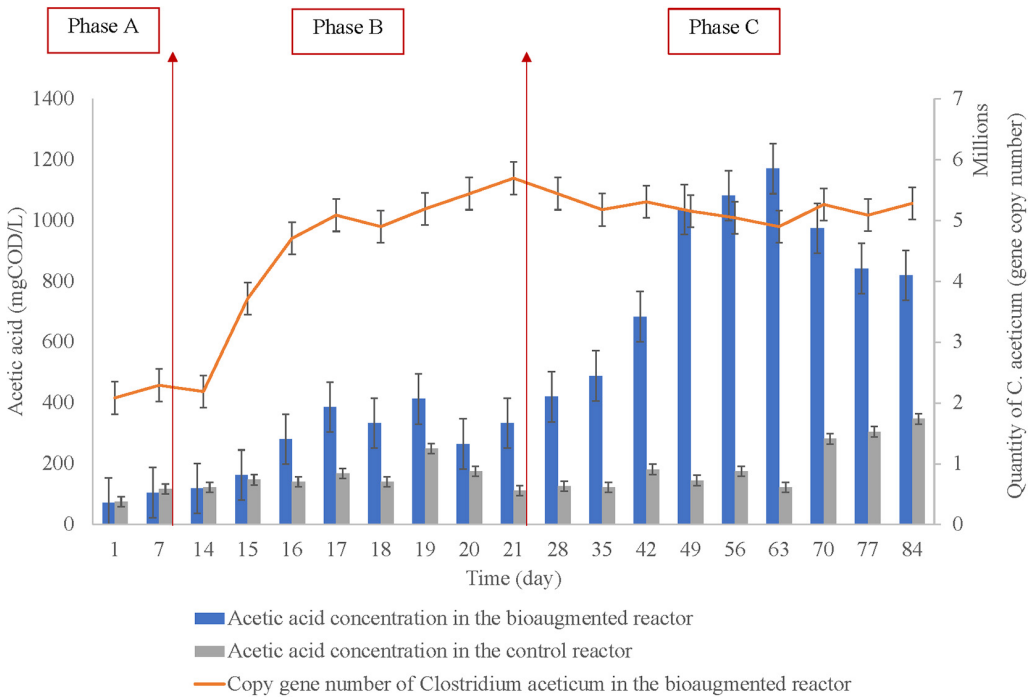

FIGURE 2 | The acetic acid concentration in the control and the bioaugmented set and quantification of *Clostridium aceticum* in the bioaugmented set (Phase A: before bioaugmentation; Phase B: during bioaugmentation, and Phase C: after bioaugmentation).

feasibility from agro-industrial waste (cucumber, tomato, and lettuce) (Greses et al., 2020). Lim et al. (2020) investigated VFA production from fermentation of palm oil mill effluent under pH 5 (Lim et al., 2020). Their results stated that the highest acetic acid concentration was obtained as 918 mg COD/L at day 30 from 33400 mg COD/L content of the substrate. She et al. (2020) used the pretreatment (freezing/thawing) for VFA production from waste activated sludge. The pretreatment increased the acetic acid production from 933 ± 46 to 1281 ± 57 mg COD/L as maximum concentration (the SCOD concentration of substrate was 5852 mg/L) (She et al., 2020). From the view of substrate concentration in terms of COD content, the bioaugmentation of *C. aceticum* enhanced acetic acid production *via* fermentation more than 10 times than other studies. Based on the calculation of acetic acid production yield, it was 0.05 gCOD/ gCOD at Phase A, 0.125 gCOD/gCOD at Phase B, and 0.181 gCOD/gCOD at Phase C, respectively in the bioaugmented reactor with the 0.21 gCOD/gCOD (day 63) maximum value. Nonetheless, it was 0.06 ± 0.02 g COD/gCOD as an average at the control reactor in all phases. The bioaugmentation of *C. aceticum* increased acetic acid production yield 3.5 times than the control reactor. Jankowska et al. (2017) stated that the acetic acid production yield from cheese whey fermentation varied under different pH: as an average acetic acid production yield was 0.056 gCOD/gCOD under acidic pH, 0.31 gCOD/gCOD under alkali pH, and 0.164 gCOD/gCOD under neutral pH.

Atasoy et al. (2019a) compared acetic acid production efficiency from monoculture and mixed culture during fermentation of milk processing wastewater under alkali pH. Higher acetic acid concentration was obtained from *C. aceticum* as 743 mg COD/L than the mixed culture as 541 mg COD/L (Atasoy et al., 2019a). The result of the current study showed that bioaugmentation of mixed culture with *C. aceticum* produced almost two times higher acetic acid concentration than monoculture fermentation. Talabardon et al. (2000) evaluated the acetic acid production from milk permeate under thermophilic (60°C) fermentation. Although many thermophilic acetogens are not able to ferment lactose, they investigated that *Clostridium thermolacticum* can convert lactate to acetate, ethanol, CO_2 and H_2 (Talabardon et al., 2000). From this point of view, our results stated that *C. aceticum* not only grew with cheese production wastewater as substrate but also it increased acetic acid production in mixed culture.

Quantification of *Clostridium aceticum* During the Reactor Operation

The efficiency of the bioaugmentation was monitored *via* acetic acid production and the adaptation of *C. aceticum* in the mixed culture. For this reason, *C. aceticum* was quantified in every phase during the operation, as represented in **Figure 2**. The results showed that the average gene copy number of *C. aceticum* was $2.2 \times 10^6 \pm 1.5 \times 10^3$ before bioaugmentation (Phase A), while it increased $4.6 \times 10^6 \pm 1.1 \times 10^4$ during the application of bioaugmentation (Phase B). After the bioaugmentation was complete (Phase C), the gene copy number increased $5.3 \times 10^6 \pm 1.6 \times 10^3$ on average. Based on the quantification of *C. aceticum*, the average copy gene number increased almost 2.5 times by

TABLE 1 | Acetic acid production by mixed microbial culture fermentation under various operational and environmental conditions.

Substrate	Operational and environmental conditions	Acetic acid production as concentration	Acetic acid production as yield	References
Cheese production wastewater	Mixed culture fermentation under pH 10 at 35°C	After bioaugmentation (Phase C) 836 ± 261 mg COD/L as average; 1170 ± 18 mg COD/L as maximum in the bioaugmented reactor; and 150 ± 80 mg COD/L as average in the control reactor	After bioaugmentation (Phase C) 0.181 gCOD/gCOD as average; 0.21 gCOD/gCOD as maximum in the bioaugmented reactor; and 0.06 ± 0.02 gCOD/gCOD as average in the control reactor	This study
Cheese whey	Mixed culture fermentation under pH 5 at 30°C	The maximum acetic acid concentration 3580 mg COD/L	0.195 gCOD/gCOD	Lagoa-Costa et al., 2020
Agro-industrial waste: lettuce waste	Mixed culture fermentation under pH 6 ± 0.4 at 25°C	The maximum acetic acid concentration 5500 ± 70 mg COD/L	0.35 gCOD/gVS	Greses et al., 2020
Palm oil mill effluent	Mixed culture fermentation under pH 4.8–5.5 at 29°C	The maximum acetic acid concentration 918 mg COD/L	0.035 gCOD/gCOD	Lim et al., 2020
Waste activated sludge	Mixed culture fermentation under pH 6.8 at 35°C (application of freezing/thawing pretreatment)	The maximum acetic acid concentration 1281 ± 57 mg COD/L	0.218 gCOD/gCOD	She et al., 2020
Cheese whey	Mixed culture fermentation under different pH at 35°C	n/a	0.056 gCOD/gCOD under pH 5; 0.164 gCOD/gCOD under neutral pH; and 0.31 gCOD/gCOD under pH 10	Jankowska et al., 2017
Semi-synthetic milk processing wastewater	Mixed culture and pure culture fermentations under pH 10 at 35°C	743 mgCOD/L acetic acid by *C. aceticum;* 541 mgCOD/L acetic acid by mixed microbial culture	n/a	Atasoy et al., 2019a

bioaugmentation. The highest gene copy number was obtained on day 21 as $5.7 \times 10^6 \pm 1.2 \times 10^2$. Nevertheless, as stated before, the highest acetic acid production was obtained at day 63.

Even though the main product of *C. aceticum* is acetic acid, there are several other products such as ethanol, butyric acid, and acetone etc., based on the metabolic pathway type (Jones et al., 2016). Arslan et al. (2019) investigated acetic acid and ethanol production by *C. aceticum* under acidic and alkali pH conditions (Arslan et al., 2019). Their results showed that C. *aceticum* had a fast biomass growth under pH 8 with 1.8 g acetic acid production in the first 44 h of the fermentation. Nevertheless, the biomass growth of *C. aceticum* gradually decreased when the pH reached acidic conditions. Additionally, they observed that *C. aceticum* converted ethanol to acetic acid in the solventogenic phase as a reverse reaction (Arslan et al., 2019). From the perspective of their results, the growth of *C. aceticum* in the mixed culture might be promoted by the alkali pH. The reverse reaction ability of *C. aceticum* could result in higher other acid types of production at *C. aceticum* in the bioaugmented reactor than the control reactor.

Clostridium aceticum has been studied mainly for autotrophic growth on carbon dioxide, carbon monoxide, and hydrogen gasses to produce acetic acid (Sim et al., 2007; Riegler et al., 2019). Nevertheless, the results of the current study revealed that *C. aceticum* adapted well to the mixed culture under high alkali pH (10) in carbon-rich substrate fermentation.

Bacterial Community Profile

Besides the quantification of *C. aceticum*, the bacterial community profile in the bioaugmented reactor was analyzed. Analysis of the sequencing data for each phase (Phase A, B, and C) were presented as phylum and family levels in **Figure 3**. The results showed that despite the most dominant phylum, members were the same in each phase (**Figures 3A,C,E**). Their relative abundance varied depending on the bioaugmentation stage. The most dominant phylum was *Bacteroidetes* in Phase A (53 ± 12%), while its relative abundance decreased to 37 ± 9 and 38 ± 16% in Phase B and in Phase C, respectively. *Firmicutes* was the second most dominant phylum member in Phase A (25 ± 7%). The relative abundance of *Firmicutes* increased by bioaugmentation: it was 45 ± 4% in Phase B and 38 ± 11% in Phase C. In this regard, the bioaugmentation effect in each phase was more distinctly based on the relative abundance of family members (**Figures 3B,D,F**).

The bacterial community profile in the control reactor was presented in our recently published study (Atasoy and Cetecioglu, 2021). The results showed that the dominant phylum members changed through the reactor operation in the control reactor. *Firmicutes* (30 ± 3%) were dominant at the beginning of the reactor operation, while *Bacteroidetes* became dominant gradually, their relative abundance increased to 35 ± 11 and 49 ± 13% after almost 4 and 21 weeks of reactor operation, respectively (Atasoy and Cetecioglu, 2021).

The most dominant family members were *Flavobacteriaceae* (15 ± 6%) in Phase A; *Thermoanaerobacterales Family III. Incertae sedis* (24 ± 6%) in Phase B and *Porphyromonadaceae* (14 ± 7%) in Phase C, respectively in the bioaugmented reactor. On the other hand, the most dominant family members in the control reactor were *Porphyromonadaceae* (12 ± 2%), *Coriobacteriaceae* (8 ± 3%), and *Flavobacteriaceae* (8 ± 5%)

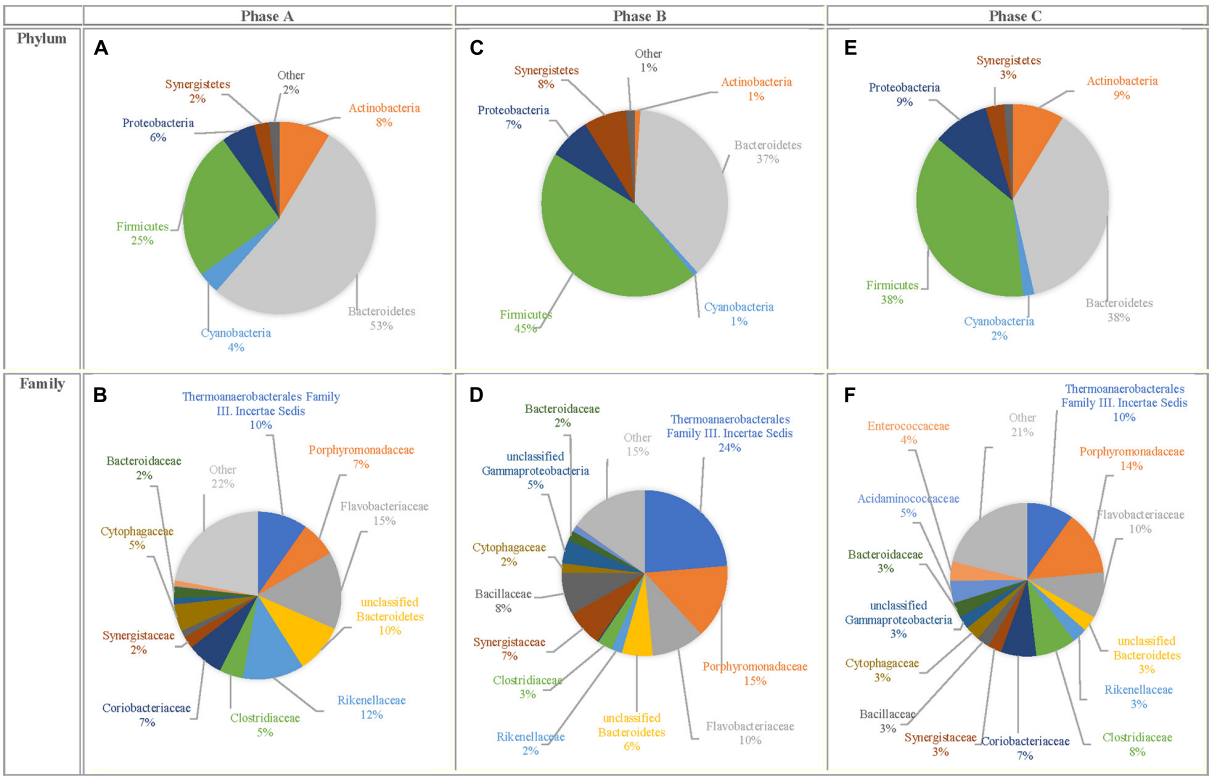

FIGURE 3 | Bacterial community profile for Phase A, Phase B, and Phase C for phylum level **(A,C,E)** and family level **(B,D,F)**.

at the beginning of the reactor operation. After 21 weeks, *Porphyromonadaceae* (27 ± 12%), *Bacteroidaceae* (17 ± 4%), and *Veillonellaceae* (11 ± 3%) became dominant in the control reactor (Atasoy and Cetecioglu, 2021).

Thermoanaerobacterales Family III. Incertae sedis belongs to the *Firmicutes* phylum, main fermentation products are acetate, succinate, ethanol and formate (Gries et al., 2019). The results revealed that the relative abundance of *Thermoanaerobacterales Family III. Incertae sedis* increased simultaneously with the gene copy number of *C. aceticum* during bioaugmentation. From this point of view, despite that, there is no study in the literature about the relations between species of the *Thermoanaerobacterales Family III. Incertae sedis* and *C. aceticum,* the results of the current study suggest that there might be a syntropy for acetic acid production.

The relative abundance of *Porphyromonadaceae,* which is a family member of *Bacteroidetes* phylum, increased by bioaugmentation. Since *Porphyromonadaceae* is mainly responsible for propionic acid production (Rios-Covian et al., 2017), an increase in propionic acid production during and after bioaugmentation might link with the high abundance of *Porphyromonadaceae.* Furthermore, *Porphyromonadaceae* (27 ± 12%) was the most dominant family member in the control reactor at the end of the reactor operation (Atasoy and Cetecioglu, 2021).

The relative abundance of *Rikenellaceae* from the phylum of *Bacteroidetes,* dramatically decreased by bioaugmentation: it was 12 ± 3% in Phase A; 2 ± 0.7% in Phase B, and 3 ± 1.02% in Phase C. Apart from the effects of bioaugmentation, the relative abundance of *Rikenellaceae* decreased by the retention time in anaerobic digesters (Nakasaki et al., 2020). *Rikenellaceae* is a well-known species in anaerobic digesters (Koo et al., 2019; Nakasaki et al., 2020; Schwan et al., 2020) and participates in easily degradable compounds (i.e., glycerol) degradation to acetic acid in fermentation (Nakasaki et al., 2020). In the current study, the decreasing relative abundance of *Rikenellaceae* in Phase B and Phase C might be caused by either rapid consumption of readily biodegradable compounds or competing with *C. aceticum* and members of the *Rikenellaceae* family.

Volatile Fatty Acid Composition Shift at the Bioaugmented Reactor

The main aim of mixed culture bioaugmentation with *C. aceticum* was to enhance acetic acid production in the VFA mixture. As stated before, acetic acid concentration was increased by bioaugmentation by *C. aceticum*: the average acetic acid percentage in the VFA mixture was 8 ± 0.2% in Phase A, 15 ± 4% in Phase B and 22 ± 5% in Phase C (**Figure 4A**). Interestingly, the results stated that the dominant acid type, which was propionic acid, did not change by bioaugmentation. Although *C. aceticum* is not responsible for propionic acid production according to its metabolic pathway (Alexander and Weuster-Botz, 2017; Arslan et al., 2019), propionic acid

production was enhanced by bioaugmentation of *C. aceticum*. The average percentage propionic acid concentration in the VFA mixture was 34 ± 23% in Phase A, 55 ± 13% in Phase B, and 49 ± 9% in Phase C. The dominant acid type was propionic acid in the control reactor during operation (**Figure 4B**). The acid composition in the control reactor as an average was: 59 ± 12% propionic acid, 13 ± 7% acetic acid, 8 ± 3% isovaleric acid, 7 ± 2% butyric acid, and 6 ± 3% isobutyric acid. The results stated that despite the propionic acid was dominant at both reactors, the bioaugmentation of *C. aceticum* suppressed the propionic acid percentage in the VFA mixture, while it increased the ratio of acetic acid.

The manipulation of the operational conditions in mixed culture fermentation can affect the acid composition (Lu et al., 2011). Nevertheless, control of the manipulation mechanism depends on thermodynamic and metabolic principles: the product mixture is specified by thermodynamic constraints and enzyme availability in pure culture fermentation, while, it is more complicated in mixed culture fermentation because of the wide range of metabolic activities and energetic considerations (Mohd-Zaki et al., 2016). Many studies have been conducted to identify metabolic flux and energy conversions in mixed culture fermentation (Lee et al., 2008; Hoelzle et al., 2014; De Vrieze and Verstraete, 2016; Cetecioglu et al., 2019). Lee et al. (2008) evaluated H_2 production from glucose fermentation under several pH conditions, thermodynamically (Lee et al., 2008). Based on their calculations, the standard Gibbs Free Energy $(\Delta G°)'$ for acetic acid and propionic acid production *via* glucose fermentation under pH 10 stated that acetic acid production has $-1{,}14$ kJ/e$^-$; propionic acid production has $-6{,}78$ kJ/e$^-$. Though thermodynamic calculations in fermentation depend on many parameters such as pH, temperature, substrate composition, therefore available electron acceptors, etc., the rough estimate would be an explanation for high propionic acid production in the bioaugmented reactor since propionic acid production provides more energy than acetic acid production.

Besides acetic and propionic acid production, other acid type production during the operation were observed: the average acid composition during Phase C was composed of 11 ± 8% of iso-valeric acid, 6 ± 4% of valeric acid, 5 ± 4% of iso-butyric acid, and 5 ± 3.2% of butyric acid in addition to acetic acid and propionic acid. Therefore, the bioaugmentation of *C. aceticum* enhanced not only acetic acid production but also increased propionic acid production indirectly and other acid productions (Alexander and Weuster-Botz, 2017). Nevertheless, the bioaugmentation of mixed culture by *C. butyricum* showed that the dominant acid type (propionic acid) was shifted to butyric acid by bioaugmentation (Atasoy and Cetecioglu, 2020). In addition, their results stated that bioaugmentation of *C. butyricum* did not only change dominant acid type but also significantly affect the VFA composition as well: propionic acid was decreased (from 60 ± 12 to 30 ± 17%) whereas, acetic (from 12 ± 7 to 20 ± 11%), butyric (from 21 ± 9 to 35 ± 4%), and valeric (from 8 ± 4 to 15 ± 5%) acids were increased by bioaugmentation (Atasoy and Cetecioglu, 2020). Therefore, despite pH (Atasoy et al., 2019b; Eryildiz et al., 2020), substrate type (Jankowska et al., 2017; Ma et al., 2017), and temperature (Jiang et al., 2013; Vanwonterghem et al., 2015) affected the VFA composition, the current results showed that type of monoculture in bioaugmentation is also one of the important parameters to effect acid type in fermentation.

Total VFA Production at the Bioaugmented Reactor

The total VFA production in the bioaugmented reactor was 1204 ± 340 mg COD/L (0.67 gCOD/gCOD yield) at Phase A, 1878 ± 338 mg COD/L (0.79 gCOD/gCOD yield) at Phase B, and 4166 ± 988 mg COD/L (0,85 gCOD/gCOD yield) at Phase C. Also, the highest total VFA production was obtained at day 70th as 5493 ± 36 mg COD/L with a 0,98 gCOD/gCOD production yield. In the control reactor, the average total VFA concentration was 1254 ± 11 mg COD/L with 0.68 ± 0.02 gCOD/gCOD yield. Thus, based on the total VFA concentration in the bioaugmented and the control reactor, the average concentration increased 3.3 times, whereas the maximum concentration increased 5 times.

The efficiency of VFA production *via* fermentation depends on several operational and environmental conditions. Jankowska et al. (2017) showed the importance of substrate type on VFA production (Jankowska et al., 2017). Their results stated that the highest VFA was obtained from microalgae biomass (0.83 gVFA/gSCOD), maize silage (0.78 gVFA/gSCOD), and cheese whey (0.71 gVFA/gSCOD), respectively, under initial alkaline pH conditions. Moretto et al. (2019) investigated the optimized conditions for VFA production under mesophilic and thermophilic conditions with different pH values by using a batch reactor and continuously stirred tank reactor (CSTR) from urban waste fermentation (Moretto et al., 2019). Their results showed that the batch reactor and CSTR produced almost the same VFA concentration with thermal pretreatment under pH 9 (41 ± 2 gCOD/L for batch; 39 gCOD/L for CSTR). The pH did not affect VFA concentration (pH 9: 30 ± 2 gCOD/L; pH 7: 27.5 ± 2 gCOD/L) as well (Moretto et al., 2019). In addition, Atasoy et al. (2019b) confirmed that the pH had almost no effect on VFA production yield. From the point of parameters that affect VFA production, the results of the current study stated that the VFA production depends on the type of bacterial strain as well as their interactions with each other and their environment.

The Correlation Analysis Between VFA Composition and Quantity of *C. aceticum*

The concentration of each acid type and quantity of *C. aceticum* was correlated during fermentation (Phase A, B, and C) to investigate their mutual effect on each other, the results are shown in **Table 2**. The correlation analysis results stated that acetic acid production positively correlated with total VFA (0.898), iso-valeric acid (0.866), propionic acid (0.789), and iso-hexanoic acid (0.720) production at a 0.01 significance level as well as the gene copy number of *C. aceticum* (0.553) at 0.05 significance level. Nevertheless, the bioaugmentation of *C. aceticum* resulted in higher propionic acid production in all phases. There was no correlation between propionic acid production and the gene copy number of *C. aceticum*. However, the total VFA

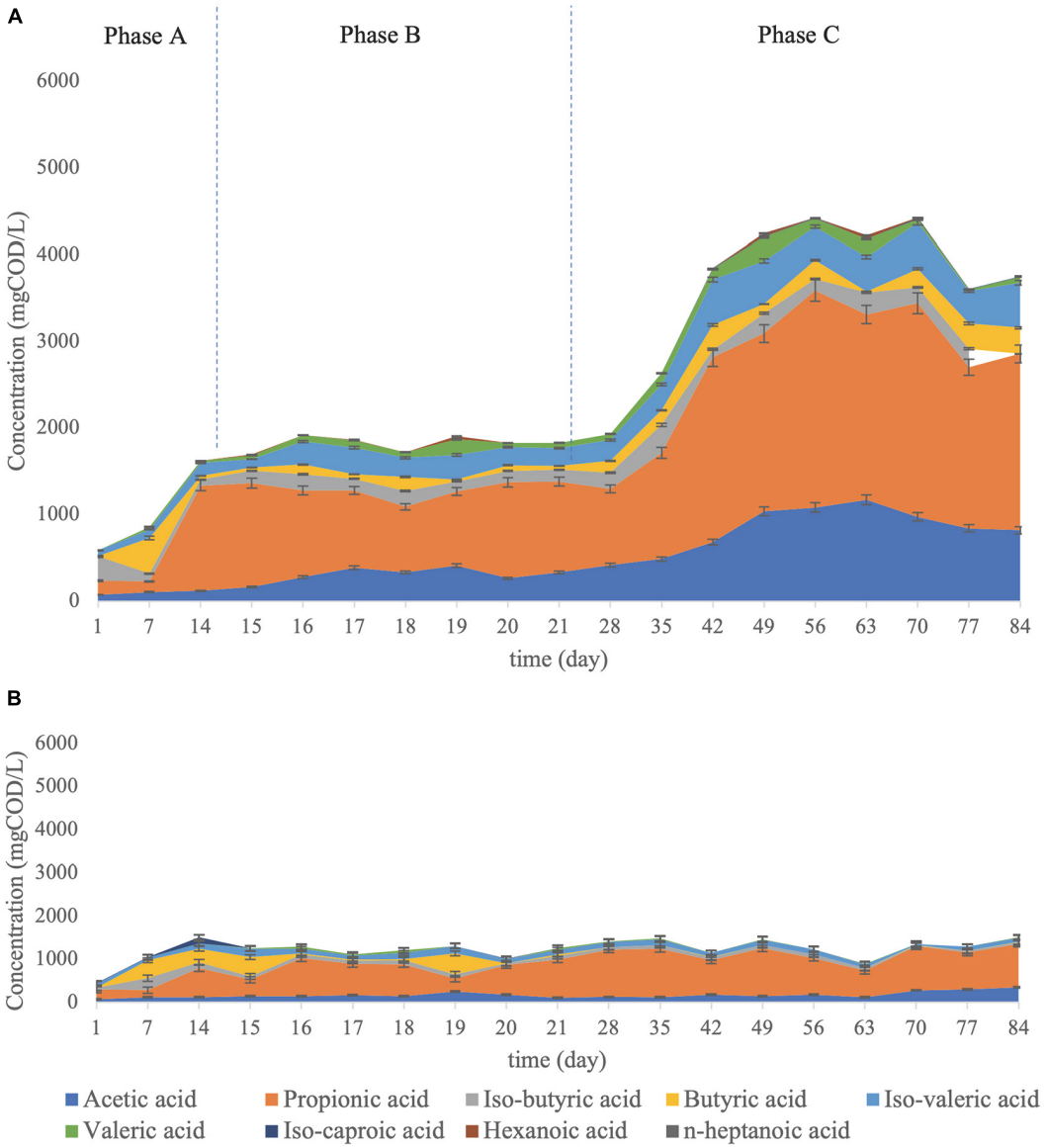

FIGURE 4 | VFA composition **(A)** in the *C. aceticum* bioaugmented reactor at Phase A: before bioaugmentation; Phase B: during bioaugmentation, and Phase C: after bioaugmentation and **(B)** in the control reactor.

production was correlated (0.490 at 0.05 significance level) with *C. aceticum*. Therefore, the correlation analysis of *C. aceticum* bioaugmentation reactor data might be explained as *C. aceticum* enhanced propionic acid production indirectly.

Cycle Analysis in the Bioaugmented Reactor

The acid composition was observed during a cycle (24-hour) to investigate the acid shift. Therefore, the cycle analysis was conducted after seven days of bioaugmentation application (day 28). The acid shift during a cycle for the bioaugmented reactor is represented in **Figure 5**.

The cycle analysis of *C. aceticum* in the bioaugmented reactor showed that almost all acid types were increased to the peak point in the first 5 h, then it was stable until the 9th hour. From the 13th hour, the production was increased again until at the end of the cycle. Mainly, acetic acid production in the 1st hour was 279 ± 17 mg COD/L, then it increased in the first 3 h to 1157 ± 29 mg COD/L. Following this, the production was almost stable in the next 14 h; afterwards, it reached 1148 ± 36 mg COD/L at the 24th hour. Propionic acid, which was the dominant acid type during a cycle, started from 1859 ± 204 mg COD/L in the 1st hour. It reached 3465 ± 108 mg COD/L at the end of the cycle (24th hour), although the highest propionic acid concentration was between the 5th and 9th hours.

TABLE 2 | Correlation coefficients between the quantification of *C. aceticum* with VFA composition after bioaugmentation.

	Acetic acid	Propionic acid	Iso-butyric acid	Butyric acid	Iso-valeric acid	Valeric acid	Iso hexanoic acid	Hexanoic acid	n-heptanic acid	Total VFA	*C.aceticum* copy number
Acetic acid	1	0.789**	0.312	0.012	0.866**	0.542*	0.720**	0.424	0.551*	0.898**	0.553*
Propionic acid	0.789**	1	0.226	0.013	0.878**	0.433	0.770**	0.383	0.197	0.968**	0.437
Iso-butyric acid	0.312	0.226	1	0.476*	0.471*	−0.095	0.583**	−0.217	0.426	0.361	0.194
Butyric acid	0.012	0.013	0.476*	1	0.073	−0.402	0.403	−0.468*	0.058	0.109	−0.33
Iso-valeric acid	0.866**	0.878**	0.471*	0.073	1	0.489*	0.729**	0.277	0.406	0.943**	0.646**
Valeric acid	0.542*	0.433	−0.095	−0.402	0.489*	1	−0.023	0.837**	0.329	0.483*	0.42
Iso hexanoic acid	0.720**	0.770**	0.583**	0.403	0.729**	−0.023	1	0.01	0.292	0.816**	0.233
Hexanoic acid	0.424	0.383	−0.217	−0.468*	0.277	0.837**	0.01	1	0.151	0.379	0.173
n-heptanoic acid	0.551*	0.197	0.426	0.058	0.406	0.329	0.292	0.151	1	0.355	0.177
Total VFA	0.898**	0.968**	0.361	0.109	0.943**	0.483*	0.816**	0.379	0.355	1	0.490*
C. aceticum copy number	0.553*	0.437	0.194	−0.33	0.646**	0.42	0.233	0.173	0.177	0.490*	1

***Correlation is significant at the 0.01 level (2-tailed); *Correlation is significant at the 0.05 level (2-tailed).*

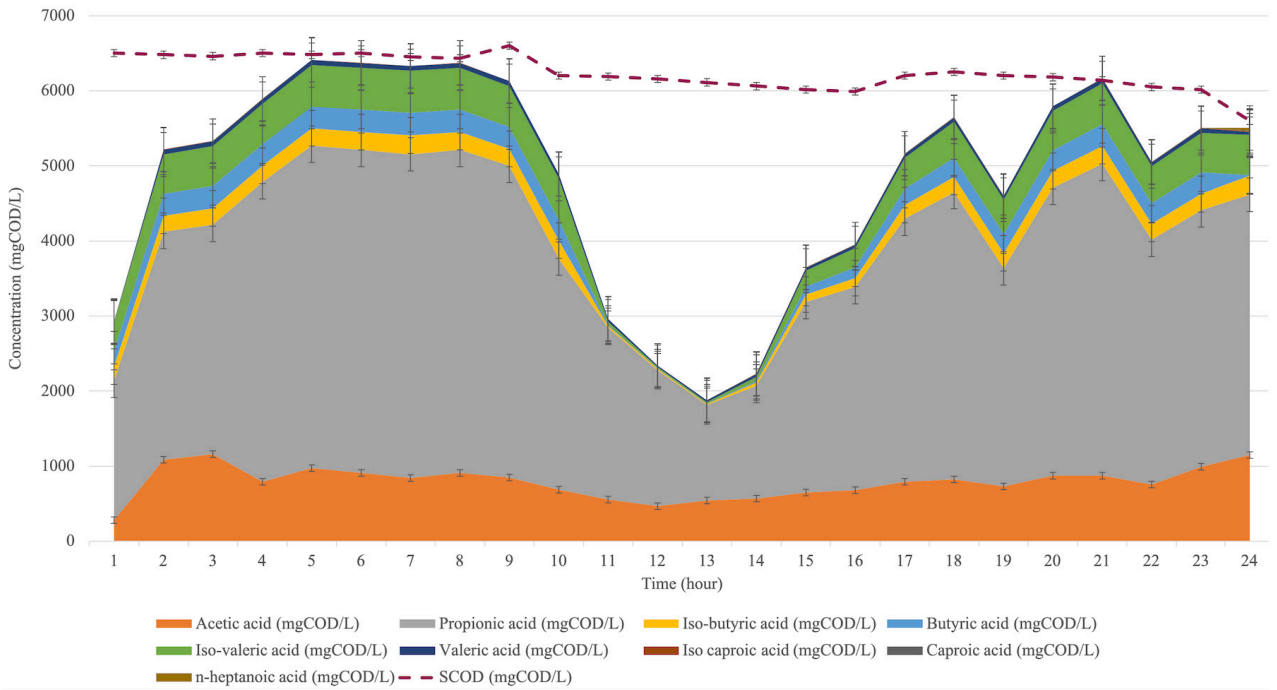

FIGURE 5 | VFA composition shift during a cycle analysis at the bioaugmented reactor for 24 h.

The sCOD concentration from the 1st hour to the 24th hour (**Figure 5**) showed that the sCOD reduction was negligible. Nevertheless, the reason for the drop in total VFA production between the 11th and 17th hours could be explained by CO_2 production. On the other hand, as described previously, the metabolic pathway of *C. aceticum* has reversible reactions from acetic acid to ethanol production as well as vice versa (Grimalt-Alemany et al., 2018). Therefore, the results might be explained by chain elongation (De Groof et al., 2019) from short-chain fatty acids (VFA) to medium or large chain fatty acids as well as ethanol or CO_2 production after the 16th hour. Following this, the reversible reactions might have increased VFA production again from the 14th hour. The cycle analysis stated that the highest VFA production, as well as acetic acid concentration, could be obtained in the first 6 h of the cycle, shortening the retention time or reduction of the reactor volume. In addition, cycle analysis was also conducted in the control reactor. The results showed that 12 h would be sufficient as a cycle duration to achieve a similar VFA

composition and production efficiency in the control reactor (Atasoy and Cetecioglu, 2020).

CONCLUSION

In this study, mixed microbial culture was bioaugmented by *C. aceticum* to obtain an acetic acid dominant VFA mixture. Despite the fact that acetic acid concentration was increased by bioaugmentation (almost 10-fold compared to the control reactor), the dominance of the propionic acid in the VFA mixture did not change. However, the effects of the bioaugmentation indicate certain unknown syntrophic relations and corresponding metabolic pathways. It is crucial to gain a deeper understanding of bioaugmentation's effects on the microbial community, particularly to establish its profile and the functions and interactions in the mixed culture. Furthermore, the identification of metabolic networks for acid production is crucial for a comprehensive view of bioaugmentation effects.

DATA AVAILABILITY STATEMENT

The datasets presented in this study can be found in online repositories. The names of the repository/repositories and accession number(s) can be found below: https://www.ncbi.nlm.nih.gov/, PRJNA667606.

AUTHOR CONTRIBUTIONS

MA: conceptualization, methodology, formal analysis, investigation, data curation, writing – original draft, and visualization. ZC: conceptualization, writing – review and editing, and supervision. Both authors contributed to the article and approved the submitted version.

FUNDING

This study was financed by the Vinnmer Marie Curie Incoming Grant (2016-04070).

ACKNOWLEDGMENTS

We would like to acknowledged support from the Science for Life Laboratory, the National Genomics Infrastructure, NGI, and Uppmax for assisting in massive parallel sequencing and computational infrastructure.

REFERENCES

Alexander, M., and Weuster-Botz, D. (2017). Reaction engineering analysis of the autotrophic energy metabolism of Clostridium aceticum. *Biochem. Eng. J.* 364:fnx219. doi: 10.1093/femsle/fnx219

Allied Market Research (2020). *World Acetic Acid Market – Opportunities and Forecasts, 2019-2026*. Available online at: https://www.alliedmarketresearch.com/acetic-acid-market (accessed March 20, 2020).

APHA, AWWA, and WEF (2012). *Standard Methods for the Examination of Water and Wastewater. Stand Methods*. Alexandria, VA: Water Environment Federation, 541.

Arslan, K., Bayar, B., Nalakath Abubackar, H., Veiga, M. C., and Kennes, C. (2019). Solventogenesis in *Clostridium aceticum* producing high concentrations of ethanol from syngas. *Bioresour. Technol.* 292, 121941. doi: 10.1016/j.biortech.2019.121941

Atasoy, M., and Cetecioglu, Z. (2020). Butyric acid dominant volatile fatty acids production: bio-augmentation of mixed culture fermentation by *Clostridium butyricum*. *J. Environ. Chem. Eng.* 8:104496. doi: 10.1016/j.jece.2020.104496

Atasoy, M., and Cetecioglu, Z. (2021). Bioaugmentation as a strategy for tailor-made volatile fatty acid production. *J. Environ. Manage* 295:113093.

Atasoy, M., Eyice, Ö, and Cetecioglu, Z. (2019a). Volatile fatty acid production from semi-synthetic milk processing wastewater under alkali pH: the pearls and pitfalls of microbial culture. *Bioresour. Technol.* 19:122415. doi: 10.1016/j.biortech.2019.122415

Atasoy, M., Eyice, Ö., and Cetecioglu, Z. (2020a). A comprehensive study of volatile fatty acids production from batch reactor to anaerobic sequencing batch reactor by using cheese processing wastewater. *Bioresour. Technol.* 311:123529. doi: 10.1016/j.biortech.2020.123529

Atasoy, M., Eyice, O., Schnürer, A., and Cetecioglu, Z. (2019b). Volatile fatty acids production via mixed culture fermentation: revealing the link between pH, inoculum type and bacterial composition. *Bioresour. Technol.* 292:121889. doi: 10.1016/j.biortech.2019.121889

Atasoy, M., Owusu-Agyeman, I., Plaza, E., and Cetecioglu, Z. (2018). Bio-based volatile fatty acid production and recovery from waste streams: current status and future challenges. *Bioresour. Technol.* 268, 0–1. doi: 10.1016/j.biortech.2018.07.042

Bhatia, S. K., and Yang, Y.-H. (2017). Microbial production of volatile fatty acids: current status and future perspectives. *Rev. Environ. Sci. Bio Technol.* 16, 327–345. doi: 10.1007/s11157-017-9431-4

Braun, M., Mayer, F., and Gottschalk, G. (1981). Clostridium aceticum (Wieringa), a microorganism producing acetic acid from molecular hydrogen and carbon dioxide. *Arch. Microbiol.* 128, 288–293. doi: 10.1007/BF00422532

Britz, T. J., and van Schalkwyk, C. (2006). Treatment of dairy processing wastewaters. *Waste Treat. Food Process. Ind.* 6, 1–28. doi: 10.1201/9781420037128.ch1

Caporaso, J. G., Lauber, C. L., Walters, W. A., Berg-Lyons, D., Lozupone, C. A., Turnbaugh, P. J., et al. (2011). Global patterns of 16S rRNA diversity at a depth of millions of sequences per sample. *Proc. Natl. Acad. Sci. U.S.A.* 108, 4516–4522. doi: 10.1073/pnas.1000080107

Cetecioglu, Z., Dolfing, J., Taylor, J., Purdy, K. J., and Eyice, Ö (2019). COD/sulfate ratio does not affect the methane yield and microbial diversity in anaerobic digesters. *Water Res.* 155, 444–454. doi: 10.1016/j.watres.2019.02.038

Chi, X., Li, J., Wang, X., Zhang, Y., Leu, S. Y., and Wang, Y. (2018). Bioaugmentation with Clostridium tyrobutyricum to improve butyric acid production through direct rice straw bioconversion. *Bioresour. Technol.* 263, 562–568. doi: 10.1016/j.biortech.2018.04.120

Ciesielski, S., and Przybylek, G. (2014). Volatile fatty acids influence on the structure of microbial communities producing PHAs. *Brazilian J. Microbiol.* 45, 395–402. doi: 10.1590/S1517-83822014000200005

Cirne, D. G., Björnsson, L., Alves, M., and Mattiasson, B. (2006). Effects of bioaugmentation by an anaerobic lipolytic bacterium on anaerobic digestion of lipid-rich waste. *J. Chem. Technol. Biotechnol.* 81, 1745–1752. doi: 10.1002/jctb.1597

Cock, P. J. A., Antao, T., Chang, J. T., Chapman, B. A., Cox, C. J., Dalke, A., et al. (2009). Biopython: Freely available Python tools for computational molecular biology and bioinformatics. *Bioinformatics* 25, 1422–1423. doi: 10.1093/bioinformatics/btp163

De Groof, V., Coma, M., Arnot, T., Leak, D. J., and Lanham, A. B. (2019). Medium chain carboxylic acids from complex organic feedstocks by mixed culture fermentation. *Molecules* 24, 1–39. doi: 10.3390/molecules24030398

De Vrieze, J., and Verstraete, W. (2016). Perspectives for microbial community composition in anaerobic digestion: from abundance and activity to

connectivity. *Environ. Microbiol.* 18, 2797–2809. doi: 10.1111/1462-2920.13437

Dietrich, K., Dumont, M. J., Del Rio, L. F., and Orsat, V. (2017). Producing PHAs in the bioeconomy — Towards a sustainable bioplastic. *Sustain. Prod. Consum.* 9, 58–70. doi: 10.1016/j.spc.2016.09.001

Du, R., Peng, Y., Ji, J., Shi, L., Gao, R., and Li, X. (2019). Partial denitrification providing nitrite: opportunities of extending application for anammox. *Environ. Int.* 131:105001. doi: 10.1016/j.envint.2019.105001

Eryildiz, B., Lukitawesa, and Taherzadeh, M. J. (2020). Effect of pH, substrate loading, oxygen, and methanogens inhibitors on volatile fatty acid (VFA) production from citrus waste by anaerobic digestion. *Bioresour. Technol.* 302:122800. doi: 10.1016/j.biortech.2020.122800

Eurostat (2020). Chemicals production and consumption statistics. *Stat. Explain.* 2009, 1–9.

Expert Market Research (2019). *Global Acetic Acid Market*. Sheridan, WY: Expert Market Research.

Fang, W., Zhang, X., Zhang, P., Wan, J., Guo, H., Ghasimi, D. S. M., et al. (2020). Overview of key operation factors and strategies for improving fermentative volatile fatty acid production and product regulation from sewage sludge. *J. Environ. Sci. (China)* 87, 93–111. doi: 10.1016/j.jes.2019.05.027

FDA (1989). Available online at: https://www.fda.gov/regulatory-information/search-fda-guidance-documents/cpg-sec-562100-acetic-acid-use-foods-labeling-foods-which-used (accessed March 20, 2020).

Greses, S., Tomás-Pejó, E., and Gónzalez-Fernández, C. (2020). Agroindustrial waste as a resource for volatile fatty acids production via anaerobic fermentation. *Bioresour. Technol.* 297, 122486. doi: 10.1016/j.biortech.2019.122486

Gries, O., Ly, T., Gries, O., and Ly, T. (2019). *The Firmicutes, Bergey's Manual of Systematic Bacteriology*, 2nd Edn. Salmon Tower Building: Springer International Publishing. doi: 10.1007/978-3-662-58219-0_26

Grimalt-Alemany, A., Łężyk, M., Lange, L., Skiadas, I. V., and Gavala, H. N. (2018). Enrichment of syngas-converting mixed microbial consortia for ethanol production and thermodynamics-based design of enrichment strategies. *Biotechnol. Biofuels* 11, 1–22. doi: 10.1186/s13068-018-1189-6

Gunjan, D., and Haresh, M. (2020). Production pathways of acetic acid and its versatile applications in the food industry. *Intech* 32, 137–144. doi: 10.5772/intechopen.92289

Hansen, R. G. (1974). "Milk in human nutrition," in *Nutrition and Biochemistry of Milk/Maintenance*, eds B. L. Larson and V. R. SMITH (Academic Press), doi: 10.1016B978-0-12-436703-6.50013-2

Herrero, M., and Stuckey, D. C. (2015). Bioaugmentation and its application in wastewater treatment: a review. *Chemosphere* 140, 119–128. doi: 10.1016/j.chemosphere.2014.10.033

Hoelzle, R. D., Virdis, B., and Batstone, D. J. (2014). Regulation mechanisms in mixed and pure culture microbial fermentation. *Biotechnol. Bioeng.* 111, 2139–2154. doi: 10.1002/bit.25321

Hong, P., Wu, X., Shu, Y., Wang, C., Tian, C., Wu, H., et al. (2020). Bioaugmentation treatment of nitrogen-rich wastewater with a denitrifier with biofilm-formation and nitrogen-removal capacities in a sequencing batch biofilm reactor. *Bioresour. Technol.* 303:122905. doi: 10.1016/j.biortech.2020.122905

Jankowska, E., Chwialkowska, J., Stodolny, M., and Oleskowicz-Popiel, P. (2017). Volatile fatty acids production during mixed culture fermentation – The impact of substrate complexity and pH. *Chem. Eng. J.* 326, 901–910. doi: 10.1016/j.cej.2017.06.021

Jiang, J., Zhang, Y., Li, K., Wang, Q., Gong, C., and Li, M. (2013). Volatile fatty acids production from food waste: effects of pH, temperature, and organic loading rate. *Bioresour. Technol.* 143, 525–530. doi: 10.1016/j.biortech.2013.06.025

Jones, S. W., Fast, A. G., Carlson, E. D., Wiedel, C. A., Au, J., Antoniewicz, M. R., et al. (2016). CO 2 fixation by anaerobic non-photosynthetic mixotrophy for improved carbon conversion. *Nat. Commun.* 7:12800. doi: 10.1038/ncomms12800

Kedia, G., Passanha, P., Dinsdale, R. M., Guwy, A. J., and Esteves, S. R. (2014). Evaluation of feeding regimes to enhance PHA production using acetic and butyric acids by a pure culture of *Cupriavidus necator*. *Biotechnol. Bioprocess Eng.* 19, 989–995. doi: 10.1007/s12257-014-0144-z

Khan, M. A., Ngo, H. H., Guo, W. S., Liu, Y., Nghiem, L. D., Hai, F. I., et al. (2016a). Optimization of process parameters for production of volatile fatty acid, biohydrogen and methane from anaerobic digestion. *Bioresour. Technol.* 219, 738–748. doi: 10.1016/j.biortech.2016.08.073

Khan, M. A., Ngo, H. H., Guo, W. S., Liu, Y. W., Zhou, J. L., Zhang, J., et al. (2016b). Comparing the value of bioproducts from different stages of anaerobic membrane bioreactors. *Bioresour. Technol.* 214, 816–825. doi: 10.1016/j.biortech.2016.05.013

Klindworth, A., Pruesse, E., Schweer, T., Peplies, J., Quast, C., Horn, M., et al. (2013). Evaluation of general 16S ribosomal RNA gene PCR primers for classical and next-generation sequencing-based diversity studies. *Nucleic Acids Res.* 41, 1–11. doi: 10.1093/nar/gks808

Koo, T., Yulisa, A., and Hwang, S. (2019). Microbial community structure in full scale anaerobic mono-and co-digesters treating food waste and animal waste. *Bioresour. Technol.* 282, 439–446. doi: 10.1016/j.biortech.2019.03.050

Küsel, K., and Drake, H. L. (2011). "Acetogens," in *Encyclopedia of Geobiology*, eds R. Joachim and T. Volker (Berlin: Springer), 928. doi: 10.1007/978-1-4020-9212-1

Lagoa-Costa, B., Kennes, C., and Veiga, M. C. (2020). Cheese whey fermentation into volatile fatty acids in an anaerobic sequencing batch reactor. *Bioresour. Technol.* 302, 5175–5181. doi: 10.1016/j.watres.2020.115633

Lee, H. S., Salerno, M. B., and Rittmann, B. E. (2008). Thermodynamic evaluation on H2 production in glucose fermentation. *Environ. Sci. Technol.* 42, 2401–2407. doi: 10.1021/es702610v

Li, Y., Zhang, Q., Li, M., Sang, W., Wang, Y., Wu, L., et al. (2020). Bioaugmentation of sequencing batch reactor for aniline treatment during start-up period: Investigation of microbial community structure of activated sludge. *Chemosphere* 243:125426. doi: 10.1016/j.chemosphere.2019.125426

Lim, J. X., Zhou, Y., and Vadivelu, V. M. (2020). Enhanced volatile fatty acid production and microbial population analysis in anaerobic treatment of high strength wastewater. *J. Water Process Eng.* 33:101058. doi: 10.1016/j.jwpe.2019.101058

Lu, H., Villada, J. C., and Lee, P. K. H. (2019). Modular metabolic engineering for biobased chemical production. *Trends Biotechnol.* 37, 152–166. doi: 10.1016/j.tibtech.2018.07.003

Lu, Y., Slater, F. R., Mohd-Zaki, Z., Pratt, S., and Batstone, D. J. (2011). Impact of operating history on mixed culture fermentation microbial ecology and product mixture. *Water Sci. Technol.* 64, 760–765. doi: 10.2166/wst.2011.699

Ma, H., Liu, H., Zhang, L., Yang, M., Fu, B., and Liu, H. (2017). Novel insight into the relationship between organic substrate composition and volatile fatty acids distribution in acidogenic co-fermentation. *Biotechnol. Biofuels* 10, 1–15. doi: 10.1186/s13068-017-0821-1

Mielcarek, A., Rodziewicz, J., Janczukowicz, W., and Bryszewski, K. (2018). Effect of acetic acid on denitrification and dephosphatation process efficiencies in sequencing batch biofilm reactor. *J. Ecol. Eng.* 19, 176–180. doi: 10.12911/22998993/89659

Mohd-Zaki, Z., Bastidas-Oyanedel, J., Lu, Y., Hoelzle, R., Pratt, S., Slater, F., et al. (2016). Influence of pH regulation mode in glucose fermentation on product selection and process stability. *Microorganisms* 4:2. doi: 10.3390/microorganisms4010002

Moretto, G., Valentino, F., Pavan, P., Majone, M., and Bolzonella, D. (2019). Optimization of urban waste fermentation for volatile fatty acids production. *Waste Manag.* 92, 21–29. doi: 10.1016/j.wasman.2019.05.010

Mussatto, S. I. (2017). Challenges in building a sustainable biobased economy. *Ind. Crops Prod.* 106, 1–2. doi: 10.1016/j.indcrop.2017.07.007

Nakasaki, K., Nguyen, K. K., Ballesteros, F. C., Maekawa, T., and Koyama, M. (2020). Characterizing the microbial community involved in anaerobic digestion of lipid-rich wastewater to produce methane gas. *Anaerobe* 61:102082. doi: 10.1016/j.anaerobe.2019.102082

OECD (2003). *Guideline For The Testing of Chemicals Proposal*. Paris: Organisation for Economic Co-operation and Development.

Poehlein, A., Cebulla, M., Ilg, M. M., Bengelsdorf, F. R., Schiel-bengelsdorf, B., Whited, G., et al. (2015). The complete genome sequence of clostridium aceticum: a missing. *MBio* 6:e01168-15. doi: 10.1128/mBio.01168-15.Editor

Riegler, P., Bieringer, E., Chrusciel, T., Stärz, M., Löwe, H., and Weuster-Botz, D. (2019). Continuous conversion of CO2/H2 with Clostridium aceticum in biofilm reactors. *Bioresour. Technol.* 291:121760. doi: 10.1016/j.biortech.2019.121760

Rios-Covian, D., Salazar, N., Gueimonde, M., and de los Reyes-Gavilan, C. G. (2017). Shaping the metabolism of intestinal *Bacteroides* population through

diet to improve human health. *Front. Microbiol.* 8:1–6. doi: 10.3389/fmicb.2017.00376

Ritchie, H., and Roser, M. (2019). *CO2 and Greenhouse Gas Emissions. Our World Data*. Available online at: https://ourworldindata.org/co2-and-other-greenhouse-gas-emissions (accessed March 20, 2020).

Schwan, B., Abendroth, C., Latorre-Pérez, A., Porcar, M., Vilanova, C., and Dornack, C. (2020). Chemically stressed bacterial communities in anaerobic digesters exhibit resilience and ecological flexibility. *Front. Microbiol.* 11:867. doi: 10.3389/fmicb.2020.00867

She, Y., Hong, J., Zhang, Q., Chen, B. Y., Wei, W., and Xin, X. (2020). Revealing microbial mechanism associated with volatile fatty acids production in anaerobic acidogenesis of waste activated sludge enhanced by freezing/thawing pretreatment. *Bioresour. Technol.* 302:122869. doi: 10.1016/j.biortech.2020.122869

Sim, J. H., Kamaruddin, A. H., Long, W. S., and Najafpour, G. (2007). Clostridium aceticum-A potential organism in catalyzing carbon monoxide to acetic acid: application of response surface methodology. *Enzyme Microb. Technol.* 40, 1234–1243. doi: 10.1016/j.enzmictec.2006.09.017

Tabatabaei, M., Aghbashlo, M., Valijanian, E., Kazemi Shariat Panahi, H., Nizami, A. S., Ghanavati, H., et al. (2020). A comprehensive review on recent biological innovations to improve biogas production, Part 2: mainstream and downstream strategies. *Renew. Energy* 146, 1392–1407. doi: 10.1016/j.renene.2019.07.047

Talabardon, M., Schwitzguébel, J. P., and Péringer, P. (2000). Anaerobic thermophilic fermentation for acetic acid production from milk permeate. *J. Biotechnol.* 76, 83–92. doi: 10.1016/S0168-1656(99)00180-7

Tang, H., Zhang, Y., Hu, J., Li, Y., Li, N., and Wang, M. (2019). Mixture of different *Pseudomonas aeruginosa* SD-1 strains in the efficient bioaugmentation for synthetic livestock wastewater treatment. *Chemosphere* 237, 1–8. doi: 10.1016/j.chemosphere.2019.124455

UNEP (2013). *Global Chemicals Outlook: Towards Sound Management of Chemicals*. Nairobi: UNEP.

UNFCCC (2015). *Paris Agreement. Conf. Parties Its Twenty-First Sess*, Vol. 32. Rio de Janeiro: UNFCCC.

United Nations (2018). *Sustainable Development Goals*. Available online at: https://sustainabledevelopment.un.org/sdgs (accessed March 20, 2020).

Vanwonterghem, I., Jensen, P. D., Rabaey, K., and Tyson, G. W. (2015). Temperature and solids retention time control microbial population dynamics and volatile fatty acid production in replicated anaerobic digesters. *Sci. Rep.* 5, 1–8. doi: 10.1038/srep08496

Vidra, A., and Németh, Á (2018). Bio-produced acetic acid: a review. *Period. Polytech. Chem. Eng.* 62, 245–256. doi: 10.3311/PPch.11004

Wu, M., Guo, X., Wu, J., and Chen, K. (2020). Effect of compost amendment and bioaugmentation on PAH degradation and microbial community shifting in petroleum-contaminated soil. *Chemosphere* 256:126998. doi: 10.1016/j.chemosphere.2020.126998

Xie, J., Duan, X., Feng, L., Yan, Y., Wang, F., Dong, H., et al. (2019). Influence of sulfadiazine on anaerobic fermentation of waste activated sludge for volatile fatty acids production: focusing on microbial responses. *Chemosphere* 219, 305–312. doi: 10.1016/j.chemosphere.2018.12.015

Xu, K., Liu, H., Du, G., and Chen, J. (2009). Real-time PCR assays targeting formyltetrahydrofolate synthetase gene to enumerate acetogens in natural and engineered environments. *Anaerobe* 15, 204–213. doi: 10.1016/j.anaerobe.2009.03.005

Yang, Z., Wang, W., Liu, C., Zhang, R., and Liu, G. (2019). Mitigation of ammonia inhibition through bioaugmentation with different microorganisms during anaerobic digestion: Selection of strains and reactor performance evaluation. *Water Res.* 155, 214–224. doi: 10.1016/j.watres.2019.02.048

Younes, M., Aquilina, G., Castle, L., Engel, K. H., Fowler, P., Frutos Fernandez, M. J., et al. (2020). Re-evaluation of acetic acid, lactic acid, citric acid, tartaric acid, mono- and diacetyltartaric acid, mixed acetic and tartaric acid esters of mono- and diglycerides of fatty acids (E 472a-f) as food additives. *EFSA J.* 18:6032. doi: 10.2903/j.efsa.2020.6032

Conflict of Interest: The authors declare that the research was conducted in the absence of any commercial or financial relationships that could be construed as a potential conflict of interest.

Publisher's Note: All claims expressed in this article are solely those of the authors and do not necessarily represent those of their affiliated organizations, or those of the publisher, the editors and the reviewers. Any product that may be evaluated in this article, or claim that may be made by its manufacturer, is not guaranteed or endorsed by the publisher.

Advantages of publishing in Frontiers

OPEN ACCESS
Articles are free to read for greatest visibility and readership

FAST PUBLICATION
Around 90 days from submission to decision

HIGH QUALITY PEER-REVIEW
Rigorous, collaborative, and constructive peer-review

TRANSPARENT PEER-REVIEW
Editors and reviewers acknowledged by name on published articles

Frontiers
Avenue du Tribunal-Fédéral 34
1005 Lausanne | Switzerland

Visit us: www.frontiersin.org
Contact us: frontiersin.org/about/contact

REPRODUCIBILITY OF RESEARCH
Support open data and methods to enhance research reproducibility

DIGITAL PUBLISHING
Articles designed for optimal readership across devices

FOLLOW US
@frontiersin

IMPACT METRICS
Advanced article metrics track visibility across digital media

EXTENSIVE PROMOTION
Marketing and promotion of impactful research

LOOP RESEARCH NETWORK
Our network increases your article's readership